THE UNIVERSITY OF OKLAHOMA

GRADUATE COLLEGE

CONTEMPORANEOUS FAULTS: A MECHANISM FOR THE CONTROL OF SEDIMENTATION IN THE SOUTHWESTERN ARKOMA BASIN, OKLAHOMA

A DISSERTATION

SUBMITTED TO THE GRADUATE FACULTY

in partial fulfillment of the requirements for the

degree of

DOCTOR OF PHILOSOPHY

BY

MICHAEL WILLIAM MCQUILLAN

Norman, Oklahoma

1977

CONTEMPORANEOUS FAULTS: A MECHANISM FOR THE CONTROL OF SEDIMENTATION IN THE SOUTHWESTERN ARKOMA BASIN, OKLAHOMA

APPROVED BY

Daniel A. Busch

Charles W. Harper

John S. Wickham

Charles J. Mankin

George G. Huffman

DISSERTATION COMMITTEE

CONTEMPORANEOUS FAULTS: A MECHANISM FOR THE CONTROL OF SEDIMENTATION IN THE SOUTHWESTERN ARKOMA BASIN, OKLAHOMA

by

Michael William McQuillan

ABSTRACT

Basal Atokan and Morrowan deposition in the Arkoma basin was influenced by three down-to-the basin growth faults similar to those which have been reported from the Gulf coast. There are abrupt increases in thickness of the lower Atokan and Morrowan strata on the downthrown sides of the faults. The increased thickness in the lower Atokan is about 2,000 feet across the Kinta fault and 3,000 to 4,500 feet across the San Bois fault; the increase in thickness in the Morrowan section is less dramatic and amounts to 100 to 200 feet. The changes in stratigraphic section in proximity to faults also occurs subjacent to the minor faults within the major blocks.

The basal Atokan sand is subdivided into a lower Spiro "B" and overlying Spiro "A" facies. The Spiro "A" is believed to be a submarine sand, deposited below wave base by density currents in trends subparallel with apleo-depositional strike. The trends of maximum Spior "A" thickness and best sorting occur subjacent to faults; the sand is thinner and more shaly over the crestal portions of fault blocks. The Spiro "B" consists of offshore bar sands which occur as pods on fault block paleotopographical highs. The distribution of the Spiro "B" facies is restricted to a 50 square mile area in Ts. 8 and 9 N., Rs. 22, 23 and 24 E. The Spiro "B" represents an interruption in the early stage of transgression over the eroded Wapanucka limestone; it was followed by a transgression and the deposition of the overlying Spiro "A" sand.

The Spiro "A" sand is very fine to medium grained (0.11 to 0.34 mm.), subangular to well rounded and poorly to well sorted. The textural maturity is poorest over the crestal portions of fault blocks and is best in proximity to the bounding faults.

Intergranular pore space in the Spiro "A" and "B" sands has been reduced by formation of secondary quartz cement. Chlorite coatings on the surface of the detrital quartz grains preserved intergranular porosity by retarding the formation of secondary quartz overgrowths. The distribution of porous versus non-porous sand due to diagenetic alteration is interpreted to be related to depositional environment. In those areas of the fault blocks where the sand is somewhat shaly (e.g., crestal portions)

the best porosities and permeabilities are preserved. Along the margins of the fault blocks where the sand is thickest and best sorted, alteration by diagenetic quartz was most severe. This resulted in the best reservoir rock (those wells with the greatest gas deliverability rates) occurring over and near the crests of fault blocks where the sand is somewhat shaly and least affected by secondary quartz cement.

The Cromwell is subdivided (in descending order), into three facies, the Cromwell I, II and III sands. All three sands were mapped subparallel to depositional strike and subparallel to the fault pattern. The distribution of the Cromwell I is limited to the area around the Kinta fault block. The Cromwell II and III sands are present throughout the area, but as a whole are quite shaly. The shaly character is related to sediment supply and rate of subsidence -- when sand supply was limited and subsidence slow, shaly and poorly developed sands were deposited. The secondary quartz cement alteration history of the Cromwell sands was interpreted to be similar to that of the Spiro sands. The best preserved porosity and permeability occurs in areas where the Cromwell is somewhat shaly; however, the overall shaly character of the Cromwell results in favorable reservoir facies of only limited extent.

The source of the Spiro sand was to the east and southeast, with a limited contribution of sediment from the north. The source of the Cromwell was probably similar to that of the Spiro; local sources however, may have contributed substantial amounts of sediment.

The Arkoma basin was an area of rapid basinal subsidence. Subsidence began as early as Morrowan time and continued during deposition of the basal Atokan sediments. The rapid rate of subsidence and growth fault controlled sedimentation continued throughout Atokan time.

The growth faults cutting the Morrowan - basal Atokan strata probably originated by movement in the basement and were perpetuated by additional basement movement and/or sedimentary loading and slumping. Contemporaneous movement along the faults continued throughout deposition of the Atokan sediments and appears to diminish and cease by the time of Hartshorne sand (Desmoinesian) deposition.

ACKNOWLEDGEMENTS

The writer wishes to extend his sincere appreciation to Dr. D. A. Busch for his knowledge and advise given freely during the course of this investigation. Grateful acknowledgement is made also to Dr. C. J. Mankin for his advise and supervision.

Special thanks are due Dr. G. G. Huffman, Dr. J. S. Wickham and Dr. C. W. Harper for their critical appraisal of the manuscript and the suggestions offered by them for its improvement.

Mechanical logs were made available (through the efforts of Mr. Ed McRae), by Galaxy Oil Company, Wichita Falls, Texas and by the Oklahoma City Geological Society Log Library. Sampled were obtained from the Oklahoma Core and Sample Library, Norman, Oklahoma.

The thin sections of the Spiro and Cromwell sands were made available by Dr. D. N. Lumsden, Dr. E. D. Pittman and Dr. R. S. Buchanan. These were from the collection that furnished the petrographic information for their publication (Lumsden, et al., 1971, "Sedimentation and petrology of Spiro and Foster sands (Pennsylvanian), McAlester Basin, Oklahoma", Am. Assoc. Petroleum Geologists Bull., vol. 55, p. 254-266.

Finally, this study could not have been brought to completion without the patience and support of my faithful wife, to her I am deeply grateful.

TABLE OF CONTENTS

SUBSURFACE GEOLOGY (continued)

LIST OF TABLES

LIST OF FIGURES

LIST OF PLATES

CONTEMPORANEOUS FAULTS: A MECHANISM FOR THE CONTROL OF SEDIMENTATION IN THE SOUTHWESTERN ARKOMA BASIN, OKLAHOMA

INTRODUCTION

Introductory Statement

The existence of contemporaneous faults (growth faults) in the Arkoma Basin has been known for several years. They are characterized by thickening of the sedimentary section on the basinward, down-thrown side where rollover (reverse drag) is commonly exhibited. The significance of contemporaneous faults and the role they play in the areas of oil and gas exploration prompted study of these phenomena.

Location

The area investigated is north of the Choctaw fault and encompasses 38 townships in contiguous portions of Pittsburg, Haskell, Latimer and LeFlore Counties, Oklahoma, within Ts. 6 to 11 N., Rs. 17 to 27 E. (Fig. 1). It is in the western part of the Arkoma Basin, a structural as well as a depositional basin extending 250 miles east-west and 50 miles north-south from east-central Oklahoma into western Arkansas. Only the Oklahoma portion of the basin was covered in this investigation.

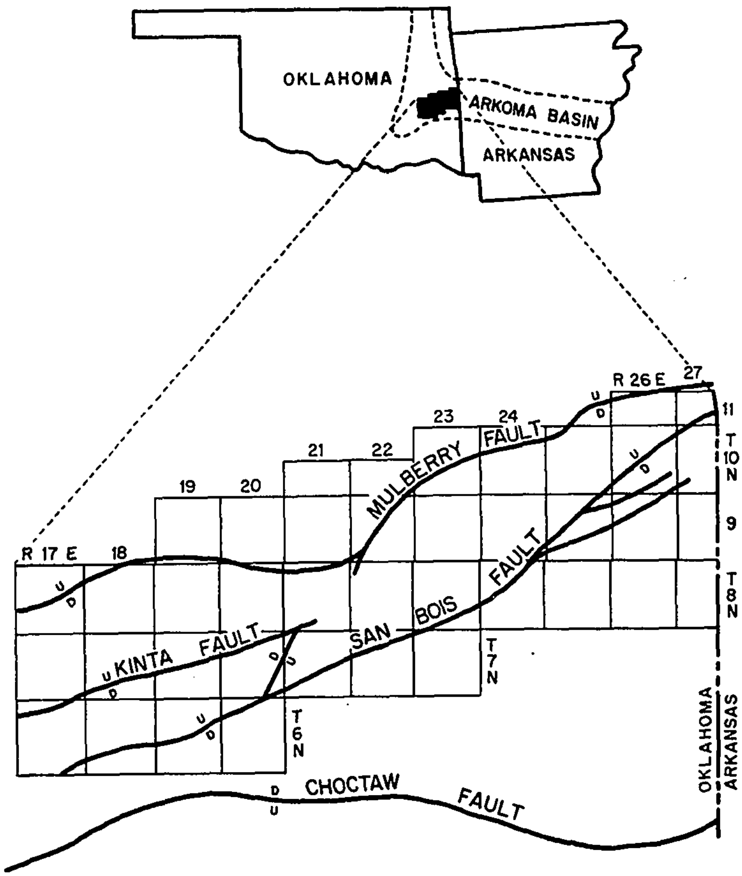

Fig. 1. Location map showing area of study in east central Oklahoma.

Purpose and Procedure

The purpose of this investigation is to determine the extent of contemporaneous faulting and its influence on the stratigraphy and petrology of Morrowan and basal Atokan strata in the southwestern portion of the Arkoma Basin.

In order to achieve this purpose it is necessary to determine (1) the occurrence and distribution of basal Atokan (Spiro) and Morrowan (Cromwell) sands; (2) the depositional environments and history of the units deposited during the interval investigated; (3) the extent to which diagenetic mineralization (secondary cementation) controlled reservoir characteristics of the sands; and (4) the significance of trapping mechanisms for commercial accumulations of hydrocarbons in the sands.

This investigation involved a complete subsurface stratigraphic and structural analysis. All available sources of information including scout cards, published reports, geophysical information, cores and samples were utilized; the main source of data being mechanical logs.

Conclustions were based mainly from interpretation of approximately 1500 mechanical logs. Permanent datum points and applicable lithologic markers were recorded for each of the logs. Thicknesses of the sand bodies under investigation were estimated from deflections of the spontaneous potential and gamma ray curves of the logs.

In order to gain meaningful results from a subsurface investigation, isopachous or structural maps must be based on a reliably correlated system of markers. Such a system of correlatable markers was established from the top of the Mississippian upward through the Morrowan and Atokan sections. Using the marker system, a well to well correlation grid was constructed.

This involved correlating from well to well along a line (two lines per township) perpendicular to the basin axis. In all, approximately 30 cross-sections were constructed, five of which are included in this report (see Plates II through VI).

In the Morrowan section, correlations were made readily throughout the study area. Correlating Atoka shales proved to be more difficult because of the faulting that affected the apparent thickness of the section. A series of 35 mechanical log markers within the Atoka sequence were correlated in order to determine the distribution and extent of the faults. Correlation of the Atoka shales (ranging in thickness from approximately 4,000 to 10,000 feet) was a painstakingly slow process, but once a marker system was established, the Atoka strata in each well could be correlated with confidence.

In order to determine whether or not the well bore had penetrated a fault, the stratigraphic section must be known. By anticipating the stratigraphic sequence that should be encountered in a well and by compairson with logs from nearby wells, the presence of a fault can be detected. Missing section is indicative of normal faulting and conversely, repeated section indicates reverse or thrust faulting.

The presence of faults is also readily indicated by geophysical means, e.g., seismic methods. Most, if not all, seismic information is in the files of petroleum exploration companies and is not freely accessible. This near paucity of available seismic information precluded its use in this investigation.

Petrographic studies of cores and cuttings aided in determining the environment of deposition, as well as diagenetic alteration features of the Spiro and Cromwell sands. Fifty-five thin section from 21 cores and cuttings of the Spiro and 15 thin sections from cores and cuttings of the Cromwell were examined and described (see Appendix for descriptions). The petrographic data were augmented by available published information on the description or petrology of the Spiro and Cromwell sands.

Previous Investigations

Regional Studies

The Morrowan rocks of the Arkoma Basin have been of interest to stratigraphers and petroleum geologists for many years. Numberous investigations of the surface geology have been made. Laudon (1958) studied the surface exposures of the Chesterian and Morrowan rocks in the McAlester Basin. A comprehensive report on the stratigraphy of the flanks of the Ozark uplift, on the north side of the Arkoma Basin was compiled by Huffman (1958). The Chester, Morrow and Atoka Series of western Arkansas and eastern Oklahoma was the subject of research by Frezon (1963). Blythe (1959) examined variations in the thickness and character of the Atoka Formation on the north side of the McAlester Basin. Paleocurrent studies in the Ouachita Mountains indicated southern and eastern source areas for Atokan sediments (Briggs, 1967).

The most recent and comprehensive biostratigraphic work on the Morrow Formation in the northeastern part of the Arkoma Basin was conducted by Rowland (1970). Henry (1973) made an in depth investigation of the brachiopod faunas of the Morrow Series of northeastern Oklahoma and northwestern Arkansas.

Subsurface investigations of the Arkoma Basin have been of interest due to the prolific gas production from Morrowan and Atokan sands. Scull

(1959) examined regional variations in the thickness of and occurrence of sands in the Atokan shales. An investigation of McAlester Basin rocks ranging in age from Cambro-Ordovician to Quaternary was completed by Disney (1960). His study was one of the first comprehensive subsurface reports on petroleum potentials of the Arkoma (McAlester) Basin.

The Oklahoma City Geological Society recognized the importance of gas producing sands in the Morrowan-Atokan sections and devoted a guidebook to the Arkoma Basin. Several excellent papers on subsurface geology of the Arkoma were presented in this publication, e.g., Berry and Trumbly (1968), Buchanan and Johnson (1968).

Lumsden, et al., (1971), published an up-to-date and comprehensive report on sedimentation and petrology of the Spiro (basal Atokan) sands in the McAlester Basin, Oklahoma. Their study was concerned with the interpretation of the depositional environment and distribution of the Spiro sand based primarily on sedimentological evidence; in so doing, it was tacitly assumed that the faulting history of the basin took place only after deposition of the Morrowan-Atokan rocks.

Contemporaneous Faults

Koinm and Dickey (1967), recognized growth faulting in the McAlester Basin and described thickening of the Atoka Formation on the downthrown side of the Kinta and San Bois faults.

More recently, Bruce (1972), discussed the mechanism for the development of regional contemporaneous faults in the Texas coastal area. Clay model studies were conducted by Cloos (1968) in his report on an experimental analysis of Gulf Coast fracture patterns.

Contemporaneous fault models based on both ancient and modern examples have been described in the literature (Curtis, 1970; Weber, 1971; Coleman and Wright, 1975). They exhibit distinctive characteristics and commonly occur in a tectonic realm of down-to-basin normal faulting. Furthermore, specific types of faults have been recognized and described. Fig. 2, is an idealized sketch of a growth fault model illustrating the various types of faults associated with a down-to-basin fault system.

Contemporaneous faults exhibit special characteristics:

(1) down-to-basin normal faults show reverse drag and rollover on the downthrown side and occur in subparallel trends on the landward side of a subsiding basin;

(2) "growth faults" (Ocamb, 1961), or "contemporaneous faults" (Hardin and Hardin, 1961), exhibit an increased sedimentary thickness on the downthrown side;

(3) they may occur as normal faults which limit or bound a graben (individual fault blocks);

(4) antithetic, crestal and flank faults bounding small horsts and grabens commonly occur within the block bounded by master faults.

The mechanism of contemporaneous faults has been discussed by Quarles (1953), Thorensen (1963) and Bruce (1972). Fig. 3 is an idealized sketch showing the development of a contemporaneous fault with related collapse structures and the associated increases sedimentary section on the downthrown side. A contemporaneous fault begins with normal displacement (Fig. 3 A), and becomes a bedding plane fault at such depth that the dip of the fault plane equals the dip of the basinward dipping beds, as in Fig. 3 C. After the dip of the fault plane is the same as the bedding plane dip, all subsequent displacement is along planes parallel with this

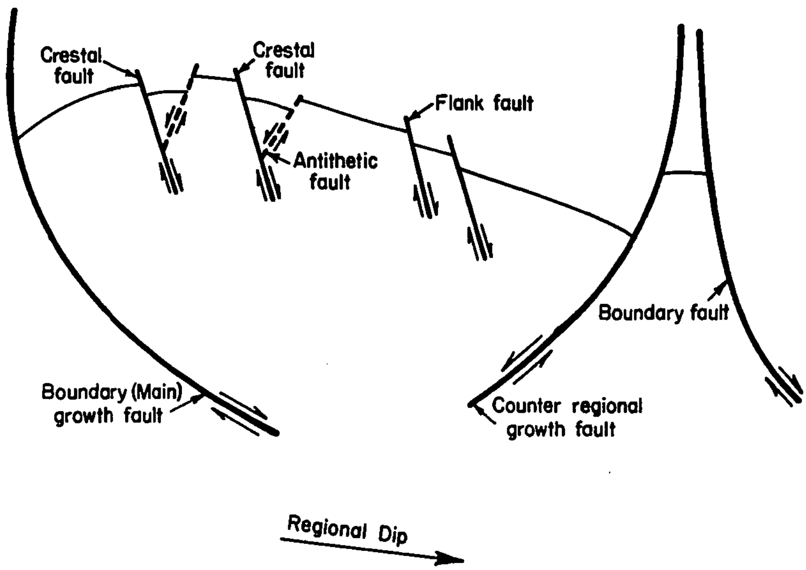

Fig. 2. Idealized sketch illustrating the types of faults associated with a down-to-basin fault system (after Bruce, 1972; Curtis, 1971; Weber, 1971).

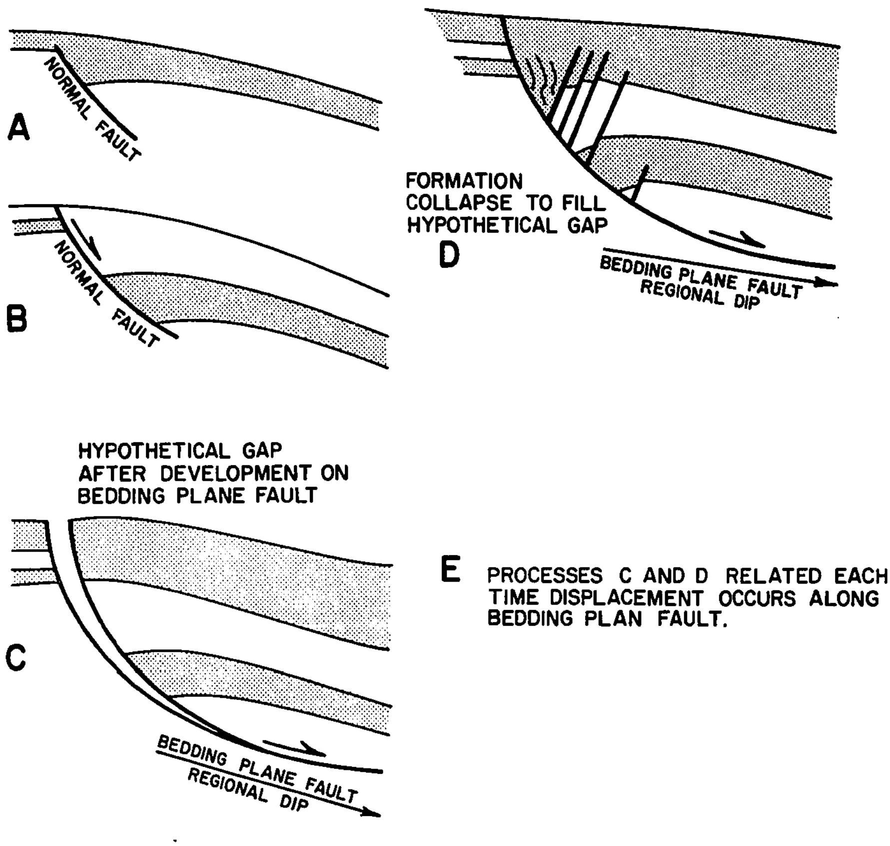

Fig. 3. Idealized sketch illustrating development of a growth fault (after Bruce, 1972).

bedding. Faulting in this matter produces a hypothetical gap, caused by normal fault movement along a curved plane, that does not develop or remain open but is filled by collapsed material from both sides of the fault zone. The collapsed portion of the gap filling is accomplished by crestal, flank and antithetic faulting.

Regional Geology

Stratigraphic Sequence

The strata in the area of investigation range in age from Cambro-Ordovician to Quaternary. In this report only the rocks of Chesterian to Atokan age were investigated; the stratigraphic units discussed are shown in Table I. The Mississippian Pitkin Limestone underlies the Morrowan strata over most of the area except perhaps in the area west of R. 19 E. In the western area, the Mississippian Pitkin grades westwardly and basinward, into a Mississippian clastic facies. The age relation between Mississippian and Morrowan rocks in eastern Oklahoma has been established by Laudon (1958). Extensive study of Mississippian rocks is beyond the scope of this investigation; brief mention is made of them here in order to establish the stratigraphic framework. Also, the Mississippian unconformity becomes less distinct westward and may actually disappear into a conformable Mississippian-Pennsylvanian clastic sequence. Morrowan rocks (as presently designated) are overlain unconformably by the thick Atoka Shale section. The Morrowan consists of shale, shelf limestone and sandstone and is divided (ascending order) into the Union Valley-Cromwell Formation, Wapanucka Shale and Wapanucka Limestone (Disney, 1960). Using surface terminology, the Morrow is divided (ascending order) into the Hale and Bloyd Formations (Laudon, 1958).

System	Series	Ozark Uplift	Arkoma Basin	Ouachita Mtns.
PENNSYLVANIAN	ATOKAN	ATOKA	ATOKA: FANSHAW SS., BRAZIL SS., RED OAK SS., SPIRO SS.	ATOKA
PENNSYLVANIAN	MORROWAN	BLOYD: KESSLER	WAPANUCKA LS.	JOHNS VALLEY
		BLOYD: SHALE		
		BLOYD: BRENTWOOD	WAPANUCKA SH.	
		HALE SS.	UNION VALLEY FM. CROMWELL SS.	
		CANE HILL SH.	CANE HILL SH.	
MISSISSIPPIAN	CHESTERIAN	PITKIN LS.	PITKIN LS.	JACKFORK
		FAYETTEVILLE	FAYETTEVILLE	
		HINDSVILLE		STANLEY
	MERAMECIAN	MOOREFIELD	MOOREFIELD	

Table 1. Stratigraphic correlation chart (adapted from Lumsden, 1971; Branan, 1968; Disney, 1960).

Morrow Series

Union Valley-Cromwell.--The Cromwell sand (Prairie Grove or Hale sandstone of surface terminology) is the basal unit of the Morrowan Series and of the Pennsylvanian System (Disney, 1960). It lies unconformably upon the Mississippian (Chester) surface, or at places is separated from the underlying Mississippian by a thin dark shale (Cane Hill Shale) which is readily identifiable on mechanical logs. Where present, the Cane Hill ranges in thickness from a "feather edge" to 30 feet. A collection of brachiopods from the Cane Hill at the surface in northwestern Arkansas is exclusively Lower Morrowan (Henry, 1973, p. 23).

The Cromwell is present everywhere in the area of investigation either as a well developed sand or as a silty or sandy shale zone. In some areas it is comprised of three distinct sands separated by thin dark shales. In this report, the individual sands have been mapped as (descending order) the first, second and third Comwell sand.

The Cromwell (Union Valley Sandstone) grades upward into the Union Valley Limestone; at places the sandstone facies is separated from the limestones facies by as much as 100 feet of dark shale.

Wapanucka Shale.--The Wapanucka Shale encompasses the predominantly shale section between the Union Valley-Cromwell and the Wapanucka Limestone; it is equivalent to part of the Bloyd Formation of surface terminology. This formation is further divided into a lower shale member, a middle limestone member (the Brentwood Limestone of surface terminology), and an upper interbedded shale and limestone member. The formation ranges in thickness from 300 to 900 feet, due mainly to the variation of the lower shale member. This variation appears to be controlled by positioning with respect to growth faults.

Wapanucka Limestone.--The Wapanucka Limestone is correlative to the Kessler Limestone Member of the Bloyd Formation in the Ozark Uplift (Laudon, 1958); it is easily recognized on well logs and marks the upper boundary of the Morrow Series. Lithologically it is a dense, spicular limestone with shale and sandy limestone lenses. According to Disney, (1960) the Wapanucka Limestone is conglomeratic (containing cobble identified as Simpson, Viola and Hunton) to the west of the study area; elsewhere the upper portion of the Wapanucka may be oolitic. A detailed study of Wapanucka lithologies in both the Ozark Uplift region and the area of the outcrops along the Choctaw fault were made by Rowland (1970) and will not be repeated here.

The upper and lower boundaries of the Morrowan strata are marked by unconformities. An unconformity within the Morrowan is present at places. This unconformity can be identified in a nine township area, between the Mulberry and San Bois faults across Rs. 22 E. through 24 E. In this area the shale and interbedded limestones above the Brentwood Limestones are missing and the Wapanucka Limestone (or Kessler) directly overlies the Brentwood (Fig. 4). The stratigraphy in this local area is further complicated by the position of the post-Morrowan, pre-Atokan unconformity; part of all of the Wapanucka Limestone is missing and the pre-Atokan unconformity cuts down into the Wapanucka shale just above the Brentwood limestone. Northward and westward from the study area the Atoka Shale overlaps the Wapanucka Limestone and rests upon the Wapanucka Shale (Disney, 1960, p. 16).

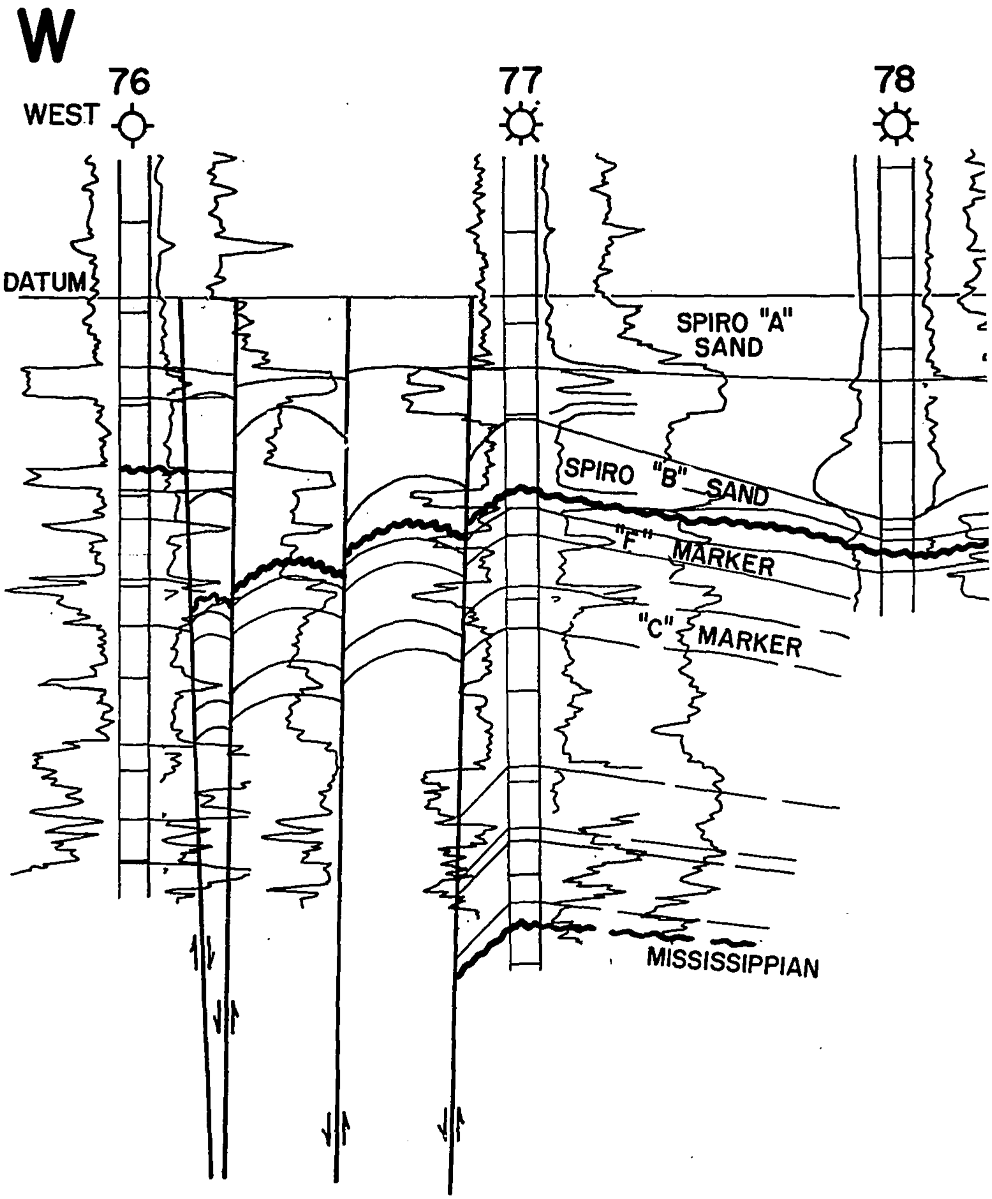
W
76
WEST
77
78
DATUM
SPIRO "A" SAND
SPIRO "B" SAND
"F" MARKER
"C" MARKER
MISSISSIPPIAN

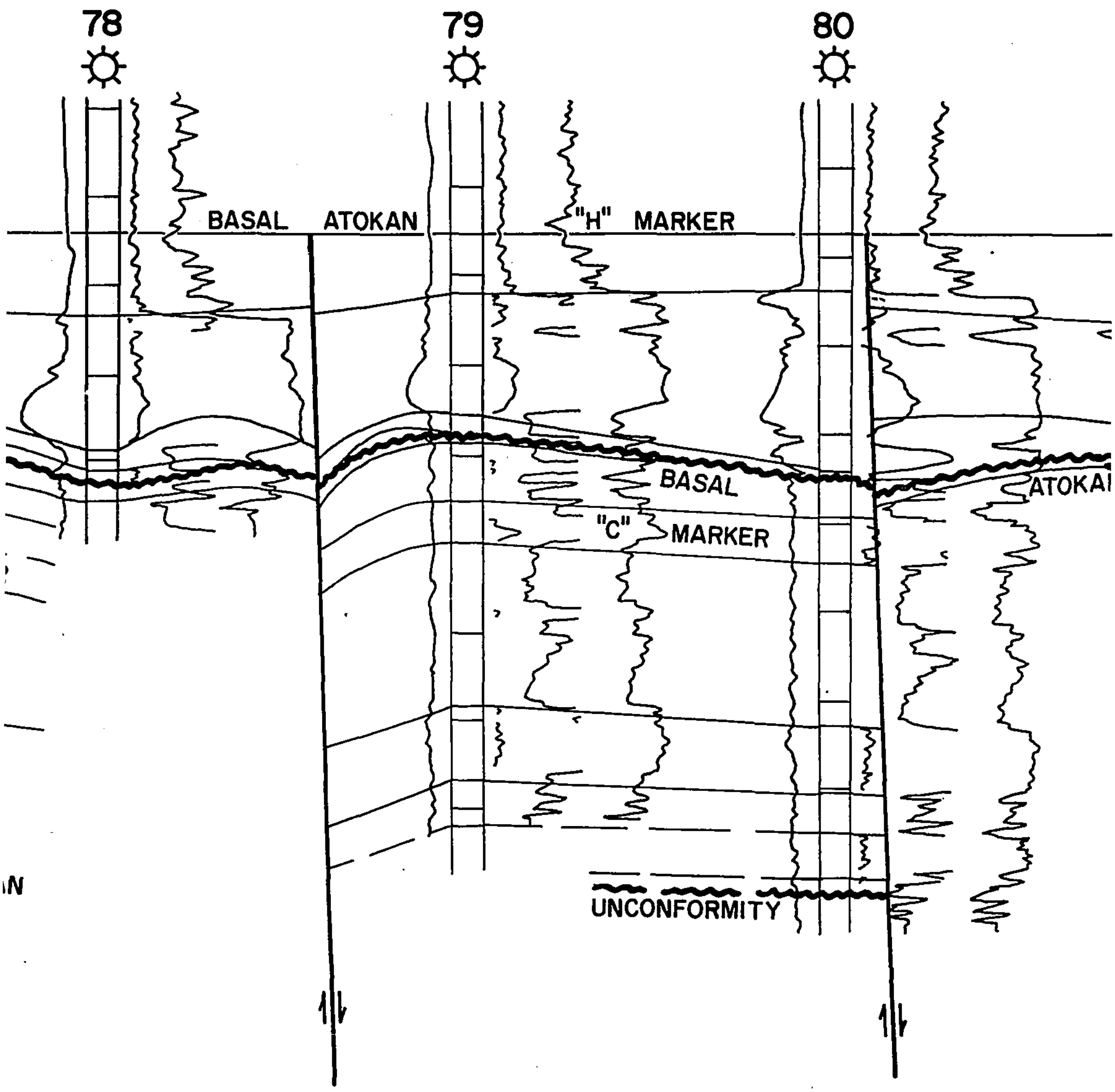

Fig. 4. East-west stratigraphic cross section W-W' (illustrating changes in Morrowan and basal Atokan stratigraphy across a series of fault blocks in Rs. 21 to 23 E.); datum basal Atokan "5" marker; refer to Plate I for location.

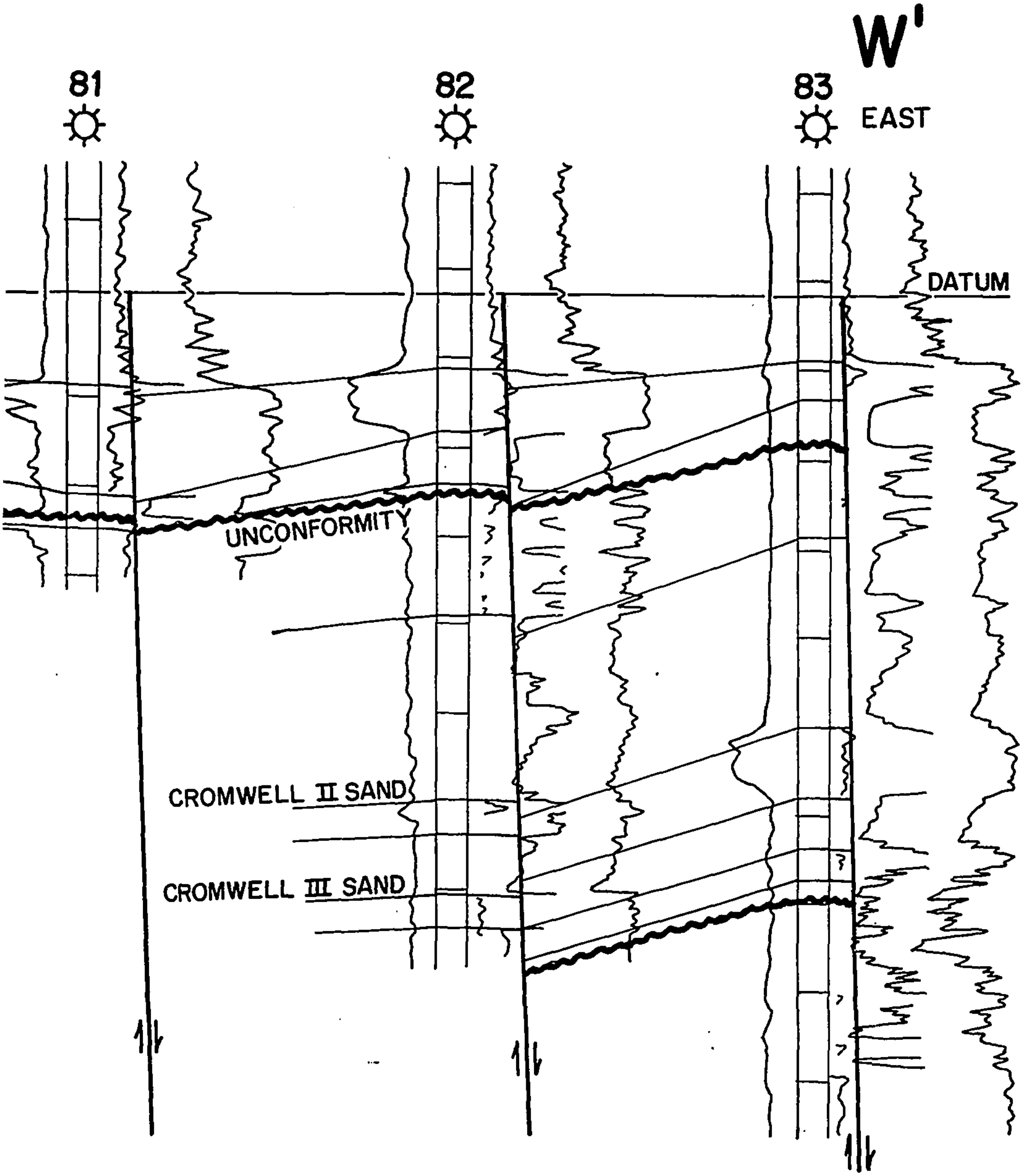

W'
81
82
83
EAST
DATUM
UNCONFORMITY
CROMWELL II SAND
CROMWELL III SAND

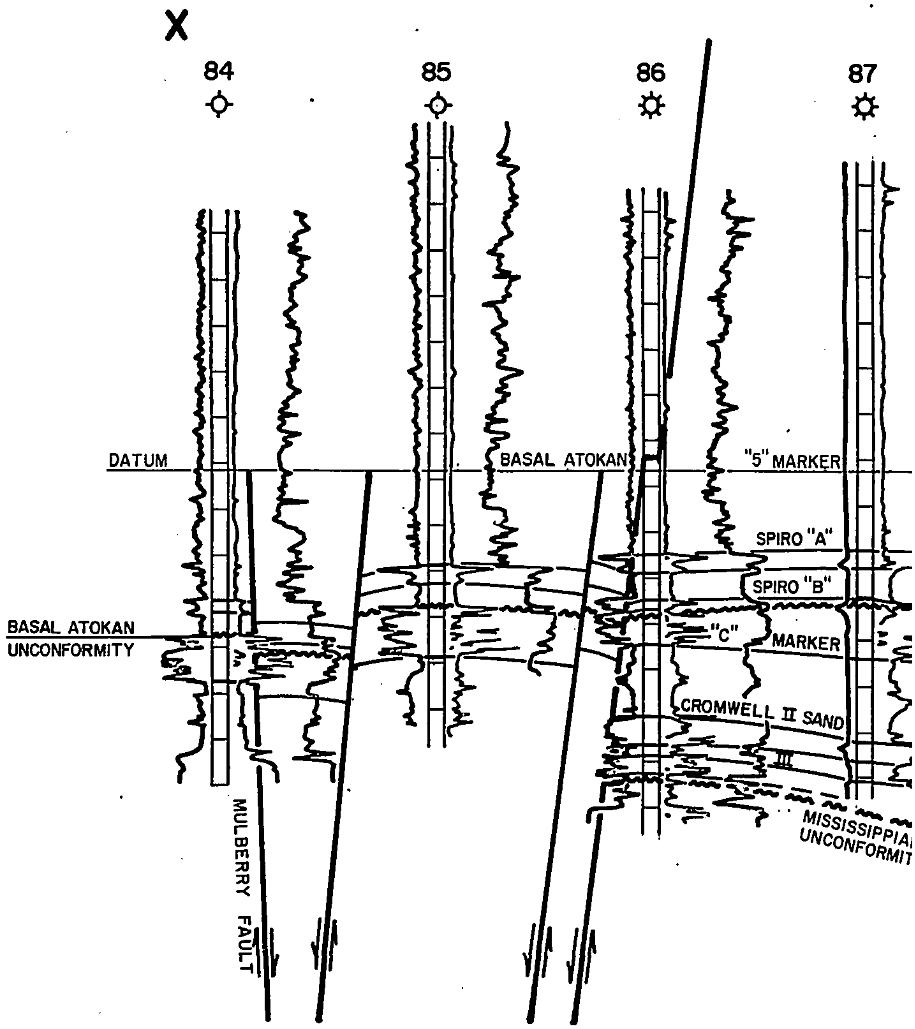

Fig. 5. North-south stratigraphic c
(illustrating changes in Mo
Atokan stratigraphy across
block); datum basal Atokan
to Plate I for location.

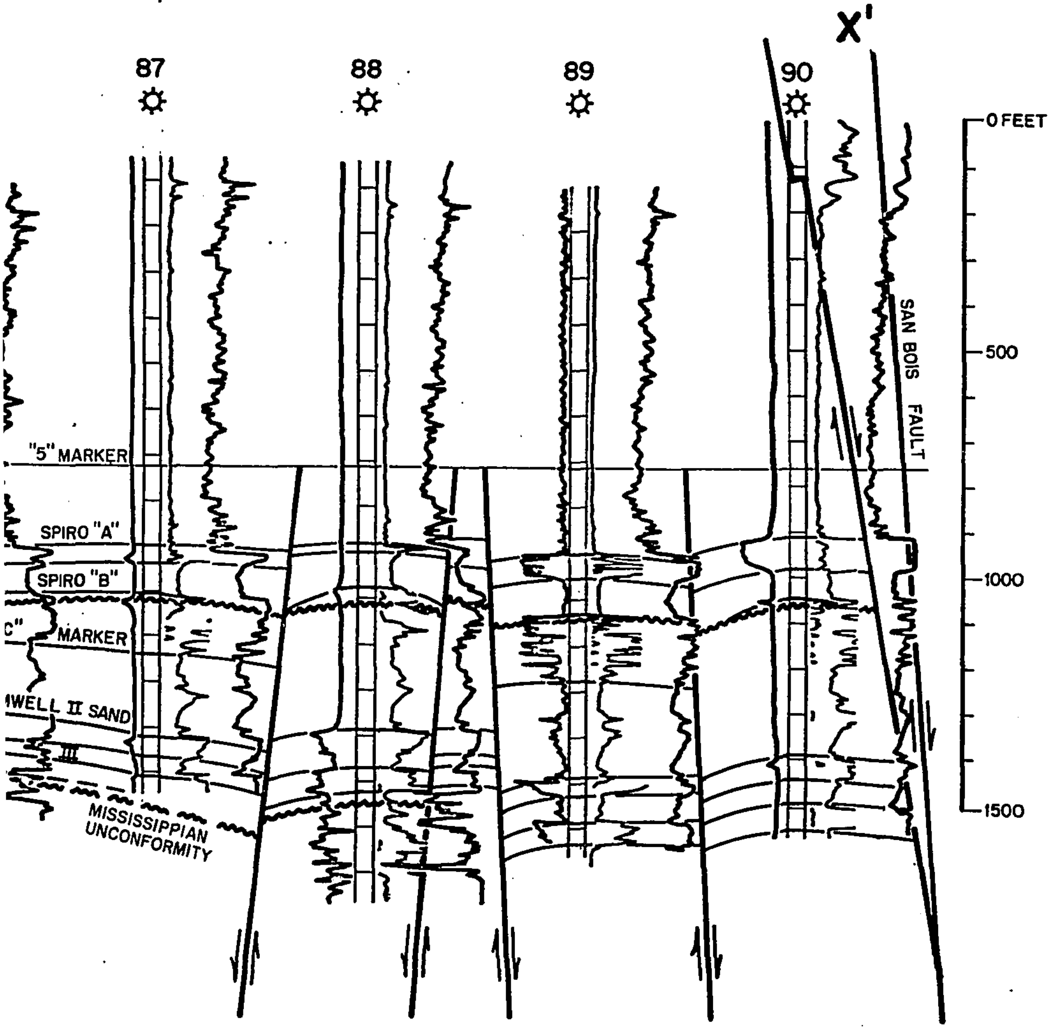

stratigraphic cross section X-X'
ng changes in Morrowan and basal
tigraphy across the Mulberry fault
um basal Atokan "5" marker; refer
for location.

Atoka Series

General Statement.--In this paper the Stoka comprises the strata which unconformably overlie the Morrow and unconformably underlie the Hartshorne in the Arkoma basin. It ranges in thickness from 2,900 feet in the extreme northern part of the study area to over 10,000 feet in the southwen (see Plates II and VI). In addition to a general thickening southward, the Atoka shows pronounced thickening as major faults are crossed from north to south, e.g., an increase in approximately 1,800 feet of lower Atoka strata across the Kinta fault (Plate II). Evidently contemporaneous faulting significantly controlled the stratigraphic thickness of the Atoka shales.

The Atoka shows a slight increase in stratigraphic thickening from west to east (Plate VI). This variation is much less pronounced than that occurring across faults and is demonstrated by the gradual increase in the interval between silt zone markers in the lower Atoka shale. Not only do the shales between markers increase in thickness, but also the amount of sand in the lower Atoka increases from west to east (Plate VI).

The lithology of the thick Atoka section is a monotonous sequence of predominantly gray to dark gray shales with minor amounts of micaceous sandy to silty gray shale and numerous interbeds of sandstone.

There are several economically important sandstone units in the Atoka Formation, e.g., Sprio, Red Oak, Brazil, Fanshaw, Cecil Spiro, "McGuire series", "Dunn series", (Branan, 1966; Six, 1968; Woncik, 1968) to name a few. Only the basal Atoka (Spiro) sand can be traced throughout the basin. The middle Atoka sands, Red Oak, Fanshaw and Brazil occur only in the basin south of the San Bois fault and were not deposited as homogeneous bodies, as evidenced by their seemingly erratic variation in distribution and thickness. Preliminary evidence indicates that their occurrence, as well as that of other Atoka sands, is related to contemporaneous faulting.

Although a study of the Atoka was not originally intended to be included as a significant part of this investigation it became apparent, after preliminary work on the structural aspect of the Morrowan units, that an understanding of the Atokan stratigraphy was essential. Only by correlating stratigraphic intervals in the Atoka shales could the presence of faults be detected. The establishment of a reliable fault pattern was essential in satisfactorily explaining the stratigraphy and sedimentation of the basal Atokan and Morrowan strata.

Sprio Sand.--The Term "Spiro Sand", herein applied to the basal unit of the Atoka Formation (Pennsylvanian) in the Arkoma Basin, is not to be confused with the younger Spiro Sandstone Member of the Savanna Formation at the surface in eastern Oklahoma (Wilson, 1935; Lumsden, et al., 1971). The Spiro sand has also been called the "basal Atokan sand", "Foster sand", or "Greenland sand"; these are all informal drillers' terms for the same basal Atokan sand unit.

Sprio-Wapanucka Relationship.--Atokan strata directly overlie the Wapanucka Limestone; the Spiro sand being the basal unit of the Atokan. Locally the Spiro rests on the Wapanucka Limestone, but usually a dark shale (sub-Spiro shale) separates the two (see Figs. 4 and 5). A disconformity separates the Morrowan and Atokan strata on the northern edge of the basin (Blythe, 1959). In the basin between the Mulberry and San Bois-Kinta fault zones, a disconformity can be recognized between the Spiro and underlying Morrowan strata. Cores from wells south of the San Bois fault show a gradational contact between the Wapanucka Limestone and the overlying sub-Sprio shale. The sub-Spiro shale then grades upward into the Spiro sand, as shown in the photograph of a Spiro-Wapanucka core (Lumsden, et al., 1971, p.258). The age relationships between the Spiro and underlying strata are questionable, but Bartlett, (1966), also Bowsher and Johnson, (1968), believed that the Spiro sand and an undetermined interval of overlying Atoka shale are of Morrowan age. The fauna in the Spiro and Wapanucka Limestone were not studied in enough sufficient detail to establish an age relation, but based on the aforementioned fossil work and the lithologic correlations made in this investigation, the Spiro sand and sub-Spiro shale are considered to be Morrowan.

Basinal Setting

The Oklahoma protion of the Arkoma basin (also referred to as the McAlester basin in earlier works) is a structural as well as a sedimentary basin. The depositional axis lies to the south of the study area 5 to 10 miles, immediately north of the frontal Ouachita belt. It is bounded on the north by the stable Ozark uplift and on the south by the mobile Ouachita geosynclinal belt. The area of investigation is situated on the northern margin of a trough that underwent rapid subsidence beginning in the Early Pennsylvanian and culminating with the Ouachita Orogeny.

The thickness of Morrowan strata increases approximately 400 feet from the northern margin southward toward the basin axis; however, the Atoka section thickens from 2,000 to more than 10,000 feet in the same distance (Plates II and III). This marked increase in sedimentary thickness indicates the area during Early Pennsylvanian time was undergoing a rapid rate of subsidence. These Mississippian and Early Pennsylvanian strata are a typical miogeosynclinal facies, i.e., shelf type limestones and shales. Their age quivalents to the south, now in the Ouachita Mountain belt, (the Stanley-Jackfork, Johns Valley sequence), comprise thick sections of turbidites and related flysch deposits of the typical eugeosynclinal facies (refer to Table 1). The area discussed in this report is located on the northern limb of the deep Ouachita geosyncline.

The axis of the geosyncline in which the Atoka was deposited was within the frontal Ouachita belt (Scull, et al., 1959); the direction of increased thickening and the change from miogeosynclinal to eugeosynclinal rock types of the Early Pennsylvanian strata also indicate the basinal axis was to the south. With a basinal setting in which there is a pronounced increase thickness of strata, a mechanism must be sought for rapid basinal subsidence. It is evident from the cross sections (Plate II and IV) that the stratigraphic intervals mentioned previously increase markedly on the downthrown side (south side) of the Mulberry and Kinta-San Bois faults. The rapid southward increase in stratigraphic section appears to be the result of movement along faults contemporaneous with deposition. This is the crux of this investigation, the cause and effect of contemporaneous faults and the variations in the associated strata.

Structural Setting

The basin can be geographically divided into three basic structural belts from south to north (Branan, 1966; Disney, 1960), ranked by degree and type of deformation (Fig. 6).

Belt I is a ten to twenty mile wide band immediately north of the Choctaw thrust. There the rocks are folded into a series of southwest-northeast trending tight folds asymmetric to the north. At depth the axes of the anticlines become the upper limits of south dipping reverse faults.

The structures common to belt II are nearly symmetrical elongate folds with little or no thrust faulting evident. Down-to-basin normal faulting is the dominant structural feature in the subsurface (Branan, 1966; p. 1624). The near surface rocks reflect a lesser degree of deformation by the Ouachita orogeny than those in belt I and the pre-Atokan rocks seem unaffected by Ouachitan movements.

Belt III is characterized by gentle folds with little or no Ouachita influence evident. This zone is outside the area of study and will not be discussed in any more detail.

The area of study is within the zone of the down-to-the-basin normal faulting. The basal Atokan and older strata are cut by southward dipping normal faults stricking southwest-northeast. The throw across the major faults (Mulberry, Kinta & San Bois) ranges from 1,800 to 6,000 feet. Between the major faults are numerous crestal, flank and antithetic faults exhibiting a throw of 100-1,000 feet. The dip of the fault planes is to the south-southeast approximately 55-65 degrees. The throw decreases upward and most of the faults die out in the Atoka Shale section 1,500 to 3,000 feet above the Wapanucka Limestone. Those faults that do reach the surface appear to represent movement during or after the Ouachita orogeny along earlier established growth faults. Reverse or thrust faults are present only in the extreme southern part of the study area; they cut only the Atoka

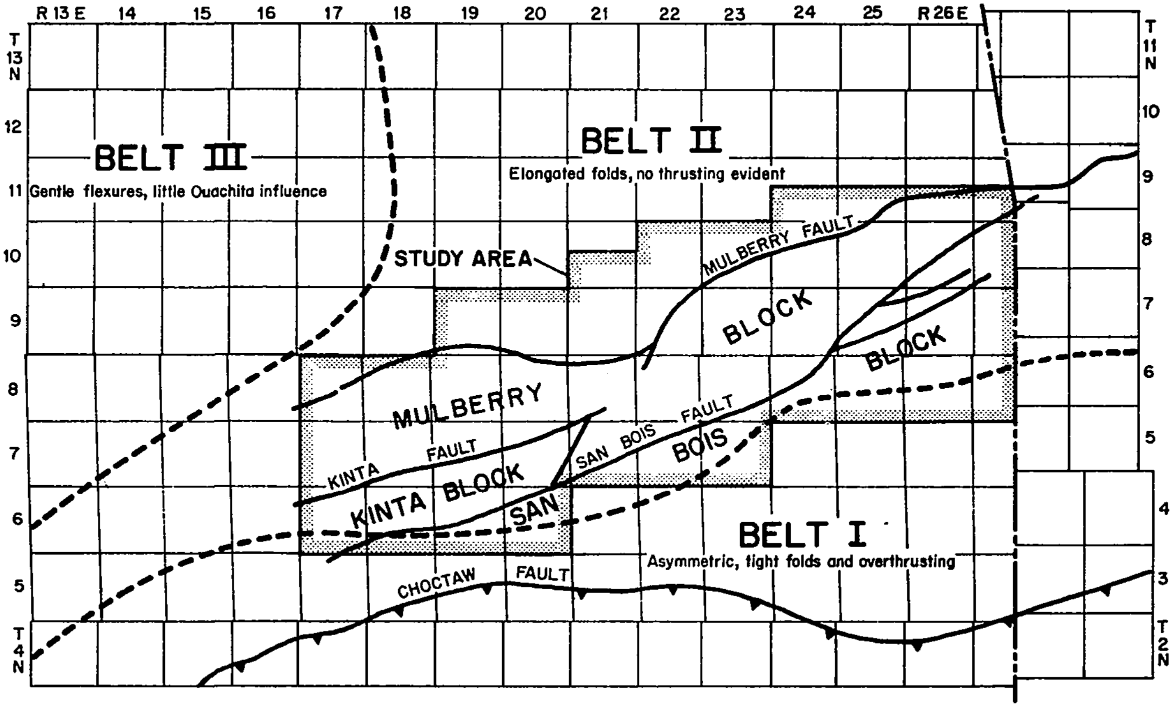

Fig. 6. Structural belts of the Arkoma Basin (Oklahoma portion, after Scull, et al., 1959).

section and the basal Atokan-Morrowan section does not seem to be affected. The maximum intensity of faulting occurs along the Kinta and San Bois faults from Rs. 19 E. to 25 E.; eastward and westward from this area the throws diminish.

SUBSURFACE GEOLOGY

Growth Fault Control on Sedimentation Concept

The existence of growth faults has been established by previous work (Koimn and Dickey, 1967), and is evident from the variation in the stratigraphic section adjacent to faults (see Structural cross-sections, particularly Plate II). It must be determined then if movement along faults affected sedimentation pattern in the basal Atokan and Morrowan strata. In order to resolve this question a comparison was made, over a limited "pilot area", between present day basal Atokan structure, the pre-unconformity structure (i.e., structural configurative predating the unconformity at the top of the Wapanucka limestone), and the Spiro sand distribution. THe idea being used here is that if there is any similarity between pre-Wapanucka unconformity structure, present day structure of the basal Atokan and Spiro sand distribution, then movement along faults cutting basal Atokan strata was contemporaneous with deposition. Conversely, if the structure prior to Wapanucka unconformity time is different than present day structure, then the faults are post-depositional in origin.

It was believed that any promising results from a study of the pilot area could be applied to the entire area of investigation in the basin and thus lead to the goal of satisfactorily explaining the geology of the Spiro and Cromwell sands.

A stratigraphic cross section (Fig. 7) and four maps were constructed covering a limited area for comparison, each of which is described separately. The maps are: (1) a present day structure map (Fig. 8); (2) a pre-unconformity structure map (Fig. 9); (3) a genetic increment map (GIS) of the interval from the basal Atokan "5" marker to the base of the Spiro sand (Fig. 10);

and (4) an isopachous map of the Spiro sand (Fig. 11).

The stratigraphic cross section Y-Y' (Fig. 7), illustrates the paleotopographic relief over a typical fault block; the basal Atokan electric log marker "5" was used as the datum of reference. The "5" marker is easily correlated throughout the area; because of this, and because the markers above and below it are subparallel, it was speculated that the marker is time consistent and serves as a reliable datum.

As can be seen on the cross section, the stratigraphic interval from the "5" marker to the base of the Spiro sand thins over the axis and thickens toward the margins of the fault block. This is due to the paleotopographical-structural relief over the structure. This anticlinal structure is caused by differential movement along the bounding faults with respect to the axial portions of the fault block.

The present day structure map (Fig. 8), shows a series of west-southwest trending fault blocks. East fault block exhibits anticlinal structure oriented subparallel with the fault system and with relief of 200' to 600'. Displacement along the bounding faults is on the order of 100' to 400' feet with a displacement of 200 feet most common.

The pre-unconformity structure map (Fig. 9), illustrates structure of the Morrowan strata prior to the time of the Wapanucka unconformity. This map was constructed by mapping the interval between the basal Atokan "5" marker and the Morrowan "F" marker, some 20 feet below the base of the Wapanucka Limestone. A thin iospachous interval indicates a pre-unconformity structural high, as opposed to a thick isopachous interval which indicates a pre-unconformity structural low. (This method of reconstructing pre-unconformity structure has been discussed by Levorsen, 1967).

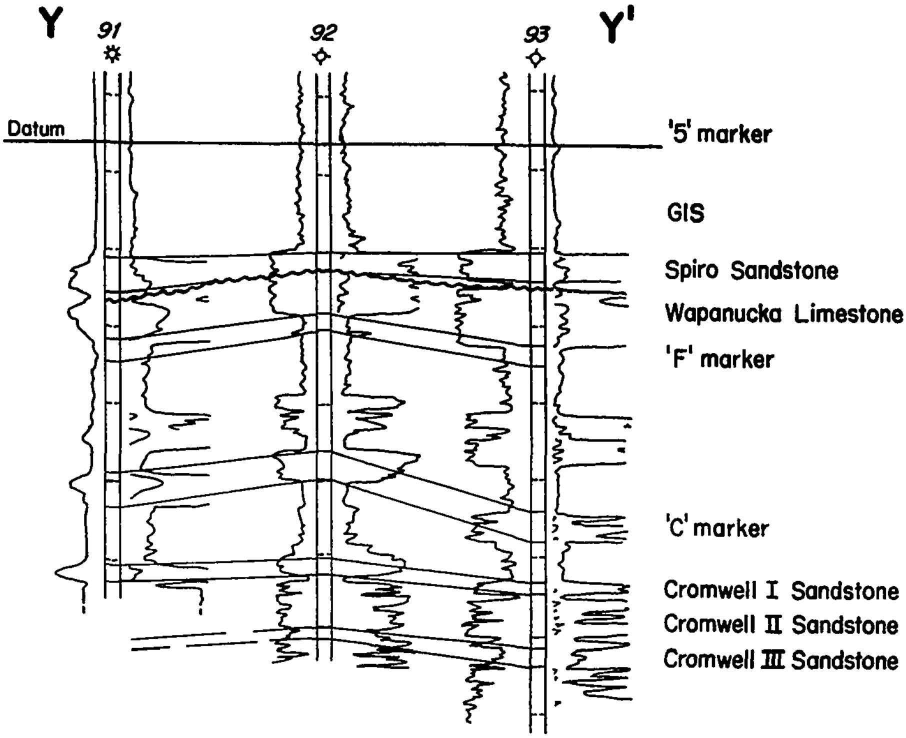

Fig. 7. North-south stratigraphic cross section Y-Y', illustrating depositional thinning over an anticlinal fault block (pilot study area, refer to Plate I for location).

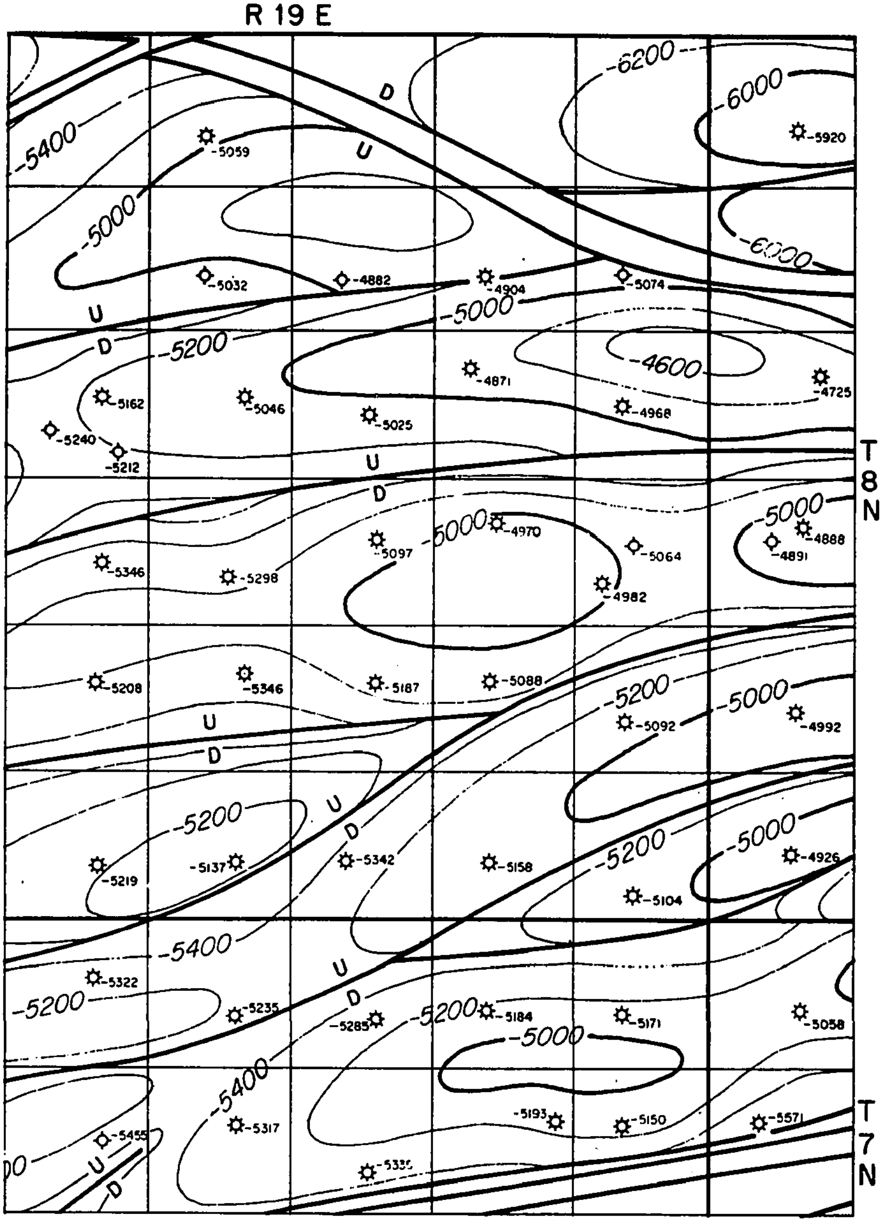

Fig. 8. Structure map of basal Atokan "5" marker illustrating present day structure (pilot study area).

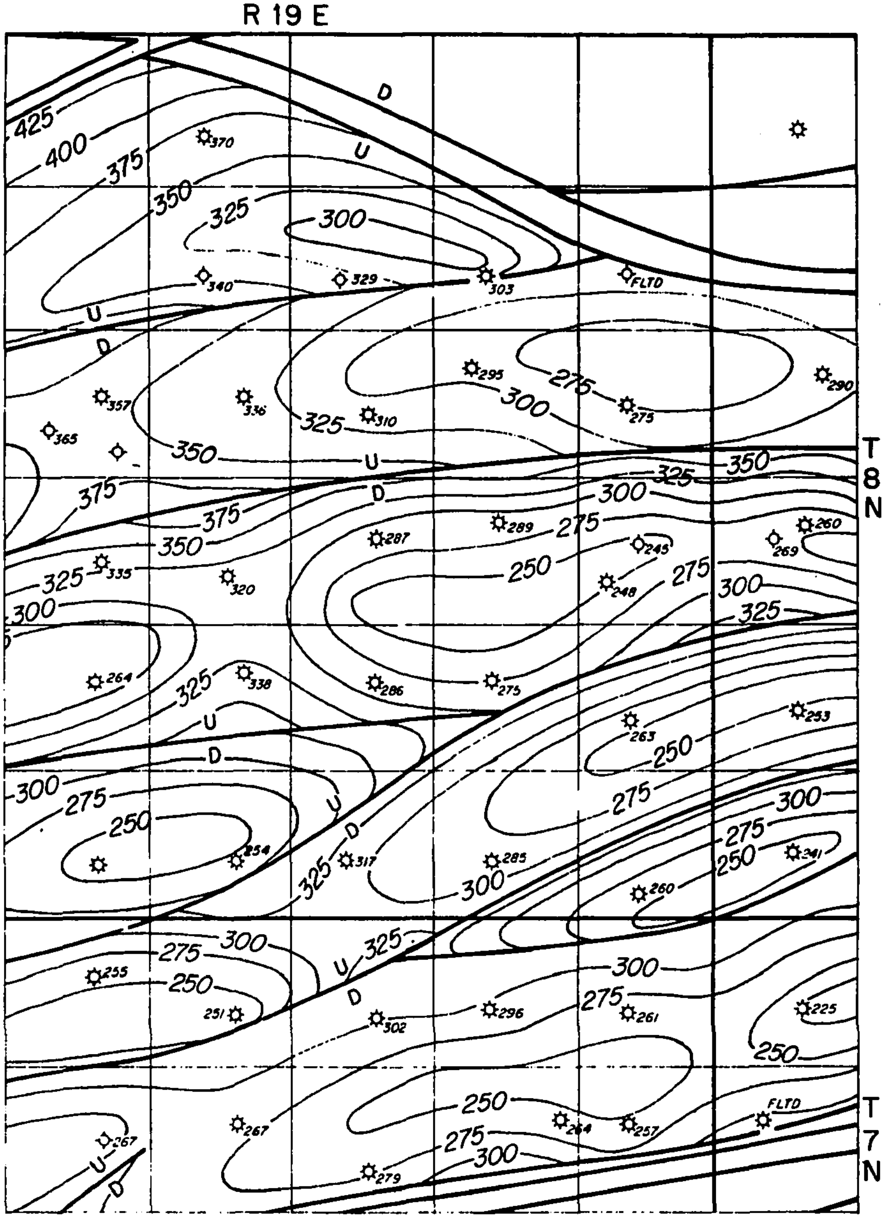

Fig. 9. Pre-unconformity structure map illustrating Morrowan structure at the time of the post-Wapanucka unconformity (pilot study area).

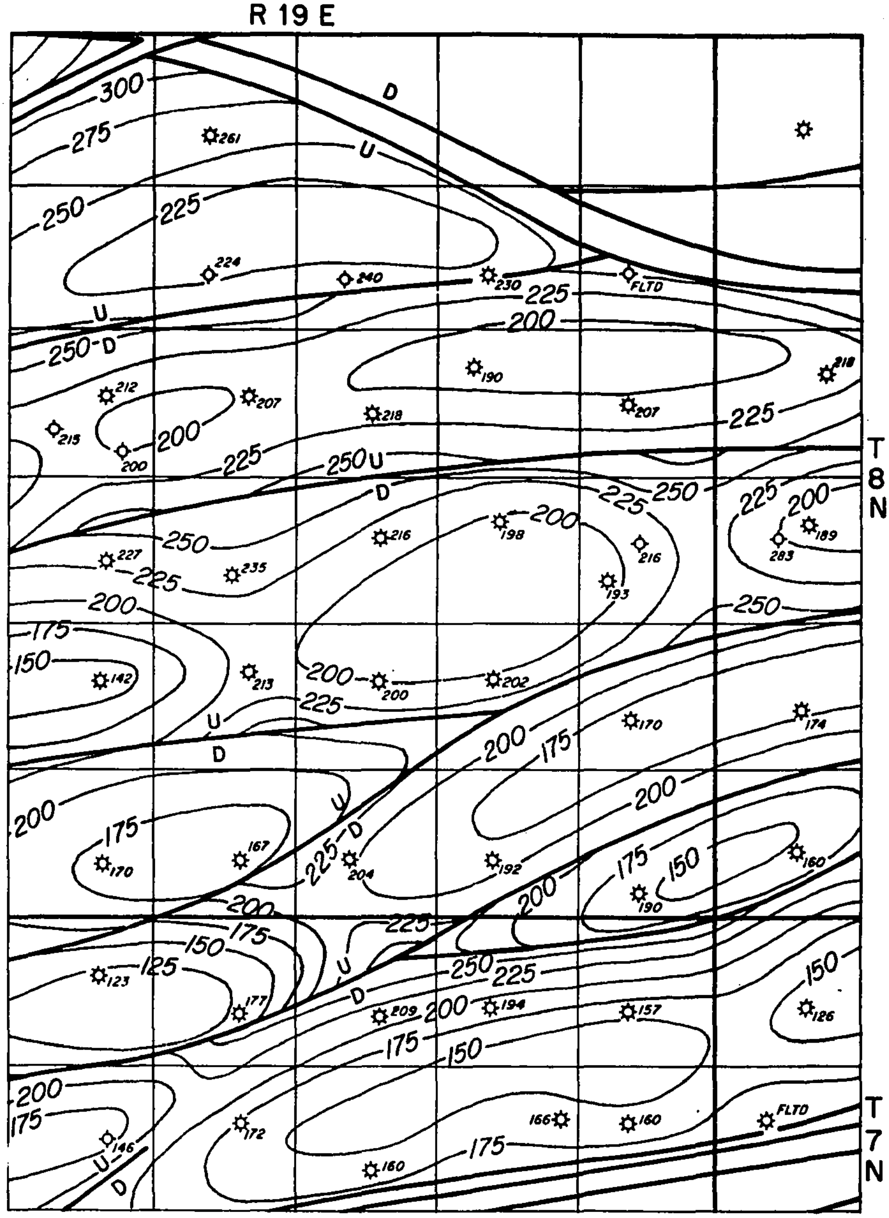

Fig. 10. GIS map: basal Atokan "5" marker to the base of the Spiro sand (pilot study area).

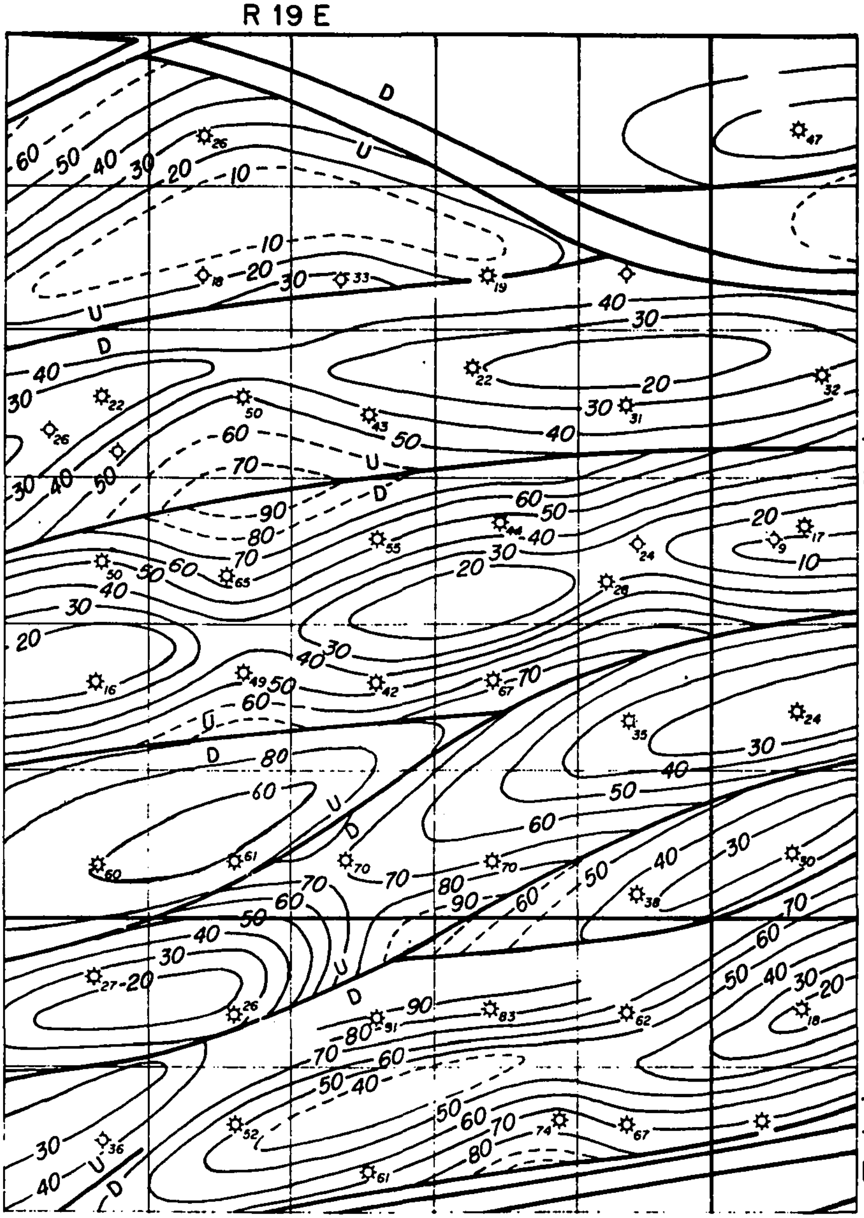

Fig. 11. Spiro sand interval isopach map (pilot study area).

The map shows that the pre-unconformity structure of the Wapanucka Limestone was a series of west-southwest trending subparallel highs and lows that are very similar to the present day structure.

A genetic increment of strata (GIS) map was constructed (Fig. 10), to show the areas of thickest Spiro sand development. The interval used is from the basal Atokan "5" marker to the base of the Spiro sand.

A GIS is defined as an interval of strata representing one cycle of sedimentation in which each lithologic component is related genetically to all others (Busch, 1971); the upper boundary must be a lithologic "time" marker and the lower boundary may be either a lithologic "time" marker, an unconformity, or a facies change from marine to nonmarine. It includes all genetically related sediments deposited during one stage of cyclic subsidence or cyclic uplift.

It is recognized there is controversy among geologists concerning the validity and use of the "lithologic time marker". Further, it is recognized that although a lithologic marker may not represent the exact same geologic instant throughout its areal extent, it is tacitly assumed that time continuity is approached. Pragmaticaly speaking lithologic time markers are valid and they are used throughout this investigation with these limitations in mind.

In this case the upper boundary is the "5" marker, a thin silt bed and the lower boundary is the base of the Spiro sand, which rests unconformably on the Wapanucka Limestone. An isopach map of this GIS (Fig. 10), shows the axis of thickening parallel with depositional strike; the thickening is coincident with the fault traces in Fig. 8, and with the pre-unconformity structural low areas at fault block margins (Fig. 9).

An isopachous map of the Spiro sand was also made for this pilot area (Fig. 11). The Spiro sand isopach is a map of the entire Spiro interval whether it be all sand, interbedded sand and shale, or shale, as indicated by the electric logs. It was thought that it was best to map the entire Spiro interval and treat it as a genetic unit, as opposed to making a net sand map. The isopachous map indicates that the Spiro sand thickens and thins consistent with the fault blocks as defined by the present day structure.

Each individual fault block has its own sand pod, or sand build-up, wherein it thins over the axial portion on the block and thickens toward the margins as the bounding faults are approached.

In comparing the three just described maps it becomes apparent that they are similar and that the pre-unconformity structure and the present day structural grain are parallel. Also the GIS map and the isopachous map of the Spiro sand conform not only to the pre-unconformity structure but also the present day structure. Because of this "hand-in-glove" match of the four different maps, it must be concluded that the present day structure and pre-unconformity structure are similar, i.e., the pre-unconformity structure is essentially the same as the present day structure and that the causes of the pre-unconformity structure were operating prior to the time of the post-Wapanucka unconformity. Therefore, we much conclude that the movement along the faults can at least be recognized prior to the time of the post-Wapanucka unconformity. Furthermore, with the conformity of the Spiro sand isopach iwth three afore mentioned maps, it also much be concluded that the movement along the faults was contemporaneous with sedimentation of the Spiro sand.

Genetic Relations Between Faults and Stratigraphic Basal Atokan Strata

Previous investigations described depositional environment models for the Spiro sand that call for channel systems (e.g., the "McCurtain channel" of Branan, 1966), or a combination of channel systems and transgressive marine bar sands (e.g., the "Foster channel facies" of Lumsden, et al., 1971).

The evidence for a north-south trending "Foster" channel facies in T. 8 and 9 N., R. 22 E. was based on questionable correclations and the occurrence of shale clasts and wood fragments in the middle part of a Spiro sand core. Shale clasts and wood fragments can occur in a marine environment and thus do not necessarily indicate a channel environment. Their channel-shaped cross section (Lumsden, et al., 1971, p. 256), was based on well control across several fault blocks where selected wells with a thick (better developed at the base) sand interval indicated a channel shape. The north-south channels they described are up to six miles wide and the individual channel facies were not mapped--only channel boundaries were projected. The width of the supposed channels seems excessive, and the same wells can be fitted into a growth fault controlled facies distribution pattern without tenuous correlations of channel versus marine facies within the same sand body. The assumption by the previous investigators that growth faulting occurred only later in Atokan time does not account for the stratigraphic changes in the basal Atokan and Morrowan section characteristic of growth faults.

the north-south channel "Foster sand" channel across T. 8 N., R. 19 E. is based on an arbitrary thickness values for channel sand versus Spiro transgressive bar sand. The boundaries of the trend were determined by assuming that the Spiro is 40 feet thick and that the rest of the sand is "Foster". Using this criterion for defining channel trends, one could assume channel trends wherever convenient.

The north-south "McCurtain channel" in T. 8 and 9 N., R. 22 E. is another name for the "Foster channel" previously discussed. According to Branan (1966, p. 1626), the Spiro is considered to be an unconformity sand at the Atoka-Morrow contact; however, there are only isolated areas where truncation of the Wapanucka Limestone below the Spiro can be demonstrated. It is in these places that the sandstone appears to have filled channels in the underlying Morrowan rocks.

Truncation of the Morrowan strata occurs over a greater area than the so-called "McCurtain channel", and can be explained as part of a regional positive condition rather than local truncation by a channel.

None of the north-south trending channel interpretations mentioned in the literature, nor channel interpretations attempted by the writer, would apply outside the pilot study area. This was due to the increased thickness toward the north of a genetic increment involving the Spiro sand and associated basal Atokan strata. This seemingly anomalous situation can be readily explained by the reverse drag and roll-over of strata in the Mulberry fault block, toward the north and into the Mulberry fault, during deposition of basal Atokan strata.

A deltaic origin for the Spiro sand was considered for the pilot study area. Again, as in the case of the channel interpretation, a deltaic model utilizing conventional mapping techniques (e.g., a GIS map of the interval of a marker above to the base of the Spiro sand) resulted in a delta distributary system building or thickening to the north. This can also be explained by the reverse drag and roll-over of the fault block northward into the Mulberry fault.

After unsuccessful attempts to develop a sedimentation model, utilizing the conventional stratigraphic methods, for the Spiro sand that would apply to the entire area of investigation, a different approach was attempted. The results from the pilot study (presented in the previous section on "Growth Fault Control on Sedimentation Concept") indicated that movement along the faults was contemporaneous with deposition of the Spiro sand. The recognition of the correlation between structural and stratigraphic variation, together with the knowledge of published accounts describing growth faults in the area (Koinm and Dickey, 1967), a depositional model compatible with contemporaneous faulting was investigated in an attempt to explain satisfactorily the stratigraphy and sedimentation of the Spiro and Cromwell sands.

The results from the pilot study indicated the Spiro sand seems to thin over the axial portion of the individual fault blocks. This provides the clue needed to determine a guide to use in mapping the sand. The present day structural attitude (Plate VII) of the basal Atokan fault blocks provides this guide. The structure of the basal Atokan, used as a guide, is the most accurate (least interpretative) method for mapping the sand. This is indicated because the area has undergone only slight westward tilting since deposition of the basal Atokan sand. Any post-depositional structural episodes either did not affect the basal Atokan section or accented slightly by mild compressive folding any previous structure.

With the growth fualt controlled sedimentation model in mind, the format for this part of the investigation became one of mapping the structure of the basal Atokan and determining the position, geographic extent and displacement the faults that cut the section.

An electric log marker less than 300 feet above the Spiro was chosen as a datum. The markers in the lower Atoka shale represent thin silty zones; these are believed to be time parallel and to reflect the same structural conditions at the time of their deposition that prevailed during sand deposition, whereas the top of the Spiro or the top of Wapanucka Limestone could be time transgressive.

In order to retain an interval of 300 feet or less between the structural datum and the Spiro sand, it was necessary to use three different electric log markers as structural planes. Different markers were used because (see cross section E-E', Plate VI), the interval between the markers increases slightly in an eastward direction. In the western portion of the area (Rs. 17 E. to 21 E.), the basal Atokan marker "5" was used as a strucutral datum; in Rs. 22 E. to 24 E., the structural datum was basal Atokan marker "4"; in the eastern portion of the area (Rs. 25 E. to 27 E.), the basal Atokan "0" marker was used as a structural datum. Although different structural datum planes were used, it is assumed the basinal subsidence mechanism controlling the structural configuration on one marker was also controlling the structure on all three markers as well as the Sprio sand, and therefore, the basinal subsidence mechanism that was active at basal Atokan time is portrayed.

Morrowan Strata

Morrowan rocks also seem to have been affected by fault movement contemporaneous with deposition. The variation in the thickness of the shale between the base of the Brentwood Limestone and the top of the Cromwell sand reflects the influence of growth faults. As in the lower Atokan, the stratigraphic interval thins over structural highs and thickens into faults. The Cromwell sand appears to be directly related to structural attitude. The thickest and best sorted sand accumulations occur off structure near faults and the thinner and shaly sand occurs over anticlinal highs.

The recognition of the relation between sand distribution and structural framework, as is the case of the Spiro sand, led to the construction of a depositional model utilizing growth faults as the mechanism for the control of sedimentation of the Cromwell sand. This approach called for the construction of a Morrowan structure map that was then used as a guide in mapping the sand.

The structure of the Cromwell sand was shown by mapping the base of the Morrowan "C" marker (base of the Brentwood limestone, Fig. 4). The base of the "C" marker was chosen as a structural datum because it is speculated to be time significant, easily recognized on electric logs and should reflect the structural conditions prevailing at the time of Cromwell deposition.

The Morrowan structure map (Plate VIII), shows essentially the same structural features as the basal Atokan structure map. The structural grain is subparallel with that of the basal Atokan structure and the fault patterns are quite similar. The position of the faults is slightly different in that they are displaced, in the direction of dip of the fault planes, a distance approximately equal to the vertical distance between the map datums. The distance between the base of the Morrowan "C" marker and the basal Atokan datum(s) is approximately 500 feet. Also, the anticlinal structures on the individual fault blocks are somewhat tighter and of greater releif.

For convenience of discussion the study area has been divided geographically into blocks bounded by the major faults, i.e., the Mulberry block, the Kinta block and the San Bois block.

Structural Framework

Mulberry Block.--The Mulberry block (Fig. 6), is bounded by major down-to-the-basin normal faults, the Mulberry fault on the north and by the Kinta and the San Bois faults on the south (Plates VII and VIII). It extends in an east-west direction, parallel with structural strike, over 50 miles across the entire area of study. The eastern and western limits may be extended as far as the bounding Mulberry or Kinta-San Bois faults are recognizable. The width of the block varies from 8 to 20 miles in a north-south direction, perpendicular to the regional structural strike. The narrowest portion of the block is between Rs. 21 and 22 E., where the Kinta and San Bois faults intersect and the Mulberry fault changes trend abruptly from a northeast-southwest to an east-west direction. The greatest width of the block is in the western portion (Rs. 18 and 19 E.) where bounding faults are on a westerly diverging trend and in the eastern portion of the area where the San Bois faults die out (Rs. 25 to 27 E.).

The displacement along the Mulberry fault averages 1,800 feet. Along the Kinta fault the displacement averages about 3,500 feet in Rs. 19 and 20 E., with it diminishing eastward toward the intersection of the San Bois and Kinta faults. The displacement across the San Bois fault varies from 4,500 to 6,500 feet in the central part of the study area and it dies out in an eastward and westward direction (Plate VII).

All three faults that bound the Mulberry block exhibit growth characteristics. Reverse drag and roll-over are well demonstrated on the down-thrown side of the Kinta fault in T. 7 N., Rs. 19 and 20 E. Plate II), and are also exhibited on the down-thrown side of the Mulberry and San Bois faults (Plates III and IV). The added stratigraphic section on the down-thrown side of the bounding faults is further evidence that movement along them was contemporaneous with deposition. Particular attention is drawn to the approximately 1,800 feet of additional stratigraphic section on the down-thrown side of the Kinta fault in cross section (A-A', Plate II).

A complex system of minor faults (Plates II and VI) occur within the Mulberry block; they trend subparallel with the major faults and form a series of horsts and grabens. The magnitude of displacement is much less on these faults than that of the main bounding faults. The displacements range from 100 to 1,000 feet, but are more commonly in the order of 200 to 400 feet. Southward dipping flank faults are more numerous than antithetic faults and are distributed on the portion of the fault block southward, or down-to-the-basin, from its axial crest. Antithetic faults occur between the structural axis and the north bounding main fault, i.e., commonly located in the roll-over region of the main fault block.

Evidently the synthetic and antithetic faults, even though of smaller magnitude, were active contemporaneous with deposition. The stratigraphic section increases in accordance with the position of these faults; however, because of the smaller magnitude of their displacement, reverse drag and roll-over in the strata dipping into the fault scarps are not exhibited to the degree as in the strata near the major faults.

In summary, the Mulberry block is an east-west trending fault block bounded on the north by the Mulberry fault and on the south by the Kinta fault of the San Bois fault. It is dissected by numerous minor faults which in turn define small anticlinal structures trending subparallel and in a west-southwesterly direction.

Kinta Block.-- The Kinta block (Fig. 6) is bounded by the Kinta fault on the north and by the San Bois fault on the south (Plates II and VII). Only the eastern portion of the block is considered in this report, as it extends westward beyond the area of study. At its widest point in Ts. 6 and 7 N., R. 19 E., it is 6 to 7 miles across and narrows eastward where the intersection of the Kinta and San Bois faults mark its eastern boundary.

The Kinta fault is the main fault bounding the block on the north. The throw of 3,000 to 4,000 feet on the fault causes the Kinta block to be 2,500-4,000 feet structurally lower than the Mulberry block to the north. Growth fault characteristics are well exhibited across the Kinta fault (Cross section A-A', Plate II); it represents a near text book example of the boundary, or master, fault in the growth fault model.

The San Bois fault, on the other hand, has a lesser magnitude of displacement than the Kinta fault. The average displacement is approximately 900 feet in T. 6 N., R. 19 E., and increases rapidly eastward to more than 3,000 feet near its intersection with the Kinta fault (Plate VII). At the point where the Kinta fault dies out in T. 7 N., R. 21 E., the San Bois fault becomes the southern boundary of the Mulberry block and is the dominant normal fault zone from there eastward.

Several minor faults form a complex horst and graben system within the Kinta block. As can be seen on the structure map (Plate VII) southward dipping flank faults are more common than antithetic faults. Here also, the displacement along the synthetic and antithetic faults is in the order to 200 to 400 feet, similar to those of the Mulberry block.

San Bois Block.--The San Bois block (Fig. 6) comprises the area of the San Bois fault. The southern boundary of the block is outside the area of study and is mentioned in a later section.

The San Bois fault is the north-bounding master fault of this block. Its displacement has been described earlier and will not be repeated here. As the San Bois fault dies out eastward the boundary between the San Bois and Mulberry blocks becomes difficult to distinguish and in all practicality the Mulberry and Kinta block may be considered one in the same from R. 25 E., eastward to the limit of the study area.

The synthetic and antithetic faults in the San Bois block are similar in nature to those already described. And again, growth fault conditions seems to have prevailed during deposition in this block as well as in the others.

Examination of the structural cross sections across the area indicates that the stratigraphic section in close proximity to the faults exhibits systematic changes. As can be seen in Cross section A-A' (Plate II) the lower Atokan stratigraphic section increases in thickness approximately 2,000 feet as the Kinta fault is crossed in a north to south direction. On the south side of the Kinta fault, lower Atokan markers "5" through "23" can be correlated throughout the area. As the Kinta fault is crossed, on the northern or upthrown side, approximately 2,000 feet of lower Atokan section is missing. The lower Atokan strata on the downthrown side, as represented by markers "14" through "23", is nowhere present to the north on the Mulberry block, and is equivalent to the lower Atokan unconformity. Not only does the section increase in thickness toward the main faults, similar changes, although not as marked, occur in proximity to the minor faults.

Summary and Discussion

Three areas of structural significance can be noted on the maps; a central area, an eastern area and a western area. Notable structural relief between these areas is evident from the map. The central area (across Rs. 22, 23 and 24 E.) is on the order to 500 to 1,000 feet structurally higher than the areas to the east or to the west (Plates VI and VII). A north-northeast trending fault between R. 24 and 25 E., with 800-1,000 feet of displacement marks the boundary of the east side of the central structural area. The western edge of the central area plunges rapidly into the structurally lower region to the west.

The trace of the Mulberry, Kinta and San Bois faults may give an indication as to why the central area is a positive feature and as will be pointed out later, was a remnant positive feature throughout Morrowan and early Atokan time. The southwest trending axis of the Ozark uplift is in alignment with the central positive area. If its axis were projected southwestward it would dissect the area between the Mulberry and San Bois faults in Rs. 22 and 23 E. The Mulberry fault changes trend abruptly to a northeast direction across T. 9 N., R. 22 E. (paralleling the projected Ozark uplift axis), and the San Bois fault trends more northerly between T. 9 N., R. 24 E., and T. 9 N., R. 29 E., becoming parallel with the projected axis of the Ozark uplift. It appears that the central positive area was a stable buttress, along either side of which the basin subsided more rapidly along the Kinta and San Bois fault zones. This would account for the abrupt changes in fault traces from an otherwise continuous east-northeastly direction. The buttressing effect could also explain the rapid increase in plunge of the Mulberry block between T. 9 N., R. 21 E., and T. 9 N., R. 22 E., and why the Mulberry block narrows at the Kinta-San Bois fault intersection in the southwest of T. 8 N., R. 22 E.

Structure on the Wapanucka Limestone is quite dissimilar to the structure of the near surface beds. The basal Atokan-Morrowan rocks are cut by a complex series of horsts and grabens that were apparently contemporaneous with deposition. The structure of the upper Atokan and younger strata is one of generally symmetrical southwest-northeast trending folds that probably were the result of differential compaction over Morrowan-aged horsts and grabens, later accentuated by compressive forces during the Ouachita orogeny.

The disparity between the subsurface structure and the near surface structure can be related to the unconformity approximately 1,200 feet above the Wapanucka Limestone, i.e., the numerous faults which form the fault block structures die out at the unconformity and do not affect the younger rocks near the surface.

From the foregoing discussion it is evident that there were two stages in the development of the structural framework. The first stage was one in which down-to-the-basin normal faulting was dominant. Movement along the faults contemporaneous with deposition is evident in Early Pennsylvanian (Morrowan) rocks and can be traced through middle to late Atokan strata. The second stage was one in which the present day structural attitude was developed during the Ouachita orogeny.

It is evident from the structural cross sections that the stratigraphic section increases in thickness significantly near the faults. The stratigraphic section between the lower Atokan markers increases quite rapidly toward the fault planes. This variation of thickness in relation to structure is most obvious in the lower Atokan section (Spiro sand upwards through marker "11", and is evident through markers "14" on the Mulberry block), and through markers "19" and "20" on the blocks south of the Kinta and San Bois faults. The stratigraphic variation is one of thinning over the anticlines and thickening into the bounding faults. The Spiro sand distribution and thickness are structurally controlled. Thicker and better sorted sand is present adjacent to structural highs and near faults. Thinner and more shaly sand is present across the structural highs.

"Growth structures" seemed to have affected the stratigraphy of the middle and upper Atokan strata. Over the Mulberry block, the distribution of the middle Atokan Tidwell sand seem sto be related to the underlying structure. As shown on the structural cross sections the middle

Atokan and younger strata thin over structural highs and become thicker over structural lows. It does not appear that the antithetic and synthetic faults forming the complex horst and graben system in the Basal Atokan and Morrowan rocks extended up through and affected the sedimentation patterns of the younger strata. Differential compaction of the shale section over the irregular unconformable surface above marker "14" undoubtedly is the cause of the stratigraphic variation rather than true growth fault control, except for some movement along the Mulberry fault. On the San Bois and Kinta blocks the lower Atokan unconformity is absent and is replaced by 2,000 feet of section (cross-section A-A', Plate II). Even though the Atokan is much thicker south of the Kinta and San Bois faults, growth faulting appeared to have controlled sedimentation patterns of the sands higher in the Atokan section (Brazil, Red Oak and Fanshaw). They appear to be present only to the south (downthrown side) of the Kinta or San Bois faults (Plates III and IV). The thickness and distribution of these sands were not studied in detail but, it appears they are directly related to growth faults. The presence of these middle and upper Atokan sands, related to growth faults and the rapidly thickening Atokan shales indicate movement contemporaneous with sedimentation was active along the San Bois and Kinta faults throughout most of Atokan time.

Stratigraphy and Sedimentation of Spiro and Cromwell Sands

Spiro Sand

The Spiro sand is present throughout the area except for a few isolated places where the Spiro interval is "shaled out". In the eastern portion, a thin black shale (sub-Spiro shale) separates the Spiro sand from the underlying the Wapnaucka Limestone; over the western portion (westward from R. 22 E.) the Sprio generally rests unconformably on top of the Wapanucka Limestone.

Herein, the Spiro is subdivided into two facies; the upper sand or Spiro "A" facies and the underlying Spior "B" facies (see Fig. 5, for stratigraphic relationships). The Spiro "A" facies occurs throughout the area, being thicker to the east and thinning to a near feather edge westward in Rs. 17 and 18 E. The Spiro "B" facies occurs in a limited area, roughly within Ts. 8 and 9 N., Rs. 22, 23 and 24 E. The Spiro "B" directly overlies the Wapanucka Limestone and is separated from the overlying Spiro "A" facies by 5 to 50 feet of shale. Recognition of the Spiro "B", where log control permits, is facilitated by the density log; there is a distinctly greater bulk density response in the underlying Wapanucka Limestone than in the Spiro "B" interval.

Spiro "A" Facies

Distribution and Thickness.--As in the pilot study, the Spiro sand interval was mapped. The total interval was used, rather than a net sand value, because it is more meaningful to treat the Spiro "A" interval as a genetic unit. The conditions controlling sedimentation of the whole interval would be better interpreted by mapping the genetic unit as opposed to an interpretation gained from a net sand map.

The Spiro "A" Iospach Map is shown in Plate IX. Generally the Spiro "A" sand exhibits thinning westward and northward from the Mulberry fault. Elsewhere the thickness ranges from approximately 40 to more than 100 feet.

Each fault block has an individual sand pod, or sand "build-up", separate and distinct from that of adjoining fault blocks. The striking similarity between different fault blocks though, is the characteristic thinning of the sand interval over the axial portions of each block. This axial thinning is not just an isolated phenomenom, but occurs on all fault blocks.

On some fault blocks, more commonly in the western part of the area where the Spiro "A" sand interval is thinner than to the east, a "shaling out" occurs over the axial portions of fault blocks. The "shaled out" areas are represented on the map by an appropriate shale lithology symbol. Where the "shaling out" occurs, the mapped interval is all silty shale or recognized as a zone on the electric logs. On a few fault blocks the Spiro "A" interval is absent and is represented by a zero line (refer to fault blocks in T. 9 N., R. 23 E., and Ts. 7 and 8 N., R. 17 E.).

Along with the thinning of the Spiro "A" interval over the axis, there is also a characteristic thickening in the interval toward the margins of the fault blocks. It is in the areas along the margins of the fault blocks, where the thickest and best developed sand occurs. This is revealed quite readily by noting the well-developed character of the electric logs of those wells located nearer the fault block margins. On some blocks near the bounding faults, the sand attains thicnesses of up to 200 feet.

Bedding and Sedimentary Structures.--The writer did not examine individual cores of the Spiro sand. However, a detailed and complete study of the petrography and petrology of the Spiro sand was reported by Lumsden, et al., (1971,"Sedimentation and Petrology of Spiro and Foster Sands (Pennsylvanian), McAlester Basin, Oklahoma"). Sedimentary structure and grain size data discussed in this and the following section, were taken freely from that report. The writer did, however, examine 35 thin sections of Spiro and Cromwell sands that were prepared by Lumsden, et al. The results of the thin section study are discussed in the section on "Petrography and Petrology".

Cores of the Spiro sand reveal massive beds with thin shale breaks and intervals of alternating sand and shale. Low amplitude cross bedding is uncommon and zones of partial homogenization that are interpreted to have resulted from burrowing organisms were revealed. A photography of a Sprio core shows some of the afore-mentioned characteristics (Lumsden, et al., 1971, p. 258). The photograph of the core shows the gradational contact between light colored Spiro sand-shale interbeds and dark colored underlying shale; the interbedded sand and shale grades upward into massive sand.

Petrography and Petrology.--Fifty-two thin sections from 19 wells were examined and supplied the information presented in this section (refer to Table 2, Plates I, IX and XIV for sample locations).

A microscopic analysis of the sand can provide evidence useful in determining a sedimentation model. Such an approach should offer an

Table 2

Sample Locations for Spiro Sand

WELL LOCATION	SECTION - TOWNSHIP-RANGE	WELL NAME	NO. OF THIN SECTION ANALYZED
1-S	11-6N-21E	Midwest Free Unit No. 1	3
2-S	3-6N-22E	Midwest Marting No. 1	1
3-S	17-6N-22E	Midwest Rider No. 1	3
4-S	10-6N-21E	Midwest Jones Unit No. 1	3
5-S	21-6N-21E	Midwest Noah Unit No. 1	3
6-S	19-6N-21E	Midwest Booth No. 1	5
7-S	16-6N-22E	Midwest Colbent No. 1	3
8-S	24-6N-20E	Midwest Sorrels	2
9-S	18-6N-21E	Midwest White	1
10-S	31-6N-21E	Pan Am Melone Unit No. 1	2
11-S	3-9N-19E	Pan Am Reusch Unit No. 1	4
12-S	32-8N-24E	Pan Am Cochran Unit No. 1	1
13-S	21-8N-20E	Superior Drain No. 1	6
14-S	33-8N-20E	Continental Ferguson No. 1	3
15-S	33-8N-20E	Ambassador Davenport No. 1	4
16-S	16-10N-20E	Mobil McAlester	1
17-S	28-7N-20E	Shell Jankowsky No. 1	5
18-S	21-6N-20E	Shell Jankowsky No. 1-21	1
19-S	33-6N-20E	Mobil Parks	1

independent line of evidence to substantiate findings based on conventional mapping techniques.

The Lumsden, et al., (1971), report was based, in part, on petrographic work from a collection of cores and thin sections of the Sprio sand. The thin sections used in their study were made available to the writer and utilized in this investigation. Diagenetic alteration features were noted; visual estimates were used in determining percentages of mineral contituents and a micrometer ocular aided in determining grain size.

Since this investigation involved a general description of the thin sections and since they were the same thin sections used in the Lumsden, et al., (1971) study, the previous report was relied upon for the statistical parameters describing grain size and sorting.

The Spiro sand is very fine to fine grained with a mean grain size ranging from 0.11 to 0.30 mm.; it is moderately to very well sorted accoring to the Friedman (1962) scale, with a range in standard deviation from 1.05 to 0.31 (Lumsden, et al., 1971). In general, the sand is compositionally immature, in the sense that unstable components survived, e.g., schist and phyllite fragments, polycrystalline quartz grains, fossil debris and carbonate rock fragments. Textural maturity varies, depending on whether the sample was located near the axis of or near the margins of a fault block. The samples positioned on or near the axial portions of fault blocks have a higher percentage of fines (silts and clays), than those located near the margins of the fault blocks.

The three Spiro sand samples shown in Fig. 12, were chosen to show the variation in sand development with respect to location on the fault blocks. The location of the samples is shown on Plates I, IX and XIV.

Fig. 12 A, B and C (samples from well 13-S), are photomicrographs of thin sections from a well located on the flank of a fault block; Fig. D, E and F (samples from well 15-S), are from a well located on the axis of a fault block; and Fig. G, H and I (samples from well 17-S), are from a well located near the margin of a fault block. In all three examples, the better sorted sand is found near the top of the Spiro interval and finer, more poorly sorted sand occurs toward the base. Fossil fragments are present in all the samples, and mya be more locally abundant as in Fig. 12 C.

Monocrystalline quartz is the most common detrital component (approximately 95%), with minor amounts of polycyrstalline quartz, metamorphic rock fragments (MRF's), detrital chlorite, carbonate rock fragments (CRF's), and fossil debris. The detrital grains are cemented by quartz or calcite, or bound by detrital clay (mostly chlorite).

The percentages of quartz cement and clay bear significatly on the reservoir properties of the rock. In the more mature, better sorted samples, quartz cement has all be obliterated original porosity. The presence of chlorite clay coating on the grains seems to have diminished or retarded the formation of secondary quartz over-growths. The thin sections from the three example wells shows this phenomenom.

Fig. 12 A, B and C, are samples of Spiro sand taken from a well on the flank (i.e., located at a position intermediate between the axis and margin) of a fault block. As shown on Fig. 12 A and C, chlorite clay is present, but quartz overgrowths are extensive, plugging the pores where the clay is not present. This well had little preserved porosity which resulted in an initial productive capacity of a few hundred MCF which was

Fig. 12 Thin sections illustrating the mineralogy and texture of Spiro sand.

A. Superior Drain No. 1
NW NW SE
Sec. 21, T. 8 N., R. 20 E.
(5,542' - Spiro sand; crossed polarizers, X 28)

The sandstone is fine, subangular, well sorted, quartz cemented, with quite extensive quartz overgrowths. The grains are comprised of monocrystalline quartz (0.2 - 0.25 mm.) 85-90%, polycrystalline quartz (0.2 - 0.25 mm.) trace, chert (± 0.25 mm.) trace, MRF's (0.2 - 0.25 mm.) trace, and altered feldspar (± 0.20 mm.) 2%. Detrital clay is not present and the rock is well sorted; quartz cement fills the pore space, hence a low order, or absence of porosity.

B. Superior Drain No. 1
Location same as above
(5,556' - Spiro sand; crossed polarizers, X 28)

The sandstone is fine, subrounded, well sorted, mostly quartz cemented, with minor calcite cement. The grain components are quartz (± 0.20 mm.) 90-95%, MRF's (± 0.20 mm.) 5%, and detrital clay 2-5%. This rock is similar to that in Fig. 12 A, except that it is finer grained; quartz overgrowths are quite extensive causing little, if any, porosity to be preserved.

C. Superior Drain No. 1
Location same as above
(5,563' - Spiro sand; crossed polarizers, X 28)

The sandstone is very fine to coarse, angular to rounded, very poorly sorted; the grain components are quartz (0.075 - 0.25 mm.) 60%, bryozoan debris (0.30 - 3.0 mm.) 15%, pelmotozoan debris (0.70 - 2.0 mm.) 10%, algal debris (± 0.3 mm.) 10%, and shell fragments (± 0.25 mm.) 5-10%. This rock is very fossiliferous, immature calcite with cemented, no quartz cement; porosity is low.

Quite a marked difference between Fig. 12 A and B, and Fig. 12 C; the 12 A and 12 B thin sections are from a quite mature rock, 12 C is from an immature and fossiliferous rock. These three samples from the same wells shows the lower part of the sand to be finer grained and more poorly sorted, and an increasing grain size and better sorting upward toward the top of the sand.

D. Ambassador Davenport No. 1
NE SW NE
Sec. 33, T. 8 N., R. 20 E.
(5,540' - Spiro sand; crossed polarizers, X 108)

The sandstone is fine, subangular and fair to poorly sorted. The component grains amount to 80%; matrix of the total rock is 5%; cement is 15%; the grains are monocrystalline quartz (± 0.2 mm.) 80%; polycrystalline quartz (± 0.15 mm.) 2%; and a trace of MRF's. Sorting is fairly good in this section; however, there is sufficient chlorite matrix to retard quartz overgrowths in places. The rock is bound by detrital chlorite and exhibits some cementation by quartz.

E. Ambassador Davenport No. 1
Location same as above
(5,540' - Spiro sand; crossed polarizers, X 275)

These are the same photomicrograph as in Fig. 12 D, but with higher magnification. This photo shows chlorite filling the pore space between quartz grains. Where this much chlorite is present quartz overgrowths are retarded; however, the chlorite plugs most of the pore space--some porosity is visible in left central portion of photo. The chlorite appears to be authigenic, but the proximity of apparently detrital chlorite leads to the assumption that the chlorite was originally detrital and authigenic growth further enriched the chlorite pore filling.

F. Ambassador Davenport No. 1
Location same as above
(5,565' - Spiro sand; crossed polorizers, X 108)

The sandstone is very fine to coarse, subrounded, poorly sorted, with a bimodal size distribution of quartz; approximately 1/3 of the grains are medium to coarse, and 2/3 are very fine to fine; the MRF's are squashed and mostly chloritized. The total rock components are monocrystalline quartz 70%; polycrystalline quartz 3%; silt and clay sized quartz and mica hash 10%; quartz cement 12%; calcite cement 2%, and MRF's 3%. Quartz overgrowths are common where matrix is not present, most of the chlorite seems to be detrital.

G. Shell Jankowsky No. 1
570' FWL and 690' FWL of NE/4
sec. 28, T. 7 N., R. 20 E.
(9,438' - Spiro sand; crossed polarizers, X 28)

The sandstone is fine, subrounded to rounded, well sorted and mature. The grains are composed of monocrystalline quartz 95-98%; a trace of polycrystalline quartz; a trace of chert and a trace of chloritized MRF's. Quartz overgrowths are extensive and abundant chlorite (50% authigenic chlorite), has caused some porosity to be preserved.

H. Shell Jankowsky No. 1
Location same as above
(9,487' - Spiro sand; crossed polarizers, X 28)

The sandstone is very fine to coarse, very poorly sorted, with a bimodal grain size distribution. The larger mode of coarse sand sized grains (0.5 - 0.6 mm.) comprises approximately 30% of the total; the smaller mode of very fine to silt sized grains amount to approximately 70%. The matrix is composed of quartz, chlorite and mica hash. The rock is immature, with a larger grained mode that is subrounded, and the small grained mode is angular to subangular; approximately 5-10% of the rock is matrix; 5% calcite cement, 5% authigenic chlorite; less than 5% MRF's and with minor quartz overgrowths.

I. Shell Jankowsky No. 1
Location same as above
(9,491' - Spiro sand; crossed polarizers, X 108)

The sandstone has a bimodal size distribution (75% coarse, 25% fine); the coarse fraction is medium sized (0.4 - 0.6 mm.), with less than a 2% matrix of quartz fines, chlorite and mica hash mostly of the cement is calcite, with some quartz overgrowths, and approximately 5% authigenic chlorite.

Sorting is best near the top of the sand, and the sand is coarser sized and better sorted in Fig. 12 G, than in 12 H or 12 I. This seems typical of a marine sand bed, i.e., more poorly sorted near the base and becoming better sorted and coarser toward the top.

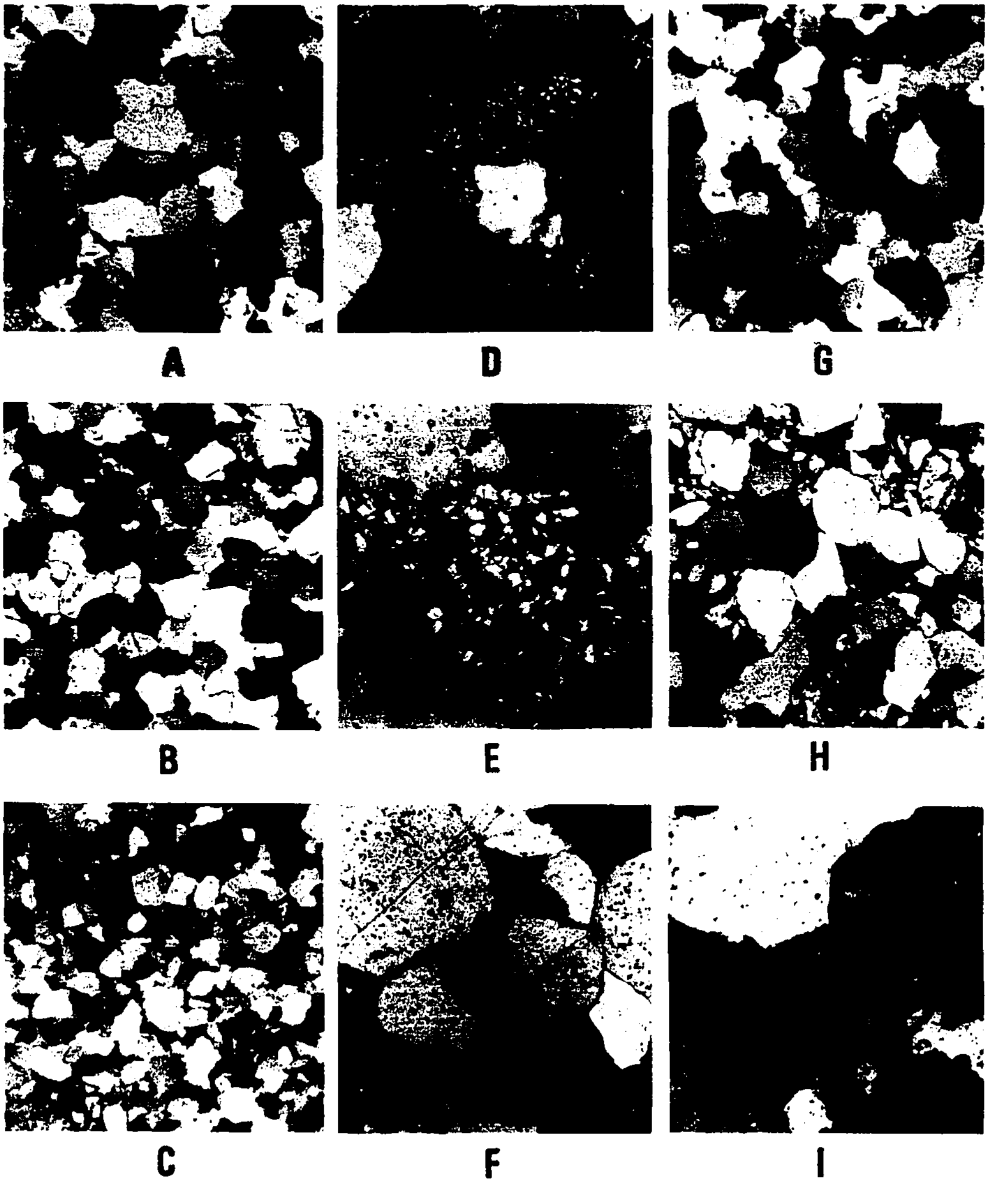
A
D
G
B
E
H
C
F
I

noncommercial. An offset well located nearer the axis of the fault block has sufficient preserved porosity to be productive.

The rocks shown in Fig. 12 D, E and F are from a well located near the axis of an anticlinal fault block. The sand has some clay coatings on the grains, thus retarding quartz overgrowths and preserving porosity. The upper portion of the sand (Fig. 12 D) is well sorted and the quartz overgrowths effectively diminish porosity.

The third example well (Fig. 12 G, H and I) is located near the margin of a fault block. As can be seen in the photomicrographs the sand is well sorted, little if any clay is present and quartz overgrowths have obliterated virtually all primary porostiy. This well is non-productive although the sand is quite thick and well sorted.

The significance of chlorite coatings on grains in preserving porosity is discussed by Pittman and Lumsden (1968). A thick coat of chlorite on detrital grains retards formation of quartz overgrowths and preserves pore space. A thin or partial coat of clay partially retards the formation of quartz overgrowths and some porosity may be preserved. In some instances the clay may be so abundant as to completely plug the interstices, thus, resulting in low effective permeability.

The abundance of clay in the otherwise well-sorted sand is anomalous and was explained by Pittman and Lumsden (1968, p. 259) as a result of filtering in after sand deposition or of diagenetic origin. They favor a diagenetic origin based on evidence of chlorite plates attached at edge normal to the surface of the detrital quartz grain. The delicate crystals show no evidence of transport, which indicates the chlorite must be authigenic.

Chlorite also is present as flakes that lack the orientation discussed. Most of this is probably detrital, but some appears to have formed after the quartz overgrowths. Perhaps the apparent second-stage chlorite in the thin sections is due to the orientation of the plane of thin section. What appears to be chlorite post-dating quartz overgrowths are in reality edges of adjoining pores filled with detrital clay. If there are two different aged chlorites, their origin is unknown. The apparently authigenic chlorite could have formed early in the diagenetic stage and before quartz cementation; the detrital chlorite in the sediment could be a source for the authigenic chlorite.

Wong (1969), observed high iron content chlorite in the Atoka sands of the Arkomas Basin. He considered the chlorite to be of detrital origin.

Although either of these explanations is plausible, a detrital origin is favored, because it is possible by a density current depositional mechanism to have a sand exhibiting these characteristics.

The presence of clay in otherwise well sorted sands can be explained by a submarine density current depositional mechanism. A density current would carry both clays and sand sized material. Near the fault block margins which were also topographically low areas, the density currents were of sufficient velocity to winnow out the clay fraction, deposition well sorted and coarser sand sized grains. Toward the topographically higher fault block axes, the density currents were of lesser velocity consequently, sand sized and clay sized material were deposited together. In some instances, over the crestal portions of the fault blocks, density current velocity was too low to carry anything but silt and clay sized material; these are areas where "shale outs" occur over the crests of fault blocks.

Depositional Environment.--A strucutral-stratigraphic framework for the Spiro "A" sand has been developed. This coupled with the petrographic analysis, provides the necessary information for a meaningful interpretation of the environment of deposition.

The Spiro "A" is interpreted to be a marine sand, deposited by density currents in a below wave base environment. The abundance of marine fossils and carbonate rock fragments (described in the previous section) is evidence for a marine origin. The Spiro isopach shows the maximum thickness of sand to be in trends parallel with structural-stratigraphic lows. The conformity of the Spiro sand with the overlying marine basal Atoka shales fits well in a marine environmental interpretation.

The depositional environment davanced here should not be confused with a turbidity current deposit although the depositing medium is thought to be due to density currents, albeit not a true turbidity current deposit. In a turbidite one should see a "Bouma sequence" in the Spiro cores. No such evidence has been observed. Harms (personal cummunication, 1972), described a density current deposit in the Guadalupe Mountains, southeastern New Mexico, where the Brushy Canyon Formation is a wedge of siltstones and sandstones with characteristics that point to deposition by nonturbid currents in deep water (± 1,000 feet).

The Spiro is thought to be analogous to this type of deposit. The lack of high energy environmental indicators suggests a subqeueous environment. The presence of soft, easily destructable grains, e.g., soft metamorphic fragments, and the presence of clay in the sand interstices lends further evidence to a below wave base marine environmental interpretation.

Spiro "B" Facies

Distribution and Thickness.--The sand occurring below the Spiro "A" and immediately above the Wapanucka Limestone is herein defined as the Sprio "B" facies. It is separated from the overlying Spiro "A" sand by a shale varying in thickness from a few feet to 50 feet. It's position immediately above the post-Morrowan (post-Wapanucka) unconformity stratigraphically characterizes this unit. Its position is unique in that it is always developed on the eroded Wapanucka surface although the shale separating it from the overlying Spiro "A" sand may be variable.

The Spiro "B" isopach map (Plate X) shows the sand occurring in a limited area in comparison to the Spiro "A" facies. It's distribution is limited to approximately nine townships in the central part of the area of study (Ts. 7 to 9 N., Rs. 22 to 24 E.).

Depositional Environment.--The thickest sand occurs on the axial portions of the fault blocks; it thins to a featheredge or shales out toward the margins of the blocks. This distribution is just the opposite of that of the overlying Spiro "A" facies. Because of this systematic increase in thickness over the axis of fault blocks, the sand is interpreted to be an "above wave base deposit". The axial protions of the fault blocks were paleotopographic highs, as well as paleostructural highs, at the time the basal Atokan sands were deposited. Water depths were sufficiently shallow over the paleotographic highs for waves to touch bottom and build marine offshore bars. It was over these "highs" that the silt and clay particles were winnowed out by wave action.

Substantiation or reinforcement of this depositional model by petrographic evidence is not possible due to the lack of samples of the Spiro "B" sand.

Interpretation of Sprio Sands

The basal Atokan sand and enveloping shales represent a genetic increment resting unconformably upon Morrowan strata (Wapanucka Limestone); it has been subdivided into two facies, the Spiro "A" and Spiro "B". The Spiro "A" is the first sand above the unconformity except in the limited area where the Spiro "B" occupies that position and is overlain by the Sprio "A" sand. The Spiro "A" sand is the basal portion of a south to north transgressive unit. The basal Atokan shales and the Spiro "A" sand locally thicken into the planes of growth faults that cut the basal Atokan strata. On the down-thrown side of the growth faults, marker beds in the basal Atokan shales are speculated to represent time lines that are diverging northward and into the fault planes.

The overall thickness of the Spiro "A" sand and overlying shales increase eastward, thus suggesting an eastern source. The basal Atokan shales continued to increase in thickness eastward into Arkansas.

The Spiro "B" sand facies is restricted to an area of approximately 50 square miles in the central portion of the Mulberry block. This sand, in contrast to the overlying Spiro "A", thickens over the axial portions of fault blocks and is interpreted to represent offshore bars developed on paleotopographical highs. This facies was deposited during a minor transgression prior to the transgression of the Spiro "A" sand.

Petrographic evidence favors an eastern source because of the abundance of soft metamorphic fragments; a source to the north could not supply the metamorphic rock fragments, although a supplementary northward source probably supplied some of the detritus. Further evidence for an eastern source may be found in the Atokan shales. Wong (1969), concluded that the suite of clay minerals found in Atokan shales in eastern Oklahoma had affinities indicative of an eastern source. However, this line of evidence may be of limited value because Wong's study was on surface exposures which were probably younger than the subsurface basal Atokan section investigated in this study. Moreover, paleocurrent studies in the Ouachita province south of the study area (Briggs, 1967; Shideler, 1970), indicate an eastern and southern source for Atokan and Johns Valley and Jackfork sediments. These indirect lines of evidence may contribute clues to the probable source of the Spiro sands.

The source of the Spiro "B" sand cannot be speculated on at any length due to the paucity of samples. A more local source would be sufficient for this sand of limited areal extent.

Cromwell Sand

The Cromwell sand(s) can be subdivided into three separate units (see stratigraphic cross section Z-Z', Fig. 13). For the purpose of this study they are named, in descending order, the Cromwell I, II and III sand(s).

The oldest of the three sands (Cromwell III) occupies the stratigraphic position immediately overlying rocks of Mississippian age (Chesterian). In the eastern part of the study area (eastward from R. 24 E.).

Cromwell I Sand Thickness and Distribution.--The uppermost Cromwell I sand (Plate XI) is restricted in distribution to the western part of the area of investigation. The eastern zero line extends from north to south subparallel with the western boundary of R. 21 E. It does not occur north of the Mulberry fault; the southern limit is unknown due to lack of control and is probably outside the area of study. The sand is thickest and best developed in Rs. 19 and 20 E.; from there it thins to the west.

The axes of thickest sand are subparallel with and adjacent to the faults that cut the Cromwell section and the sand thins over the axial high areas away from the fault traces.

The eastern boundary of the sand is of particular interest and it seems significant that it is coincident with the western boundary of a structurally positive area. The localized structurally high area, within Ts. 8 and 9 N., R. 22 through 24 E., is bounded on the south by the San Bois fault and on the east by a down to the east fault along the east side of R. 24 E. To the north the high area plunges rapidly northward (rolls over) into the Mulberry fault. The western edge of the structurally higher area also plunges rapidly westward in R. 22 E.

The positive feature has 200 to 500 feet of structural relief with respect to the surrounding areas to the north and west; the relief is much greater (e.g., 1,000 to 4,000 feet) to the east and south respectively. It is believed that this was an area that remained structurally as well as topographically high during deposition of the Cromwell I sand, thus, causing the absence of the sand due to non deposition.

Cromwell II Sand Thickness and Distribution.--The isopachous map of the Cromwell II sand is shown in Plate XII. The sand is present throughout the area of study. The southern limit is not known for sure due to lack of control in the southern and deeper portions of the basin; it is present northward beyond the boundary of the mapped area. To the east, the sand seems to be thickest and best developed; although it extends beyond the western boundary of the mapped area, it does appear to thin and become more shaly in a westward direction.

As in the case of the Cromwell I sand, the Cromwell II sand thickens and thins according to position on the individual fault blocks. Trends of maximum thickness are oriented east-west subparallel with the fault system that cuts the horizon. Also, the sand interval shows significant thinning and shaling out over the structural anticlines on the fault blocks.

The occurrences of best sorted and thickest sand development are in the west central (Rs. 19 through 21 E.), and eastern (Rs. 25 through 27 E.), portions of the area. Over the central portion, the interval thins and becomes quite shaly, in fact, there are only few areas of limited extent where the interval can be called "sand". In this central area it is predominantly a siltstone or sandy shale zone with true sand being present in only a few narrow trends subparallel with and adjacent to the faults. The reason for the thinning and shaling out of the sand over the central area is thought to be the influence of the structurally high area in Rs. 22 E. through 24 E. If the area were structrually and topographically higher than the surrounding area during depositon, the sand would thin and/or shale out in a manner similar to that observed over the axial portions of the fault blocks.

Cromwell III Sand Thickness and Distribution.--The Cromwell III sand is present throughout the area of investigation (Plate XIII); its distribution if quite similar to that of the Cromwell II sand. However, the quality of sand development is much poorer than that of the Cromwell II. The Cromwell III interval is mostly a silty or shaly zone over most of the area west of the north-south trending fault on the west side of R. 25 E. (to the east) the sand is well developed and exhibits the same thickening and thinning characteristics according to position on the fault blocks, as is the case for the overlying Cromwell II sand.

Over the central area (Rs. 22 E. through 24 E.) the interval thins and is nearly all a shaly zone. Again, this area seemed to have been positive during the time of sand deposition and only silts and clays were deposited.

Petrography and Petrology of Cromwell Sand.--Ten thin sections from four wells were examined and supplied the information from which a general description of the Cromwell sand is based (refer to Table 3, and Plate I for sample locations).

The Cromwell sand is generally very fine grained, subangular, moderately to poorly sorted. The mineral constituents are quartz (75 - 95%), and minor subequal amounts of metamorphic rock fragments, fossil fragments, and carbonate rock fragments (all totaling 5-25%).

Four photomicrographs (Fig. 14) from two different wells were chosen to illustrate the mineralogy and texture of the Cromwell sands.

All four photomicrographs were from shaly portions of the Cromwell interval, sample of the better sorted sand facies were not available.

Table 3

Sample Locations for Cromwell Sand

WELL LOCATION	SECTION-TOWNSHIP-RANGE	WELL NAME	NO. OF THIN SECTIONS ANALYZED
18 C	2-7N-20E	Warren B-1	3
19 C	25-8N-22E	Krisher	4
20 C	31-9N-20E	Abbie	1
21 C	20-11N-25E	Helm	2

Fig. 14 Thin sections 9llustrating the mineralogy and texture of Cromwell Sand(s).

A. Warren B-1
C SW sec. 2, T 7 N., R. 20 E.
(7,320' - First Cromwell sand; white light, X 108)

The sandstone is very fine to fine, subangular to subrounded and moderately well sorted. Detrital components consist of: monocrystalline quartz 90-95%; trace polycrystalline quartz; trace chert; detrital clay 5%, and a trace of fossil fragments. Cementing agents are quartz 75%; calcite 20-25%; trace dolomite cement, with the remainder bound by clay. The thin section is from the top of the Cromwell I sand; some porosity is present, but most pore space is filled by secondary quartz overgrowths.

B. Warren B-1
Location same as above
(7,440' - Second Cromwell sand; white light, X 108)

The sandstone is very fine to silt sized, poorly sorted, subangular and quartz cemented. Detrital components are monocrystalline quartz 85-90%; trace of polycrystalline quartz; trace of chert; mica 2-5%; carbonate rock fragments 2-5% and detrital clay 2-5%. This sample is typical of the fine grained second Cromwell sand; its location is from the shaled out portion of a fault block (see Plate I for location).

C. Pan Am Krisher
SE NW sec. 25, T. 8 N., R. 22 E.
(5,900' - Second Cromwell sand; white light, X 108)

The sandstone is very fine to silt sized, subangular, poorly sorted, clay bound and quartz cemented. The detrital components are: quartz 80%; mica hash and MRF's 5%; detrital clay 15%. This sample is from the basal portion of the Cromwell II sand, on a fault block that is "shaled out" (see Plate I for location).

Another example of the fine grains ("shaled out") facies of the second Cromwell sand. Note the abundance of clay pore filling and the slightly altered MRF in the center of the photo.

D. Pan Am Krisher
Location same as above
(6,010' - Third Cromwell sand; white light, X 108)

The sandstone is very fine to silt sized, poorly sorted, with abundant fossil fragments--sample from near the Mississippian unconformity. The detrital components are: quartz 75%; fossil fragments and carbonate rock fragments 10-15%; detrital clay and MRF's 9-10%. The location of this sample is on the "shaled out" portion of the third Cromwell (see Plate I for location).

A

C

B

D

Only one sample (Fig. 14 A.) approaches reservoir quality rock; in those samples where the rock is coarser grained or better sorted, quartz overgrowths obliterate most pore space. The reduction of porosity by diagenetic quartz cement results in low productive capability.

Depositional Environment.--Petrographic evidence indicates an environment of deposition that can be best described as a below wave base marine deposit, i.e., density current deposit. Density currents transporting clay and silt rich sediment deposited their load over and near the crestal portions of fault blocks. As shown on the Cromwell sand maps thick, well sorted sand is present near the margins of fault blocks where the transporting and sorting power of the density current were greatest.

Interpretation of Cromwell Sands.--The interval including the base of the 'C' marker (Brentwood Limestone) the the base of the Cromwell sands (Fig. 4) represents a lower Morrowan GIS. The upper boundary of the GIS is the time parallel Brentwood Limestone and represents a time consistent unit; the lower boundary is the base of the Cromwell sand, which overlies the Mississippian-Pennsylvanian unconformity. The GIS represents an episode of continuous transgressive sedimentation commencing with marine encroachment on the Mississippian unconformity.

The lowermost Cromwell III sand is poorly developed, but present throughout the area. It is overlain by the Cromwell II sand that is also present over the entire area. The Cromwell II is thicker and better developed, except for the localized central area. The uppermost Cromwell I sand is less extensive and confined to the western portions of the area.

Due to the presence of marine fossils, the orientation and geometry of the sands, all three units are thought to have been deposited in a marine environment. The abundance of silt, clay and fine sized rock particles suggest a low energy environment of deposition. The petrographic evidence, coupled with a depositional model controlled by growth faults, indicates deposition by subamrine density currents in an environment similar to that described for the basal Atokan Spiro "A" sand.

The question may arise, "Could the thinning of the Cromwell II and III sands and the limited distribution fo the Cromwell I sand be due to erosion after deposition of the Cromwell sands"? The lack of evidence for abrupt changes in thickness by erosion or channeling and the gradual thinning or pinching out of the sands seem to rule out this possibility. The abundance of shale and paucity of sand can be explained best by sediment supply versus rate of subsidence. During deposition of the Cromwell III the sand supply was low and the rate of subsidence moderate; later, during the deposition of Cromwell I the rate of deposition was much less than before so that the available sand by-passed the structurally high topographic areas and was deposited in areas undergoing subsidence near major faults.

Fig. 13, the north-south stratigraphic cross section 'Z-Z', across the Mulberry and Kinta blocks, illustrates the influence of differential subsidence on lower Morrowan stratigraphy. The following discussion summarizes the events causing the variation in Cromwell sand stratigraphic relationships. The observed variations are as follows:

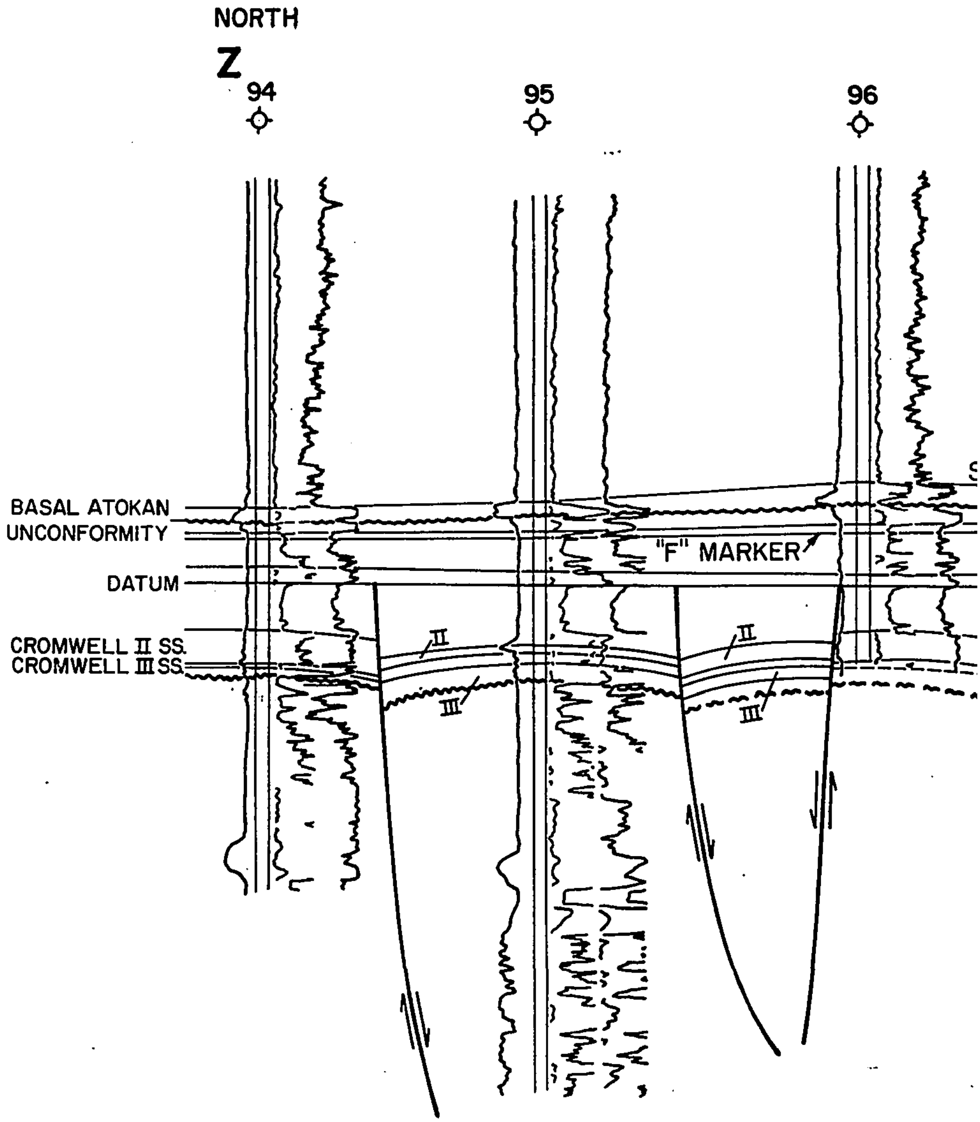

NORTH
Z
94
95
96
BASAL ATOKAN
UNCONFORMITY
"F" MARKER
DATUM
CROMWELL II SS.
CROMWELL III SS.
II
III

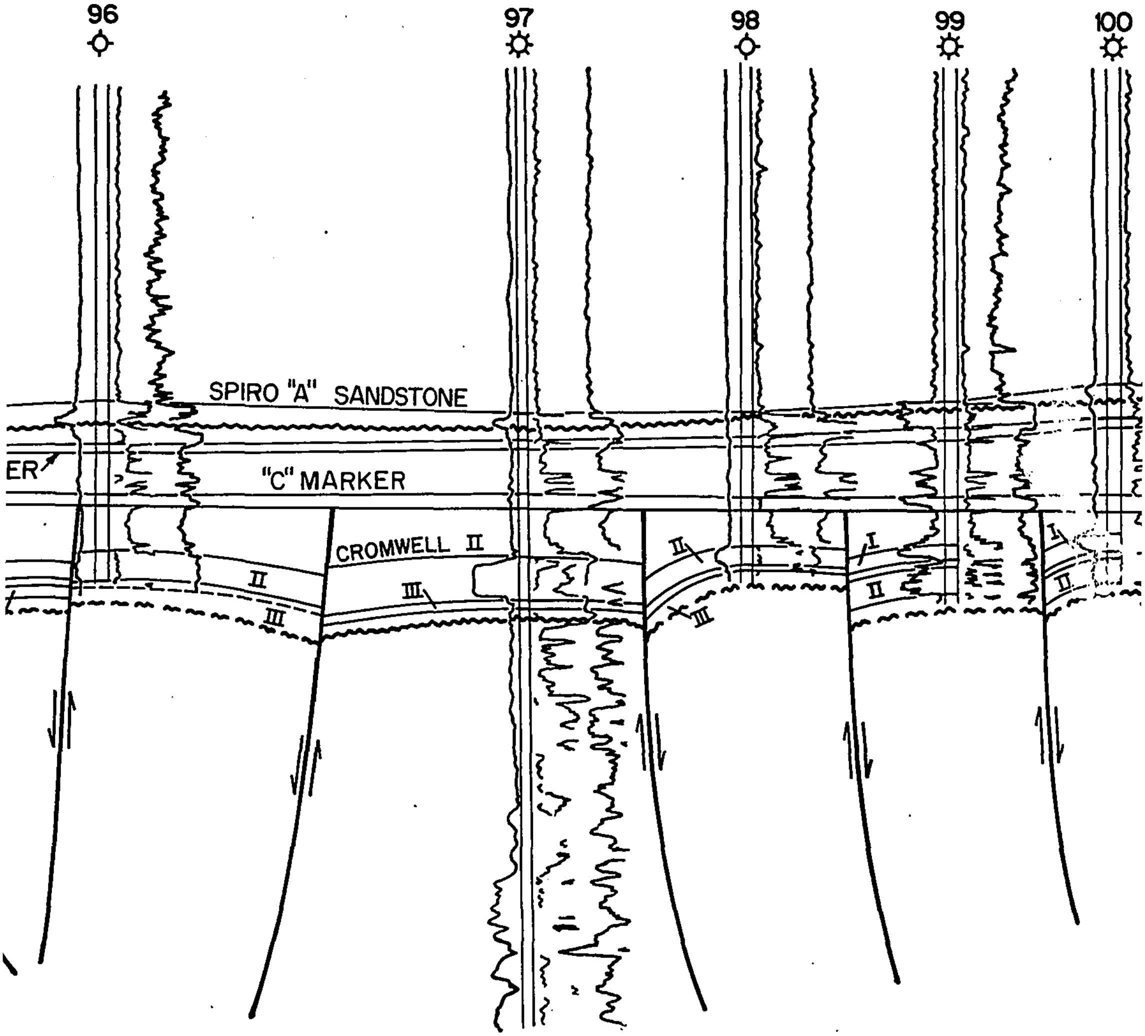
96
97
98
99
100
SPIRO "A" SANDSTONE
ER
"C" MARKER
CROMWELL II
II
III
III
II
III
I
II
I
II

Fig. 13. No
il

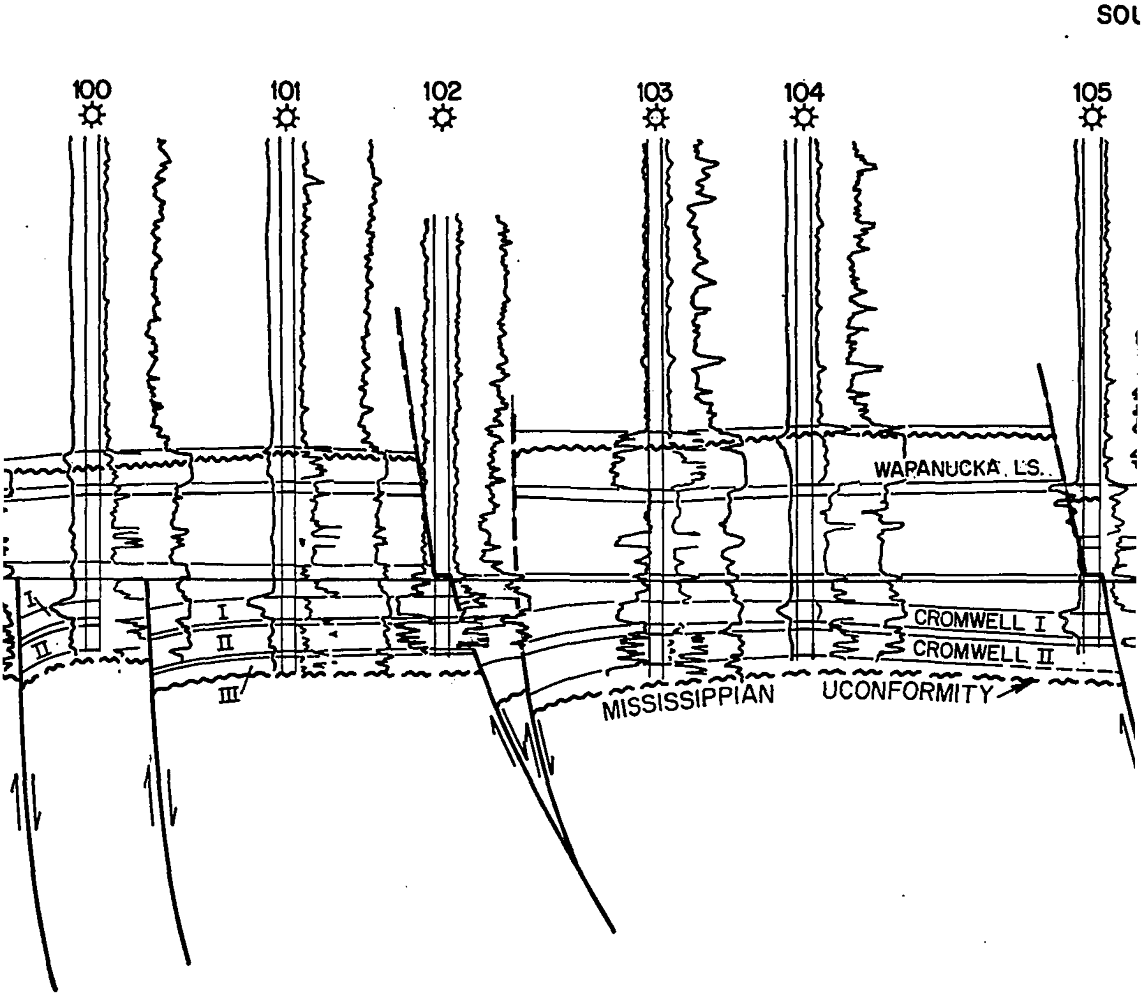

g. 13. North-south stratigraphic cross section Z-Z', illustrating Morrowan and Cromwell sand stratigraphy.

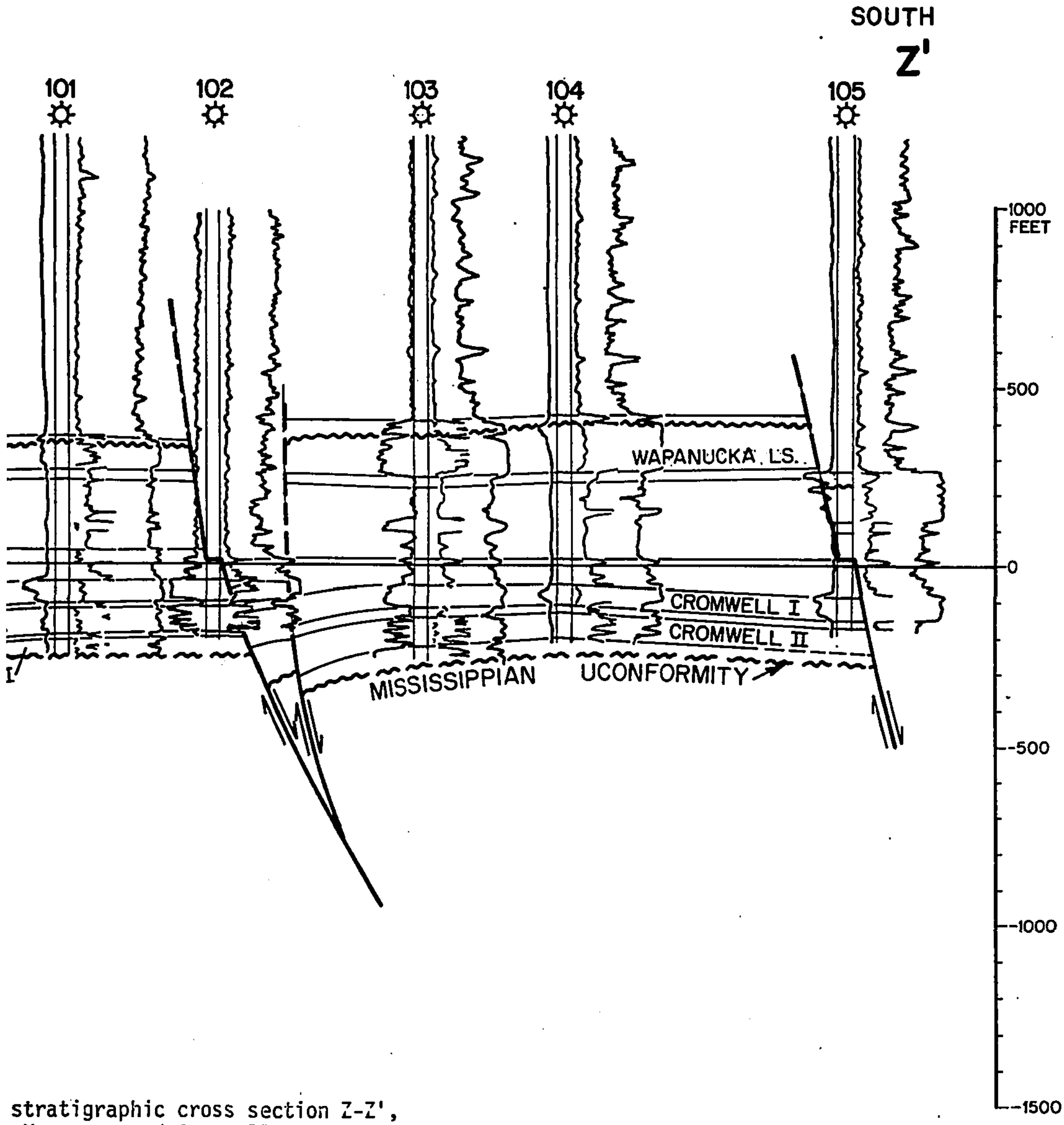

stratigraphic cross section Z-Z',
; Morrowan and Cromwell sand stratigraphy.

The Cromwell I sand is not present north of well 99 in sec. 30 T. 8 N., R. 20 E. The interval from the base of the 'C' marker to the base of the massive Wapanucka Limestone is subequal from north to south across faults where the Cromwell I is present. South of the Kinta fault, the Cromwell I sand and thin overlying shale between it and the 'C' marker are time equivalent to the thick shale between it and the Cromwell II sand and the base of the 'C' marker to the north.

The history of these events may be described as follows. The Cromwell III and II were deposited with the best sorted and thickest sands occurring close to faults, especially to the north. Subsidence was greatest during Cromwell II time to the north. The block north of the Kinta fault stabilized and south block subsided leading to the deposition of the Cromwell I sand; this was followed by deposition of the 'C' marker over both blocks.

During deposition of Morrowan strata between the 'C' marker and the massive Wapanucka Limestone, the area to the south subsided rapidly relative to the stable fault block north of the Kinta fault. This led to a thicker Wapanucka Shale (shale between 'C' marker and Wapanucka Limestone) and thicker total Morrowan section south of the fault as compared to the Mulberry block on the north. Rapid subsidence in post 'C' marker time explains the lower limestone - shale ratio in the strata south of the fault.

South of the Kinta fault the 'C' marker is thin and close to the top of the Cromwell sand; this appears to be a miscorrelation when compared to the thickness between the base of the 'C' marker and the Cromwell sand to the north. However, to the north the Cromwell I sand is absent and is correlative to the shale above the Cromwell II sand. The Cromwell I is only present to the south where subsidence was more rapid.

The petrographic evidence and the distribution of the Cromwell sands indicate a source area similar to that of the Spiro "A" sand. The eastern Oklahoma platform would have to be crossed by sediment supplying drainage systems. No channel deposits seem to be present in that area but, that does not necessarily rule out a northern source for some of the sediment. The Ozark uplift area would probably be a favorable source area, and also to some extent the area toward the Hunton arch.

The presence of soft metamorphic rock fragments indicates a metamorphic source. Perhaps a southern source supplied the soft metamorphics. An eastern source must be a favored due to the slight thickening of the Cromwell sands to the east. Probably eastern and south-eastern areas were the major sources contributing to the sediemnt supply of the Cromwell sands.

Reservoir Characteristics of Spiro and Cromwell Sands

A comparison of the productive capabilities of different wells reveals an interesting situation. The thickest and best developed sands are not always the best gas producers. In fact, the opposite seems to be the case, the wells that have a somewhat shaly sand seem to be the better producers. This observation, along with the preservation of porosity in shaly sands revealed by the thin section analysis prompted the construction of an isopotential map for each of the production Spiro and Cromwell sands.

The isopotential map was constructed by plotting values of the initial potential (I.P.) test in MMCFGPD, of each gas well. The idea advanced here is that the initial potential of each well should be an indication of the effective porosity and permeability of the producing sand in that well. Those wells with high initial potential tests are direct evidence of a more porous and permeable reservoir rock; likewise, those wells with lower initial potential tests are indicative of lesser porosity and permeability.

Not all wells were completed in the same manner. Some well were acidized or fracture treated, whereas some did not require stimulation before potential testing. Experience has shown that regardless of the type or amount of treatment on completion, the well with poor reservoir qualities results in a lower potential deliverability rate and those wells in porous and permeable reservoirs have high potential flows, although enchanced some by treatment. Therefore, it was assumed that the initial potential tests are direct measurement of effective porosity and permeability in a well.

The distribution of preserved porosity and permability apparently is a direct result of the diagenetic history of the sand. Also, it has been suggested that the diagenetic growth of guartz can be attributed to the depositional environment of the sand. Here we see that the highest I.P.'s, indicative of porous and permeable sand seem to be the result of preserved porosity caused by a clay coating on sand grains. In turn, the occurrence of clay in the sand seems to be a result of the location of a well on individual fault blocks, i.e., the shaly sands occur nearer the axial portions and the better developed, cleaner sands occur near the margins of the fault blocks.

The isopotential map is a valuable prospecting tool in that is defines trends, or fairways, where the best reservoir rock might be encountered.

Spiro "A" Isopotential Map

The Spiro "A" isopotential map (Plate XIV) reveals that the districtuion of the best productive capabilities is systematic and that the best wells are located on the crests or near the crests of the individual fault blocks. Conversely, the wells with lower I.P.'s are located away from the high portions of the fault blocks, near the margins. But as pointed out earlier, the wells located near the margins of the fault blocks have the thickest and best developed sand. This relationship between a thinner, shaly sand and high I.P., versus a thicker, better sorted sand and a lower I.P. indicates the best reservoir rock occurs away from the margins of the fault blocks albeit thinner and more shaly.

On some fault blocks where the Spiro is of sufficient thickness, although somewhat shaly, the best wells are located on the crestal portions of the structure, e.g., wells in T. 8 N., R. 19 E. On other fault blocks, where the sand is too thin and shales out over the crestal portions, the best wells (and best reservoir rock) define a "halo of production). This "halo of production" is bounded by a shale out on the axis of the block and by poor (tight) reservoir rock on the margin near the bounding faults.

Spiro "B" Isopotential Map

An isopotential map of the Spiro "B" facies (Plate XV) indicated that the highest productivity rates are from wells nearer the margins of each sand body. This is opposite the relationship observed in comparison of the I.P.'s of the wells in the Spiro "A" sand. Here again diagenetic alteration seems to be the controlling factor in productivity rates. The thickest and best sorted sand occurs over the axis of the fault blocks. Due to the absence of clay in the best sorted sand, it is most altered by secondary quartz, which reduces its effective porosity and permeability.

Cromwell I Sand Isopotential Map

The isopotential map of the Cromwell I sand is shown in Plate XVI. The wells with higher initial potentials are located on or near the crests of the anticlinal structures on each of the fault blocks. Where the sand over the axial portions of the fault block shales out the highest initial potentials outline a halo of good productivity around the crests of the fault blocks. The thickest sand near the margins of the fault blocks is also where initial potentials are lower. This can be explained by the diagenetic history of the Cromwell I sand. The best developed and thickest sands near the margins of the fault blocks is where secondary quartz cement is the most abundant; hence, it is here where the least amount of porosity and permeability are preserved.

Cromwell II Isopotential Map

Plate XVII is the isopotential map of the Cromwell II sand. The areas of highest productivity occur in the western (west of R. 22 E.), and the extreme easterns portions of the mapped area (east of R. 24 E.).

This obviously is due to the development of favorable reservoir rock. In the central portion of the map (R. 22 through 24 E.), the sand is not developed sufficiently to be productive, i.e., the Cromwell II interval is predominantly a shaly sand, or a silty zone. Only in very limited areas, near the faults, in the central portion of the map, is the Cromwell II sand sufficiently developed to be productive.

As in the case of the Spiro "A" and "B" sands, and the Cromwell I sand, the Cromwell II sand productive capability is controlled by the amount of secondary quartz cement present. The best initial potential tests were from wells near the axis of the fault blocks. This is true except where the sand is shaled out and then the best productivity is from wells between the shale out areas and the margins of the fault blocks.

An isopotential map of the Cromwell III sand was not constructed due to the very limited number of wells in which it is productive. As can be seen on the isopachous map of the Cromwell III sand, it is mostly shaly or silty zone throughout the area. Outside the area of investigation the sand may be productive and the factors controlling the productive capabilities of the other two Cromwell sands probably apply to the Cromwell III sand.

Gas Accumulation and Origin

The Arkoma basin is a dry gas province; no oil is being produced in the area of investigation.

Gas has been produced from shallow sands in the Arkoma basin since the early part of the twentieth century. Since 1954, the deeper Spiro and Cromwell sands have become important exploration targets where commercial quantities of dry gas were discovered. The height of drilling activity for the deep Spiro sand was during the 1960's. The shallow, easily found gas areas have been drilled (less than 7500' depths); the remaining exploration targets would be in areas where the drilling depths are in excess of 10,000 feet.

Gas accumulations in both the Spiro and Cromwell sands are due primarily to stratigraphic traps which ahve little or no relation to structural features. Production seems to be dependent on porosity development within the sand. In come areas water is present, but as a rule the sand, where present, is either non-porous or gas productive.

Definite closed structure is required to form a trap in the shallow shelf areas to the north and in the eastern part of the basin (Branan, 1966, p. 1629). In the producing areas to the east in Arkansas, some of the productive zones or structures are associated with water, but others are not. THese fields may be classed as combination structural and stratigraphic accumulations.

In the Oklahoma portion of the basin and within the area of investigation, those areas where gas-water contacts are present, the fields may be classed as combination structural and stratigraphic accumulations.

Gas-water contacts are shown for the Spiro "A" sand in Plate VIII. North of the Mulberry fault, water in the Spiro "A" sand is quite extensive; however, there are areas in T. 9 N., R. 20 and 21 E. where structural relief is sufficient for gas production.

South of the Mulberry fault water is much less extensive than to the north, but there are fault blocks with gas-water contacts. These are located near the major faults, for example near the Mulberry fault in secs. 1 through 6, T. 8 N., R. 20 E., and south of the fault in T. 10 N., R. 24 and 25 E. In the central part of the mapped area, secs. 9 through 12, 24 32 and 33, T. 9 N., R. 23 E., the gas-water contacts are at different levels on different fault blocks. The large graben structure covering the north side of T. 9 N., R. 26 and 27 E., is wet.

Evidence for the generation of hydrocarbons soon after sediment burial has been presented by Kidwell and Hunt (1958), Smith (1954), Price (1976), and is correlated with the dewatering history of swelling clays (Burst, 1969, Powers, 1967; Weaver, 1960, 1967).

The origin and migration of petroleum by aqueous solutions is the most up-to-date explanation to the problem and is presented by Price (1976). His model utilizes faults as providing the main path way for the vertical movement of water and dissolved hydrocarbons from great basinal depths. Eventually the fluids are focused into shallower reservoir sands when the fault becomes impermeable to further fluid movement. The carrying capacity for petroleum by a small amount of hot water is many times that of a much larger amount of cold water. Thus, primary migration by molecular solution may be operable at depths of as much as 40,000 feet until all deep basinal pore water has been removed by compaction.

The just described mechanism for hydrocarbon generation and migration should apply to the Arkoma basin. The prerequisites for the utilization of such a model are present, e.g., deep basinal sediments in excess of 15,000 feet, faults as a pathway for the movement of dissolved hydrocarbons, and ample reservoir sands at shallower depths.

Hydrocarbons probably were generated soon after sediment burial. With increasing depth of burial, and after critical temperatures are reached for petroleum to be soluble with water, hydrocarbons migrated up along the numerous faults in the basin. Gas, or the lighter fraction of petroleum would be the first to migrate. As each reservoir sand was filled to spill point, later generated hydrocarbons (heavier fractions, including oil), could not be trapped in the previously filled gas saturated sands. The heavier fractions bypassed the deeper sands (Spiro, Cromwell), and were trapped in shallow sands updip.

This explains the absence of oil in the area of study. Also, this might explain the areas of water occurring structurally higher than gas accumulations, e.g., Spiro water sand north of the Mulberry fault and approximately 2,000 feet high to gas south of the Mulberry fault. Apparently the gas migrated into the Spiro sand and displaced the connate water after movement along the faults; thus, the different gas-water movement along the faults; thus, the different gas-water contacts for different individual fault blocks.

GEOLOGIC HISTORY

History of Faulting

It has been demonstrated that faulting occurred contemporaneous with deposition of the Morrowan and basal Atokan strata. Moreover, the evidence that growth faulting continued through deposition of the thick Atoka shale section is demonstrated in this investigation and documented by earlier work (namely Koinm and Dickey, 1967). Growth faulting is the mechanism preferred for basinal subsidence necessary to explain the thick Atokan clastic wedge that increases in thickness to the south from less than 5,000 to over 10,000 feet.

Fig. 15 , is a schematic structural cross section across the central part of the Arkoma basin showing the relative location of faults and sequence of faulting during basinal subsidence. Figs. 15 A-E depict subsidence of the basin by using key log markers, representing events (1) through (5), as datums of reference.

Movement occurred along the northernmost fault (Mulberry fault) first (Event (2), Fig. 15 B). The Mulberry fault acted as the master fault in a typical growth fault model (see Fig. 3 A). Relative down to the basin movement was greatest on the downthrown side of the fault. This is reflected by the increase in thickness

EVENT 1

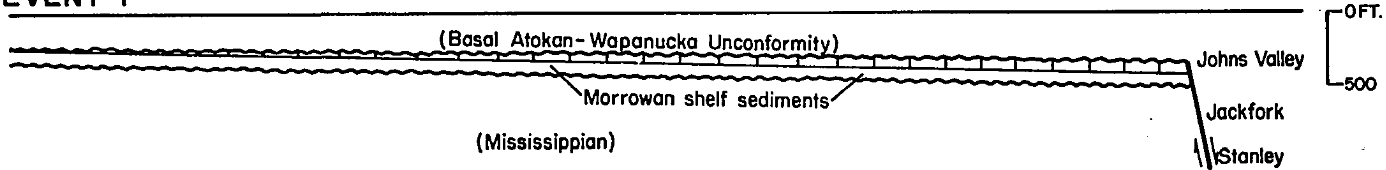

Fig. 15 A. Basinal subsidence at Event 1: "late Morrowan (post-Wapanucka Limestone)".

EVENT 2

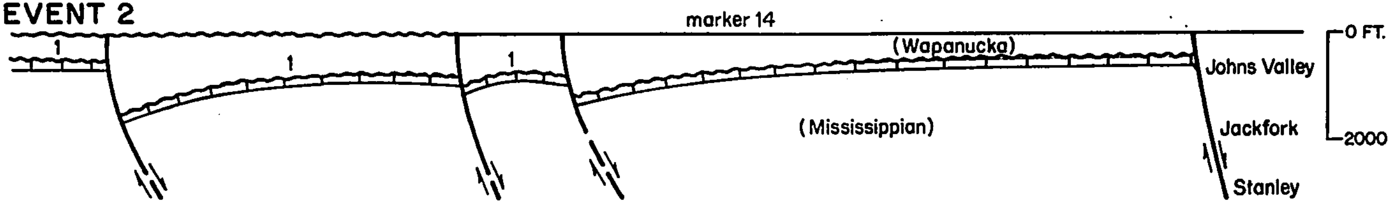

Fig. 15 B. Basinal subsidence at Event 2: "Atokan marker "14" event to south and age equivalent lower Atokan unconformity to north".

EVENT 3

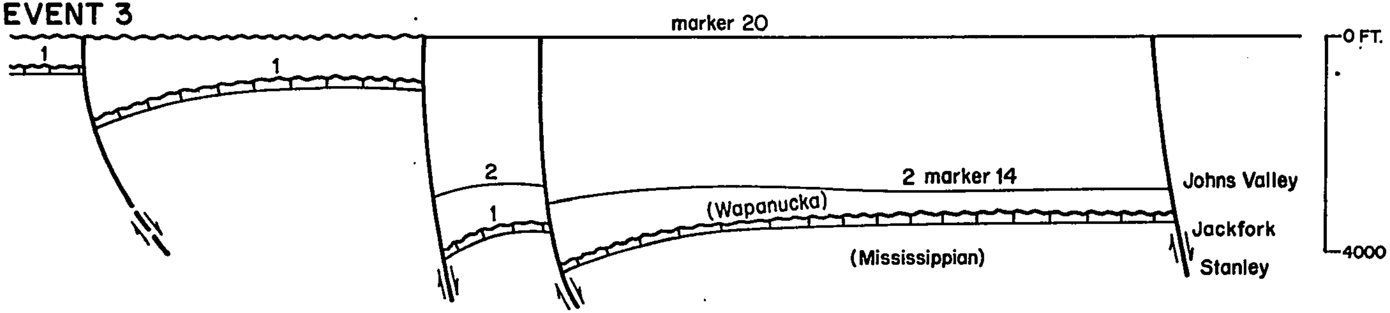

Fig. 15 C. Basinal subsidence at Event 3: "Atokan marker "20" event to south and age equivalent lower Atokan unconformity to north".

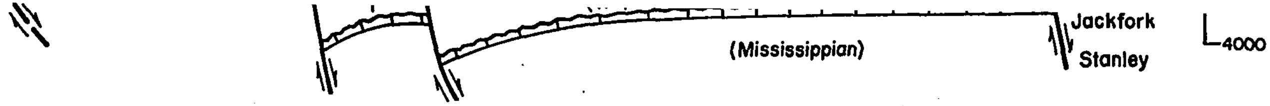

Fig. 15 C. Basinal subsidence at Event 3: "Atokan marker "20" event to south and age equivalent lower Atokan unconformity to north".

EVENT 4

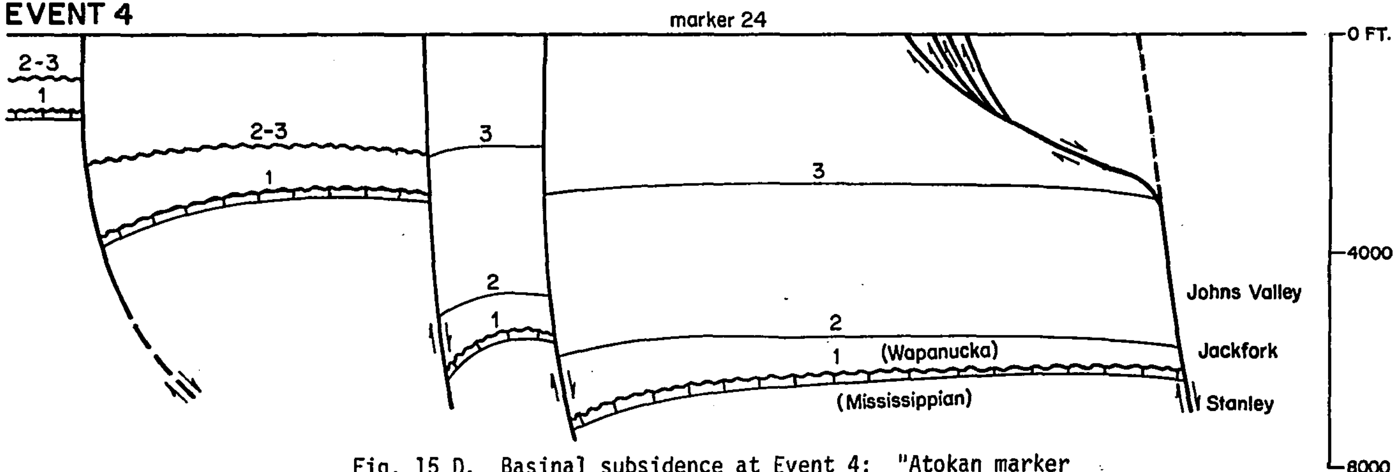

Fig. 15 D. Basinal subsidence at Event 4: "Atokan marker "24" event (approximately middle Atokan)".

EVENT 5

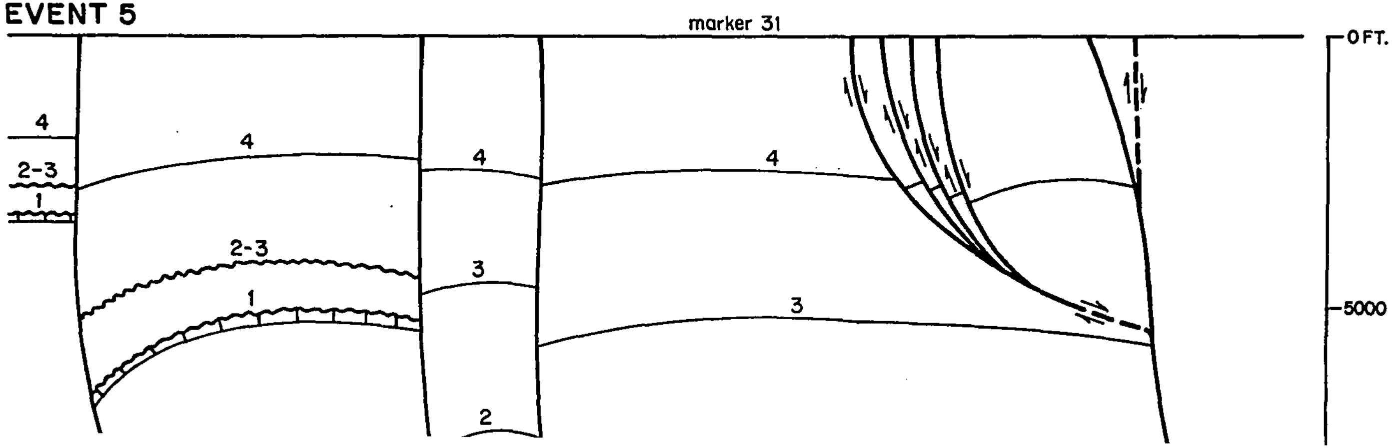

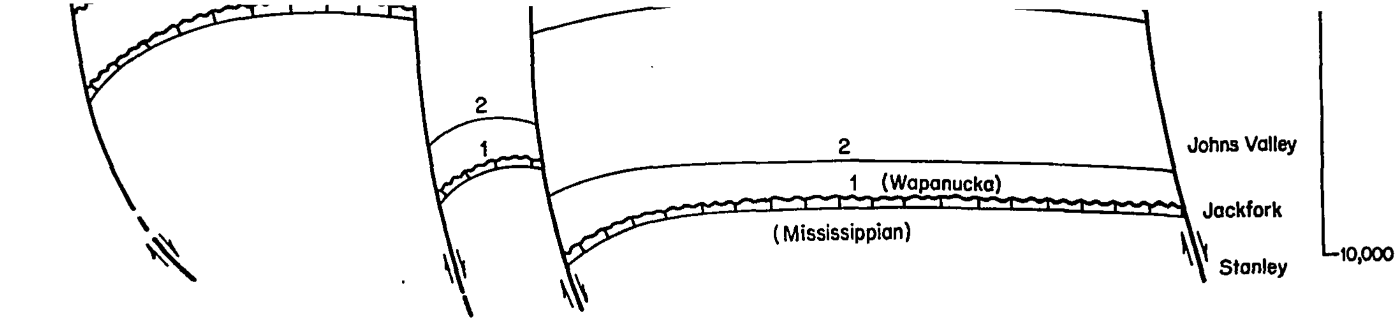

Fig. 15 E. Basinal subsidence at Event 5: "Atokan marker "31" event (approximately late Atokan)".

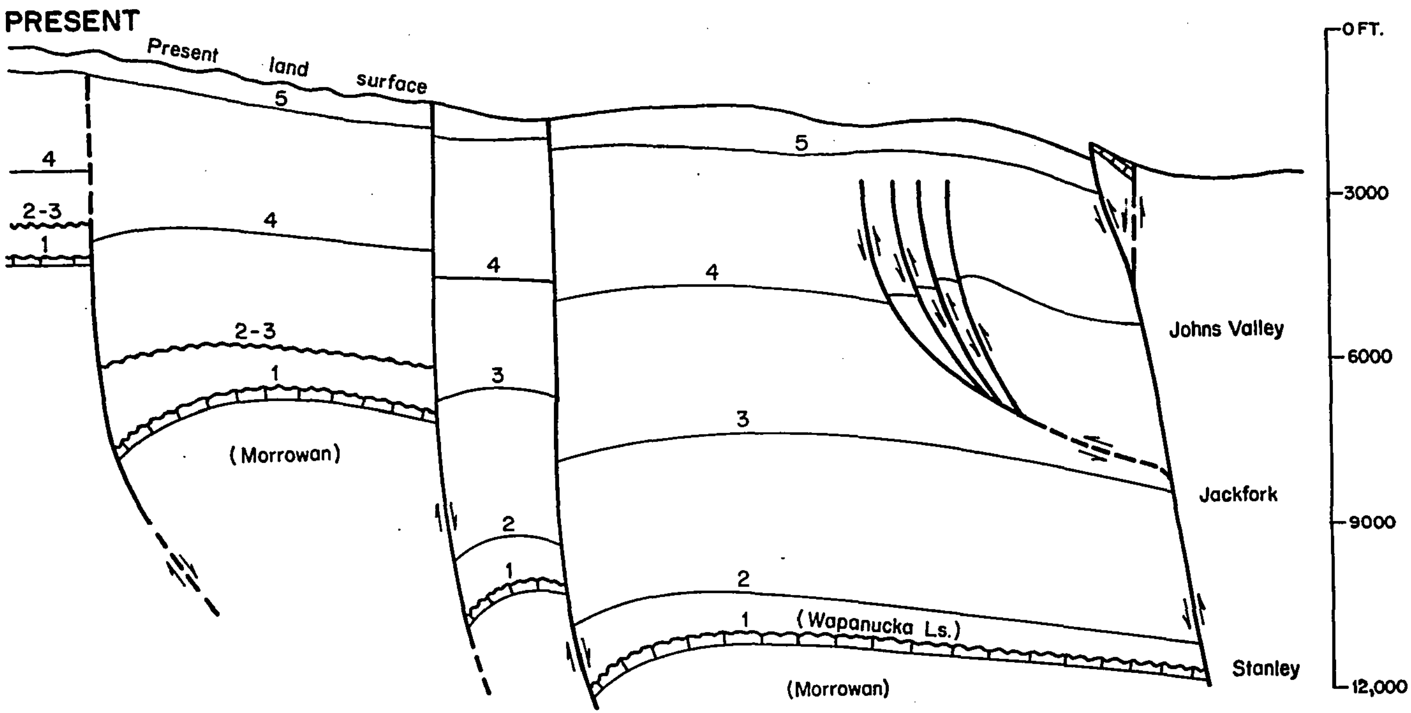

Fig. 15 F. Present day structural-stratigraphic relations.

Fig. 15 E. Basinal subsidence at Event 5: "Atokan marker "31" event (approximately late Atokan)".

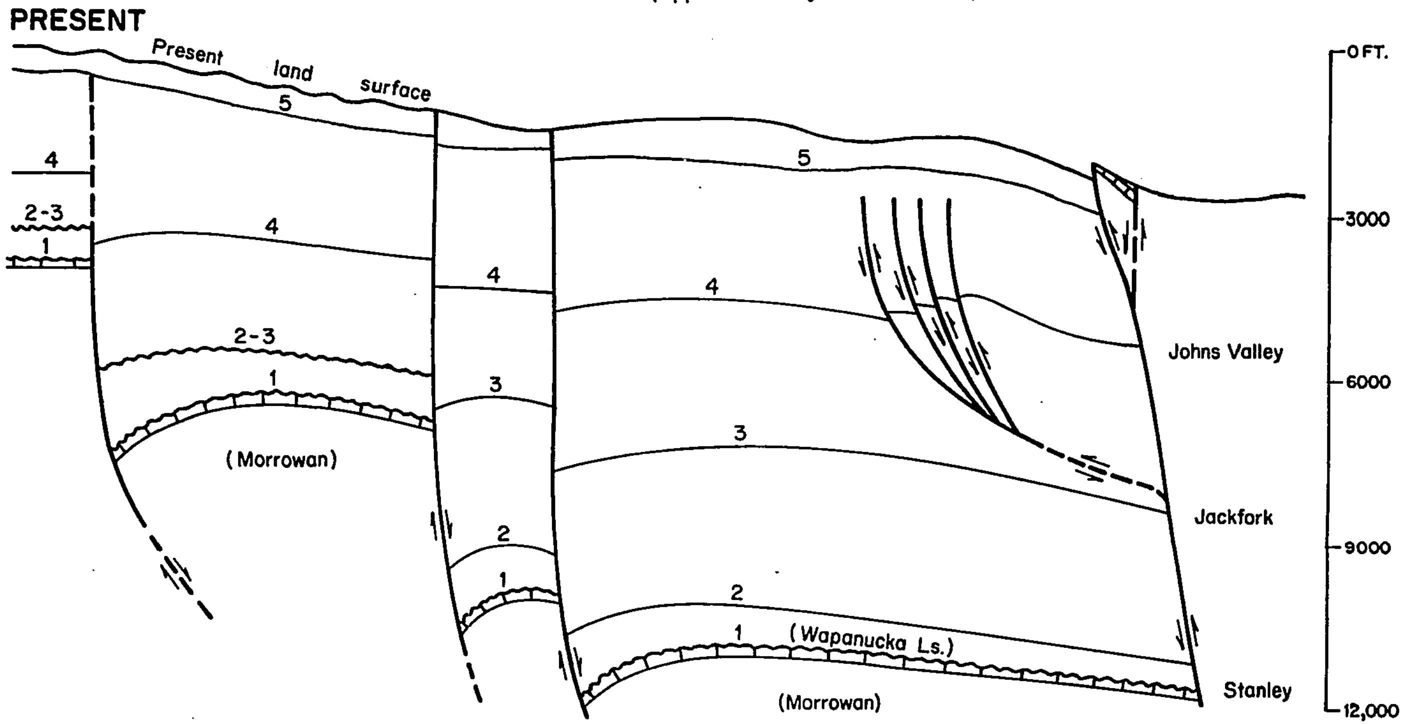

Fig. 15 F. Present day structural-stratigraphic relations.

Fig. 15. Schematic north-south cross sections illustrating stages of basinal subsidence from Morrowan to present. Horizontal distance approximately 40 miles, not to scale.

of the basal Atokan shales northward into the fault plane. The area south of the Mulberry fault acted as a relatively stable block; however, there was some minor movement along the Kinta and San Bois fault planes. Although the principal movement along these latter two faults was later, some movement occurred soon after movement was initiated along the Mulberry fault.

Event (3), Fig. 15 C, depicts increased movement along the Kinta fault; from north to south it is approximately 2,000 feet. Between the Mulberry and Kinta faults the lower Atokan markers "14" through "20" are not present and this interval is represented by the lower Atokan unconformity.

By Middle Atoka time, represented by event (4) in Fig. 15 D, the movement along the Kinta and San Bois faults was at a maximum. Northward on the Mulberry block, slight movement resumed as the Middle Atokan shales are present, but thinner than basinward to the south.

During events (3) and (4) growths faults were initiated in the Atoka shales, south of the San Bois and Kinta faults. Próbably these faults were first formed during event (3) approximately middle Atoka time.

Event (5), Fig. 15 E, shows continued movement across the major fault zones. Movement along the southern faults exceeded that along the northern faults as the upper Atoka shales thicken southward.

Post event (5) marks the time of the Ouachita movement. The Ouachita orogeny resulted in uplift south of the area and thrrusting northward of the Morrowan strata over Atokan shales. Fig. 15 F, shows the present day structural configuration across the area of study and south to the Ouachita mountains.

History of Sedimentation

Following depsoition of the Chesterian rocks the area of investigation underwent a period of minor uplift and erosion. The Morrowan seas transgressed a port-Mississippian surface of low relief and the Cromwell sands were deposited. During deposition of the Cromwell, faulting contemporaneous with deposition influenced the stratigraphy and sedimentation of these sands.

During deposition of the Morrow movement along the faults apparently was of lesser magnitude than movement during deposition of lower Atokan strata. The abrupt and rapid changes in thickness of the lower Atokan versus the more subtle and less marked thickness variations in the Morrowan strata is a reflection of fault movement during deposition. Undoubtedly the history of growth faulting affected strata older than Morrowan -- perhaps even as old as Hunton.

Deposition continued through Morrowan time while stable shelf shales and limestones were deposited. This represents a quiescent period in the history of growth fault movement; the youngest Morrowan unit, the Wapanucka limestone was deposited at this time. After deposition of the Wapanucka Limestone the area underwent an episode of emergence and erosion. The eroded Wapanucka Limestone surface shows little angularity and is best described as a disconformity between it and the overlying basal Atoka shale.

In the central area (R. 22 E. through 24 E.) the percentage of shale is less between the base of the "C" marker (base of Brentwood Limestone), and the thick upper limestone (Wapanucka Limestone), and the Morrowan section is slightly thinner. To the west and to the east, the thick (80 - 100 feet) Wapanucka Limestone is separated from the Brentwood Limestone by mostly shale with some thin limestones. Over the central area the interval above the base of the Brentwood Limestone to the Wapanucka unconformity is mostly limestone (refer to Fig. 4 and Plate VI). This apparent change in the Morrowan strata may be explained in two ways.

One explanation is that the central area remained a positive feature, in comparison to the surrounding area, throughout Morrowan time. The strata above the Brentwood Limestone, by virtue of facies change from shale to limestone, contains less shale because the area was more stable and conducive to carbonate deposition. After its deposition the thick upper Wapanucka Limestone member was partially removed by erosion, down to the limy facies abvoe the Brentwood Limestone.

The other explanation is that the increased percentage in limestone above the Brentwood is due to facies changes only. By this explanation the upper Wapanucka, as recognized to the west or to the east, is present but not separated from the underlying units by a shale break. This explanation also indicates the central area was more stable and positive to the surrounding area, thus conducive to carbonate deposition.

Either explanation for the Morrowan Limestone facies in the central area may be valid; a detailed biostratigraphic investigation could resolve the question, but the paucity of cores though the Morrowan strata precludes such an undertaking. Whichever explanation is favored, both point to the same conclusion that the central area was a remnant positive feature through Morrowan time while the adjacent area subsided more rapidly. The indication of a stable central area by the facies relationship of the Morrowan strata is also reflected in the underlying Cromwell sand facies. The Cromwell II and III sands are poorly developed or represented by a shaly zone in the central area. The youngest (Cromwell I) sand is not present over the central area. The facies relationships of the Cromwell II and III sands also indicate the central area was a positive feature, consequently silts and clays were deposited there while the adjacent area subsided differentially and received more sand-sized material.

After exposure and erosion of the Wapanucka Limestone the basin was stable or subsided slowly and the dark gray to black sub-Spiro shale was deposited. Over the central area the sub-Spiro shale is not present and the Spiro "B" sand was deposited on the topographically high anticlinal axes of fault blocks. The Spiro "B" sand is an above wave base deposit. In the adjacent area the dark sub-Spiro shale was deposited in a quite water or lagoonal environment.

The increased movement along growth faults after deposition of the sub-Spiro shale marks the beginning of the deposition of the Spiro "A" sand. As the seas encroached from south to north the Spiro "A" sand was deposited as part of this transgression. Contemporaneous movement along faults controlled the thickness and distribution of the Spiro "A" sand as described earlier.

Continued rapid subsidence along the fault zones resulted in locally increased thickness of the basal Atoka shales toward and into the fault planes. During this time sediment supply was abundant and the amount of mud was far in excess of sand, thus the thick basal Atoka shales with thin silty or sandy zones.

South of the Kinta and San Bois faults, rapid subsidence and sedimentation continued through the time of marker '14'. North of the faults, a hiatus or disconformable situation prevailed from the time of marker '14' through marker '20', as represented by the lower Atokan unconformity.

Subsidence continued south of the Mulberry block through marker '20' time. An increase in the amount of sand in the sediment supply resulted in the deposition of the Panola, Brazil and Red Oak sands south of the Kinta and San Bois faults. The stable Mulberry block might have been eroded and contributed some of the sediment supply to the south, this contribution to the sand supply was probably minor because there was little sand present in the lower Atokan shales.

Movement along the Mulberry fault resumed, along with continued subsidence south of the Mulberry block and is represented by the interval between markers '20' through '24' marker. Along with rejuvenated subsidence, the sand supply increased resulting in deposition of Tidwell sand immediately underlying the 24' marker. Apparently, movement along the Mulberry fault was greatest at this time because the thickest Tidwell sand is found on the downthrown side of the Mulberry fault. In comparison, thin sands or no sand is present at this stratigraphic level to the south near the Kinta and San Bois faults.

Throughout the time represented by markers 25 through 31, subsidence continued basinwide. During this time the upper Atoka shales and sands were deposited. Basinal subsidence continued through deposition of the Desmoinesian Hartshorne Sandstone.

SPECULATIONS AND PROBLEMS

In a study of this scope and magnitude it is difficult to summarize the geologic history of an area by developing a basinal subsidence model without stepping out of bounds in terms of area investigation, or evidence presented. This can also be carried a step further in that conclusions applicable to the area of investigation might also explain specific problems outside the area and furthermore in arriving at these possible conclusions, evidence is used that is not presented in the pater, but is part of the information gained during research. Some examples of "speculations and problems" are discussed in this section.

Comparison of Fig. 15 A, with the sequence Fig. 15 F, illustrates an interesting situation. The present day Ouachita thrust system and the Red Oak thrusts, are hypothesized to be former down to the basin growth faults. These old growth faults were zones of weakness along which reverse movement occurred during the Ouachita uplift. Admittedly the evidence for this hypothetical history of a region outside the area of study is tenuous, but the hypothetical events are compatible with a basinal subsidence model for the region.

It is hypothesized that under the influence of Atokan growth faults, the Red Oak sands were deposited. This hypothetical situation is based on interpretation of cross sections and maps, not included in this presentation, of the area of the Red Oak gas field (Ts. 6 and 7 N., Rs. 22

to 24 E.) approximately 10 miles south of the San Bois fault.

The growth fault mechanism, might offer a unique explanation for the rapid transition from the shelf and miogeosynclinal facies on the north to the eugeosynclinal facies to the south of the Choctaw fault. Perhaps the Choctaw fault was an ancient growth fault, on the down-thrown side of which accumulated the thick Stanley, Jackfork and Johns Valley sequence that is believed to be age equivalent to the Late Mississippian and Early Pennsylvanian (Morrowan) to the north. Movement along the fault was later reversed during the Ouachita disturbance.

Facies relations, sedimentary petrology and paleocurrent studies indicate that the Ouachita geosyncline derived its sediments from marginal sources. A turbidity flow mechanism dominated during sediment transport.

Briggs and Cline (1967), presented evidence from the source areas and paleocurrent data on the late Mississippian and Pennsylvanian flysch sediments of the Ouachita fold belt. They found that directional readings on sandstones of the Jackfork, Johns Valley and lower Atoka sequence show that the sediment transport was westward, down the axis of the geosyncline and that current directions remained essentially constant during the deposition of 13,000 feet of sediment.

Shideler (1970), on provenance studies of Johns Valley boulders in the Ouachita facies, concluded that the exotic boulders had a nearby source, and were possibly due to erosion of an escargement or area of high relief.

The just described sedimentologic and stratigraphic evidence suggest a depositional environment involving a basinal subsidence model with which the Choctaw fault, postulated as a former growth fault, is compatible.

Future work in the Red Oak area involving the depositional environment of the Red Oak sand and associated strata may determine if a growth fault mdel explains their depositional mechanism. Further work on the surface and subsurface geology of the area near the Choctaw thrust will test the hypothesis that it may at an early time was a growth fault.

SUMMARY AND CONCLUSIONS

The subsurface structure of the southwestern Arkoma basin is dominated by three large down-to-the basin growth faults. Growth faults are uniquely characterized by having a substantial increase in throw with depth and across which, from the upthrown to the downthrown block, there is a rapid thickening of correlative section. Growth faulting was the mechanism for basinal subsidence during deposition of Morrowan and basal Atokan strata; a depositional model compatible with growth faulting was developed for the basal Atokan (Spiro) and Cromwell sands. The growth fault system in the Arkoma basin is similar to the numerous examples along the Gulf Coast described by Thorsen (1963), and Bruce (1972).

The basal Atokan sand has been mapped as two separate units, the uppermost Spiro "A" and the underlying Spiro "B" facies.

The Spiro "A" sand is well to moderately well sorted and is present throughout the area. It is believed to occur in thick trends subparallel to the depositional strike and fault system. The Spiro "A" is believed to be a below wave base sand deposited by a density current medium coincident with paleotopographical/paleostructural low areas. Each fault block has its own sand buildup that is characteristically thickest and better sorted adjacent to the bounding faults; the thinner and more shaly sand occurs over the crestal portions of the fault blocks.

The Spiro "B" sand is present in only a limited central portion of the area and characteristically underlies the Spiro "A" and directly overlies the post-Wapanucka unconformity. It occurs as pods over individual fault blocks and exhibits thickening over the crestal protions with thinning to a feather edge or to zero toward the fault block margins.

The Spiro "B" is an above wave base marine sand deposit that accumulated in thick pods over paleotopographic/paleostructural high areas. Over the paleotopographic highs waves touched bottom and the sand was winnowed and distributed into deposits that thicken over the highs and thin toward subjacent low areas.

The Spiro "A" and "B" sands are cemented predominantly by quartz, with minor amounts of calcite and chlorite. Porosity and permeability have been reduced by secondary quartz cementation that most adversely affected the best sorted and thickest sands. Where chlorite coatings on the sand grains are well formed, the growth of secondary quartz cement was retarded and the sandstone retained good porosity and permeability.

The diagenetic alteration history is interpreted to be related to the depositional history in that the best sorted and thickest sands that accumulated along fault block margins were affected more by secondary quartz cement. The thinner, more shaly sands common to the crestal portions of the fault blocks were less affected by secondary quartz cement and retained the best porosity and permeability. Therefore, the sand with the most favorable reservoir characteristics is not the thickest and best sorted, but the somewhat shaly sand.

Both the Spiro "A" and "B" are interpreted to be marine sands deposited subparallel with paleodepositional strike. There is no evidence for a north-south trending facies as previously reported in the literature e.g., the north-south "Foster" channel facies of Lumsden, et al., (1971).

The source of the Spiro sand is believed to be to the east and southeast, with a limited contribution of sediment from the north.

The Cromwell sand is subdivided (in descending order) into three facies, the Cromwell I, II and III. The Cromwell sands and overlying Morrowan shales exhibit stratigraphic changes characteristic of a growth fault control sedimentation pattern. All three sands are interpreted to be marine deposits and were mapped subparallel to the depositional strike and subparallel with the fault system.

The distribution of the Cromwell I sand is limited to the area around the Kinta fault block. The Cromwell II and III sands are present throughout the area, but as a whole are quite shaly. The shaly character is related to sediment supply and rate of subsidence -- when sand supply was low and subsidence slow, shaly and poorly developed sand was deposited.

The secondary quartz cement alteration history of the Cromwell sands is believed to be similar to that of the Spiro sands. The best preserved porosity and permeability occur in areas where the Cromwell is somewhat shaly; however, the overall shaly character of the Cromwell results in favorable reservoir facies of only limited extent.

The source of the Cromwell is interpreted to be to the east and southwest, similar to that of the Spiro sand; however, local sources may have contributed substantial amounts of sediment.

The southwestern Arkoma basin was an area that underwent a rapid rate of subsidence beginning at least as early as Morrowan and continued through deposition of the basal Atokan. The rapid rate of subsidence and growth fault controlled sedimentation continued throughout deposition of the Atokan section.

In many respects, the growth faults of the southwestern Arkoma basin resemble those of the Gulf coast. The Gulf coast growth faults are believed to result from tension and gravity slide, caused partly by subsidence of the basin floor, and partly by the rapid compaction of the recently deposited sediments. It may be supposed that the southwestern Arkoma basin faults had a similar origin.

The growth faults cutting the Morrowan and basal Atokan section probably originated at depth, due to basement movements. This is thought to be the case because a thick shale below the Morrow is not present to act as a glide plane for the faults as they flatten and become bedding plane faults at depth. Moreover, examination of seismic profiles by the writer (not shown here) revealed that the faults that cut the Morrowan strata do not flatten at depth, but continue downward at a nearly constant dip rate until they can no longer be recognized.

The growth faults occurring higher in the Atokan shale section are due to loading or slumping by rapidly deposited sediment. These faults flatten and become bedding faults in the Atoka shales.

BIBLIOGRAPHY

Bartlett, C. S., 1966, Arkoma's search for porosity broadens: Oil and Gas Jour. (Jan.), p. 126-144.

Berry, R. M. and Trumbly, W. D., 1968, Wilburton gas field, Arkoma Basin, Oklahoma, in Cline, L. M., ed., Guidebook to the geology of the western Arkoma Basin and Ouachita Mountains, Oklahoma: Okla. City Geolo. Soc., p. 86-99.

Blythe, J. G., 1959, Atoka Formation on the north side of the McAlester basin: Okla. Geol. Survey Circ., p. 47, 74.

Bowsher, A. L. and Johnson, N. L., 1968, Road log for second day, in Cline, L. M., ed., Guidebook to the geology of the western Arkoma Basin and Ouachita Mountains, Oklahoma: Okla. City Geol. Soc. Guidebook, p. 30-54.

Branan, C. B., Jr., 1968, Natural gas in Arkoma Basin of Oklahoma and Arkansas, in Beebe, B. W. and Curtis, B. F., eds., Natural Gases of North America--a symposium: Am. Assoc. Petroleum Geoloists Mem. 9, v. 2, p. 1616-1655.

Briggs, G. and Cline, L. M., 1967, Paleocurrents and source areas of late Paleozoic sediments of the Ouachita Mountains, southeastern Oklahoma: Jour. Sed. Petrology, v. 37, p. 985-1000.

Bruce, C. H., 1972, Pressure shale and related sediment deformation; a mechanism for development of regional contemporaneous faults: Gulf Coast Assoc. Geol. Socs. Trans., v. 22, p. 23-31.

Buchanan, R. S. and Johnson, F. K., 1968, Bonanza gas field--a model for Arkoma Basin growth faulting, in Cline, L. M., ed., Guidebook to the geology of the western Arkoma Basin and Ouachita Mountains, Oklahoma: Okla. City Geol. Soc., p. 75-85.

Burst, J. F., 1969, Diagenesis of Gulf Coast clayey sediments and its possible relation to petroleum migration: Am. Assoc. Petroleum Geologists Bull., v. 53, p. 73-93.

Busch, D. A., 1971, Genetic units in delta prospecting: Am. Assoc. Petroleum Geologists Bull., V. 55, p. 1137-1154.

__________, 1975, Influence of growth faulting on sedimentation and prospect evaluation: Am. Assoc. Petroleum Geologists Bull., v. 59, p. 217-230.

Cloos, E., 1968, Experimental analysis of Gulf Coast fracture pattersn: Am. Assoc. Petroleum Geologists Bull., v. 52, p. 420-444.

Coleman, J. M. and Wright, L. D., 1975, Modern river deltas: variability of processes and sand bodies, in Broussard, M. L., ed., Deltas, Models for Exploration: Houston Geol. Soc., p. 99-149.

Curtis, D. M., 1970, Miocene deltaic sedimentation, Louisiana Gulf Coast, in Morgan, J. P. and Shaver, R. H., eds., Deltaic Sedimentation Modern and Ancient: Soc. Econ. Paleontologists and Mineralogists Special Pub. 15, p. 293-308.

Disney, R. W., 1960, The subsurface geology of the McAlester basin, Oklahoma: Unpublished Ph. D. Dissertation, The University of Oklahoma, Norman, Oklahoma.

Frezon, S. E., et al., 1963, The Chester, Morrow and Atoka Series in western Arkansas and eastern Oklahoma: Shale Shaker, October, 1963, p. 4.

Friedman, G. M., 1962, On sorting, sorting coefficients and the log normality of the grain size distribution of sandstones: Jour. Geol. v. 70, p. 737-756.

Henry, T. W., 1973, Brachiopod biostratigraphy and faunas of the Morrow Series (Lower Pennsylvanian) of northwestern Arkansas and northeastern Oklahoma: Unpublished Ph. D. Dissertation, University of Oklahoma, Norman, Oklahoma.

Huffman, G. G., 1958, Geology of the flanks of the Ozark uplift, northeastern Oklahoma: Okla. Geol. Surv. Bull., p. 77, 271.

Kidwell, A. L. and Hunt, J. M., 1958, Migration of oil in recent sediments of Pedernales, Venezuala, in Weeks, L. G., ed., Habitat of Oil--a symposium: Am. Assoc. Petroleum Geologists, Tulsa, Oklahoma, p. 790-817.

Koinm, D. N. and Parke A. Dickey, 1967, Growth faulting in McAlester Basin of Oklahoma: Am. Assoc. Petroleum Geologists Bull., v. 51, p. 710-718.

Laudon, R. B., 1958, Chesterian and Morrowan rocks in the McAlester Basin of Oklahoma: Okla. Geol. Surv. Circ., p. 30, 46.

Levorsen, A. I., 1967, Geology of Petroleum: W. H. Freeman and Company, San Fransicso, p. 724.

Lumsden, D. N., et al., 1971, Sedimentation and petrology of Spiro and Foster sands (Pennsylvanian) McAlester Basin, Oklahoma: Am. Assoc. Petroleum Geologists Bull., v. 55, p. 254-266.

Ocamb, R. D., 1961, Growth faults of south Louisiana: Gulf Coast Assoc. Geol. Socs. Trans., v. 2, p. 139-173.

Pittman, E. D. and Lumsden, D. N., 1968, Relationship between chlorite coatings on quartz grains and porosity, Spiro sand, Oklahoma: Jour. Sed. Petrology, v. 38, p. 668-670.

Powers, M. C., 1967, Fluid-release mechanisms in compacting marine mudrocks and their importance in oil exploration: Am. Assoc. Petroleum Geologists Bull., v. 51, p. 1240-1254.

Price, L. C., 1976, Aqueous solubility of petroleum as applied to its origin and primary migration: Am. Assoc. Petroleum Geologists Bull., v. 60, p. 213-244.

Quarles, M., Jr., 1953, Salt ridge hypothesis on origin of Texas Gulf Coast type of faulting: Am. Assoc. Petroleum Geologists Bull., v. 37, p. 489-508.

Rowland, T. L., 1970, Lithostratigraphy and Carbonate Petrology of the Morrow Formation (Pennsylvanian), Braggs-Cookson Area, Northeastern Oklahoma: Unpublished Ph. D. Dissertation, University of Oklahoma, Norman, Oklahoma.

Scull, B. J., et al., 1959, The Atoka of the McAlester Basin--Arkansas Valley Region, in Cline, L. M., Hilseweek, W. J. and Feray, D. E., eds., The geology of the Ouachita Mountains--a symposium: Dallas, Texas, Dallas and Ardmore Geol. Socs., p. 166-172.

__________________, 1960, A comparison of Plio-Miocene sedimentation of the Gulf Coast with Atoka sedimentation in the Arkoma Basin: 7th Bienn. Geol. Symposium, School of Geology, University of Oklahoma, Norman, Oklahoma.

Shideler, G. L., 1970, Provenance of Johns Valley boulders in late Paleozoic Ouachita facies, southeastern Oklahoma and southwestern Arkansas: Am. Assoc. Petroleum Geologists Bull., v. 54, p. 789-806.

Six, D. A., 1968, Red Oak-Norris gas field, Brazil anticline, Latimer and LeFlore Counties, Oklahoma, in Beebe, B. W. and Curtis, B. F., eds., Natural Gases of North American--a symposium: Am. Assoc Petroleum Geologists, Mem. 9, v. 2, p. 1644-1657.

Smith, P. V., Jr., 1954, Studies on origin of petroleum--occurrence of hydrocarbons in recent sediments: Am. Assoc. Petroleum Geologists Bull., v. 38, p. 377-404.

Thorsen, C. E., 1963, Age of growth faulting in southeast Louisiana: Gulf Coast Assoc. Geol. Socs. Trans., v. 13, p. 103-110.

Weaver, C. E., 1960, Possible uses of clay minerals in search for oil: Am. Assoc. Petroleum Geologists Bull., v. 44, p. 1505-1518.

Weber, K. J., 1971, Sedimentological Aspects of Oil Fields in the Niger Delta: Geologie en Nijnbouw, v. 50 (3), p. 559-576.

Wilson, C. W., Jr., 1935, Age and correlation of the Pennsylvanian surface formations and of oil and gas sands of Muskogee County, Oklahoma: Am. Assoc. Petroleum Geologists Bull., v. 19, p. 503-520.

Woncik, John, 1968, Kinta gas field, in Beebe, B. W. and Curtis, B. F., eds., Natural Gases of North America--a symposium: Am. Assoc. Petroleum Geologists, Mem. 9, v. 2, p. 1636-1643.

Wong, H. Y., 1969, Clay petrology of the Atoka formation, eastern, Oklahoma: Unpublished Ph. D. Dissertation, The University of Oklahoma, Norman, Oklahoma.

APPENDIX A

CROSS SECTION IDENTIFICATION AND LOCATION INDEX

The wells included in the stratigraphic and structural cross sections that appear in this report are listed below. The location of the wells on each profile section is shown on Plate I. The wells used on these cross sections are identified by a number which appears above each well on the various sections. The wells are listed in order of positioning on the profile section by the indentification number; section, township, range and spot location.

Identification Number		Location
	Cross Section A-A'	
1	32, T. 8 N. - R. 20 E.	NW SE
2	5, T. 7 N. - R. 20 E.	C N/2
3	8, T. 7 N. - R. 20 E.	W/2 W/2 SW NE
4	17, T. 7 N. - R. 20 E.	NE SW
5	20, T. 7 N. - R. 20 E.	C SW
6	29, T. 7 N. - R. 20 E.	C SW
7	32, T. 7 N. - R. 20 E.	C NW
8	5, T. 6 N. - R. 20 E.	C NW
	Cross Section B-B'	
9	32, T. 9 N. - R. 21 E.	SE SE SE
10	4, T. 8 N. - R. 21 E.	C SE
11	9, T. 8 N. - R. 21 E.	NW NW SE
12	16, T. 8 N. - R. 21 E.	SW NE
13	16, T. 8 N. - R. 21 E.	C SE
14	22, T. 8 N. - R. 21 E.	C W/2
15	27, T. 8 N. - R. 21 E.	SE SW NE
16	34, T. 8 N. - R. 21 E.	SE NW
17	2, T. 7 N. - R. 31 E.	SE NW
18	11, T. 7 N. - R. 21 E.	NW SW NE
19	14, T. 7 N. - R. 21 E.	C NW

Identification Number		Location
	Cross Section C-C'	
20	11, T. 10 N. - R. 23 E.	NE SE
21	23, T. 10 N. - R. 23 E.	NW SE
22	26, T. 10 N. - R. 23 E.	C SE
23	35, T. 10 N. - R. 23 E.	C NE
24	1, T. 9 N. - R. 23 E.	NW SE
25	12, T. 9 N. - R. 23 E.	NW SE
26	18, T. 9 N. - R. 24 E.	SE NW
27	19, T. 9 N. - R. 24 E.	SE NW
28	30, T. 9 N. - R. 24 E.	SE NW
29	31, T. 9 N. - R. 24 E.	NE SE
30	6, T. 8 N. - R. 24 E.	S/2 S/2 SW
31	7, T. 8 N. - R. 24 E.	NW SE
32	18, T. 8 N. - R. 24 E.	SE NW
33	19, T. 8 N. - R. 24 E.	C NW
34	29, T. 8 N. - R. 24 E.	NW SE
35	32, T. 8 N. - R. 24 E.	SW NE
	Cross Section D-D'	
36	20, T. 11 N. - R. 26 E.	SE SE
37	33, T. 11 N. - R. 26 E.	C SW
38	2, T. 10 N. - R. 26 E.	NE SW SW
39	11, T. 10 N. - R. 26 E.	SW NE
40	12, T. 10 N. - R. 26 E.	NE SW
41	18, T. 10 N. - R. 27 E.	NW SE
42	19, T. 10 N. - R. 27 E.	C NE
43	29, T. 10 N. - R. 27 E.	NE SW
44	31, T. 10 N. - R. 27 E.	NW SE
45	6, T. 9 N. - R. 27 E.	E/2 W/2
46	12, T. 9 N. - R. 26 E.	SE SW NE
47	13, T. 9 N. - R. 26 E.	SE NE
48	13, T. 9 N. - R. 26 E.	NW SW SE
49	24, T. 9 N. - R. 26 E.	SW NE
50	29, T. 9 N. - R. 27 E.	NW SE
51	32, T. 9 N. - R. 27 E.	C SE
52	4, T. 8 N. - R. 27 E.	NE SW NW
53	4, T. 8 N. - R. 27 E.	NW SE
54	9, T. 8 N. - R. 27 E.	C NE

Identification Number		Location
	Cross Section E-E'	
55	10, T. 8 N. - R. 17 E.	W/2 SE
56	19, T. 8 N. - R. 19 E.	SW SW NE
57	27, T. 8 N. - R. 19 E.	SE NW
58	30, T. 8 N. - R. 19 E.	SE NW
59	9, T. 7 N. - R. 19 E.	SW SE NE
60	25, T. 8 N. - R. 19 E.	NE SW
61	22, T. 8 N. - R. 20 E.	SE NW
62	17, T. 8 N. - R. 21 E.	SE NW
63	23, T. 8 N. - R. 21 E.	NE SW
64	17, T. 8 N. - R. 22 E.	SW NE
65	13, T. 8 N. - R. 22 E.	S/2 N/2
66	9, T. 8 N. - R. 23 E.	NW SE
67	34, T. 9 N. - R. 23 E.	SE NE SW
68	19, T. 9 N. - R. 24 E.	SE NW
69	13, T. 9 N. - R. 24 E.	S/2 S/2 NW
70	4, T. 9 N. - R. 25 E.	NW NW SE
71	1, T. 9 N. - R. 25 E.	NE SW NE
72	32, T. 10 N. - R. 26 E.	NW SW
73	23, T. 10 N. - R. 26 E.	N/2 S/2
74	18, T. 10 N. - R. 27 E.	NW SE
75	9, T. 10 N. - R. 27 E.	S/2 N/2
	Cross Section W-W'	
76	24, T. 8 N. - R. 21 E.	SE SE NW
77	29, T. 8 N. - R. 22 E.	SW NE
78	22, T. 8 N. - R. 22 E.	NW NE SW
79	26, T. 8 N. - R. 22 E.	SW NE SW
80	25, T. 8 N. - R. 22 E.	SE NW
81	30, T. 8 N. - R. 23 E.	NE NE SW
82	29, T. 8 N. - R. 23 E.	SW NE
83	28, T. 8 N. - R. 23 E.	SW NE
	Cross Section X-X'	
84	9, T. 9 N. - R. 22 E.	SE NW
85	28, T. 9 N. - R. 22 E.	1933' FSL & 2083' FEL
86	34, T. 9 N. - R. 22 E.	660' S & 660' E of C
87	6, T. 8 N. - R. 23 E.	153' E & 125' S of C
88	7, T. 8 N. - R. 23 E.	SW NE
89	20, T. 8 N. - R. 23 E.	SW NE
90	29, T. 8 N. - R. 23 E.	SW NE

Identification Number		Location
	Cross Section Y-Y'	
91	23, T. 8 N. - R. 19 E.	600' N & 50' W of C
92	24, T. 8 N. - R. 19 E.	SE SE NW
93	27, T. 8 N. - R. 19 E.	SW NE
	Cross Section Z-Z'	
94	19, T. 9 N. - R. 20 E.	SW NE SW
95	31, T. 9 N. - R. 20 E.	NE NE NE
96	5, T. 8 N. - R. 20 E.	1320' S & 1220' E of C
97	18, T. 8 N. - R. 20 E.	NW SE NE
98	19, T. 8 N. - R. 20 E.	SE SE NW
99	30, T. 8 N. - R. 20 E.	950' E of C
100	31, T. 8 N. - R. 20 E.	NW NW SE
101	6, T. 7 N. - R. 20 E.	C NW SE
102	7, T. 7 N. - R. 20 E.	SE NW
103	18, T. 7 N. - R. 20 E.	150' NW of C NE SW
104	19, T. 7 N. - R. 20 E.	C SE NW
105	25, T. 7 N. - R. 19 E.	NW NE SW

APPENDIX B

SPIRO THIN SECTION DESCRIPTIONS

Midwest Free Unit No. 1
SE NW SE
Sec. 11, T. 6 N. - R. 21 E.

BA-2 (11,845'-11,846'): Sandstone, fine, subangular to subround, moderate to well sorted, 10 - 15% fossil fragments (bryozoan, pelmatazoan, algal debris (fossil fragments 0.2 - 0.3 mm. diameter), mostly CO_3 cement, some areas (less than 5%) have stained clay filling between pores, stain probably bitumen or oil residue; porosity before cement 25-30%, porosity after cement 2-5%. Overall, homogeneous fossiliferous sand; where clay absent and in clacite cemented areas, some quartz overgrowths.

Midwest Free Unit No. 1
SE NW SE
Sec. 11, T. 6 N. - R. 21 E.

BA-3 (11,851'-11,852'): Sandstone, fine, subrounded, fairly well sorted, fossiliferous, calcite cemented (less than 5%). Monocrystalline quartz 80%; chert 2%; MRF's 3%; clay 5%, mostly detrital -- grain coating has retarded quartz overgrowths. Fossil fragments are bryozoan, pelmatozoan, algall fragments, shells (all 0.25 - 0.35 mm. in diameter). Rock similar to BA-2, less fossil fragments, more clay content, come quartz overgrowths (only present where clay absent).

Midwest Free Unit No. 1
SE NW SE
Sec. 11, T. 6 N. - R. 21 E.

BA-4 (11,861'-11,862'): Sandstone, fine to medium, subangular to subrounded, bimodal size distribution (75% - 0.2 mm., 25% - 0.325 mm.), larger grains more rounded, less than 5% detrital clay, some authigenic chlorite retarding quartz overgrowths. Quartz 95%; chert - trace; MRF's 2 to 5%; clay 2 to 5%. Mostly calcite cemented, quartz overgrowths thin or absent depending on amount of clay present, trace CRF's, trace fossil fragments. Fairly loose pakcing; $\emptyset_{bc}$ 25%, $\emptyset_{ac}$ 2-5%, if clay does not plug pores, calcite cement does.

Midwest Martin No. 1
C SW NE
Sec. 3, T. 6 N. - R. 22 E.

BA-5 (11,209'-11,210'): Sandstone, bimodal size distribution (50% fine, 50% medium to coarse), fine grains--subangular, larger grains--subround to round. All quartz monocrystalline, poorly sorted, very fossiliferous. Quartz: 60%; fossil fragments: 40%; carbonate rock fragments: trace (?).

Midwest Rider No. 1
277' E and 499' S of C
Sec. 17, T. 6 N. - R. 22 E.

BA-7 (11,991'): Sandstone, fine subangular to subround fair sorting, tightly packed, 80% quartz cemented, rest $CaCO_3$ cemented, very minor amount of clay matrix, 98% quartz (monocrystalline), ± 2% MRF's, some clay coating on grains, occasional piece of altered MRF (altered to chlorite). Trace CRF's or fossil debris, stylotites cutting across thin sections.

Midwest Rider No. 1
277' E and 499' S of C
Sec. 17, T. 6 N. - R. 22 E.

BA-8 (12,009'): Sandstone, very fine, angular to subangular, moderate sorting, 10-15% matrix of chlorite and micaceous hash, 5% MRF's, quartz grains 80% (97% monocrystalline, trace polycrystalline, trace chert). Sediment seems disturbed, probably bioturbated (medium to coarse sand grains mixed with very fine sand grains in disturbed zones).

Midwest Rider No. 1
277' E and 499' S of C
Sec. 17, T. 6 N. - R. 22 E.

BA-9 (12,011'): Sandstone, same as before but not bioturbated as much as in BA-8. Some laminations preserved, also trace large (0.3 to 0.6 mm.) byrozoan and pelmatozoan fragments.

Midwest Jones Unit No. 1
1540 FWL and 1540 FEL
SE NW SE
Sec. 10, T. 6 N. - R. 21 E.

BA-10 (11,852'): Sandstone, very fine to fine, subangular, moderately, sorted, quartz cemented, some patchy calcite cement (± 25%), 5-10% CRF's and fossil debris (pelmatozoan and bryozoan). ϕ_{bc} 15-20%, ϕ_{ac} 5%. Where calcite cemented, have some porosity, if quartz cemented, no porosity. MRF's: 2-5%, and less than 1% clay matrix, abundant quartz overgrowths. Some laminations, with concentration of fossil debris in the laminations.
Note: ϕ_{bc} - porosity before cement.
ϕ_{ac} - porosity after cement.

Midwest Jones Unit No. 1
1540' FWL and 1540' FEL
SE NW SE
Sec. 10, T. 6 N. - R. 21 E.

BA-11 (11,860'): Sandstone, fine to medium, subrounded, well sorted in laminations, otherwise poorly sorted, loosely packed, concentration of MRF's in laminations, MRF's: 2-5%. Between some laminations poorly sorted--larger (0.3 mm. grains of quartz and rounded MRF's with finer quartz (0.15 to 0.2 mm.). Very fine sand to silt sized quartz and mica hash laminae (± 0.35 mm. wide). Less than 2% clay matrix, due to lack of clay coating, rock mostly quartz cemented and therefore little porosity. ϕ_{bc} 25%, ϕ_{ac} 2-5%.

Midwest Jones Unit No. 1
1540' FSL and 1540' FEL
SE NW SE
Sec. 10, T. 6 N. - R. 21 E.

BA-12 (11,880'): Shale, dark gray to brown, contains chlorite similar to that found in sandstone thin sections; foraminifera present.

Midwest Noah No. 1
790' FNL and 2440' FWL
Sec. 21, T. 6 N. - R. 21 E.

BA-13 (12,303'): Sandstone, fine, poorly to moderately sorted, subangular to subrounded, calcite cemented, loosely packed, fossil fragments present (25% of grains), quartz 72%, ± 2% MRF's, trace clay matrix. Laminated (2-4 mm. apart), abundant sand laminations with abundant fossil debris. Fossiliferous laminations coarser grained (coarse to very coarse sand size). Most quartz monocrystalline, trace polycrystalline quartz, trace chert. Fossil debris: 75% bryozoan; 25% pelmatozoan, algal plates and shell fragments.

Midwest Noah No. 1
790' FNL and 2440' FWL
Sec. 21, T. 6 N. - R. 21 E.

BA-14 (12,328'): Sandstone, very fine to fine, moderately to well sorted, 5% chlorite matrix, authigenic chlorite on quartz grains, retarded quartz overgrowths in places, 2-5% MRF's, where chlorite matrix not between grains (± 50% of grain contacts) have quartz overgrowths; less than 5% calcite cement in patches, 2-5% pelmatozoan and bryozoan debris.

Overall, better sorted rock than BA-13, lesser percentage of fossil debris, but still has enough clay matrix to retard quartz overgrowths and therefore rock may be classified as immature to submature.

Midwest Noah No. 1
790' FNL and 2440' FWL
Sec. 21, T. 6 N. - R. 21 E.

BA-15 (12,344'): Sandstone, very fine, subangular fairly well sorted, mostly quartz cemented, 5-10% calcite cemented. 5-10% bryozoan, pelmatozoan, and algal debris. Where calcite cemented, some porosity preserved--otherwise quartz cement and no porosity.

Midwest Booth No. 1
1896' FEL and 2148' FSL
Sec. 15, T. 6 N. - R. 21 E.

BA-16 (12,075'): Sandstone, very fine to silt sized, angular to subangular, poorly sorted, immature, fossiliferous. Bryozoan and pelmatozoan debris. (± 2%). Overall, poorly sorted muddy rock.

Monocrystalline quartz 98%, polycrystalline quartz - trace, chert - trace.

Midwest Booth No. 1
1896' FEL and 2148' FSL
Sec. 15, T. 6 N. - R. 21 E.

BA-17 (12,105'-12,106'): Sandstone, fine, subangular, moderately sorted, occassional fine lamination of chlorite mud, mostly calcite cemented, minor quartz overgrowths. Minor MRF's (less than 1%), less than 2% mud matrix, 5-10% of quartz grains 0.5 to 1.5 mm.; trace bryozoan and pelmatozoan debris, and trace carbonate rock fragments (0.5 - 1.5 mm).

Midwest Booth No. 1
1,896' FEL and 2,148' FSL
Sec. 15, T. 6 N. - R. 21 E.

BA-18 (12,108'-12,109'): Sandstone, very fine to fine, subangular to rounded (larger grains more rounded), poorly sorted,; MRF's 10%, chlorite mud matrix 15-20%, 2-5%: carbonate rock fragments and carbonate intraclasts, pelmatozoan and bryozoan debris (1.0 - 4.0 mm.). About 25% calcite cement, 5-10% quartz overgrowths.

Rock is immature and has bimodal size distribution of grains, muddy matrix has retarded quartz overgrowths, but still low porosity, due to poor sorting.

Midwest Booth No. 1
1,896' FEL and 2,148' FSL
Sec. 15, T. 6 N. - R. 21 E.

BA-19 (12,109'-12,110'): Sandstone, fine moderately sorted, subrounded; 5-10% MRF's, 5-10% chlorite matrix, 2% pelmatozoan and bryozoan debris, and carbonate rock fragments.

Midwest Booth No. 1
1,896' FEL and 2,148' FSL
Sec. 15, T. 6 N. - R. 21 E.

BA-20 (12,114'-12,115'): Sandstone, fine, subrounded, moderately to well sorted; 2-5% MRF's, 5% chlorite matrix and quartz grain coating, mostly quartz cement, clay coating of quartz grains contributed to the preservation of porosity.

Midwest Colbentz No. 1
SW SW NE
Sec. 16, T. 6 N. - R. 22 E.

BA-21 (12,049'-12,050'): Sandstone, fine (mean 0.15 - 0.17 mm.), subangular to subrounded (coarser fraction $\pm$ 0.3 mm., subrounded to rounded), moderate to well sorted. Monocrystalline quartz 90%, polycrystalline quartz - trace, chert - trace, bryozoan debris - 5%, pelmatozoan debris - 2%, shell fragments - 2%. Fabric of alternating bands (about 2.0 mm. apart) of coarse and fine sand sized fraction (coarse fraction 0.25 - 0.3 mm., fine fraction 0.125 - 0.15 mm.), fossiliferous. $\emptyset_{bc}$ 15-20%, $\emptyset_{ac}$ 2-5%; calcite cement 75-80%, quartz cement (overgrowths) 20-25%. No clay, well washed sediment, submature.

Midwest Colbentz No. 1
SW SW NE
Sec. 16, T. 6 N. - R. 22 E.

BA-22 (12,068'-12,069'): Sandstone, fine, subangular to subrounded, moderately to well sorted, no clay matrix. Calcite cement 90%, quartz cement 10%; 2-5% bryozoan debris, loosely packed submature. $\emptyset_{bc}$ 25%, $\emptyset_{ac}$ less than 2%.

Midwest Colbentz No. 1
SW SW NE
Sec. 16, T. 6 N. - R. 22 E.

BA-23 (12,080'-12,081'): Sandstone, very fine to fine, angular to subangular, very poorly sorted; laminated, laminations composed of fine, and very fine, to silt sized sand grains, laminations seem disturbed, bioturbated (?); 10-15% detrital chlorite and mica hash matrix; about 5% fossil fragments (0.5 - 1.5 mm.) composed of bryozoan and pelmatozoan debris. Occasional shale lamination, some laminations bioturbated.

Overall, rock is poorly sorted, dirty, increase in amount of mud in this rock as opposed to others in this well that are well washed. Sediment is immature, probably grading downward into shale.

Midwest Sorrels
NE SW NE
Sec. 24, T. 6 N. - R. 20 E.

BA-24 (13,696'-13,697'): Quartz 95%; MRF's 2-5%; clay 3%. Sandstone, very fine to medium, subrounded to rounded, well sorted; 75-80% calcite cement, remainder quartz cement, pressure solution present; trace fossil fragments, ± 2% authigenic chlorite, mature sediment.

Midwest Sorrels
NE SW NE
Sec. 24, T. 6 N. - R. 20 E.

BA-25 (13,697'-13,698'): Sandstone, fine, subangular to subrounded, poorly sorted; quartz grains up to 1.5 mm., clasts of limestone (1.5 - 2.0 mm. and some 22.0 mm. X 5.0 mm.) well washed--absence of detrital fines and clay, near erosion zone of underlying limestone.

BA-27 (13,701'): Wapanucka Limestone.

Midwest Sorrels
NE SW NE
Sec. 24, T. 6 N. - R. 20 E.

BA-28 (13,721'): Wapanucka limestone.

Mobil Parks No. 1
SE SW SW
Sec. 33, T. 6 N. - R. 20 E.

BA-29 (13,104'-13,106'): Sandstone, fine, poorly sorted, subangular to subrounded, immature rock. Monocrystalline quartz 80%; polycrystalline quartz - trace; MRF's 5%; detrital clay 7%; pelmatozoan debris 5%; bryozoan debris - trace, shells and algal fragments - trace. Mostly clay bound, trace quartz and calcite cement.

Midwest White
Sec. 18, T. 6 N. - R. 21 E.

BA-30 (12,689'): Quartz 97% (monocrystalline 98%, polycrystalline 2%); MRF's 2%; detrital clay - trace; zircon - trace. Sandstone, fine, subrounded, well sorted; calcite cement 90-95%; remainder quartz overgrowths; less than 2% clay matrix. Well sorted, mature sediment. Interesting rock because nearly all calcite cement, maybe if all clay is winnowed out will have quartz cement, which is then replaced by calcite.

Shell Jankowsky No. 1-21
350' N of C
Sec. 21, T. 6 N. - R. 20 E.

BA-31 (13,659'): Sandstone, fine to medium, subrounded to rounded, moderately to well sorted, $\emptyset_{bc}$ 20%, $\emptyset_{ac}$ 10%. Quartz 85%; MRF's - trace; CRF's - trace; detrital clay 2-5%; quartz cement 5-10%; calcite cement 2-5%.

Thin coating of clay on most quartz grains has retarded quartz overgrowths.

BA-32 (13,701'): Wapanucka Limestone.

Pan American Reusch Unit No. 1
1320' NSL and 1320' EWL of NW
Sec. 3, T. 5 N. - R. 19 E.

BA-38 (11,491'): Quartz 90-95%; MRF's 2-5%, fossil fragments 5-10%. Sandstone, fine (0.15 to 0.20 mm.), well sorted, subrounded, some detrital and authigenic chlorite pore filling, fossiliferous; calcite cement (less than 5%), rest quartz cement (overgrowths), chlorite rims common; submature to mature sediment, chlorite pore filling seems secondary, i.e., after quartz overgrowths. Fossils: Bryozoan fragments 75%; algal fragments 15%; shells 10%.

Pan American Reusch Unit No. 1
1320' NSL and 1320' EWL of NW
Sec. 3, T. 5 N. - R. 19 E.

BA-39 (11,500'): Quartz: 60%, fossil debris 40%; no detrital clay. Sandstone, fine ($\pm$ 0.2 mm.), poorly sorted, some quartz grains of very coarse (3.0 mm.) sand size, no detrital or authigenic chlorite, very fossiliferous, all calcite cement. Fossil debris: pelmatozoan, bryozoan, and some algal plates.

Pan American Reusch Unit No. 1
1320' NWL and 1320' EWL of NW
Sec. 3, T. 5 N. - R. 19 E.

BA-40 (11,505'): Quartz 85-90%; MRF's 2-5%; chlorite and fine quartz matrix 5-10%. Mostly quartz cement (overgrowths), occasional patches of calcite cement. Laminations 2.0- 3.0 mm. thick with concentration of fines at laminae boundaries. Immature sediment. Summary: rock gets finer downward--probably grades into shale. Clasts of rock type in BA-40 found in BA-30--possible indication of reworking of underlying, older, rock.

Pan American Melone Unit No. 1
NW NW SE
Sec. 31, T. 6 N. - R. 21 E.

BA-41 (12,600'): Sandstone, fine, subrounded, moderately well sorted, mostly quartz cement, but some patches of calcite cement. Monocrystalline quartz 80%; polycrystalline quartz 4%; chert - trace; MRF's 7%; CRF's 3%; detrital clay 5%. Where clay coats grains, quartz overgrowths retarded. Most grains had clay coating before overgrowth, but authigenic quartz surrounded by clay rim in lots of places, explanation(?). At breakover between immature and mature sediment. Here the clay coating is not as effective in preserving porosity as in other samples. $\emptyset_{bc}$ 10%, $\emptyset_{ac}$ $\pm$ 2%.

Pan American Melone Unit No. 1
NW NW SE
Sec. 31, T. 6 N. - R. 21 E.

BA-42 (12,628'): Sandstone, fine to coarse, bimodal size distribution (fine mode 0.15 mm. - 70%, coarse sand mode 30%). Monocrystalline quartz 65-70%; polycrystalline quartz 5%; chert - trace; MRF's occurring in both large and small size modes 10%; CRF's, pelmatozoan debris, algal plates, bryozoan debris in equal porportion 5%; detrital clay 10-15%. Poorly sorted, calcite cement 25%, quartz overgrowths 5-10%, remainder clay matrix binding rock, immature. Much more poorly sorted than samples from higher in section-accounts for increase in gamma ray curve.

Superior Drain No. 1
NW NW SE
Sec. 21, T. 8 N. - R. 20 E.

BA-51 (5,534'-5,535'): Monocrystalline quartz (0.20 - 0.25 mm.) trace, chert (± 0.25 mm.) trace, MRF's (0.25 - 3.0 mm.) 2-5%; CRF's and limestone intraclasts (± 0.20 mm.) trace. Sandstone, fine to medium, well sorted, well washed (no clay), quartz cemented (quartz overgrowths quite extensive). Intraclasts of carbonate mud with quartz grains imbedded in carbonate mud.

Superior Drain No. 1
NW NW SE
Sec. 21, T. 8 N. - R. 20 E.

BA-52 (5,541'-5,542'): Sandstone (same as BA-51), except 2% altered feldspar; 8% MRF's, no CRF's. If anything rock better sorted and cleaner than BA-51; also, perhaps slightly finer grained (± 0.2 - 0.25 mm.). Both BA-51 and BA-52 mature rocks.

Superior Drain No. 1
NW NW SE
Sec. 21, T. 8 N. - R. 20 E.

BA-53 (5,548'-5.549'): Quartz 60-65%; fossil fragments (mostly algal fragments 0.5 - 4.0 mm.), subequal minor proportions of pelmatozoan (± 1.0 mm.) and bryozoan debris (0.3 - 2.0 mm.) 30-35%; calcite cemented sandstone fragments and matrix: 2-5%. (Sandstone clasts: clasts of very fine to fine grained sandstone, subangular to subrounded, fairly well sorted, calcite cemented.)

Sandstone, coarse to silt sized (0.05 - 1.00 mm.), very poorly sorted, angular to very well rounded (larger quartz grains very well rounded, others subangular to angular), 10-15% calcite cement, remainder quartz cement.

Superior Drain No. 1
NW NW SE
Sec. 21, T. 8 N. - R. 20 E.

BA-54 (5,555'-5,556'): Quartz 90-95%; MRF's 5%; detrital clay 2-5%.
Sandstone, fine (0.2 mm.), well sorted subrounded; mostly quartz cemented, minor calcite cement. Well sorted, mature rock, finer than BA-51 or BA-52.

Superior Drain No. 1
NW NW SE
Sec. 21, T. 8 N. - R. 20 E.

BA-55 (5,562'-5,563'): Quartz 60%, fossil fragments 40% (bryozoan debris (0.3 - 3.0 mm.) 15%; pelmatozoan debris (0.7 - 2.0 mm.) 10%; algal debris (± 0.3 mm.) 10%; shell fragments (2.0 - 4.0 X 0.25 mm. - 5%).
Sandstone, very fine to coarse, angular to rounded very poorly sorted, immature, very fossiliferous--almost a limestone; calcite cemented, no quartz cement.

Superior Drain No. 1
NW NW SE
Sec. 21, T. 8 N. - R. 20 E.

BA-56 (5,564'-5,565'): Quartz 90-95%; fossil fragments 5-10%.
Sandstone, fine (0.175 - 2.0 mm.), moderately to poorly sorted, fossil fragments--bryozoan debris (0.5 - 0.75 mm.); mostly calcite cemented, minor quartz overgrowths.

Superior Drain No. 1 summary: quite a marked difference between BA-51 and BA-52, BA-53, BA-54, BA-55 and BA-56; the former thin sections are from a quite mature rock, the latter four thin sections are very immature and fossil bearing rock.

Pan American Cochran Unit No. 1
200' N of C SW NE
Sec. 32, T. 8 N. - R. 24 E.

BA-59 (10,770'-10,790', cuttings): Quartz 95-98%, MRF's (chloritized) 2-5%; bryozoan fragments - trace. Sandstone, fine, subangular to subrounded, moderately to well sorted; trace calcite cement, mostly quartz cement (overgrowths).

Continental Ferguson No. 1
SW SE NE
Sec. 33, T. 8 N. - R. 20 E.

BA-67 (5,570'-5,575'): Quartz: 75-80%; MRF's (mostly phyllite); 5-10%; matrix 15-20% (90% quartz and mica hash of fine silt to clay size, 10% detrital chlorite). Sandstone, fine to medium (30% quartz grains 0.25 - 0.3 mm., 70% quartz grains 0.15 mm. or less; 2% polycrystalline quartz, 1% chert, remainder of quartz, monocrystalline), subangular to subround, poorly sorted. Rock is mostly quartz cemented (about 5% of cementing material is calcite), original porosity nearly obliterated.

Continental Ferguson No. 1
SW SE NE
Sec. 33, T. 8 N. - R. 20 E.

BA-68 (5,575'-5,580'): Rock description: sandstone, fine, subangular to subrounded, well sorted, quartz cemented.
Mineralogy of grains: 90% monocrystalline quartz; 2-5% MRF's (schist and phyllite); minor altered feldspar; minor polycrystalline quartz.

Continental Ferguson No. 1
SW SE NE
Sec. 33, T. 8 N. - R. 20 E.

BA-69 (5,593'-5,596'): Grains: 96% monocrystalline quartz 0.25 mm.; 1% polycrystalline quartz 0.15 - 2.0 mm,; 1-2% MRF's 0.2 mm.; trace altered feldspar. Sandstone, fine to medium subrounded, well sorted, quartz cemented (less than 5% porosity).

Continental Ferguson No. 1 summary: better sorted, cleaner sand at base of section; fines increase upwards; with increase of fine matrix, have less quartz overgrowths.

Ambassador Davenport No. 1
NE SW NE
Sec. 33, T. 8 N. - R. 20 E.

BA-70 (5,535'-5,540'): Sandstone, fine, subangular, fair to poorly sorted. Sorting not bad in this rock, maybe some authigenic chlorite pore filling, possibly reworked sandstone aggregates. Grains (80%): monocrystalline quartz (0.2 mm.) 97%; polycrystalline quartz (0.15 mm.) trace; MRF's (0.2 mm.) trace; matrix (fine quartz and mica hash) 5%; cement (all quartz where not bound by chlorite clay matrix) 15%.

Sorting not bad in this section, however, enough chlorite matrix to retard quartz overgrowths in places; possibly some reworked sandstone aggregates.

Ambassador Davenport No. 1
NE SW NE
Sec. 33, T. 8 N. - R. 20 E.

BA-71 (5,540'-5,545'): Grains: quartz 80%; matrix: silt and clay sized quartz and chlorite 15%; cement: calcite 2-5%, quartz 1-5%. Monocrystalline quartz (0.25 - 0.35 mm.) 98%; polycrystalline quartz (0.2 mm.) - trace; MRF's (0.20 - 0.25 mm.) - trace; matrix (silt and clay sized chlorite and quartz).

Summary: minor percentage of authigenic chlorite (2-5%), the pore filling is fine matrix, quartz overgrowths fairly common.

Ambassador Davenport No. 1
NE SW NE
Sec. 33, T. 8 N. - R. 20 E.

BA-72 (5,560'-5,565'): Sandstone, fine, subrounded, well sorted, quartz cemented; some MRF's altered to chlorite. Grains: 75% (monocrystalline) quartz 96%; polycrystalline quartz 1-2%; MRF's 2-3%; matrix 5%; cement 20%.

Ambassador Davenport No. 1
NE SW NE
Sec. 33, T. 8 N. - R. 20 E.

BA-73 (5,570'-5,575'): Sandstone, very fine to coarse, subrounded, fair sorting, bimodal distribution of quartz; approximately 33.0% is medium to coarse, 67.0% is very fine to fine. Grains: 75% (monocrystalline quartz 95%; polycrystalline 2-5%; MRF's - trace); matrix 10% (silt and clay sized quartz and mica hash); cement 15% (quartz 98% calcite - trace). MRF's squashed, mostly chlorite. Quartz overgrowths common where matrix not present, most chlorite seems to be detrital.

Ambassador Davenport No. 1 summary: overall, not much difference between BA-71, BA-72 and BA-73; BA-70 is quite different--possibly represents a zone of reworking. More matrix in BA-72--because getting near the base of the sand (?).

Mobil McAlester
C SW NE
Sec. 16, T. 10 N. - R. 20 E.

BA-75 (2,476'): Sandstone, fine, poorly sorted, angular to very well rounded, fossiliferous. Grains: 80-85%; monocrystalline quartz (0.035 - 1.5 mm.) 75-80%; polycrystalline quartz (0.2 - 0.3 mm.) 2%; MRF's (0.2 - 0.3 mm.) 2%; fossil fragments (algal debris 75%; pelmatozoan debris 70%; bryozoan debris 5%); matrix 10-15% (silt to clay sized quartz and mica hash--some chlorite authigenic, mostly detrital); cement less than 5% (less than 5% calcite cement, no quartz cement or overgrowths).

Quite immature rock, could represent eroded and reworked top of Wapanucka limestone--may be what is referred to as Spiro "B" to the south in T. 8 N. - R. 24 E. and T. 8 N. - R. 25 E.; this is definitely a sandstone, and probably not a facies of the Wapanucka, but an eroded zone.

Shell Jankowsky No. 1
570' FWL and 690' FWL of NE/4
Sec. 28, T. 7 N. - R. 20 E.

BA-90 (9,438'): Sandstone, fine (0.20 - 0.25 mm.), subrounded to rounded, well sorted, mature. Extensive quartz overgrowths, abundant chlorite coatings (50% detrital chlorite, 50% authigenic chlorite) on grains causing some porosity to be preserved. 95-98% monocrystalline quartz, trace polycrystalline quartz, trace chert, trace chloritized MRF's. Laminations of fine grained, iron strained chlorite, and mica fines.

Shell Jankowsky No. 1
570' FSL and 690' FWL of NE/4
Sec. 28, T. 7 N. - R. 20 E.

BA-91 (9,460'): Sandstone same as in BA-90; cleaner, more mature, extensive quartz overgrowths, trace calcite cement.

Shell Jankowsky No. 1
570' FSL and 690' FWL of NE/4
Sec. 28, T. 7 N. - R. 20 E.

BA-92 (9,478'): Sandstone, fine (0.15 - 0.20 mm.), subrounded, fair to well sorted (fair sorting in streaks, well sorted in others), mostly quartz cemented; about 5% MRF's (chlorite), up to 10% matrix (silt and clay sized chlorite and quartz fines). Some authigenic chlorite preserving pore space. Rock seems more poorly sorted and less mature than BA-90 or BA-91, increase in fines explains depression of S.P. curve. Laminations of iron stained chlorite and quartz fines; in this section chlorite rims appear to be after quartz overgrowths (?).

Shell Jankowsky No. 1
570' FSL and 690' FWL of NE/4
Sec. 28, T. 7 N. - R. 20 E.

BA-93 (9,487'): Sandstone, very fine to coarse, very poorly sorted, bimodal grain size distribution (larger mode of coarse sand sized grains (0.5 - 0.6 mm.) approximately 30%, smaller mode of very fine to silt sized grains, approximately 70%), martix of quartz and chlorite, and mica hash; immature sediment, large grained mode subrounded, small grained mode angular to subangular; approximately 5-10% matrix, 5% calcite cement, 5% authigenic chlorite, less than 5% MRF's, minor quartz overgrowths.

Shell Jankowsky No. 1
570' FSL and 690' FWL of NE/4
Sec. 28, T. 7 N. - R. 20 E.

BA-94 (9,491'): Sandstone, bimodal size distribution (75% coarse - 25% fine), coarse fraction medium (0.4 - 0.6 mm.), finer fraction very fine to silt sized (0.05 - 0.10 mm.); less than 2% matrix of quartz fines and chlorite and mica hash; mostly calcite cement, some quartz overgrowths, about 5% authigenic chlorite.

Shell Jankowsky summary: BA-94 a little better sorted than BA-93; BA-93 has more percentage of fines or matrix, also BA-93 more stongly bimodal; BA-92 similar to BA-90 and BA-91, but more fine grained and a greater percentage of fines present. Both BA-91 and BA-90 very mature rocks, more so than the other three (BA-92, BA-93 and BA-94). Perhaps this is like a texture in marine sand bodies should be, i.e., more poorly sorted near the base and becoming cleaner and coarser toward the top.

APPENDIX C

CROMWELL THIN SECTION DESCRIPTIONS

Warren B-1
Sec. 2, T. 7 N. - R. 20 E.

(7,310' - 7,320;): Sandstone, very fine to fine, subangular to subrounded, moderately well sorted. Grains: 75% (monocrystalline quartz 98%; polycrystalline quartz - trace; chert - trace; bryozoan fragments - trace); matrix 5% (detrital clay); cement 20% (quartz cement 79%; calcite cement 25%; trace dolomite (?) cement). Thin section from top of Cromwell I sand.

Warren B-1
Location - same as before

(7,380' - 7,390'): Sandstone, very fine, subangular, moderately sorted quartz cemented. Fine grained rock causes depressed S.P. curve.

Warren B-1
Location - same as before

(7,430' - 7,440'): Sandstone, very fine to silt sized, poorly sorted, subangular, quartz cemented. Grains (85% (monocrystalline quartz 73%; polycrystalline quartz - trace; chert - trace; CRF's 10%; matrix 5% (detrital clay); cement 10% (all quartz). Fine grained rock and detrital clay cause depressed S.P. curve.

Krisher
Sec. 25, T. 8 N. - R. 22 E.

(5,802' - 5,830'): Quartz 95%; mica hash and MRF's 2-5%; detrital clay 2-5%. Sandstone, very fine, subangular, moderately sorted, quartz and calcite cement (50/50).

Krisher
Sec. 25, T. 8 N. - R. 22 E.

(5,890' - 5,900'): Quartz 80%; mica hash and MRF's 5%; detrital clay 15%. Siltstone to very fine sand, subangular, poorly sorted, quartz cement and clay cemented. This rock more fine grained than that of 5,820'-5,830'.

Krisher
Location - same as before

(5,930' - 5,940'): Quartz 85-90%; detrital clay 2-5%; MRF's 2-5%; fossil fragments and CRF's 2-5%. Sandstone, very fine, moderately to poorly sorted, subangular, clay bound, calcite and quartz cemented. From electric log: interbeds of sandstone and shale in zone between second and third Cromwell sands.

Krisher
Location - same as before

(6,000' - 6,010'): Quartz 75%; fossil fragments and CRF's 10-15%; detrital clay and MRF's 5-10%. Sandstone, very fine to silt sized, poorly sorted; abundant fossil as get nearer to top of Mississippian unconformity.

Abbie
Sec. 31, T. 9 N. - R. 20 E.

(4,410' - 4,415'): Quartz 75-80%; fossil fragments 10-15%; bryozoan 90%; algal 10%; detrital clay 2-5%. Sandstone, fine, subangular to subround, moderately to poorly sorted, clay bound and calcite cemented.

Abbie
Location - same as before

(4,470' - 4,475'): Quartz 80-90%; fossil fragments 10-15%; detrital clay 2-5%. Sandstone, fine, subangular to subround, moderately to poorly sorted, some clay binding--mostly calcite cemented. Rock similar to that of (4,410' - 4,415;), but less percentage of detrital clay. Sample from upper Chester (?).

Helm
Sec. 20, T. 11 N. - R. 25 E.

(3,045' - 3,050'): Carbonate rock, wackestone. Grains are fragments of bryozoans and pelmatozoans, with some algal plates; recrystallized lime mud matrix between grains.

Helm
Location - same as before

(3,050' - 3,060'): Sandstone, fine, subangular to subrounded, well sorted, calcite (with trace of dolomite) cemented. Up to 10% bryozoan fragments, also fragments of carbonate rock, same as 3,045' - 3,050'.

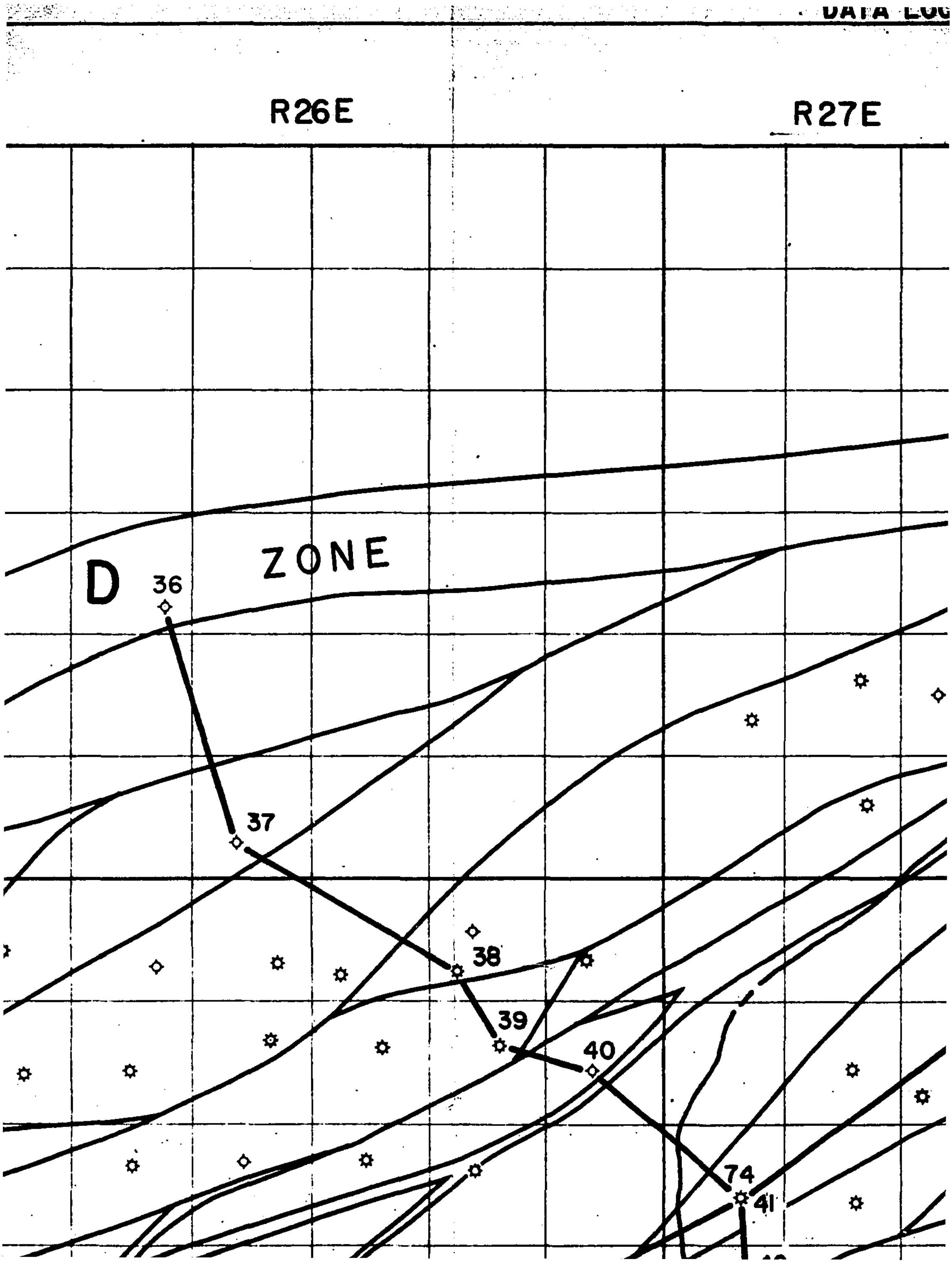

DATA LOG
R26E
R27E
ZONE
D
36
37
38
39
40
74
41

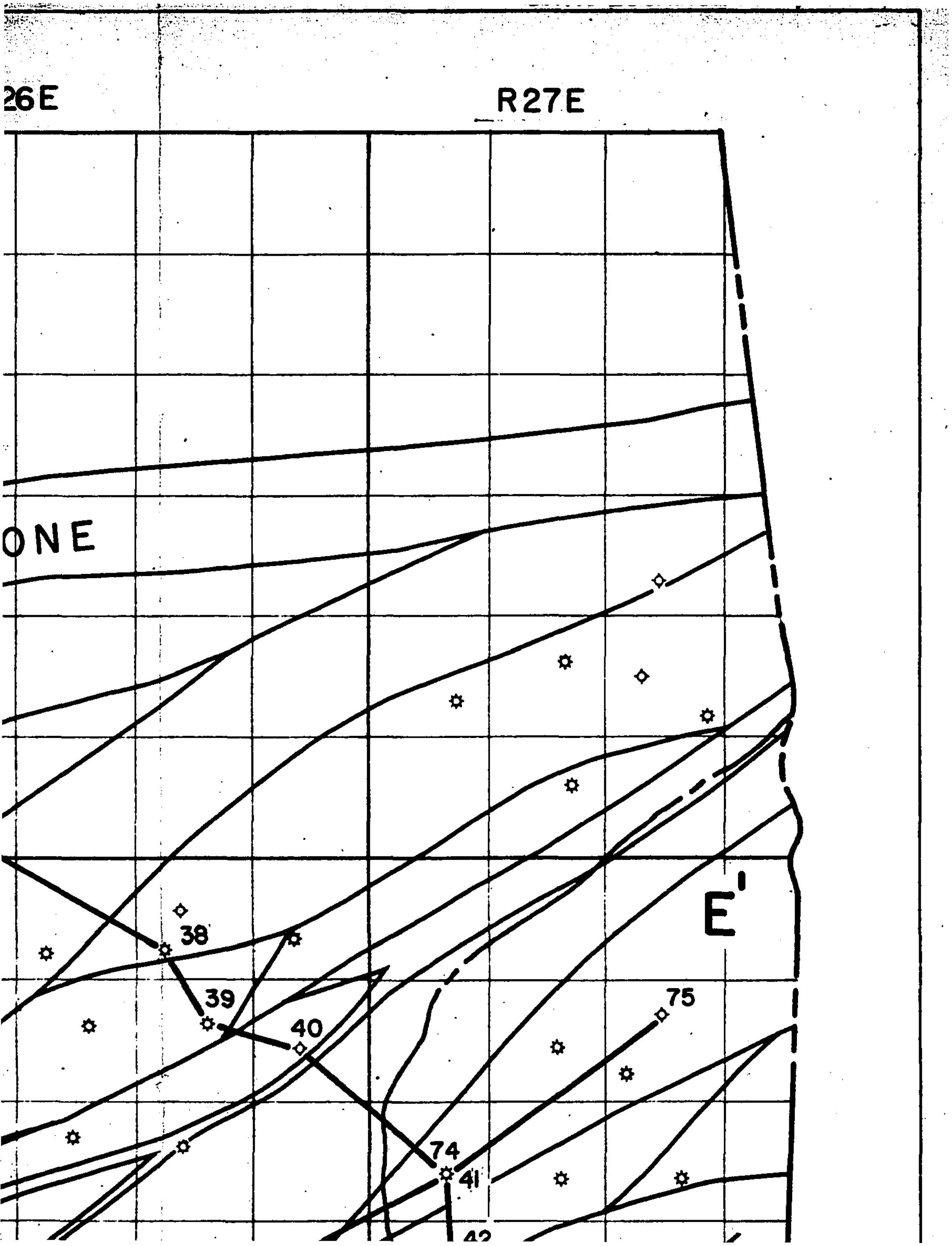

26E
R27E
ONE
E'
38
39
40
75
74
41
42

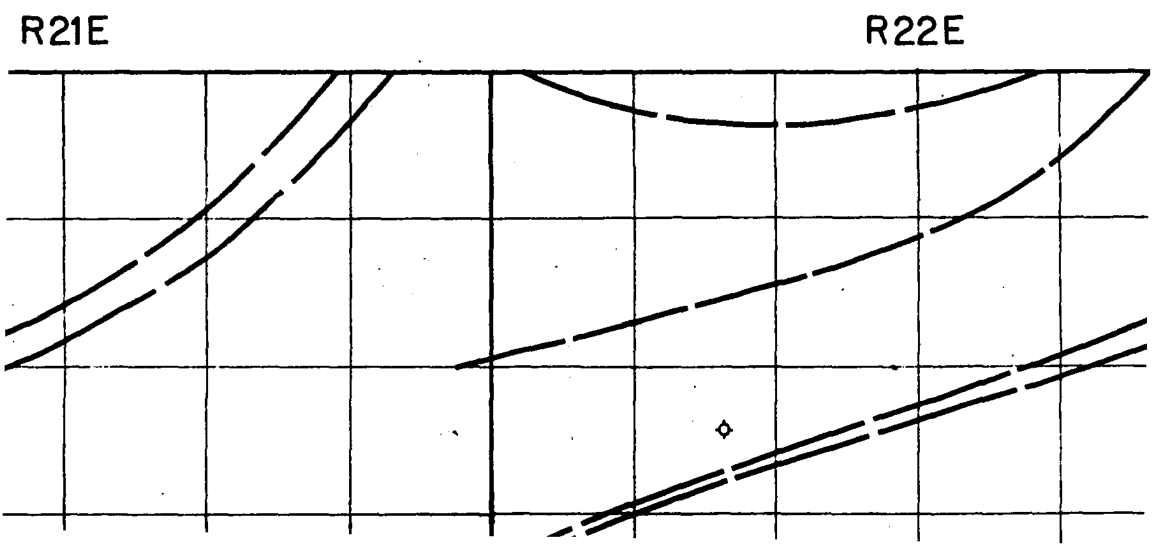
R21E
R22E

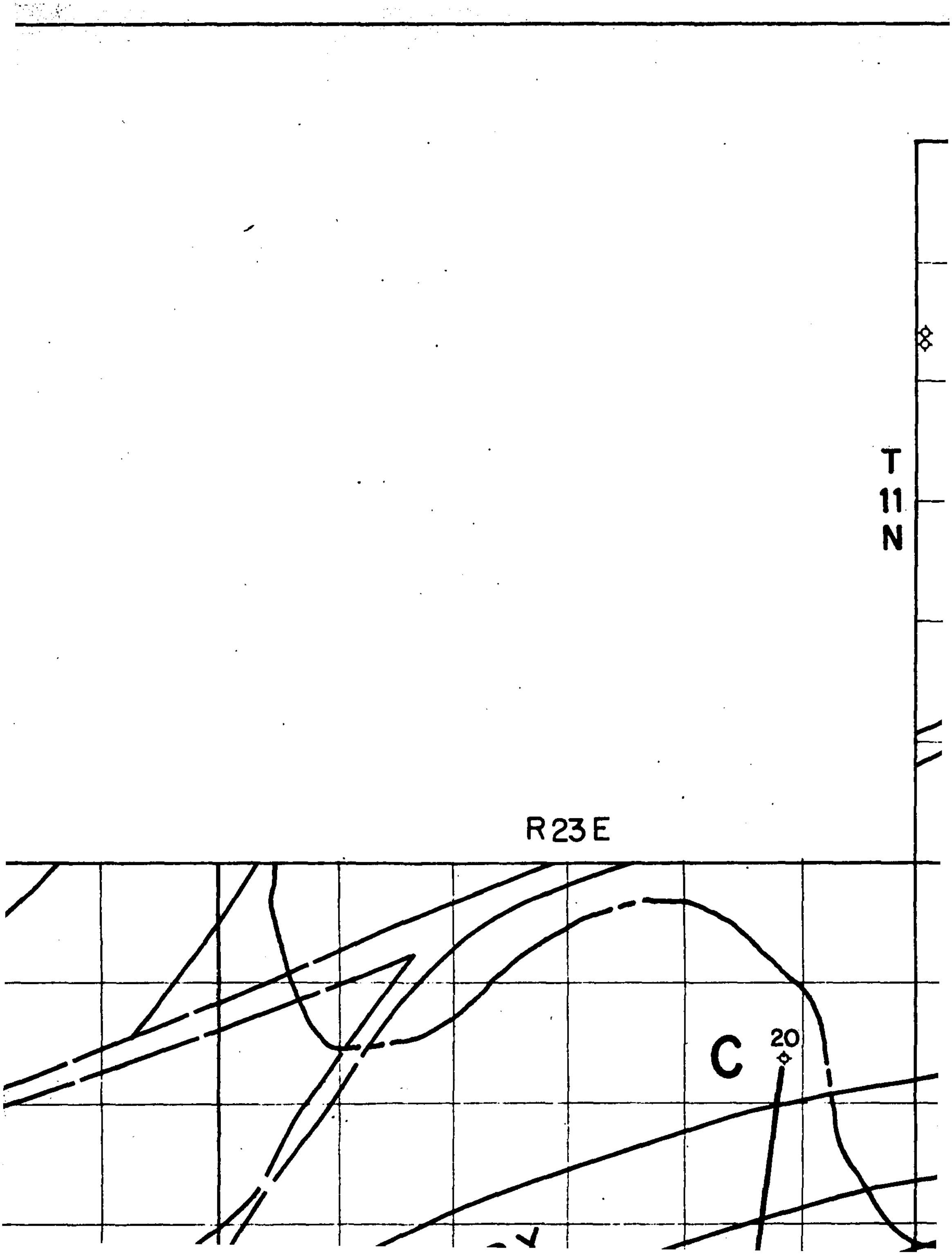
T
11
N
R23E
C
20

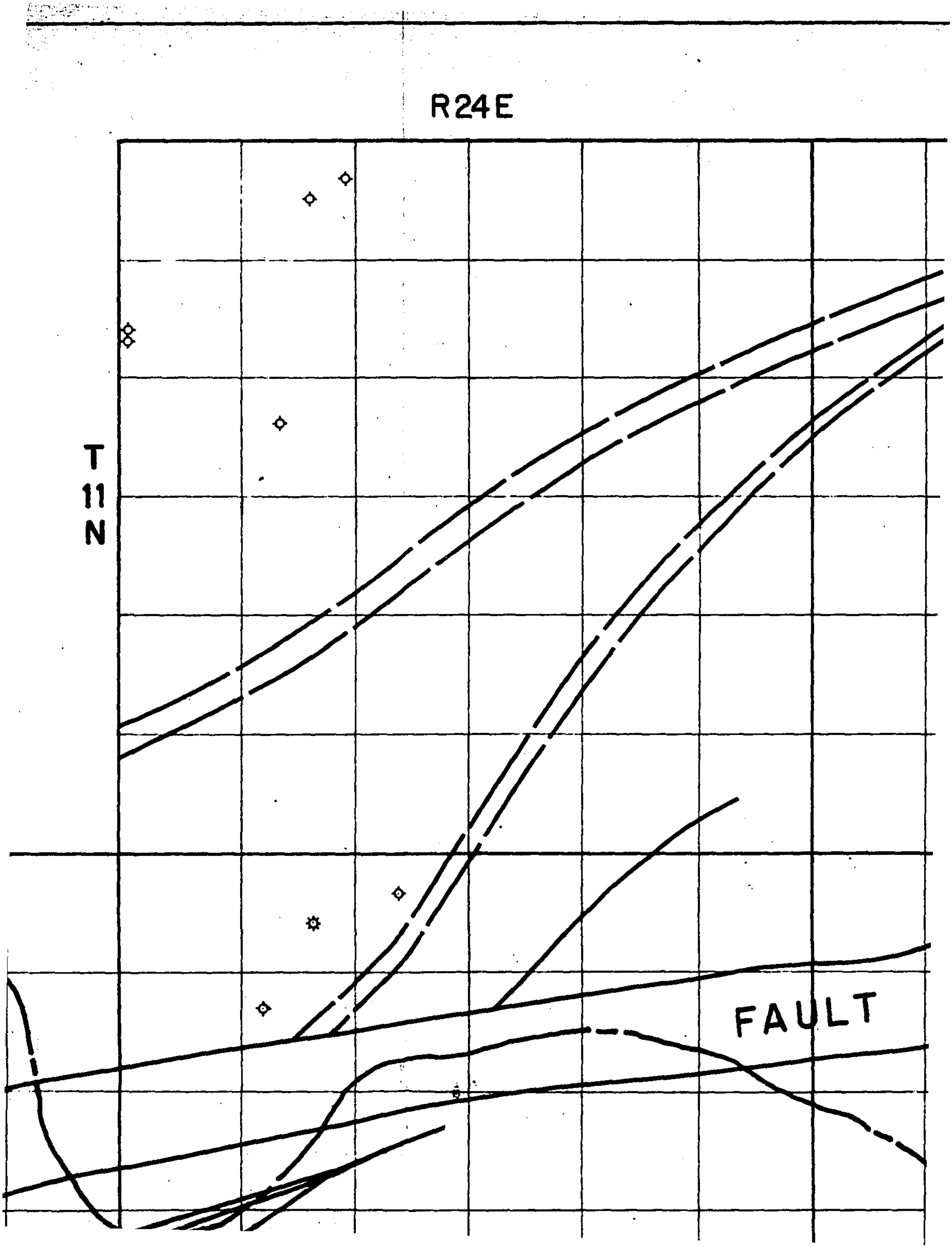
R24E
T
11
N
FAULT

R25E
HELM
D
36
3

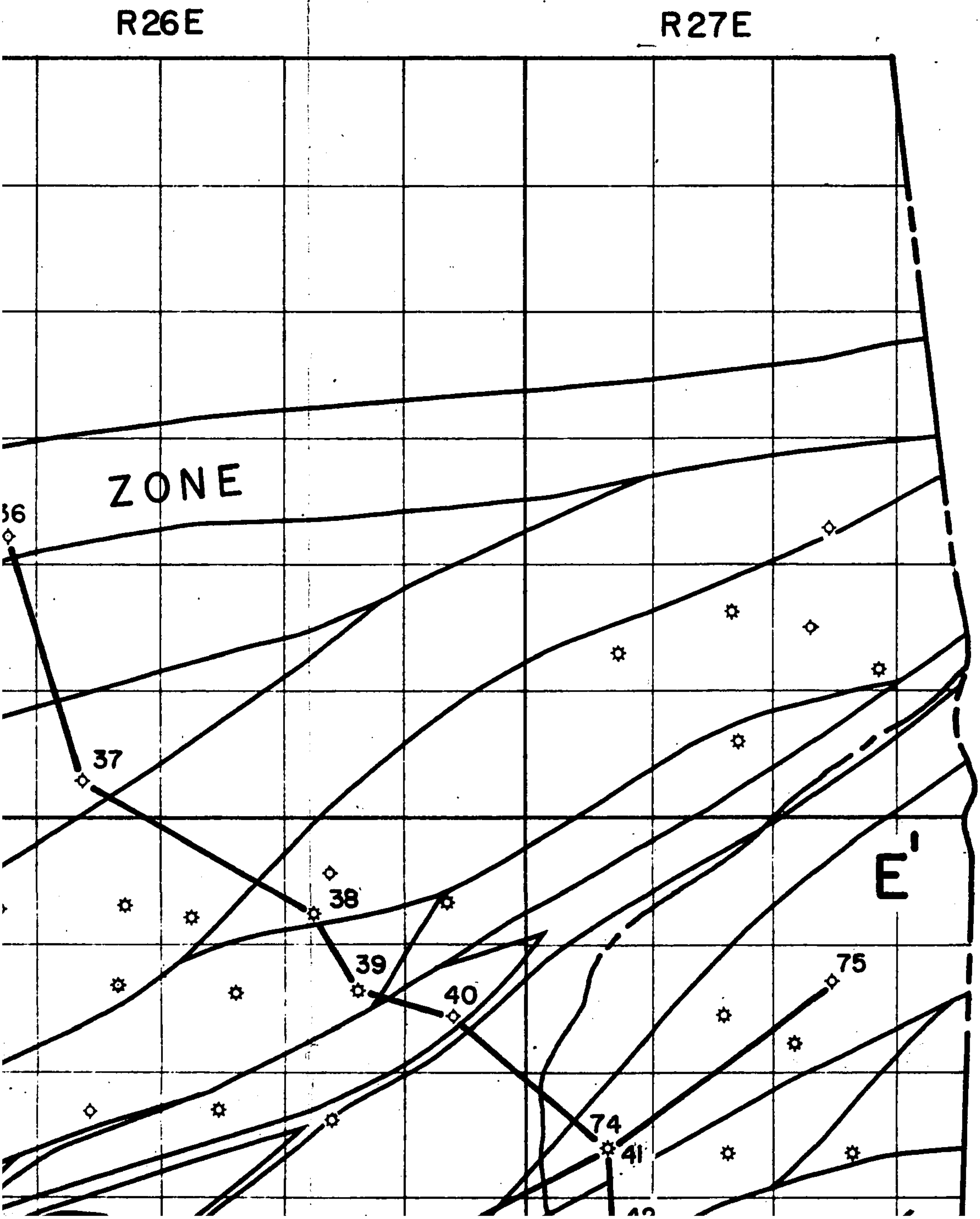
R26E
R27E
ZONE
36
37
38
39
40
74
41
75
E'

DATA LOCATION MAP, Plate I

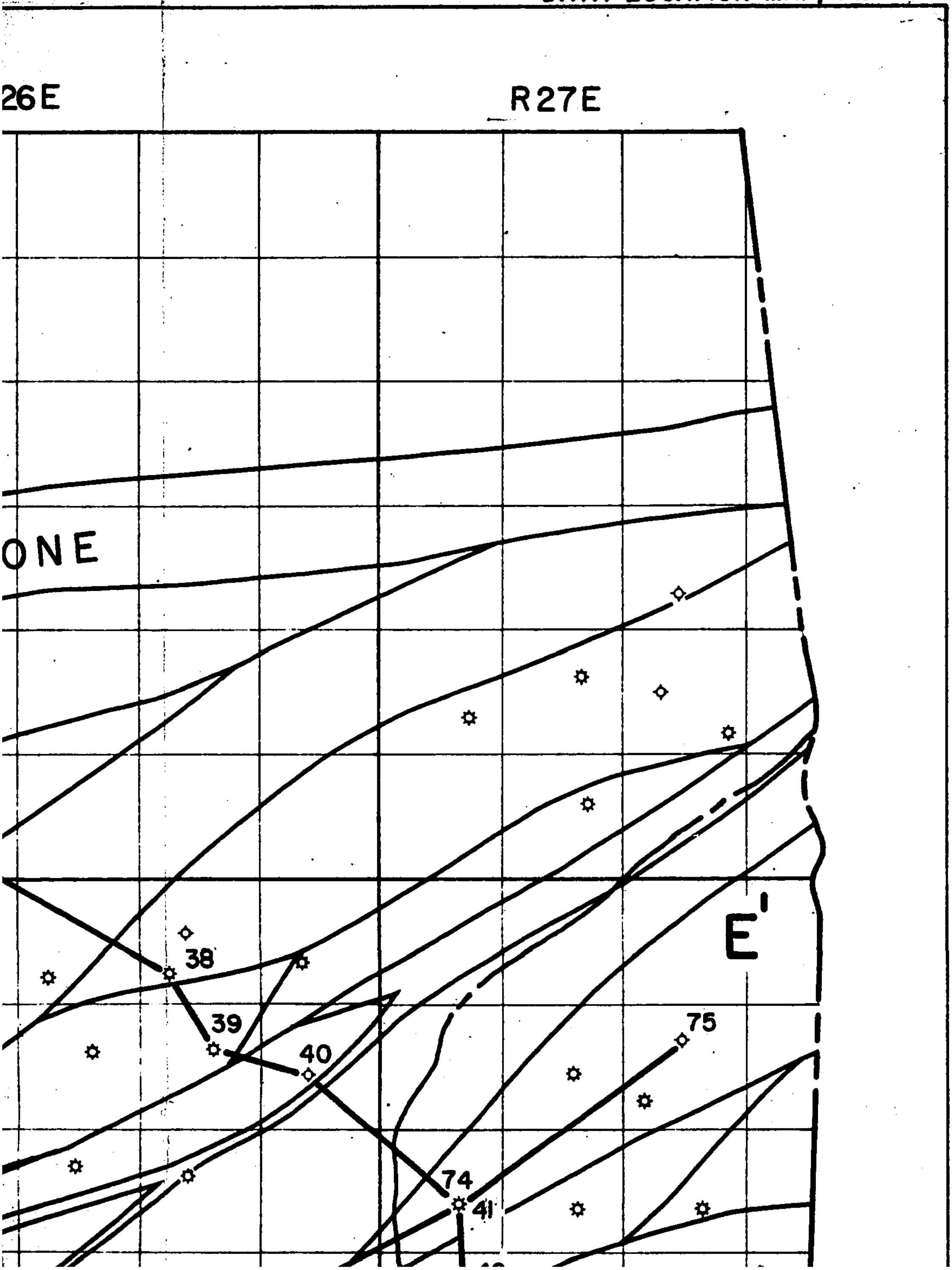

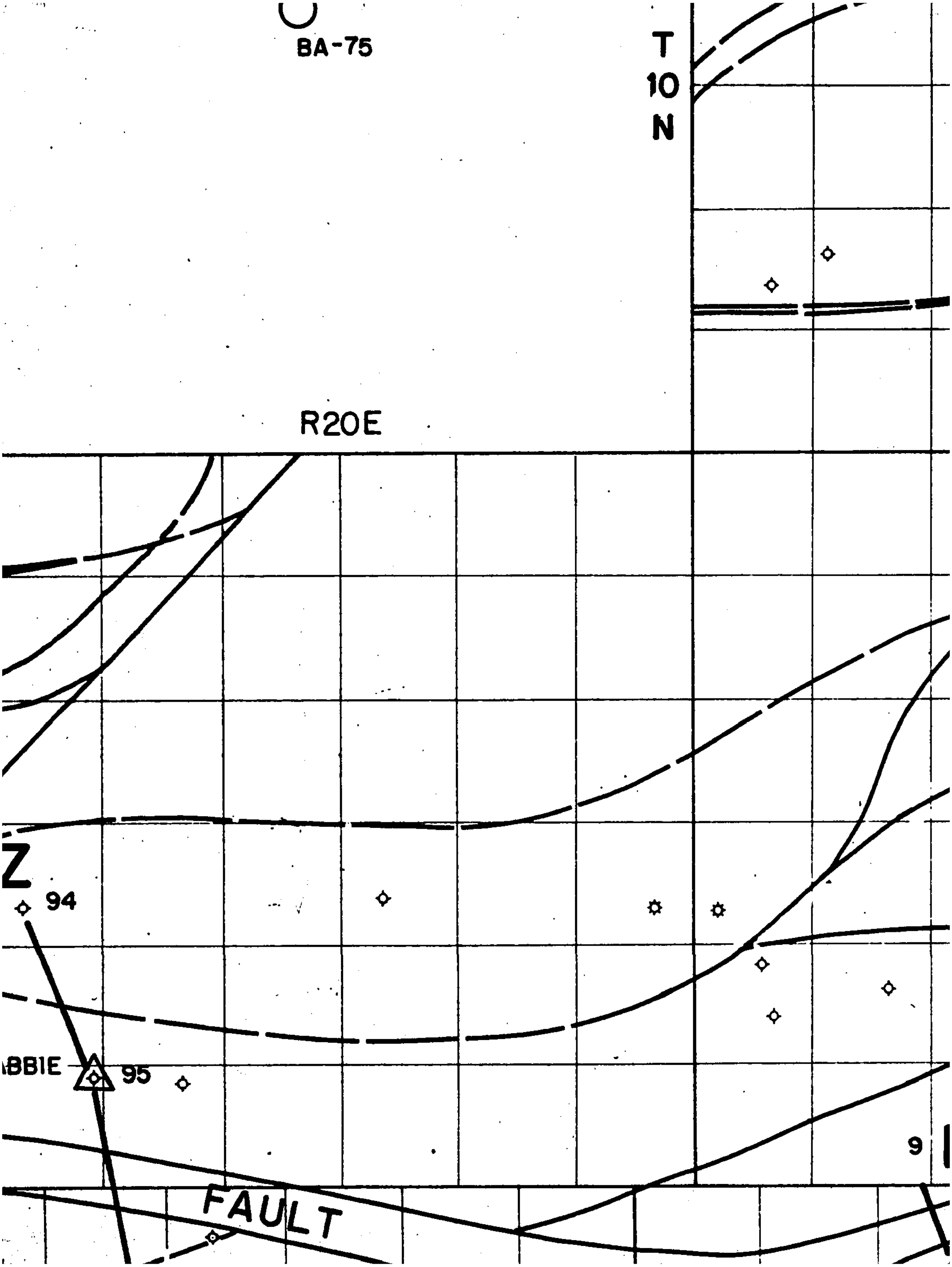
BA-75
T
10
N
R20E
Z
94
ABBIE
95
9
FAULT

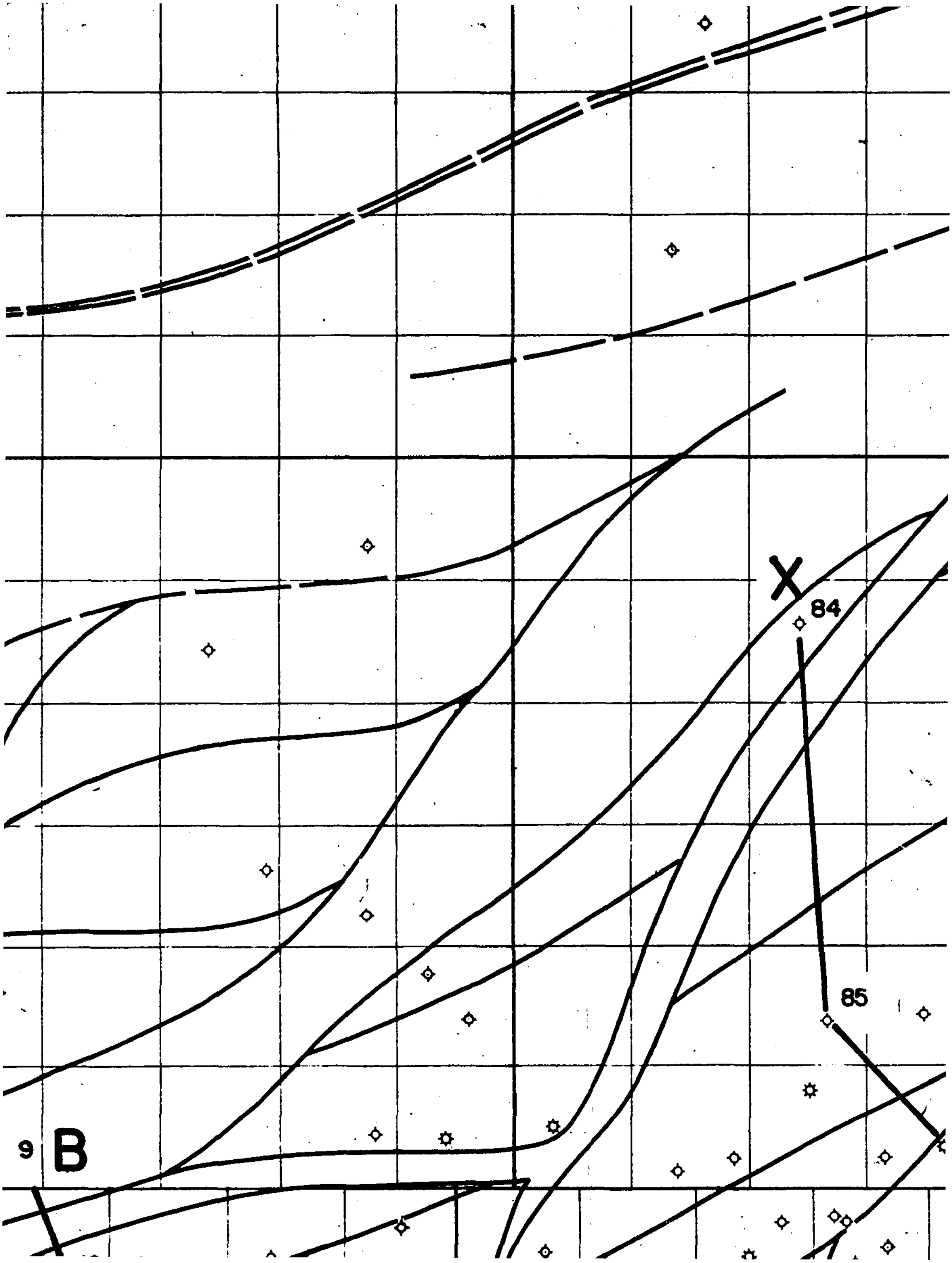
X
84
85
9
B

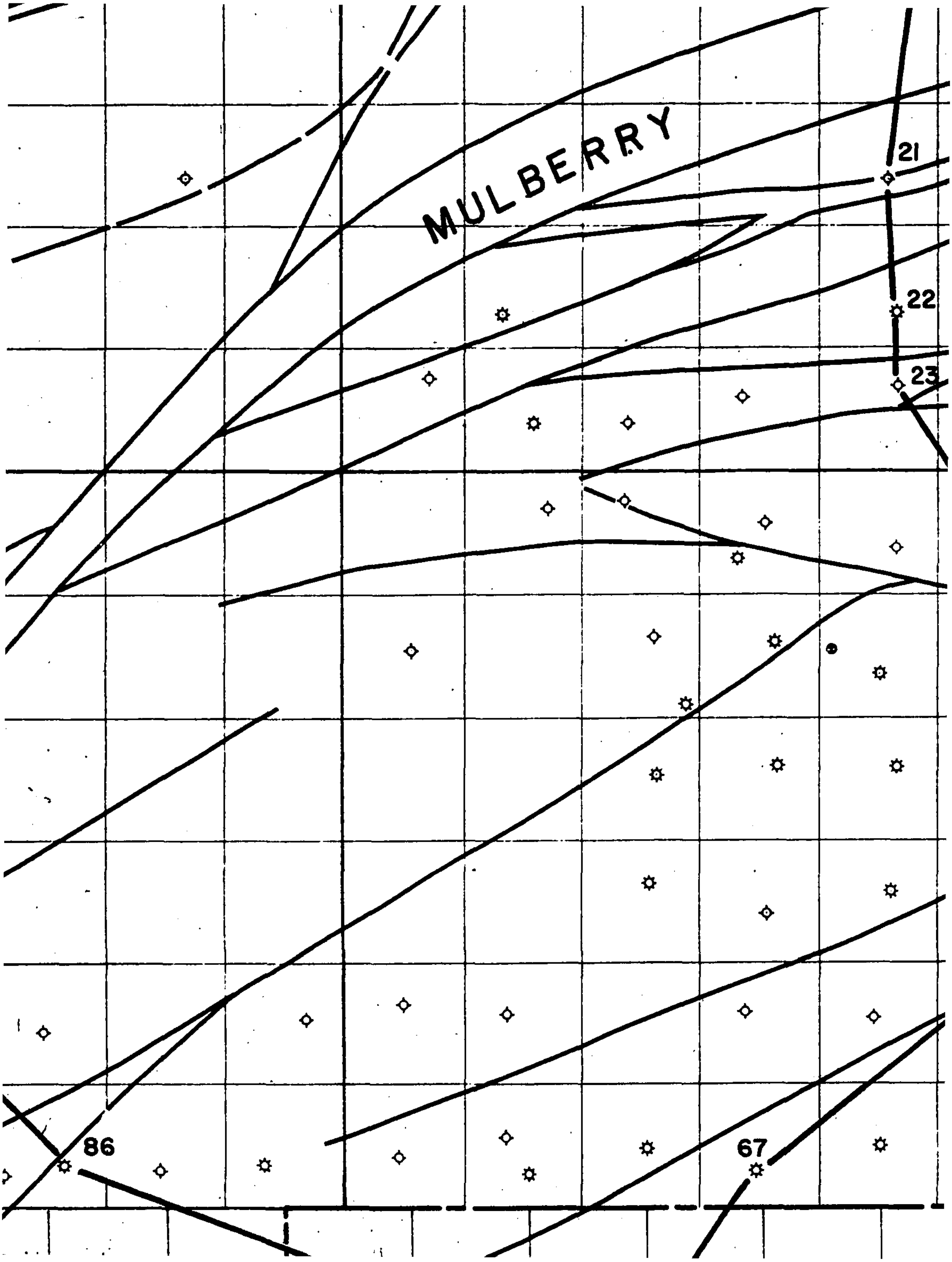
MULBERRY
21
22
23
86
67

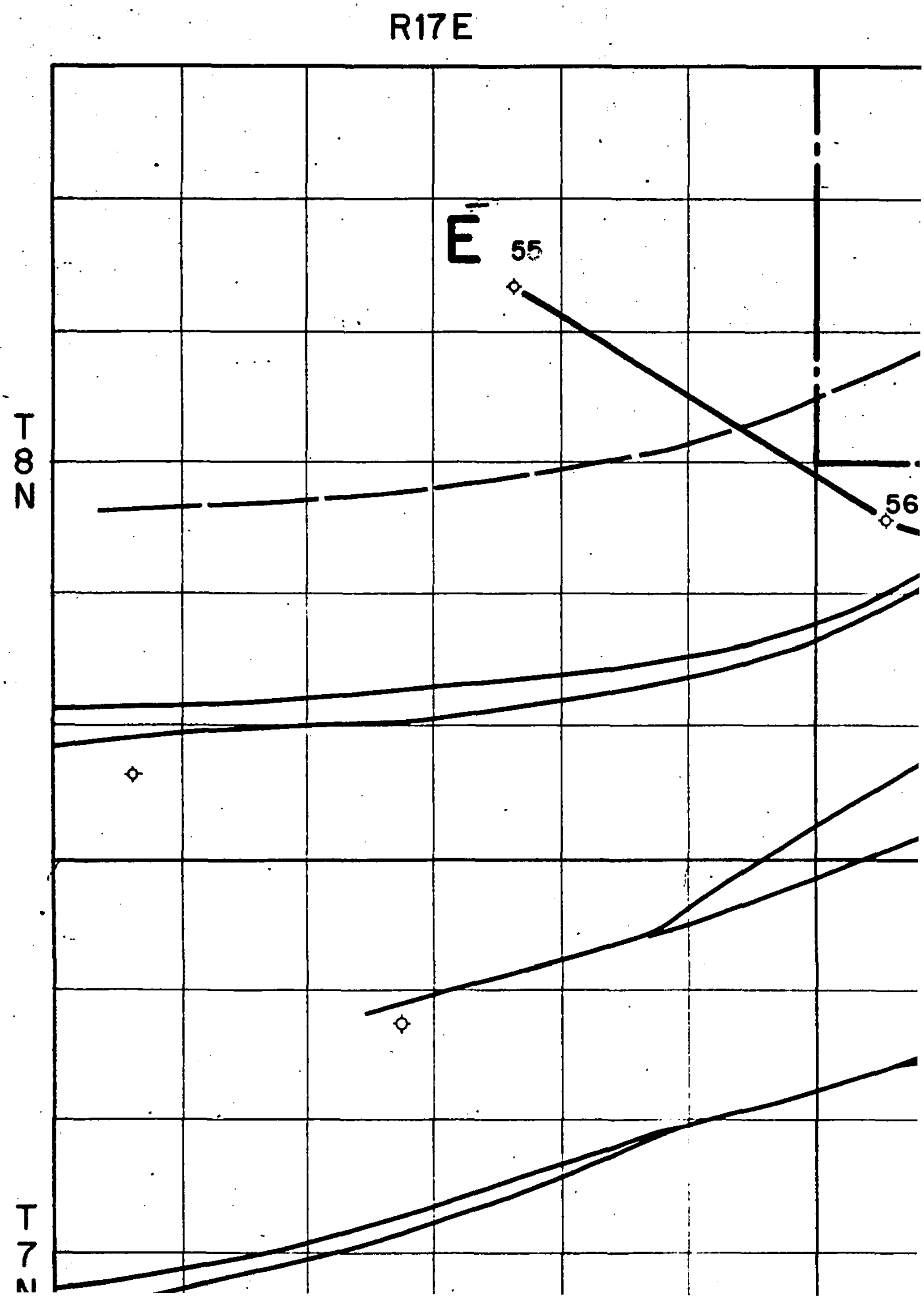

R17E
E
55
56
T 8 N
T 7 N

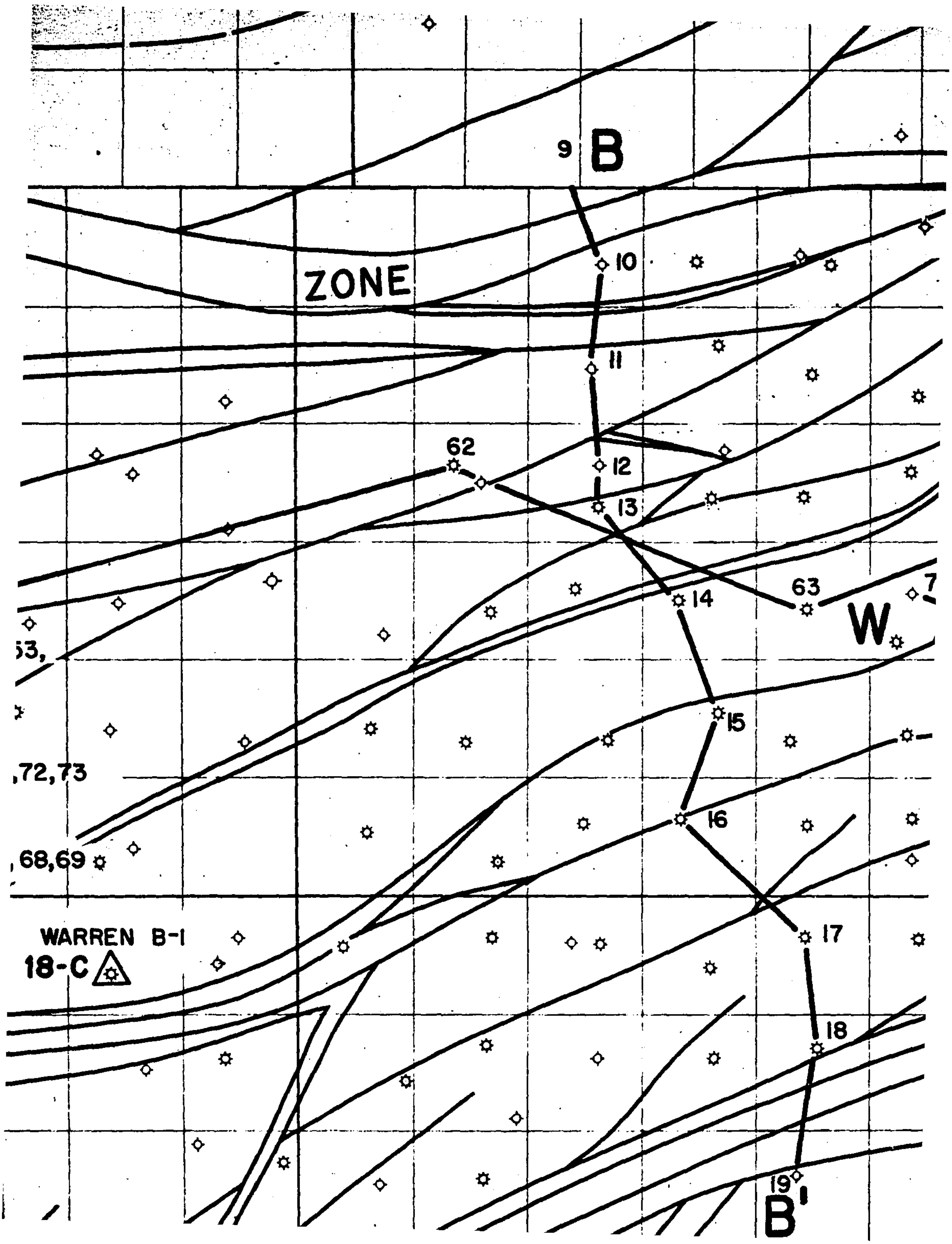

9 B
ZONE
10
11
62
12
13
14
63
W
53,
15
,72,73
16
,68,69
17
WARREN B-1
18-C
18
19
B'

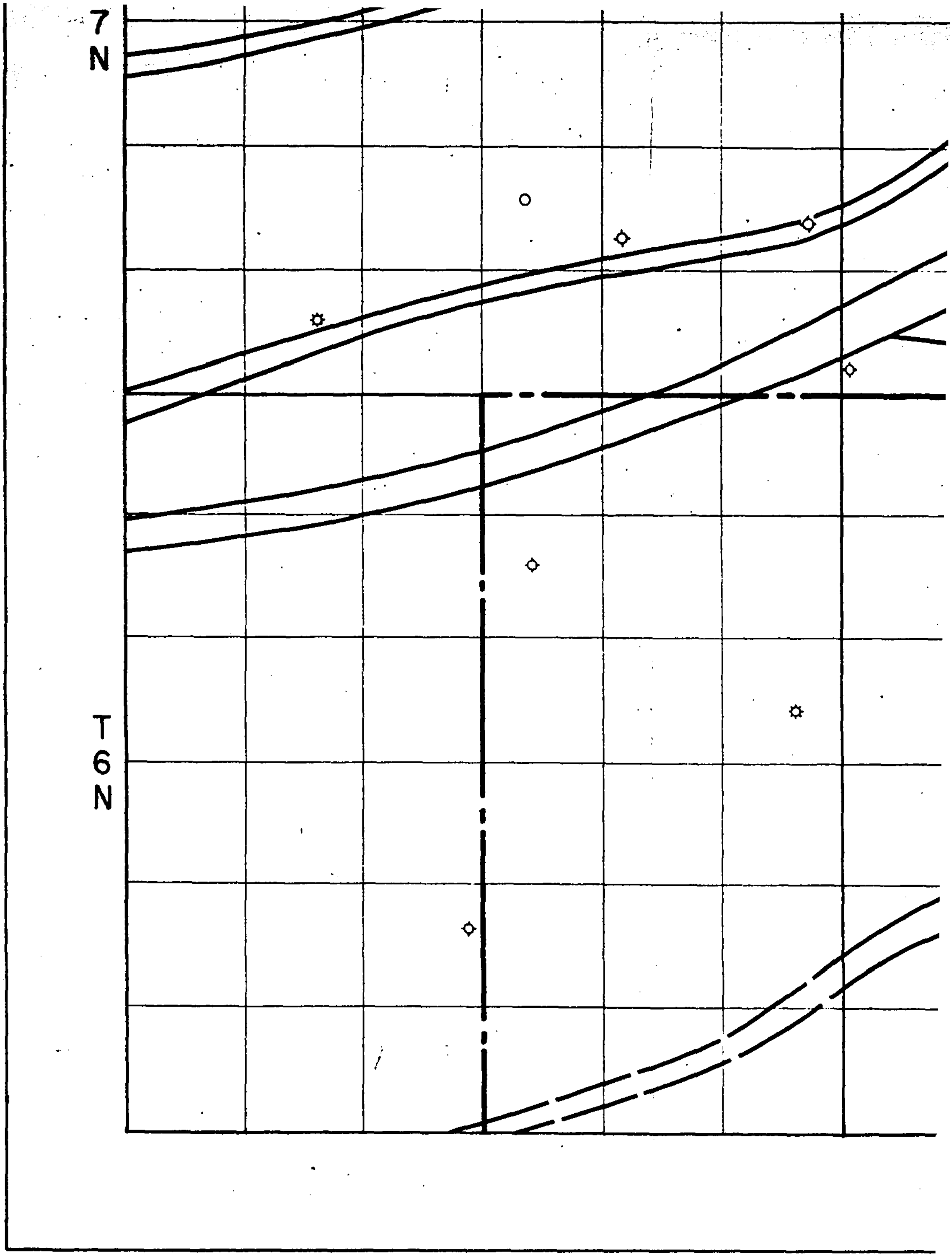
7
N
T
6
N

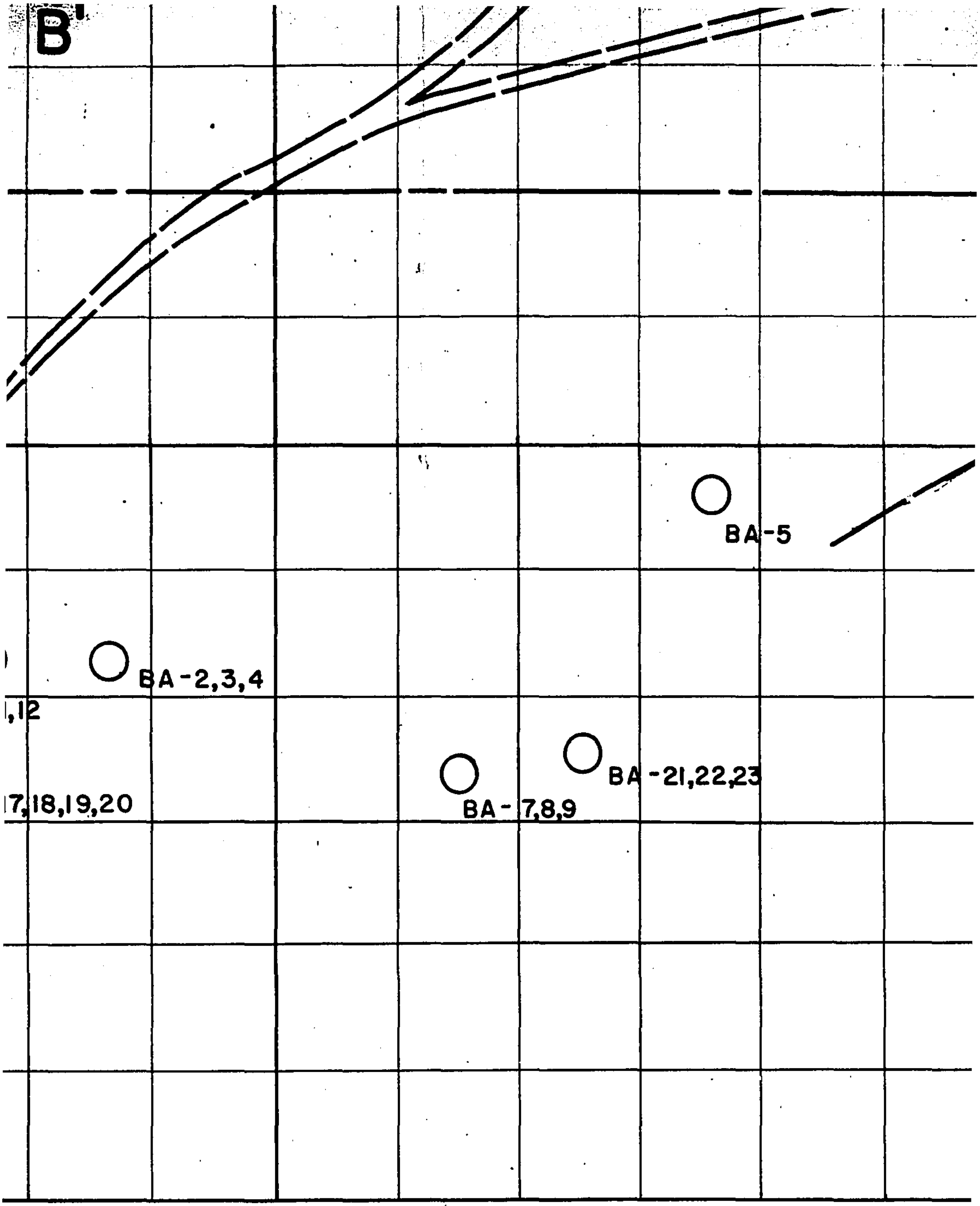
B'
BA-5
BA-2,3,4
,12
BA-21,22,23
17,18,19,20
BA-7,8,9

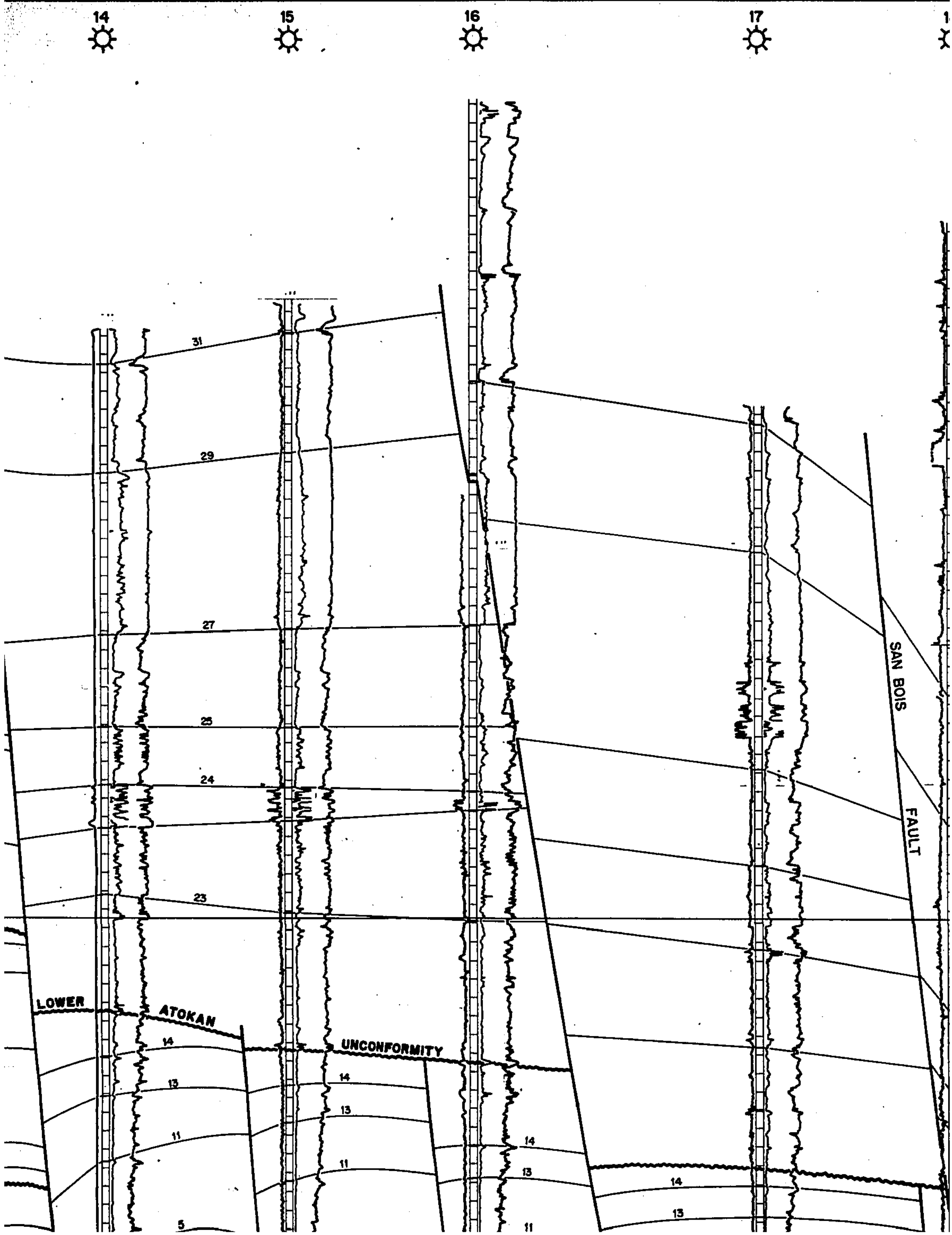
14
15
16
17
31
29
27
25
24
23
LOWER ATOKAN UNCONFORMITY
14
13
11
5
SAN BOIS FAULT

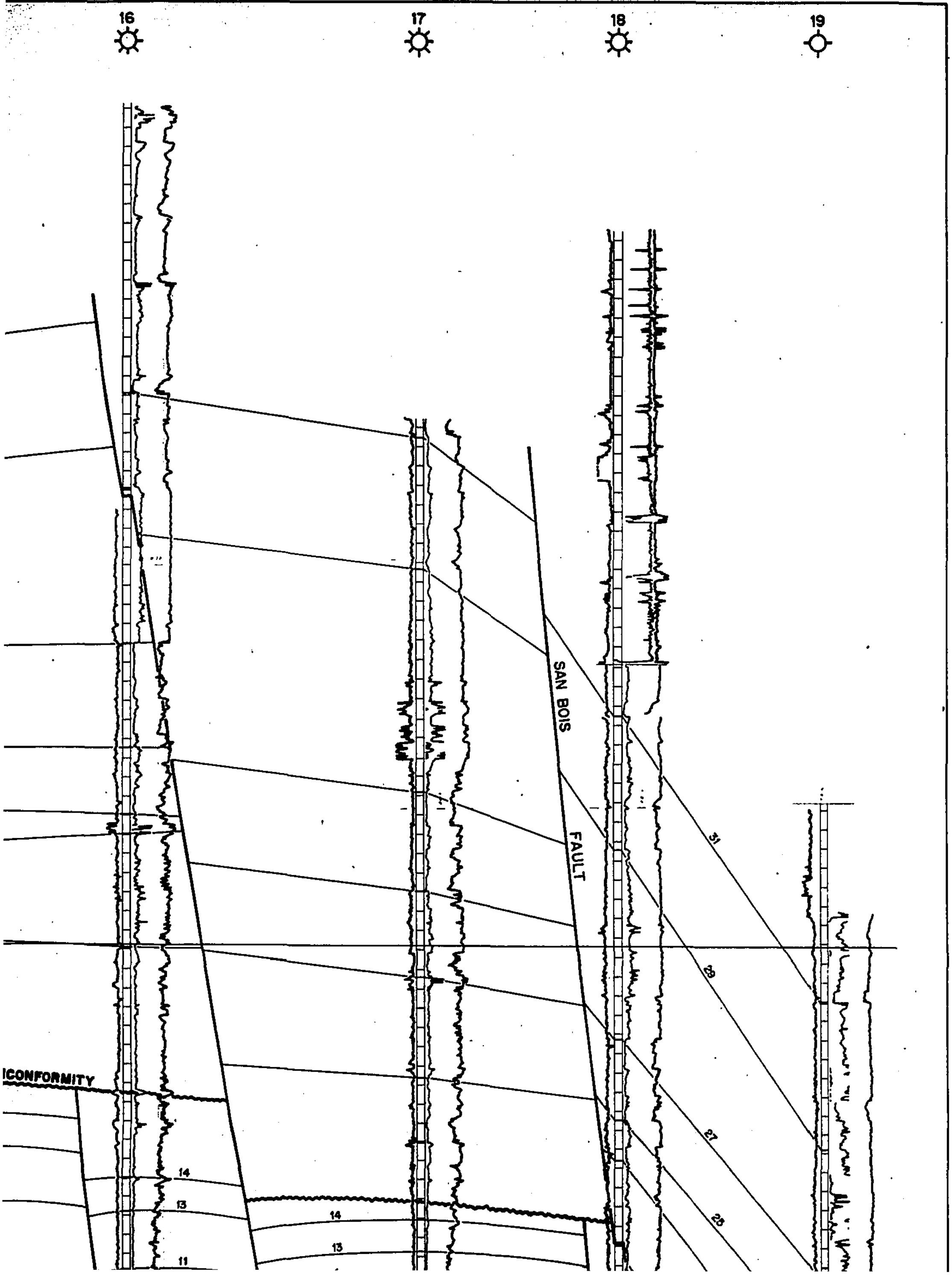
16
17
18
19
SAN BOIS
FAULT
UNCONFORMITY
31
29
27
25
14
13
11
14
13

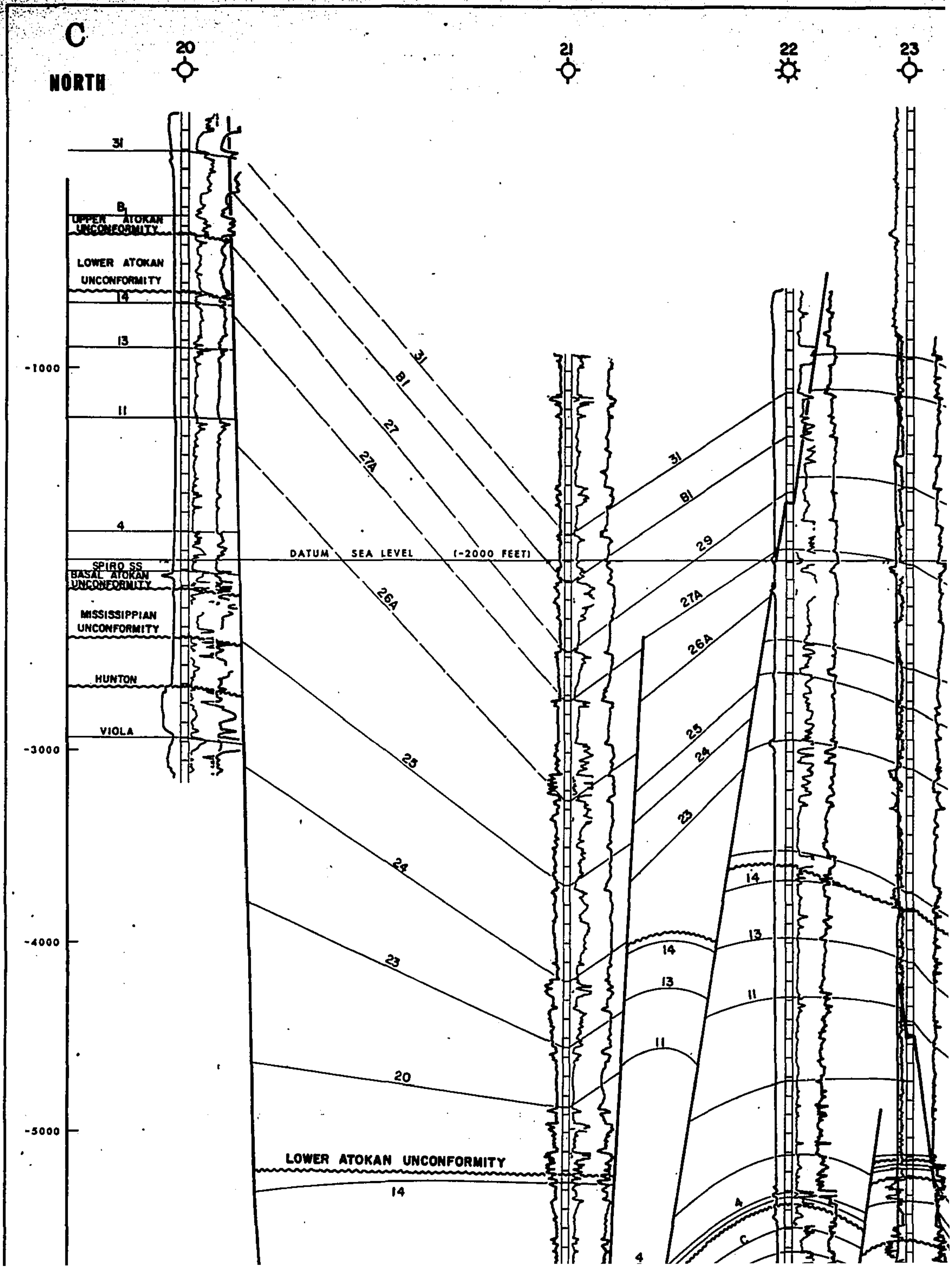

C
NORTH
20
21
22
23
31
B1
UPPER ATOKAN UNCONFORMITY
LOWER ATOKAN UNCONFORMITY
14
13
11
4
SPIRO SS
BASAL ATOKAN UNCONFORMITY
MISSISSIPPIAN UNCONFORMITY
HUNTON
VIOLA
-1000
-3000
-4000
-5000
DATUM SEA LEVEL (-2000 FEET)
27
27A
29
26A
25
24
23
20
LOWER ATOKAN UNCONFORMITY
C

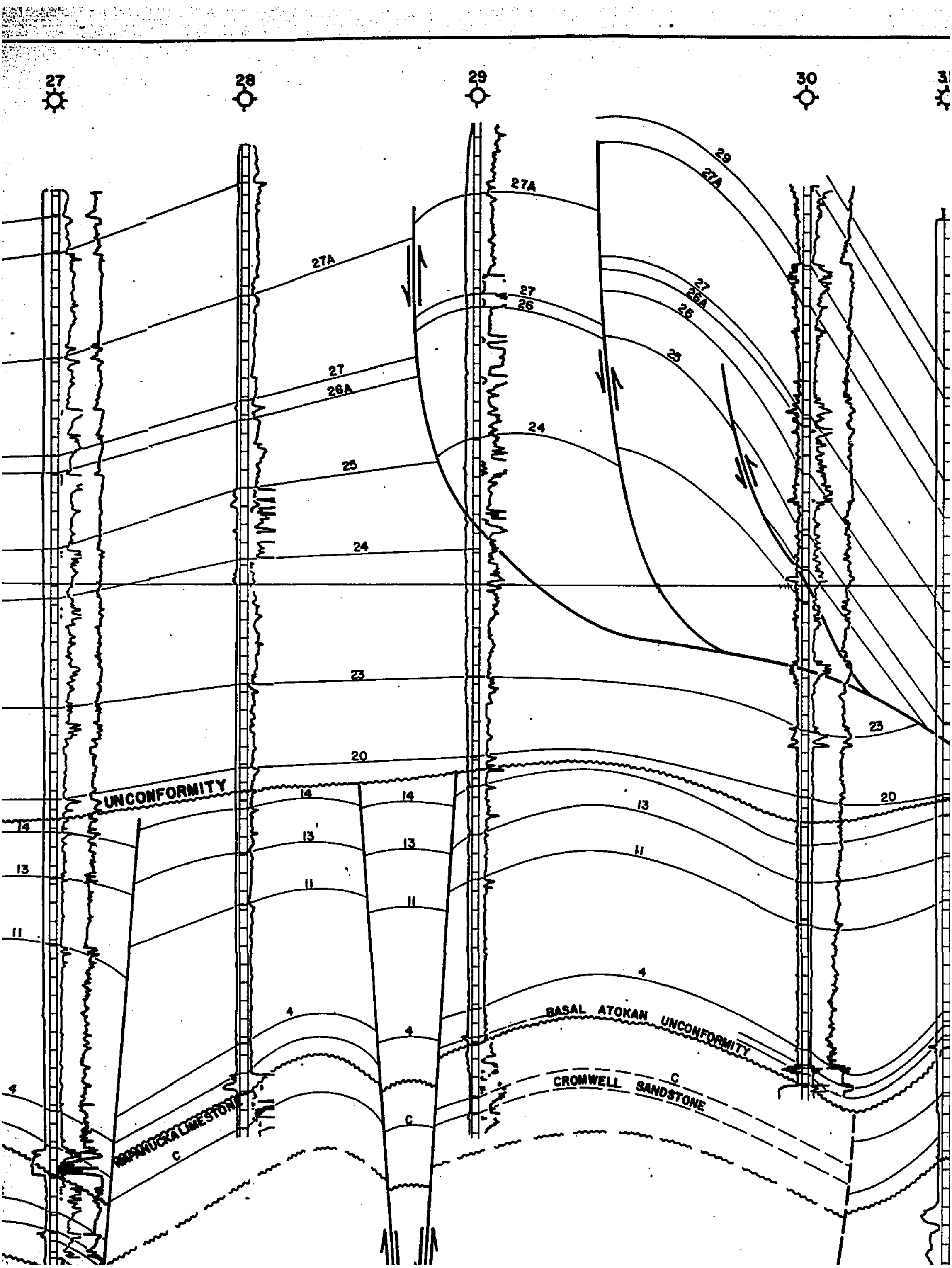

27
28
29
30
29
27A
27
26A
26
25
24
23
20
UNCONFORMITY
14
13
11
4
C
BASAL ATOKAN UNCONFORMITY
CROMWELL SANDSTONE
WAPANUCKA LIMESTONE

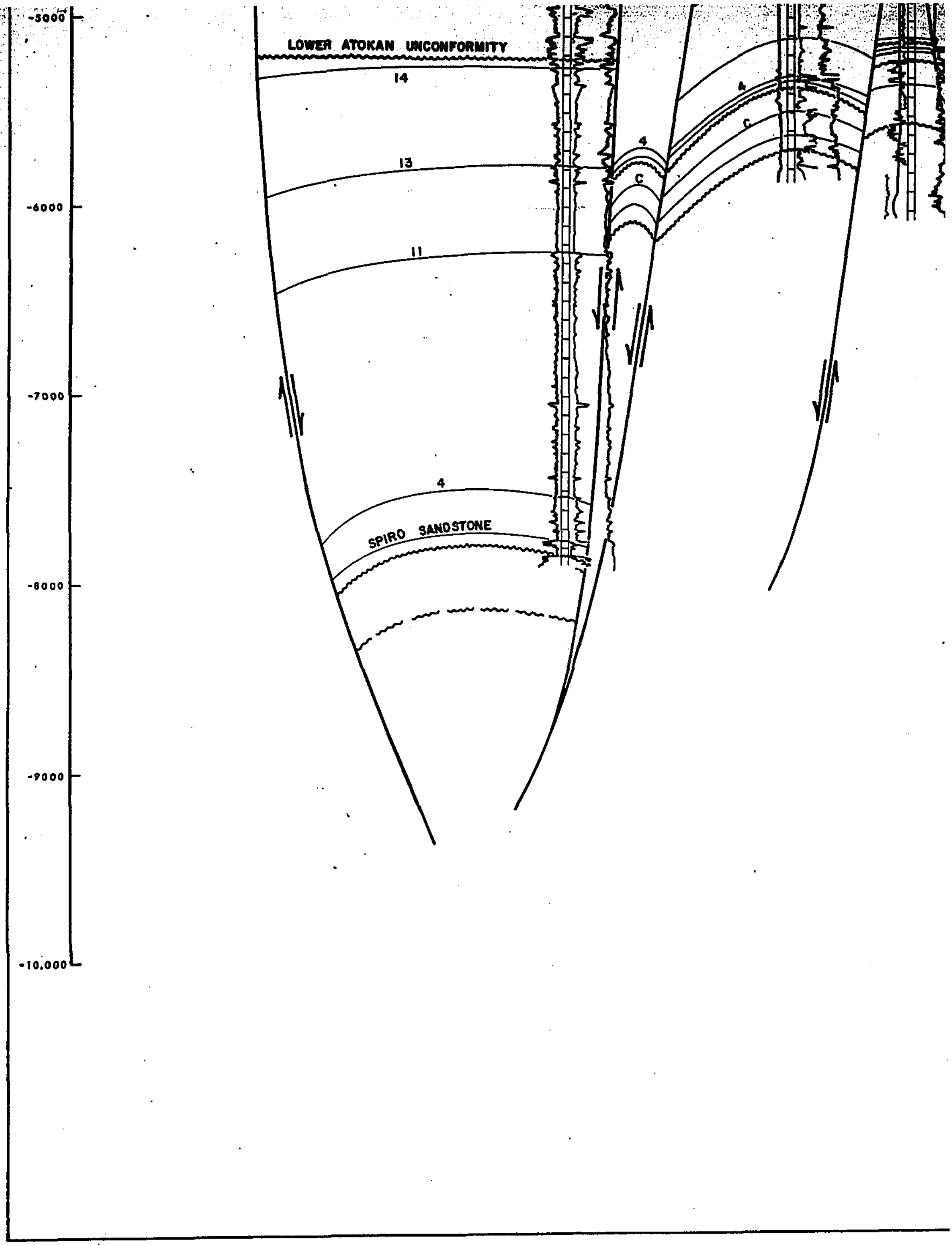

-5000
-6000
-7000
-8000
-9000
-10,000
LOWER ATOKAN UNCONFORMITY
14
13
11
4
SPIRO SANDSTONE
4
C
A
C

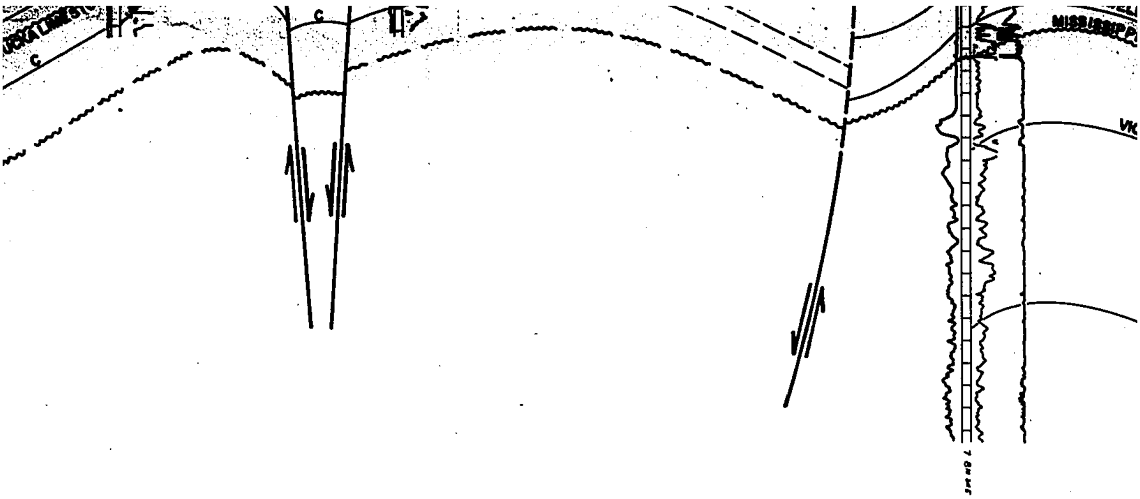

PLATE IV

STRUCTURAL CROSS SECTION C-C′

DATUM SEA LEVEL (-2000 FEET)

University of Oklahoma Ph.D. M.W. McQuillan

1976

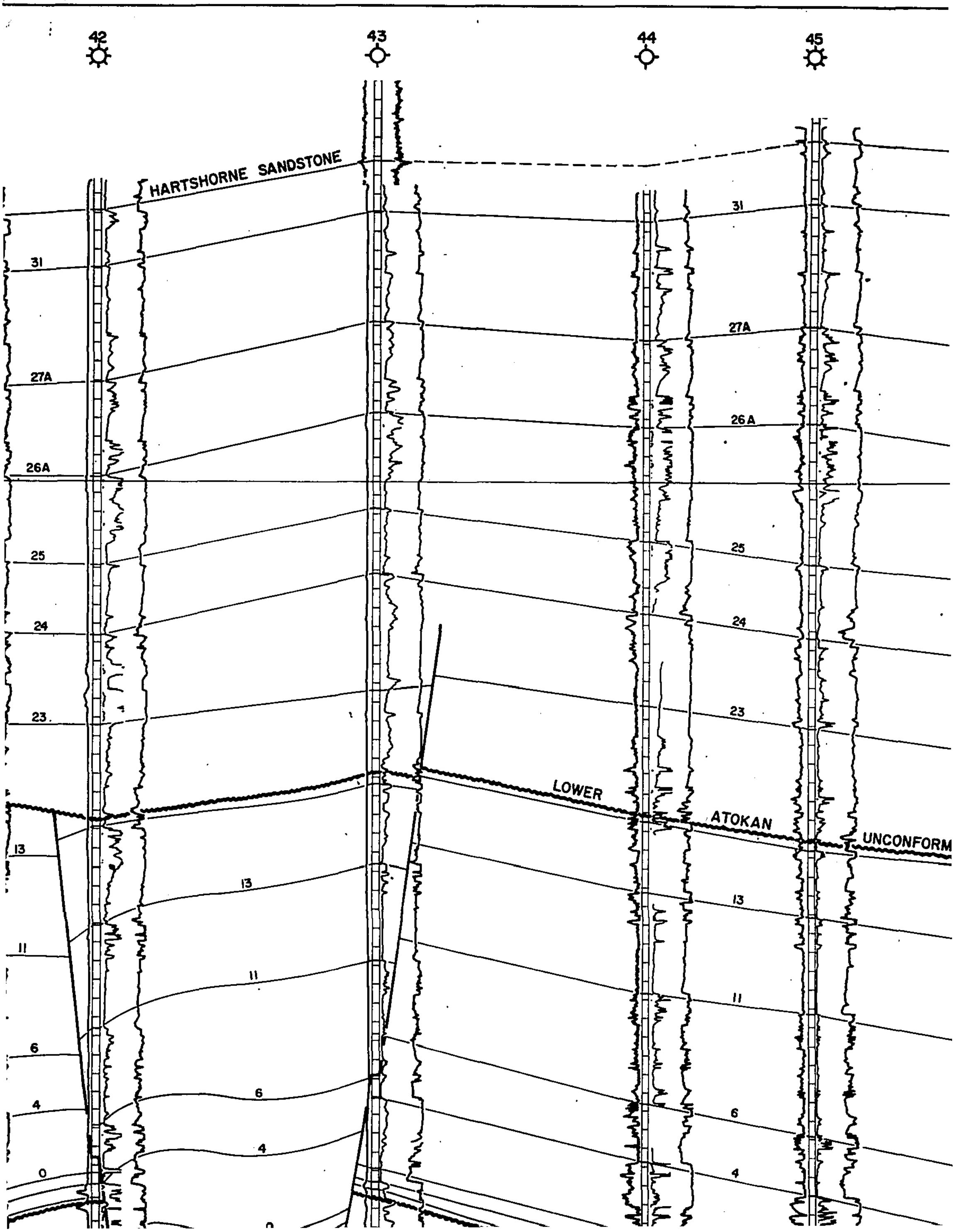
42
43
44
45
HARTSHORNE SANDSTONE
31
27A
26A
25
24
23
LOWER
ATOKAN
UNCONFORM
13
11
6
4
0

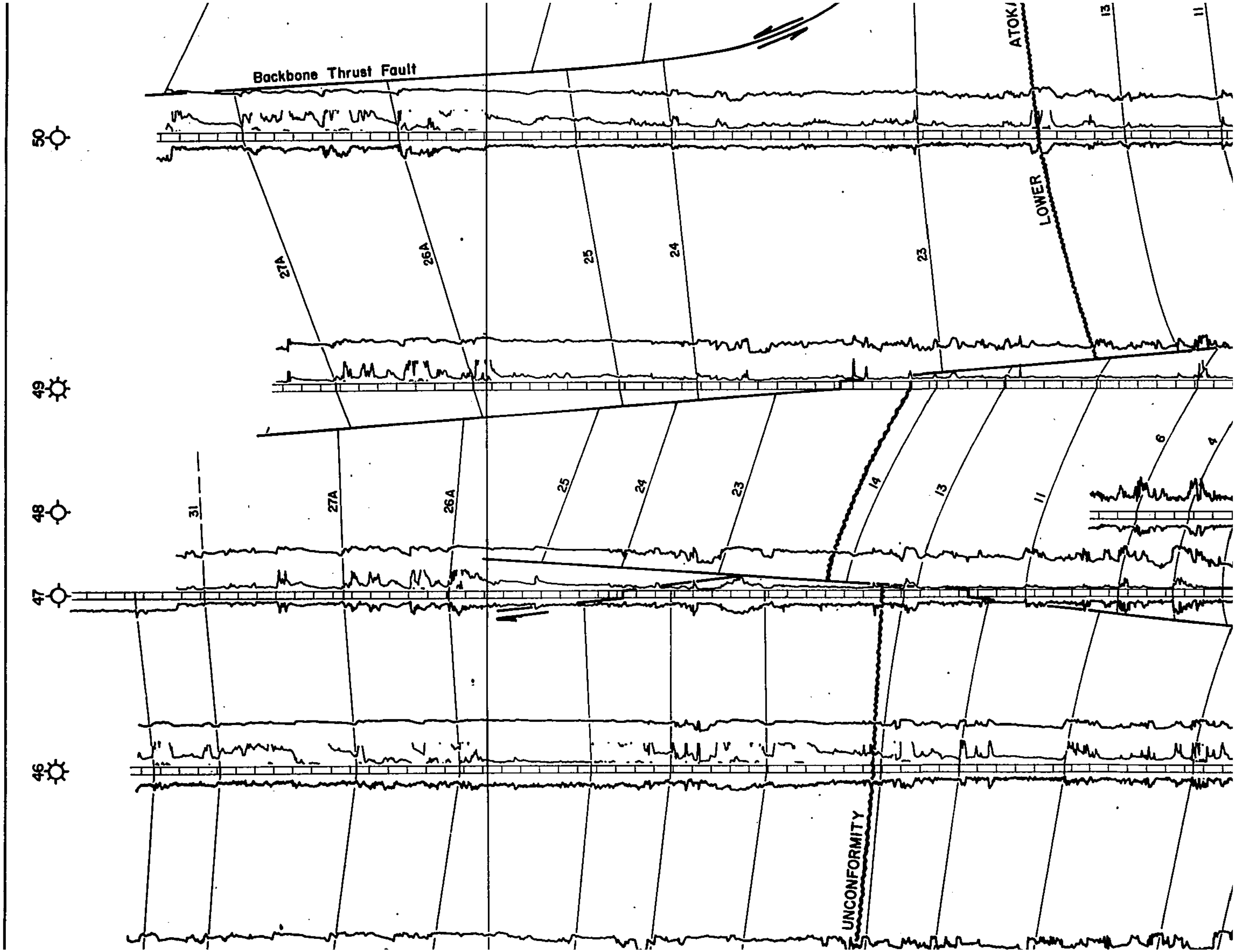
Backbone Thrust Fault
50
49
48
47
46
27A
26A
25
24
23
14
13
11
6
4
31
LOWER
UNCONFORMITY

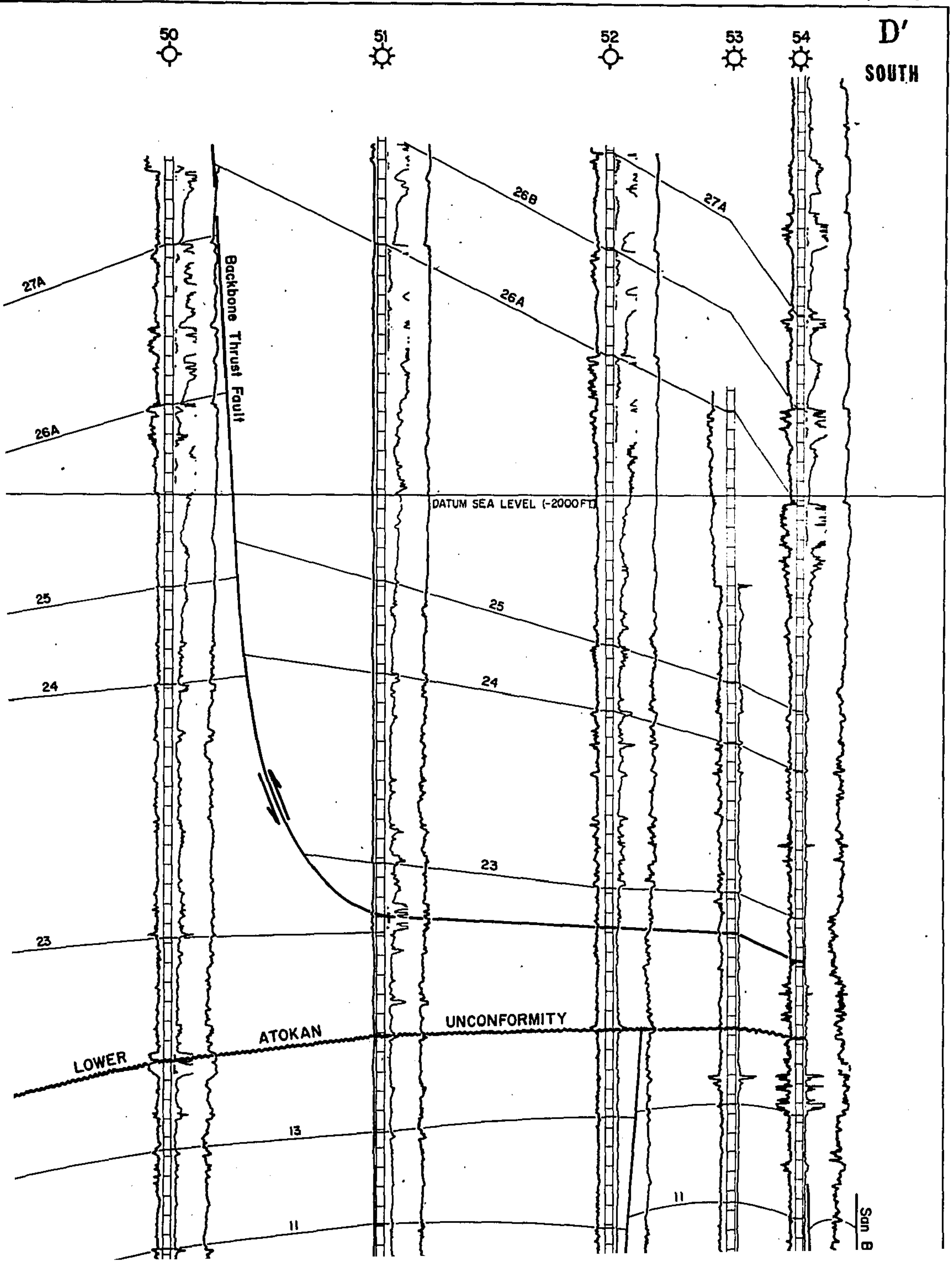

D'
SOUTH
50
51
52
53
54
27A
26B
27A
26A
26A
Backbone Thrust Fault
DATUM SEA LEVEL (-2000FT)
25
25
24
24
23
23
LOWER
ATOKAN
UNCONFORMITY
13
11
11
San B

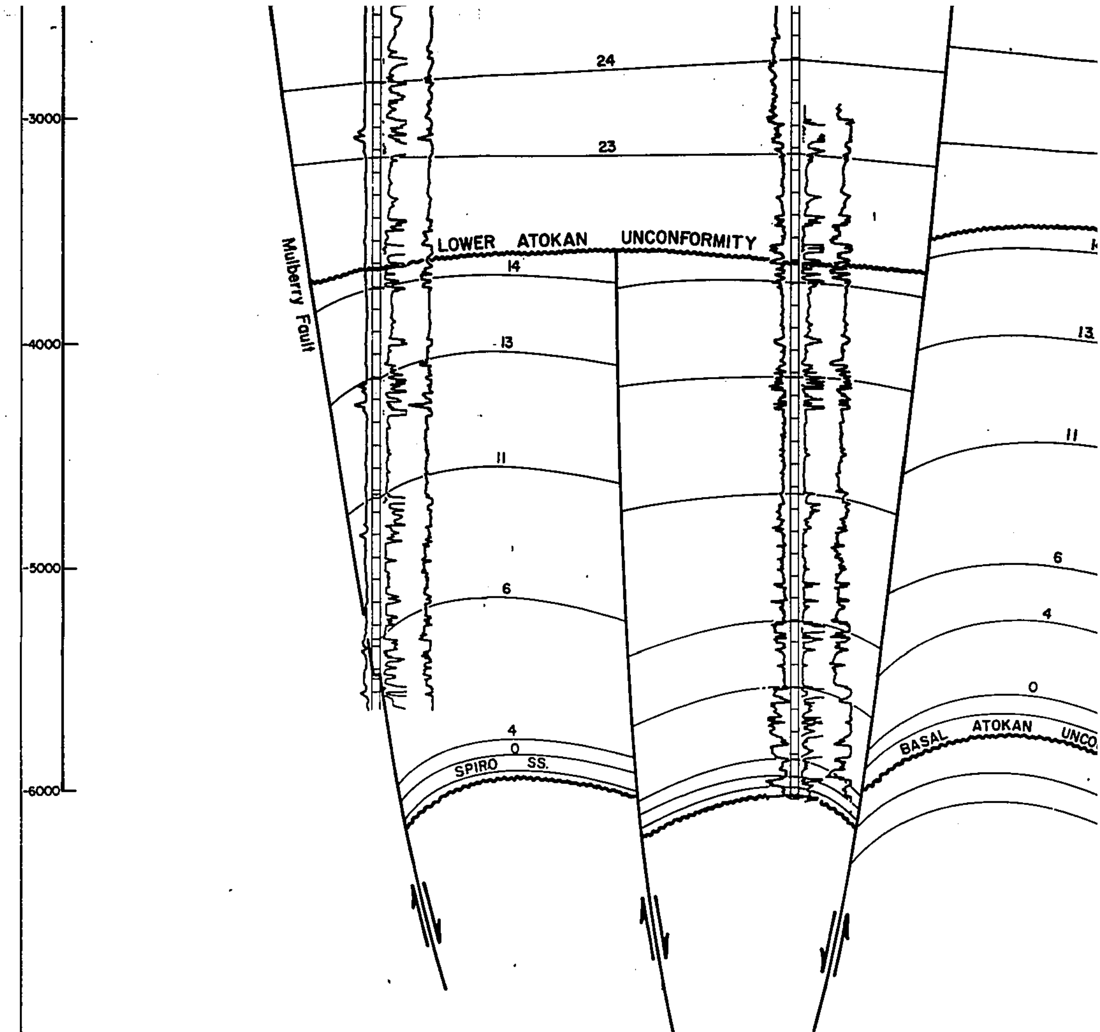

PLATE V

STRUCTURAL CROSS SECTION D-D'

DATUM SEA LEVEL (-2000 FEET)

University of Oklahoma Ph.D. M.W. McQuillan

1976

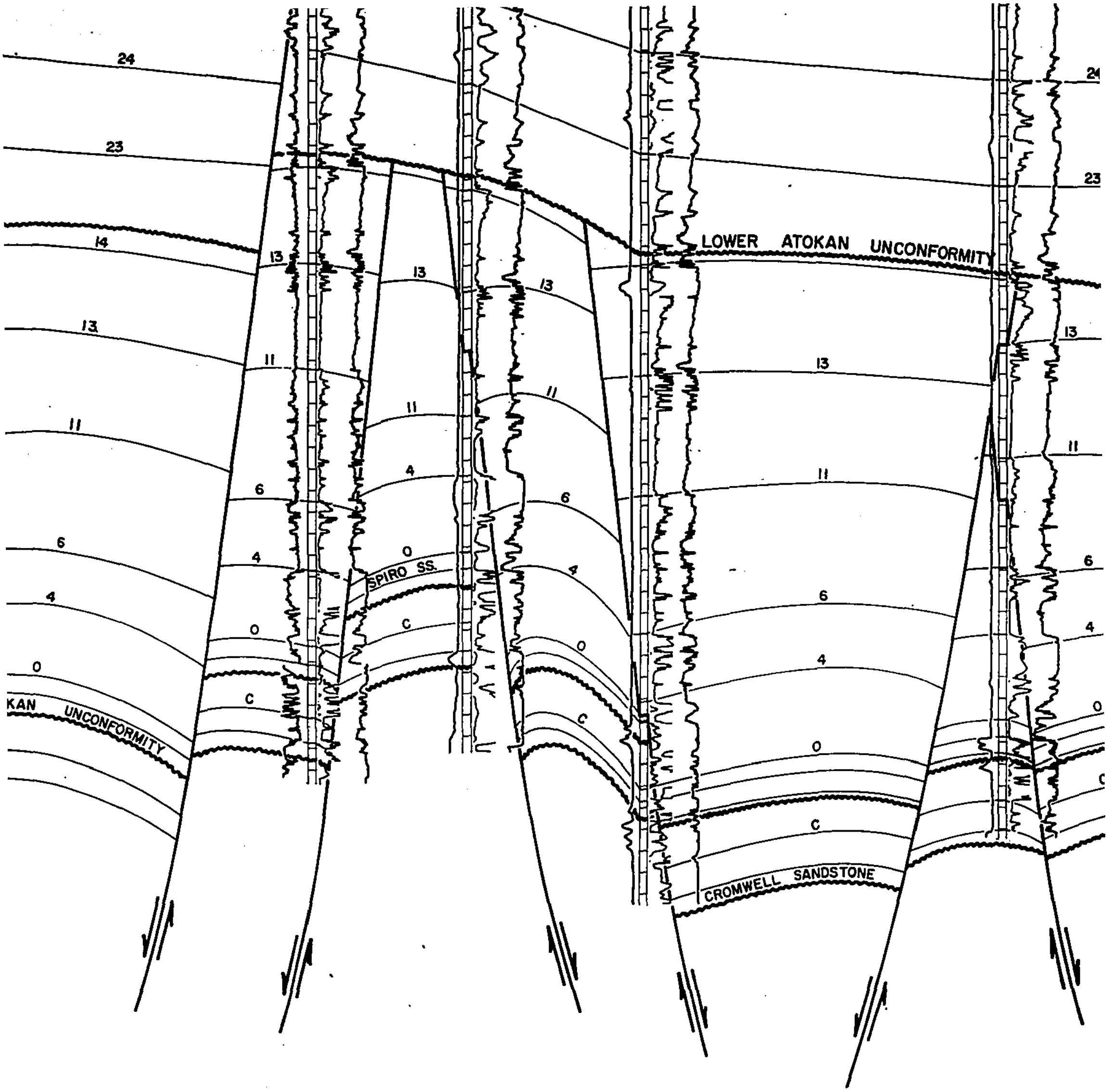
24
23
LOWER ATOKAN UNCONFORMITY
14
13
11
6
4
0
C
SPIRO SS.
KAN UNCONFORMITY
CROMWELL SANDSTONE

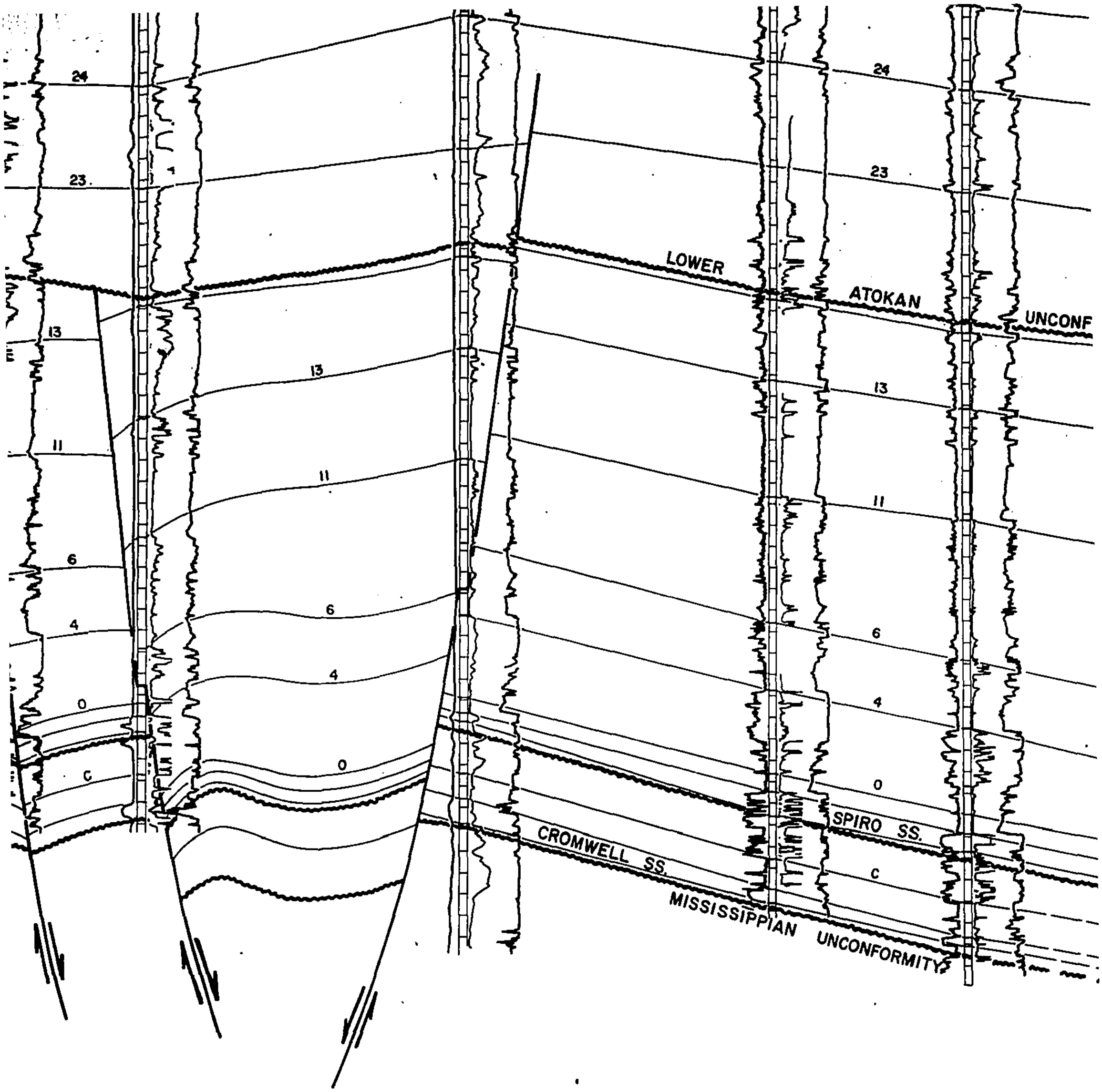

24
23
LOWER ATOKAN UNCONF
13
11
6
4
0
C
SPIRO SS.
CROMWELL SS.
MISSISSIPPIAN UNCONFORMITY

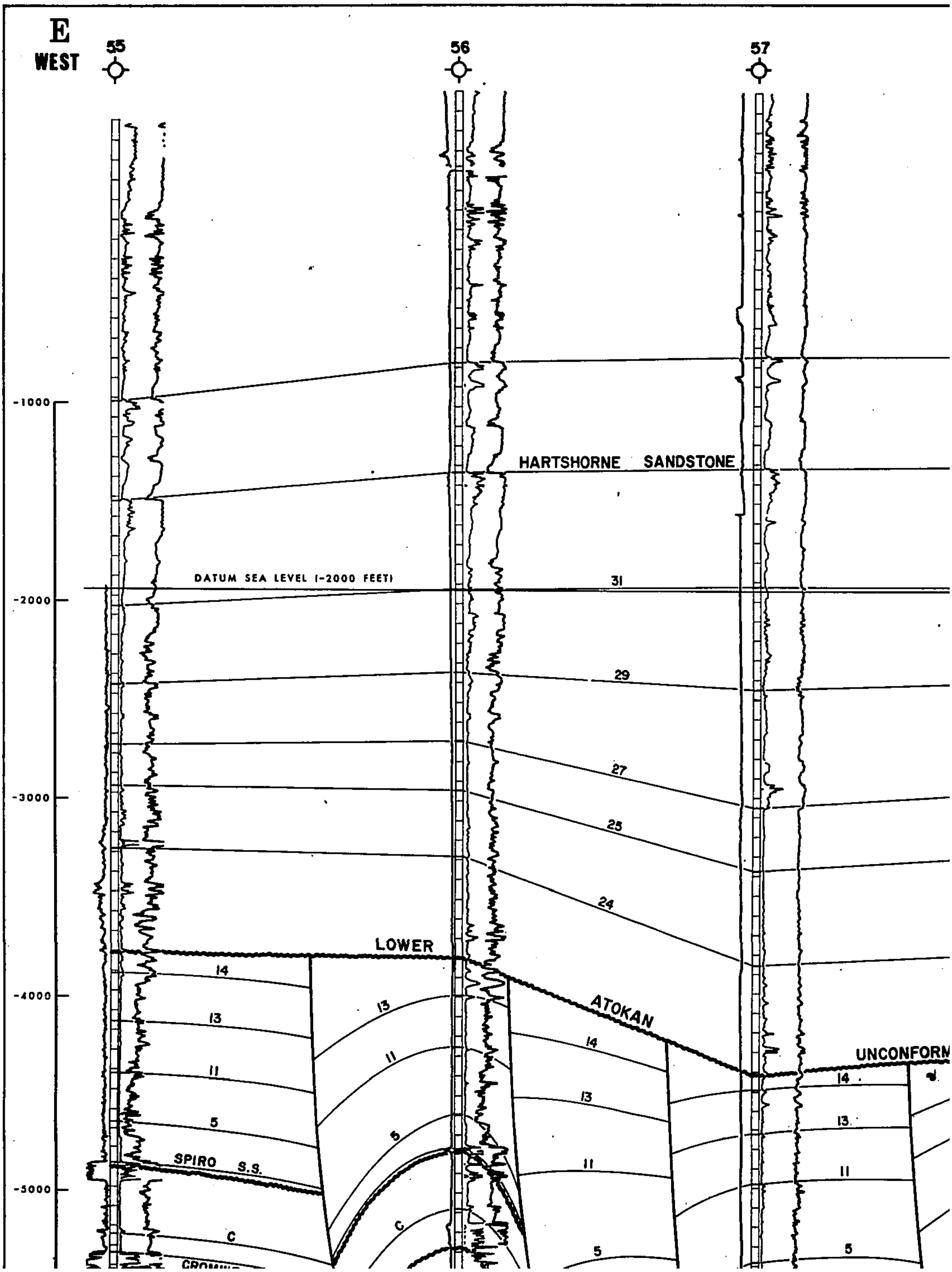

E
WEST
55
56
57
-1000
-2000
-3000
-4000
-5000
HARTSHORNE SANDSTONE
DATUM SEA LEVEL (-2000 FEET)
31
29
27
25
24
LOWER
ATOKAN
UNCONFORM
14
13
11
5
SPIRO S.S.
C

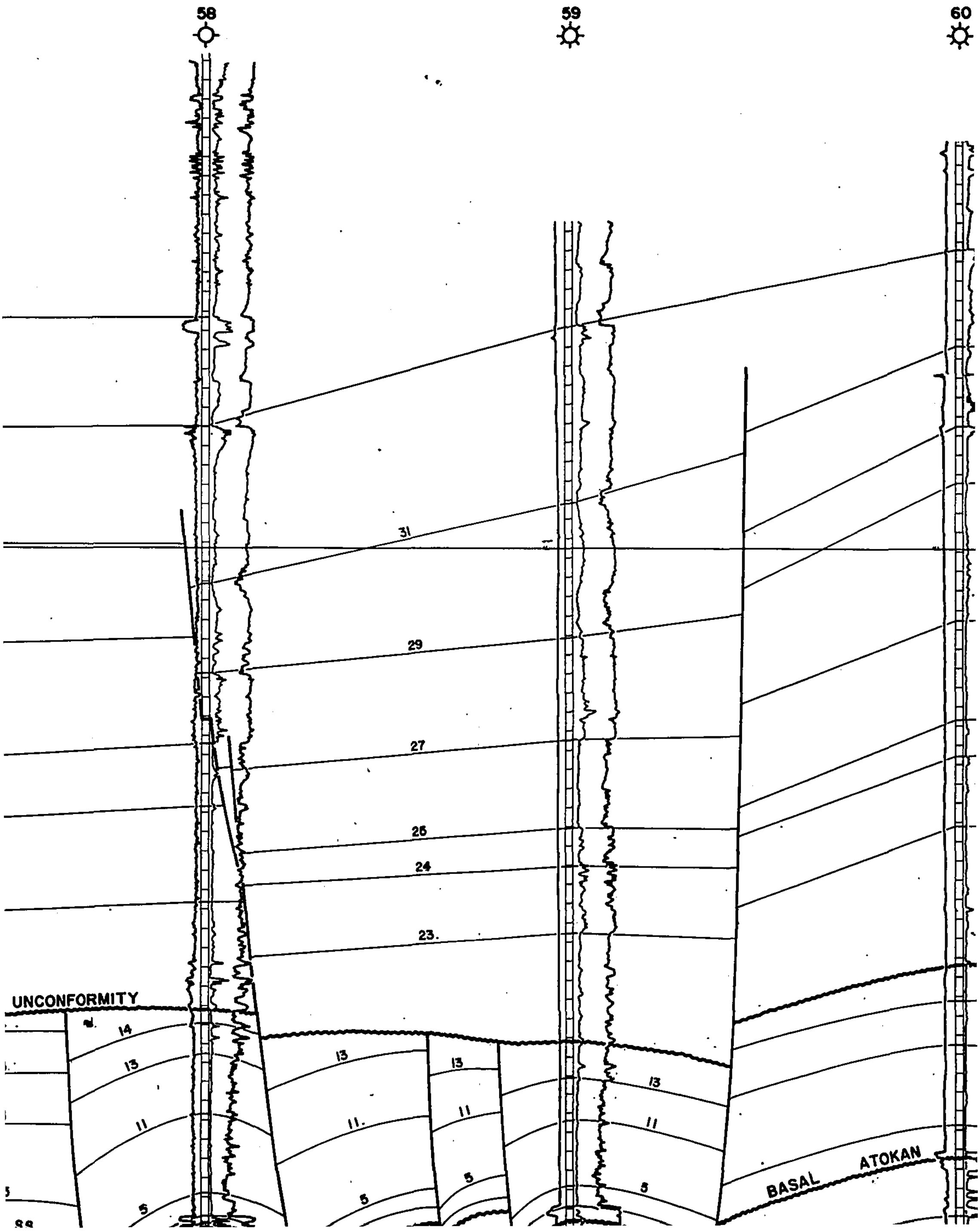
58
59
60
31
29
27
26
24
23.
UNCONFORMITY
14
13
11
5
BASAL ATOKAN

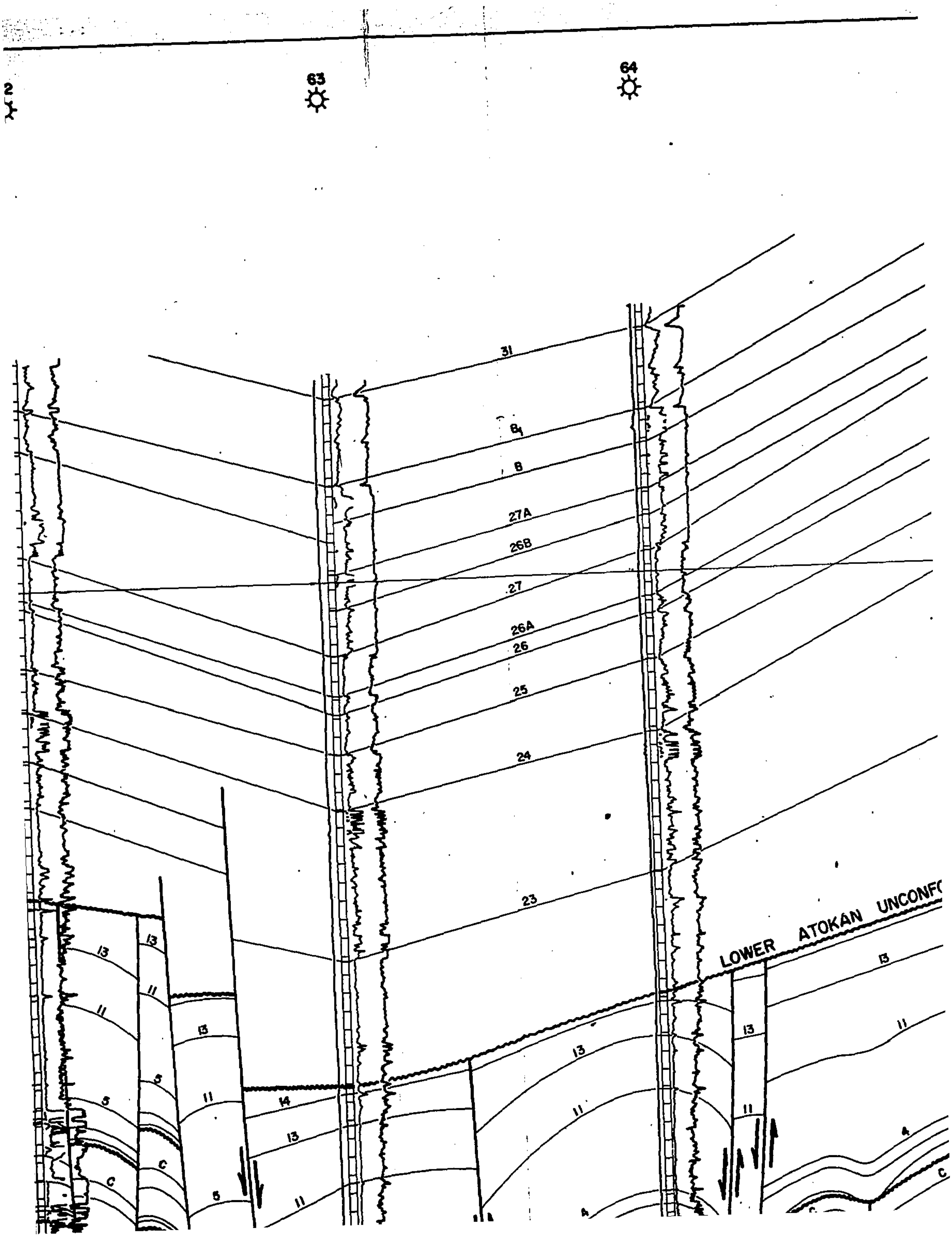

2
63
64
31
B1
B
27A
26B
27
26A
26
25
24
23
LOWER ATOKAN UNCONF
13
11
5
C
14
4

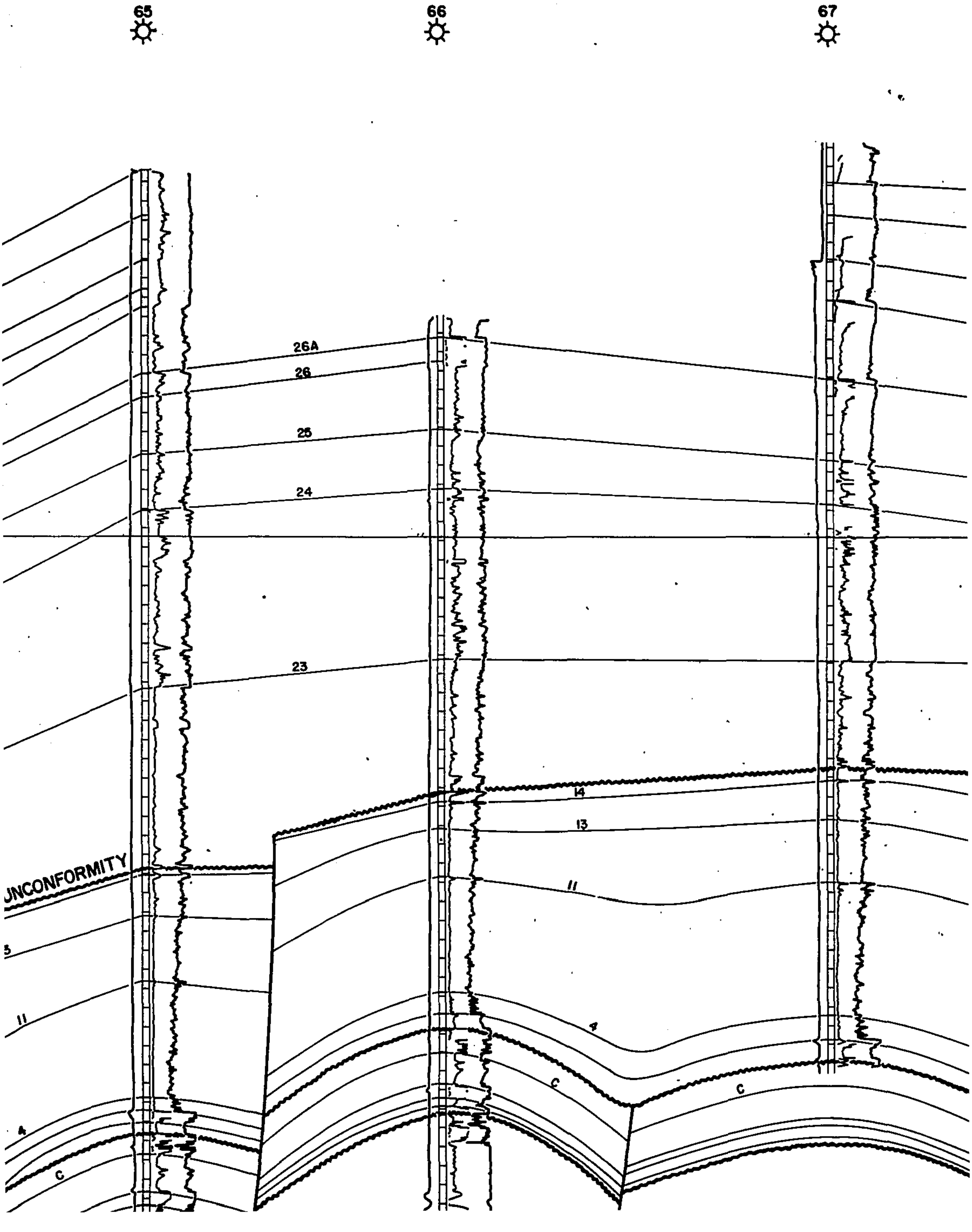

65
66
67
26A
26
25
24
23
14
13
11
UNCONFORMITY
5
11
4
4
C
C
C

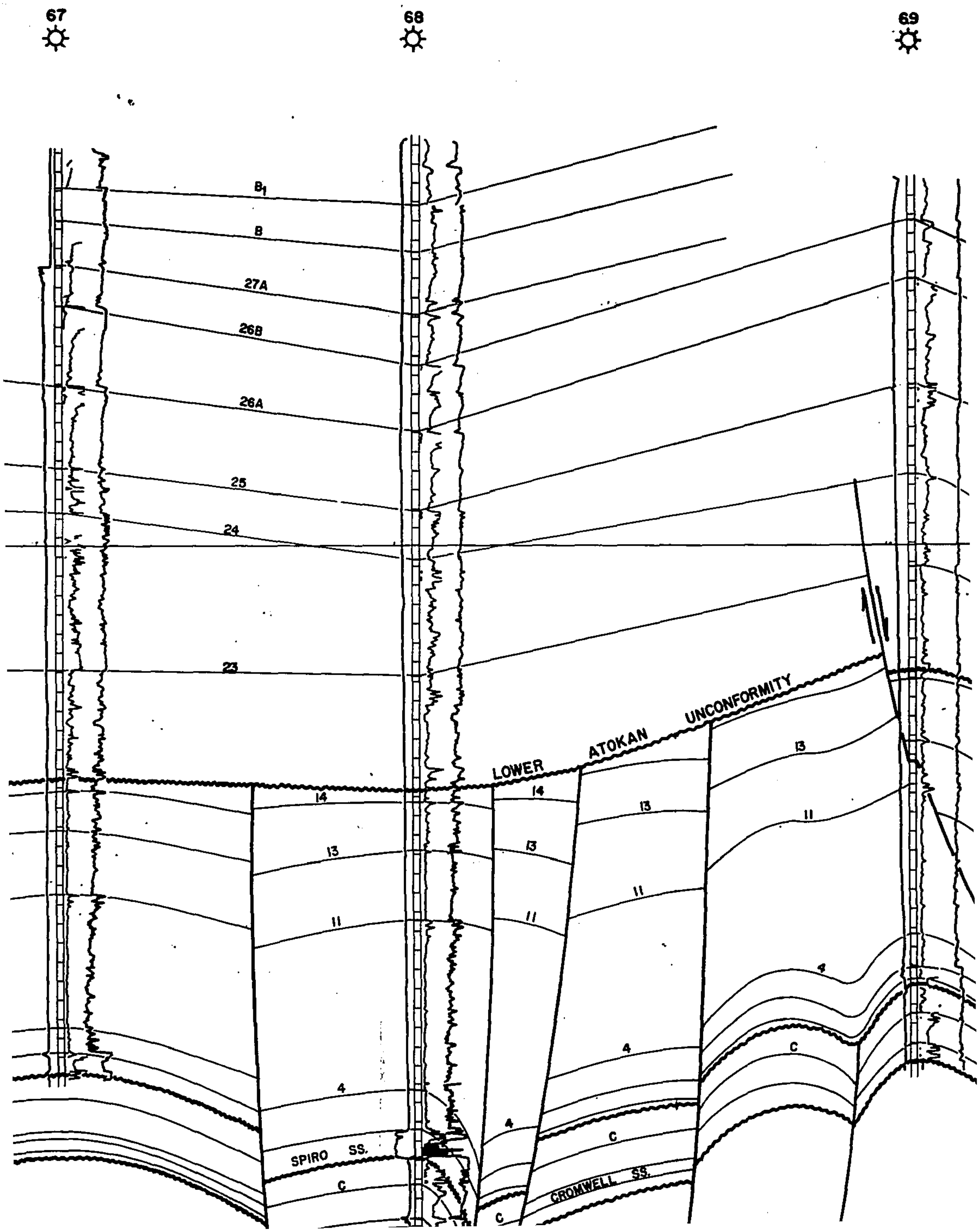

67
68
69
B1
B
27A
26B
26A
25
24
23
LOWER ATOKAN UNCONFORMITY
14
13
11
4
SPIRO SS.
C
CROMWELL SS.

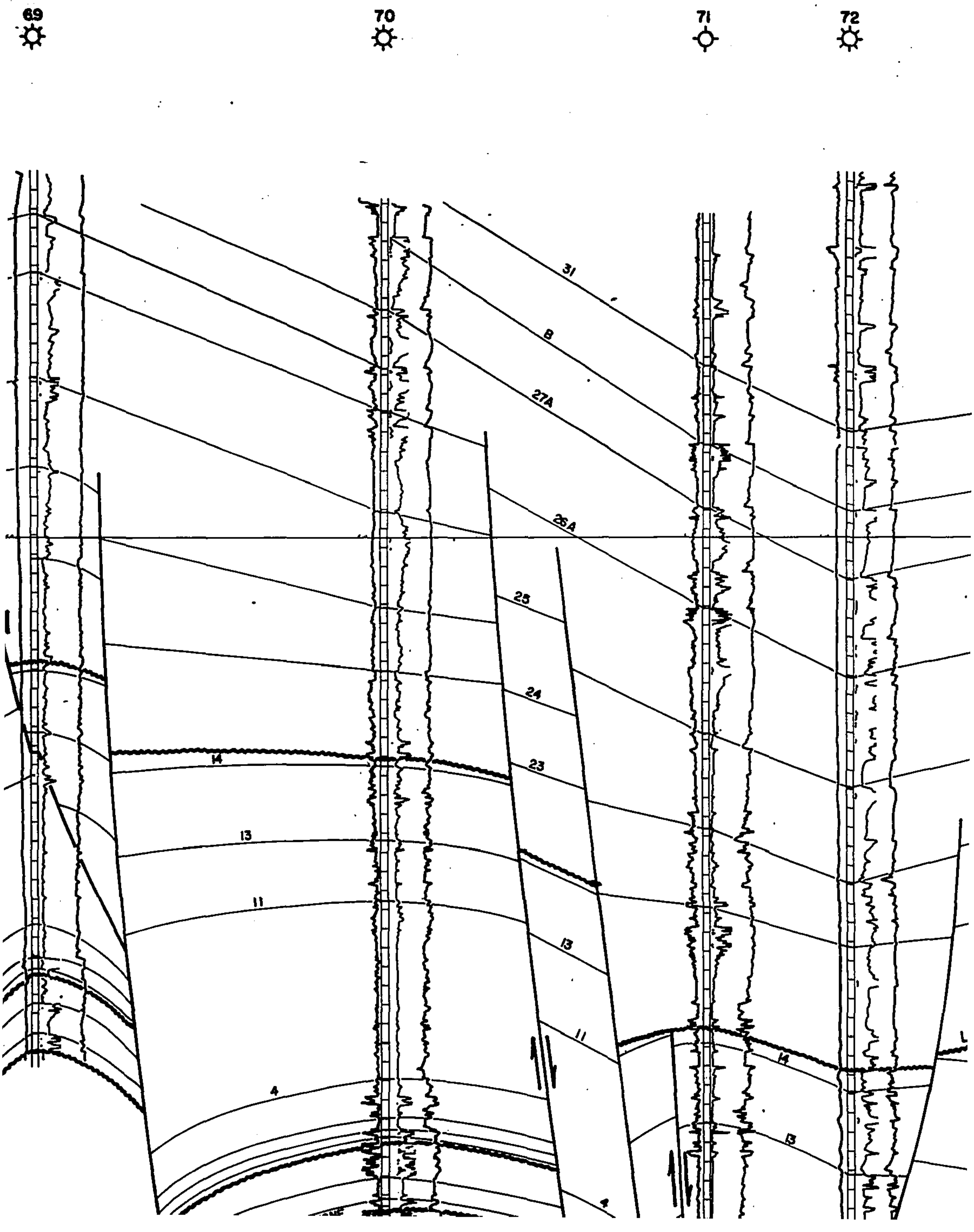

69
70
71
72
31
B
27A
26A
25
24
23
14
13
11
4

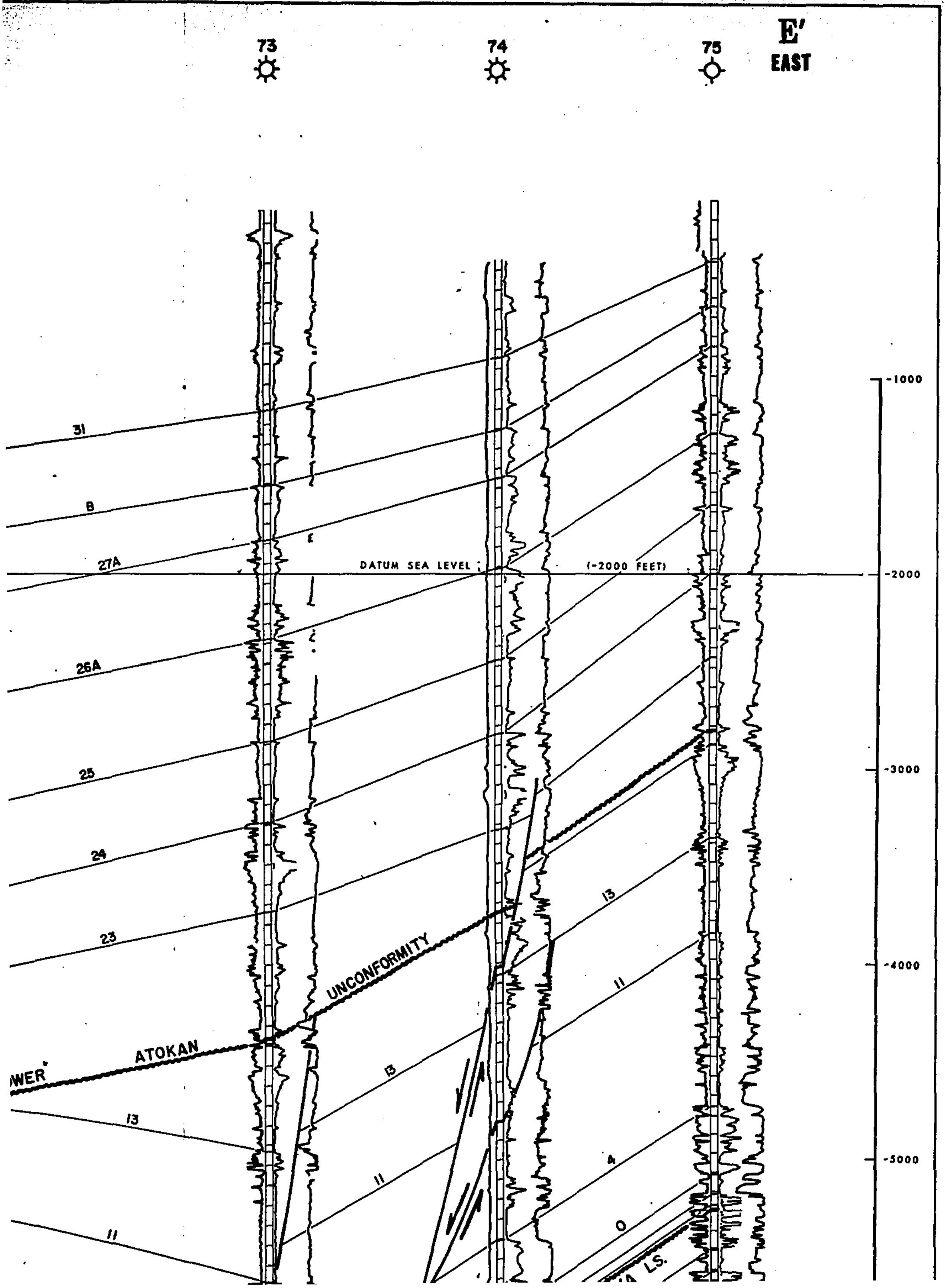
E'
EAST
73
74
75
31
B
27A
DATUM SEA LEVEL
(-2000 FEET)
26A
25
24
23
UNCONFORMITY
ATOKAN
WER
13
11
13
11
4
O
LS.
-1000
-2000
-3000
-4000
-5000

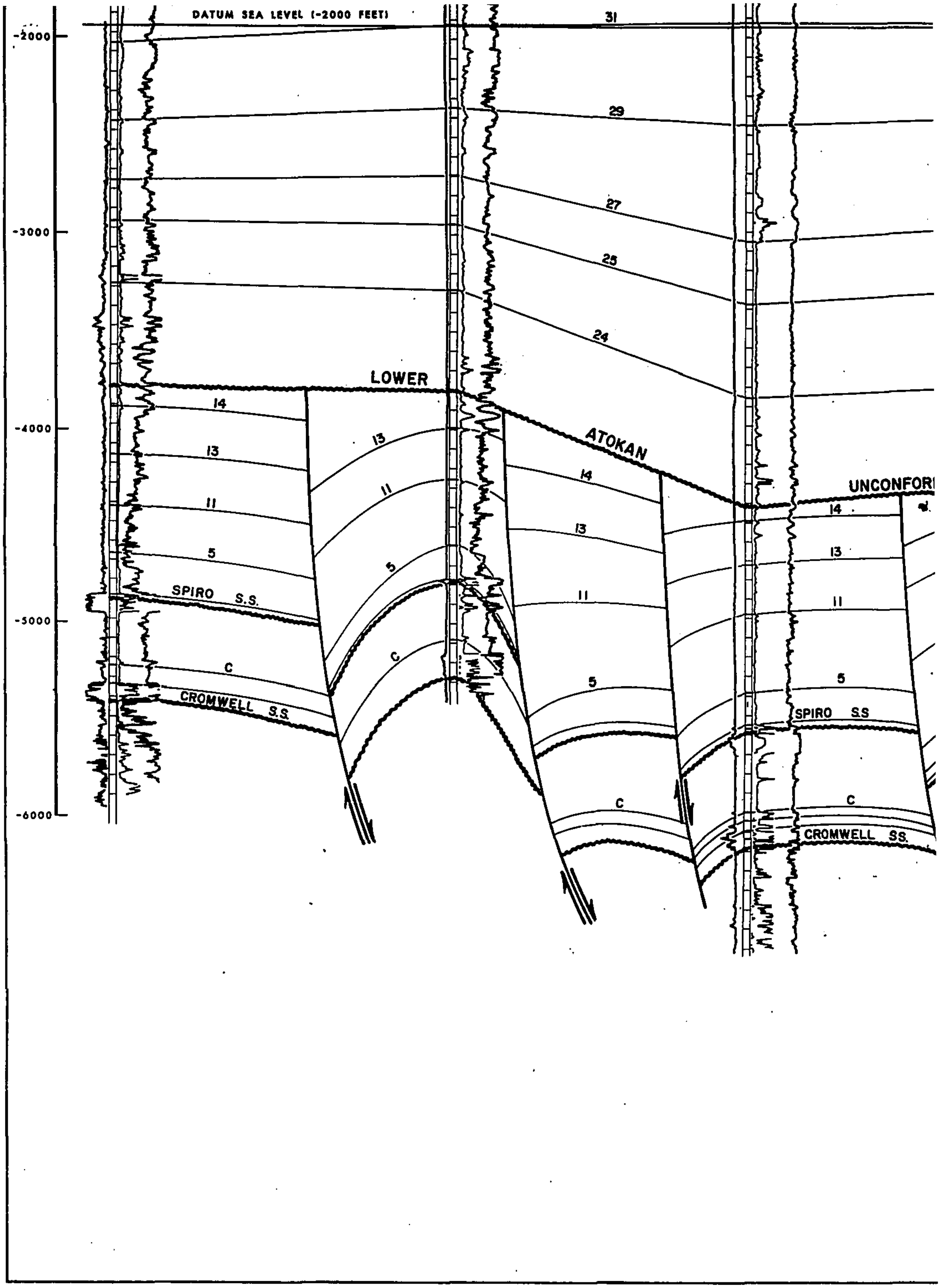
DATUM SEA LEVEL (-2000 FEET)
-2000
-3000
-4000
-5000
-6000
31
29
27
25
24
LOWER
ATOKAN
UNCONFOR
14
13
11
5
SPIRO S.S.
C
CROMWELL S.S.
SPIRO SS
CROMWELL SS.

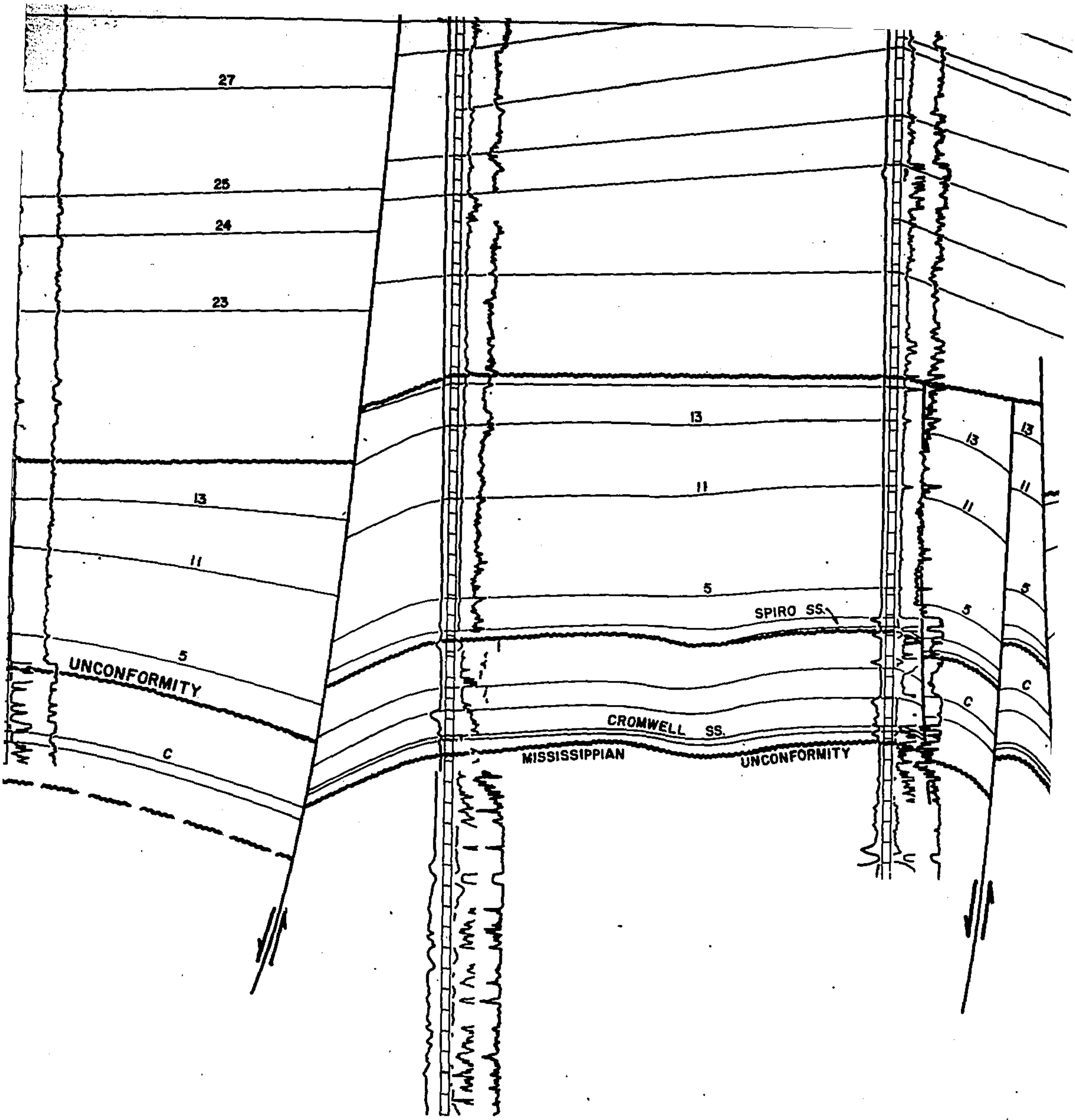

27
25
24
23
13
11
5
UNCONFORMITY
C
SPIRO SS.
CROMWELL SS.
MISSISSIPPIAN
UNCONFORMITY

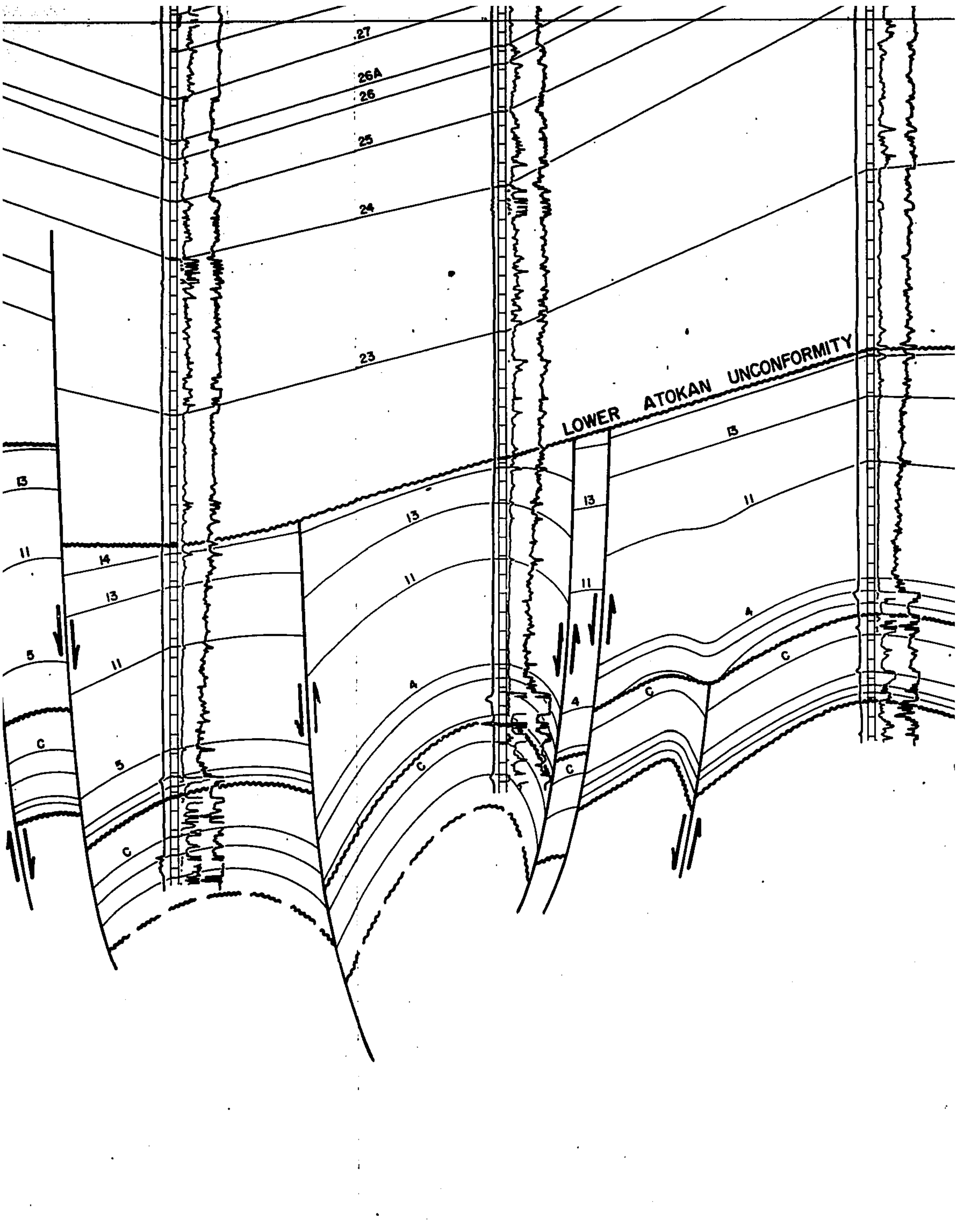

27
26A
26
25
24
23
LOWER ATOKAN UNCONFORMITY
13
11
14
13
5
11
C
5
C
13
11
4
C
13
11
4
C
13
11
4
C
C

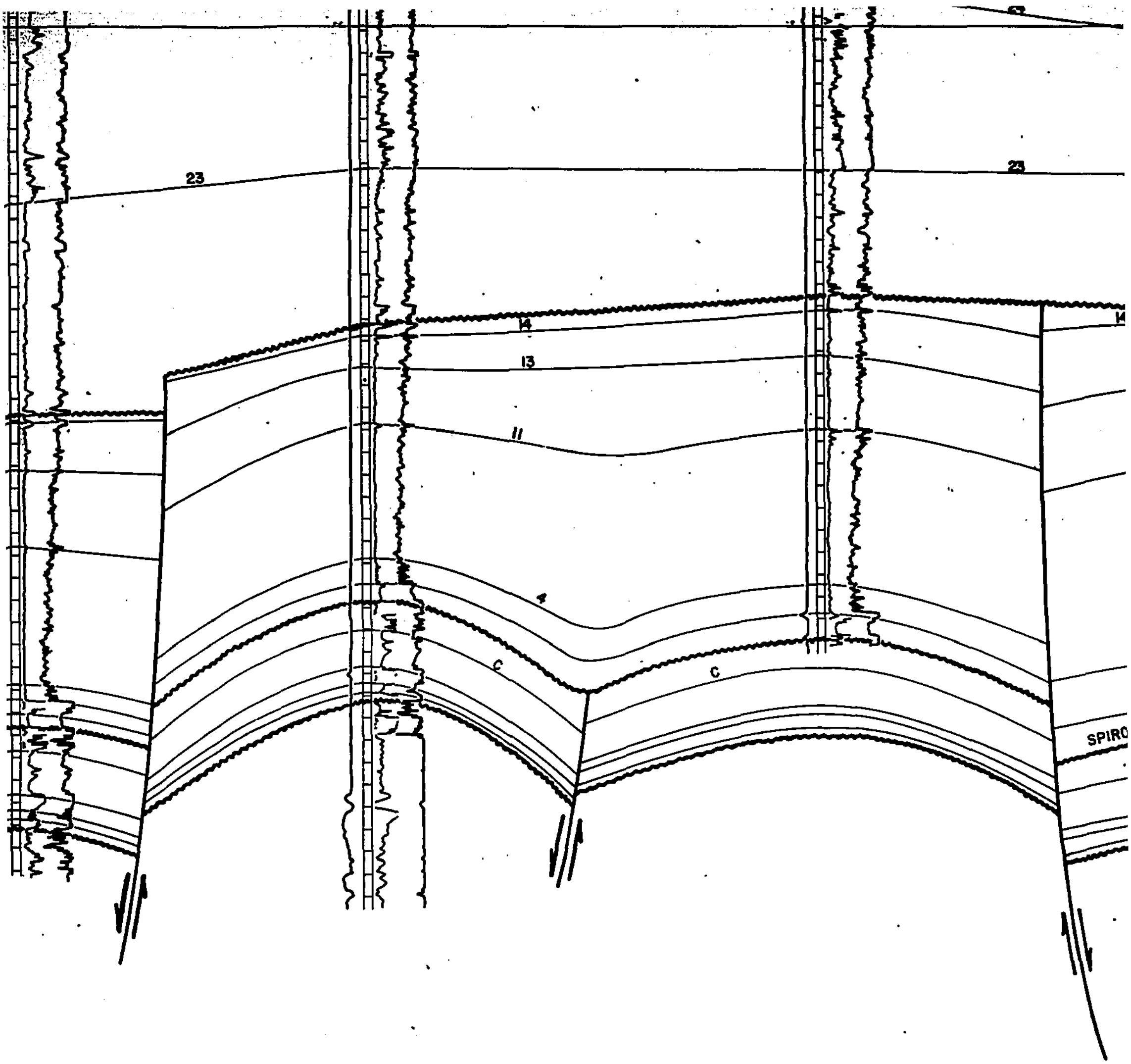

PLATE VI

STRUCTURAL CROSS SECTION E-E'

DATUM SEA LEVEL (-2000 FEET)

University of Oklahoma Ph.D. M.W. McQuillan

1976

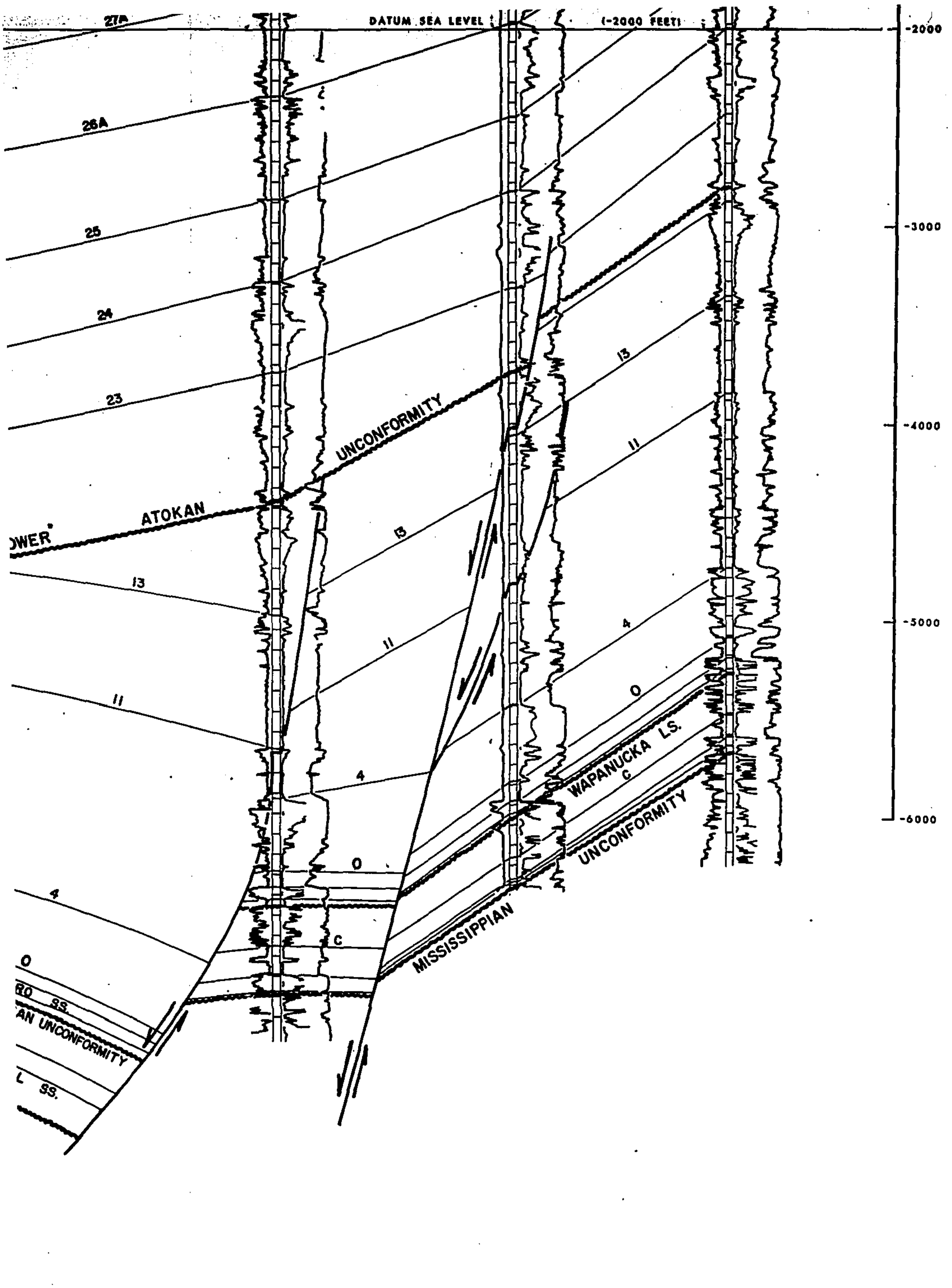

DATUM SEA LEVEL
(-2000 FEET)
-2000
-3000
-4000
-5000
-6000
27A
26A
25
24
23
13
11
4
O
C
LOWER ATOKAN UNCONFORMITY
WAPANUCKA LS.
MISSISSIPPIAN UNCONFORMITY

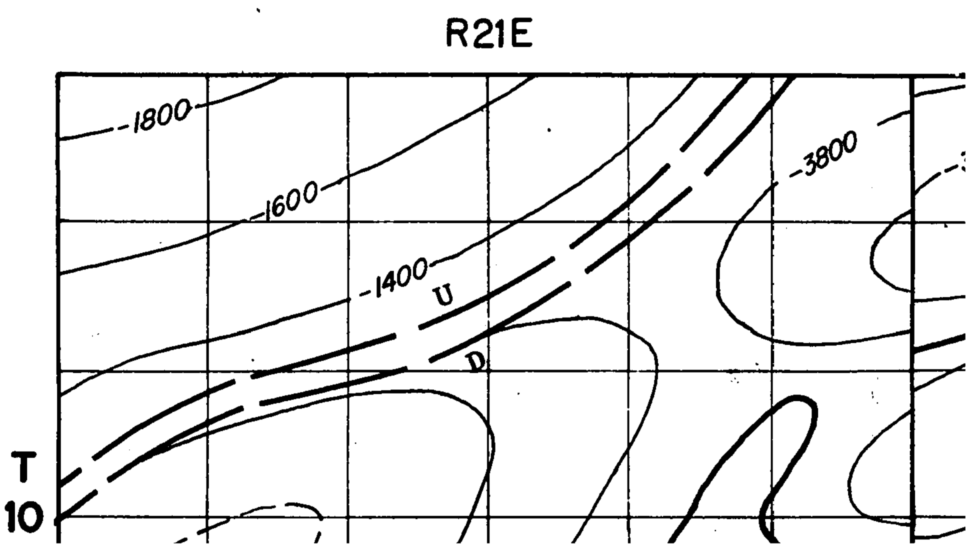
R21E
-1800
-1600
-1400
U
D
-3800
T
10

R22E

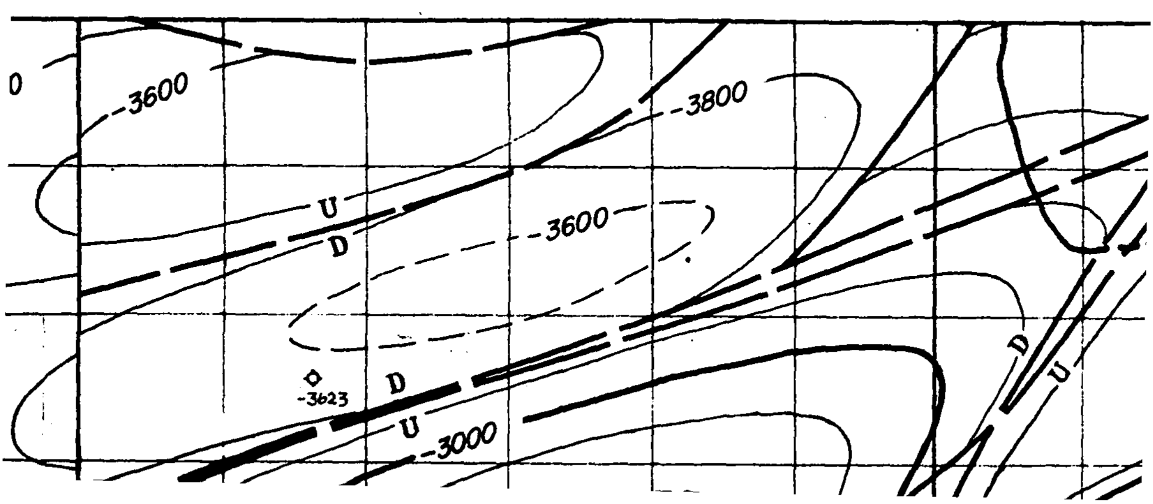

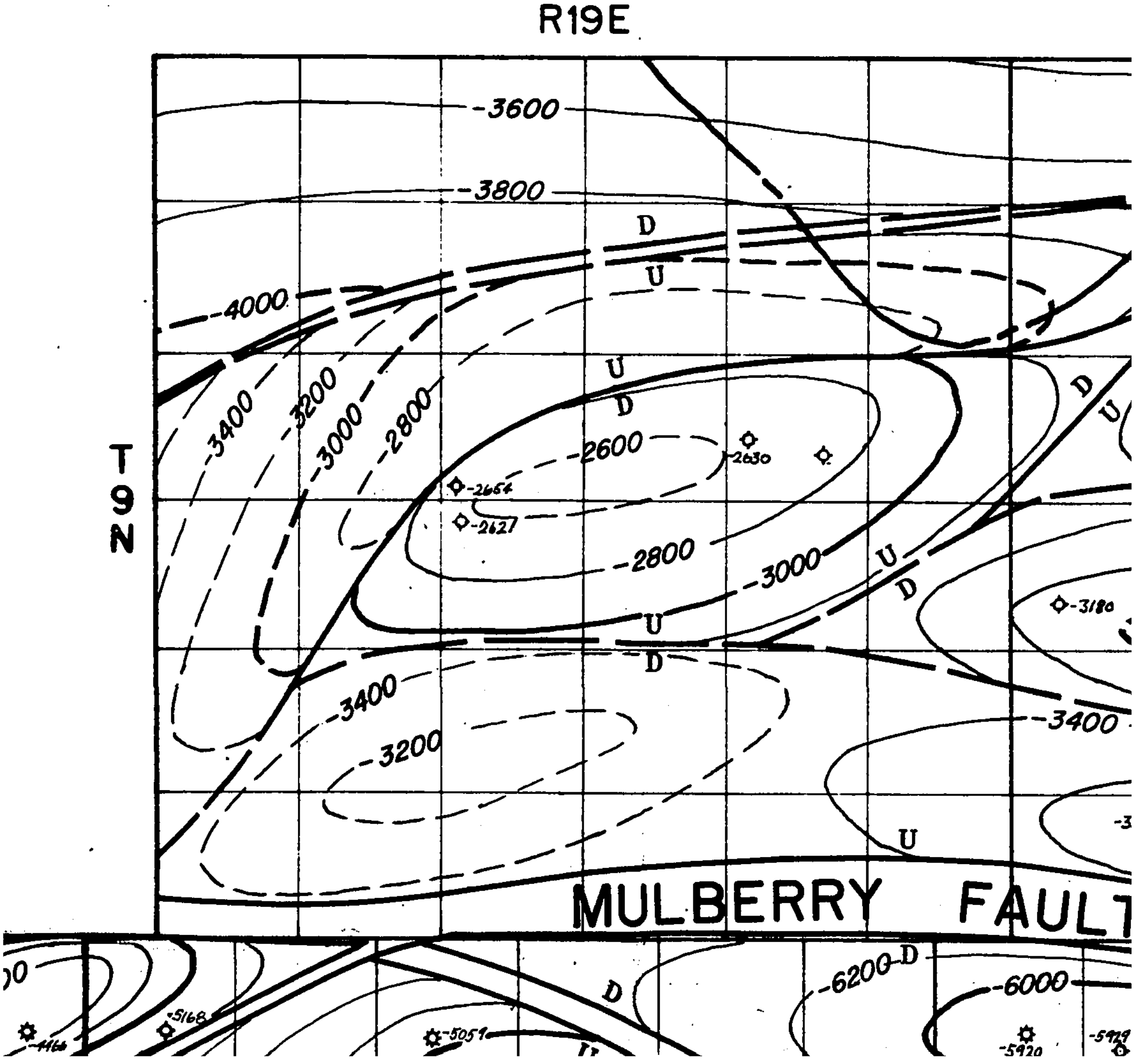

R19E
T9N
-3600
-3800
-4000
D
U
U
D
-3400
-3200
-3000
-2800
-2600
-2654
-2627
-2630
-2800
-3000
U
D
U
D
D
U
-3180
-3400
-3200
-3400
U
MULBERRY FAULT
-5168
-5059
D
-6200
D
-6000
-5920

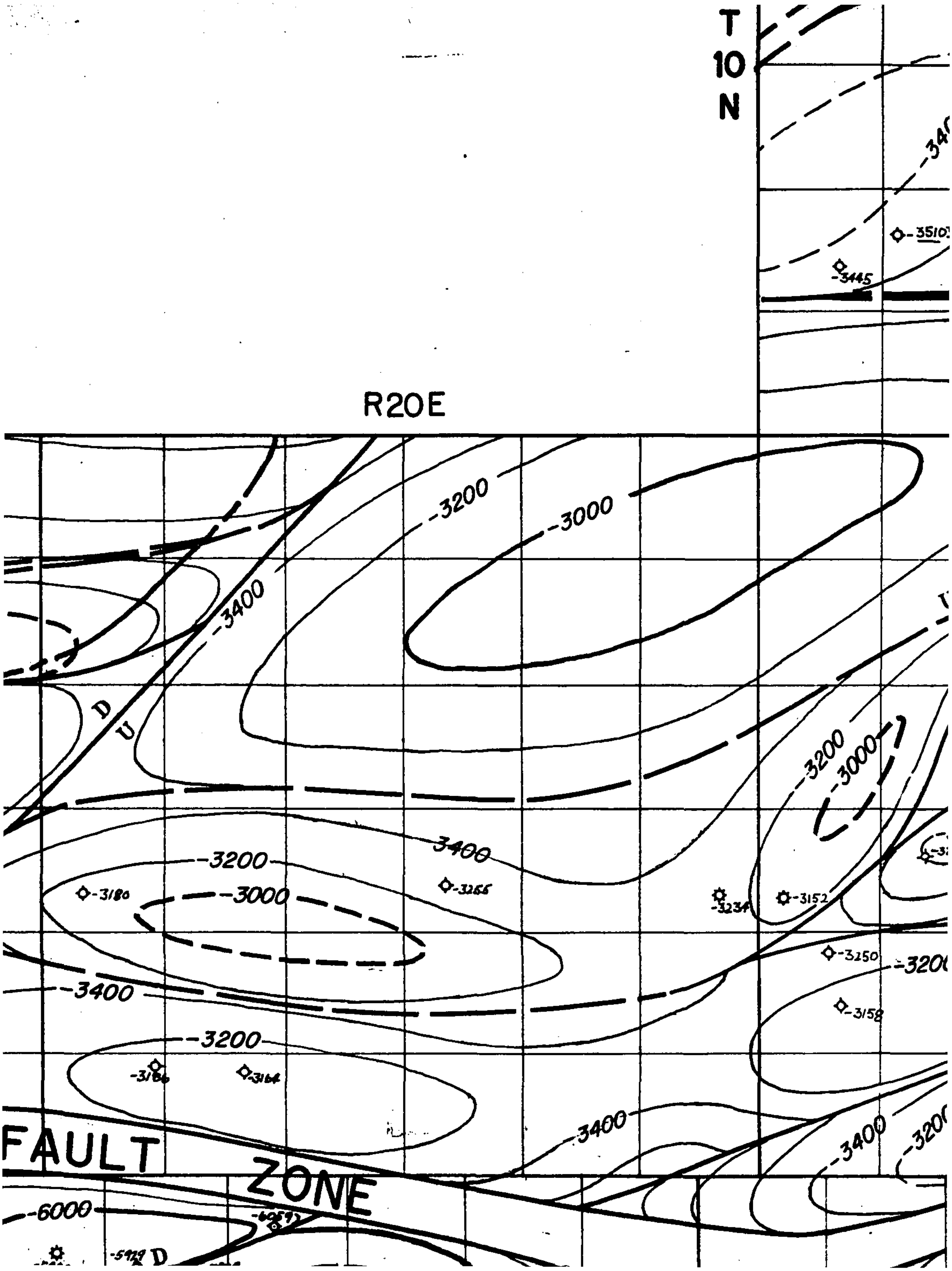
T
10
N
R20E
-3200
-3000
-3400
D
U
-3445
-3180
-3000
-3266
-3234
-3152
-3250
-3158
-3186
-3164
-3200
FAULT
ZONE
-6000
-5929
D

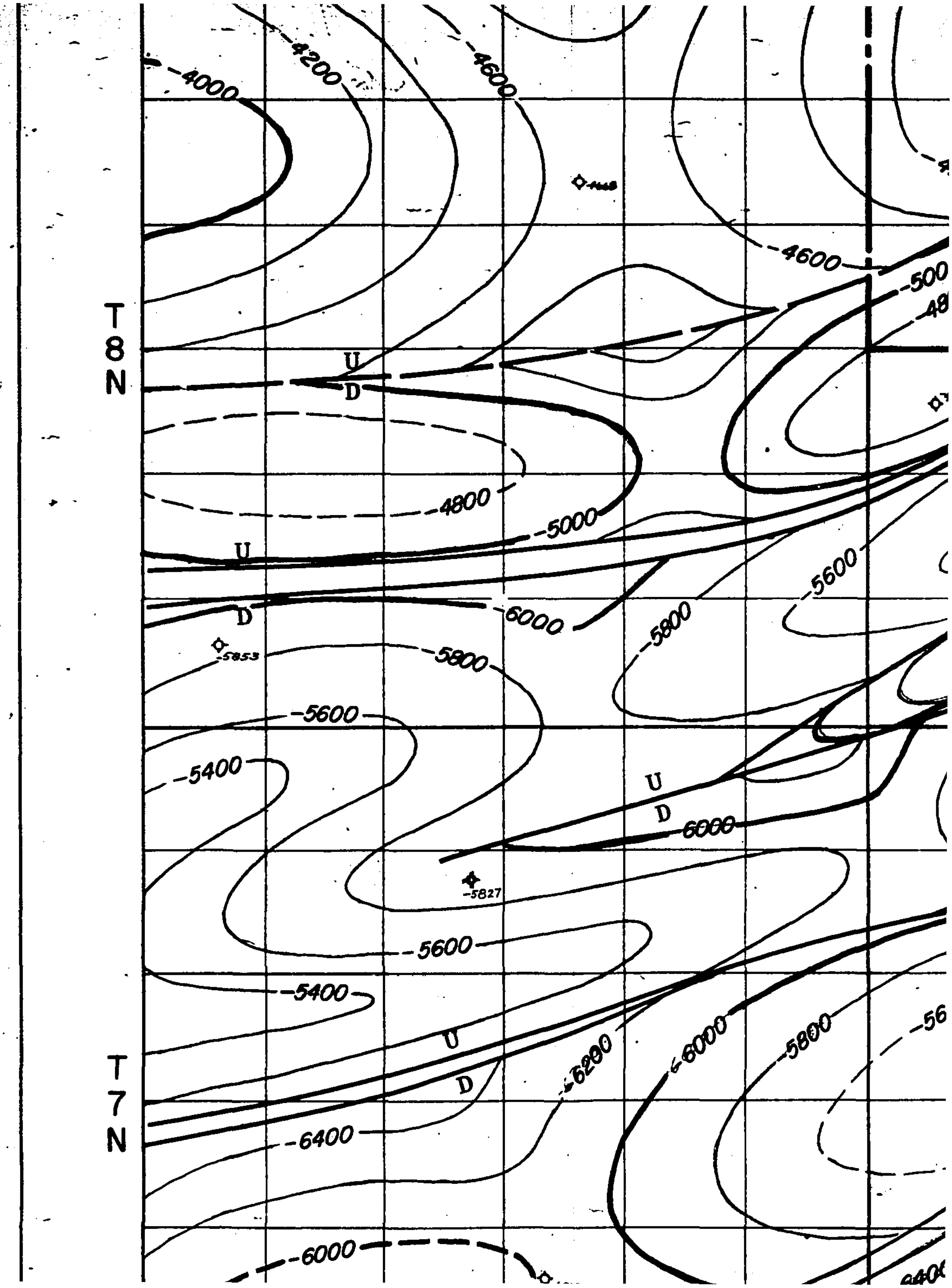
T 8 N
T 7 N
-4000
-4200
-4600
-4600
U
D
-4800
-5000
U
D
-6000
-5600
-5800
-5853
-5800
-5600
-5400
U
D
-6000
-5827
-5600
-5400
U
D
-6200
-6000
-5800
-6400
-6000

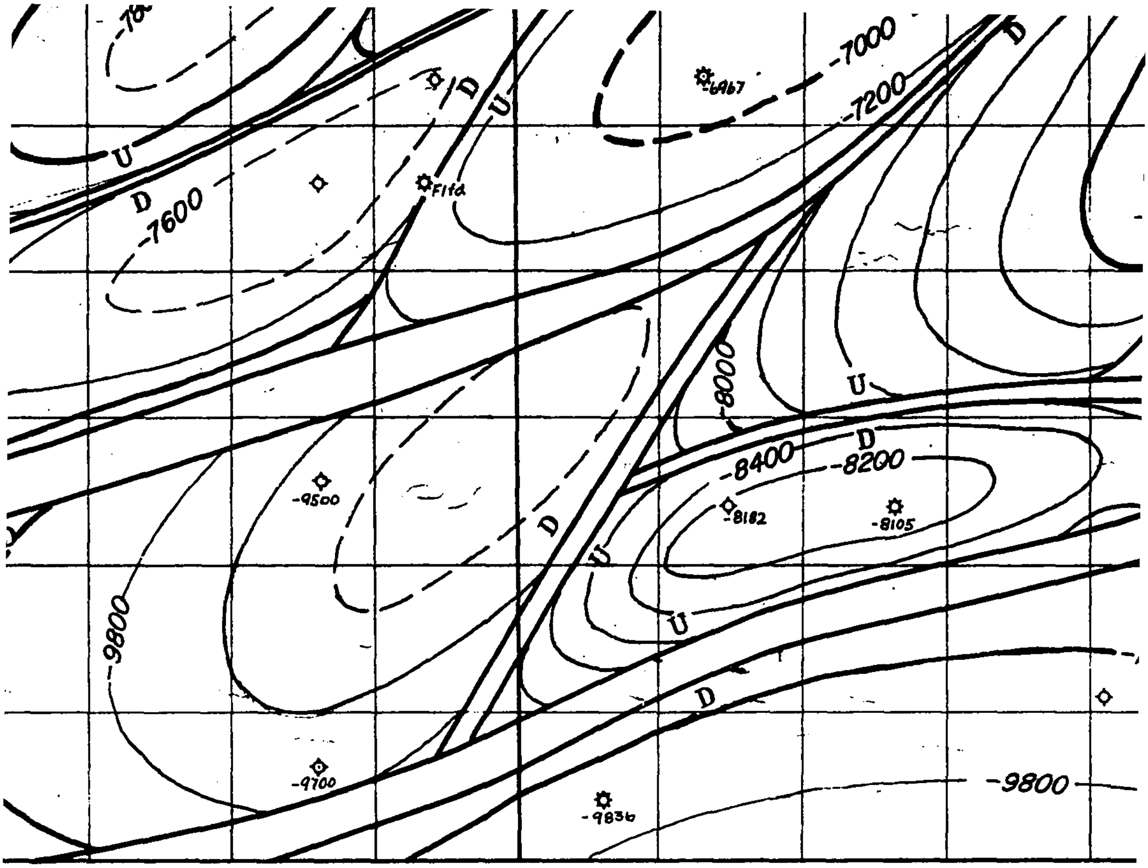
-7000
-7200
-7600
-8000
-8400
-8200
-9800
-9800
-6967
-9500
-8182
-8105
-9700
-9836
U
D

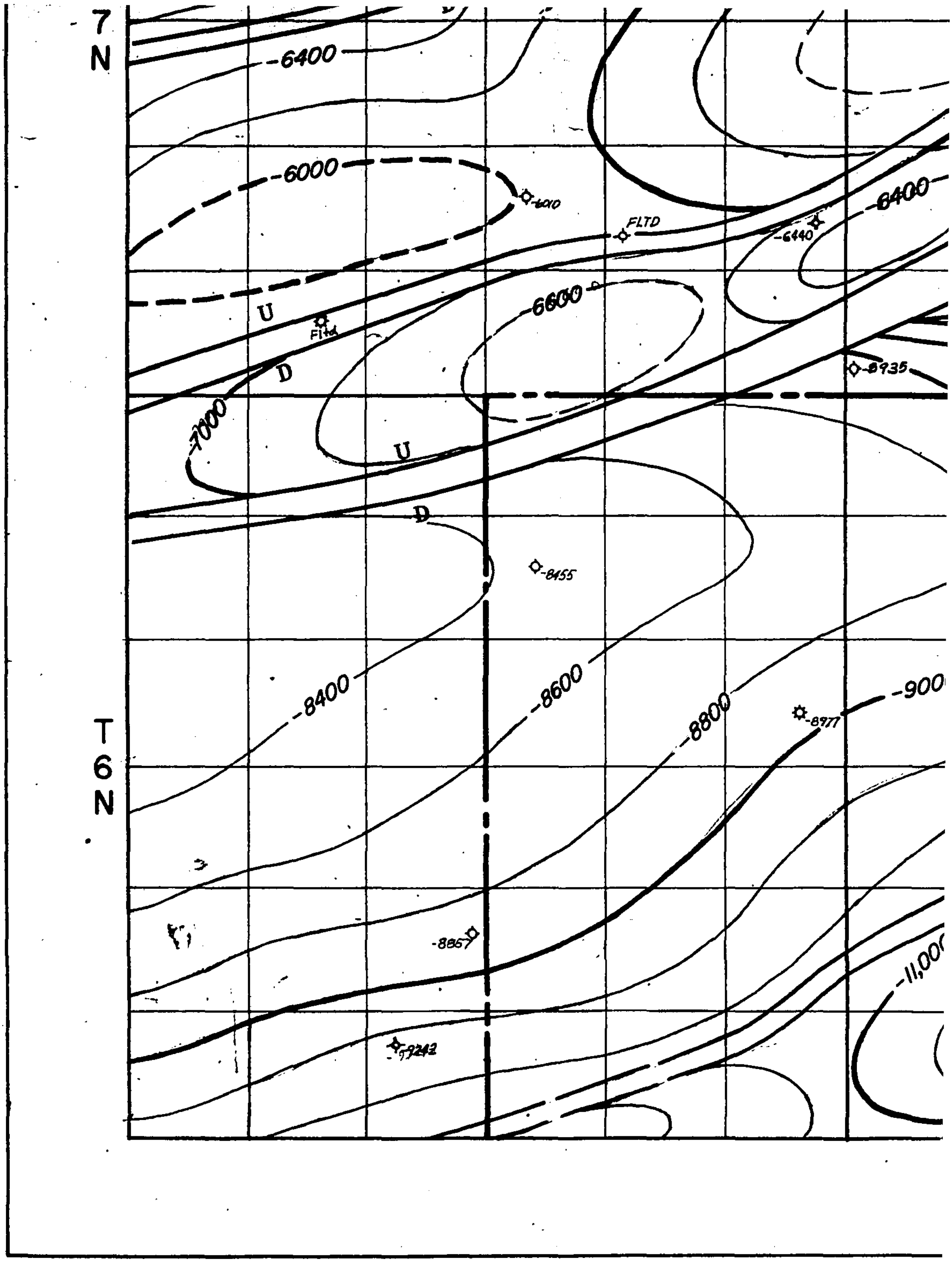
7
N
T
6
N
-6400
-6000
-6010
FLTD
-6440
6400
U
Fltd
-6600
D
-8935
7000
U
D
-8455
-8400
-8600
-8800
-8977
-8867
-9242

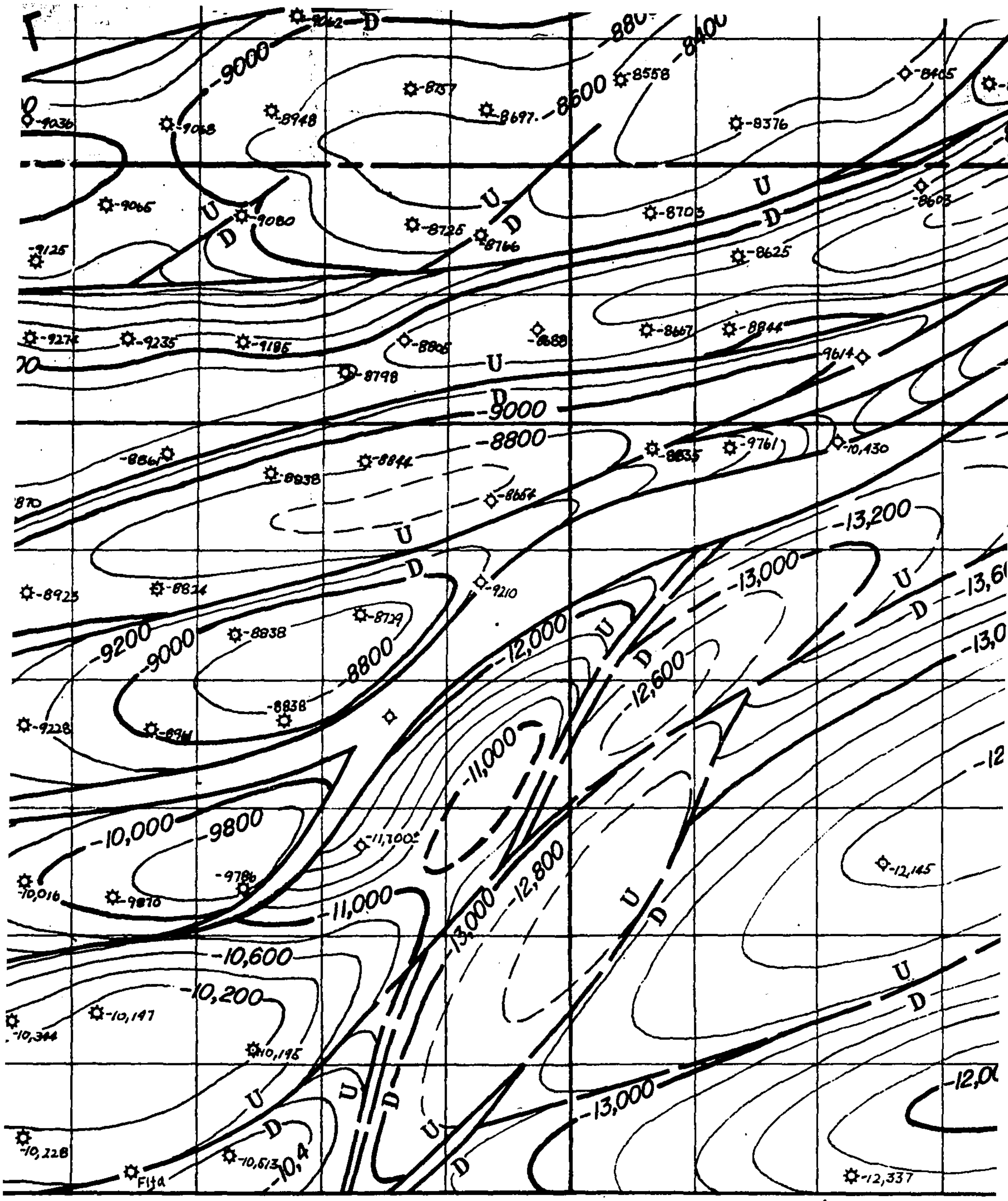

-9062
-9000
-8800
-8400
-8600
-8558
-8405
-8757
-8697
-8376
-9036
-9068
-8948
-9065
-9080
-8726
-8766
-8703
-8608
-9125
-8625
-9274
-9235
-9186
-8808
-8688
-8667
-8844
9614
-8798
-9000
-8800
-8861
-8838
-8844
-8835
-9761
-10,430
-8664
-13,200
-13,000
-8925
-8824
-9210
-8729
-9200
-9000
-8838
-8800
-12,000
-12,600
-8838
-9228
-11,000
-10,000
-9800
-11,300
-9786
-10,016
-9870
-11,000
-13,000
-12,800
-12,145
-10,600
-10,200
-10,147
-10,344
-10,195
-13,000
-10,228
-10,613
-10,4
Fita
-12,337
U
D

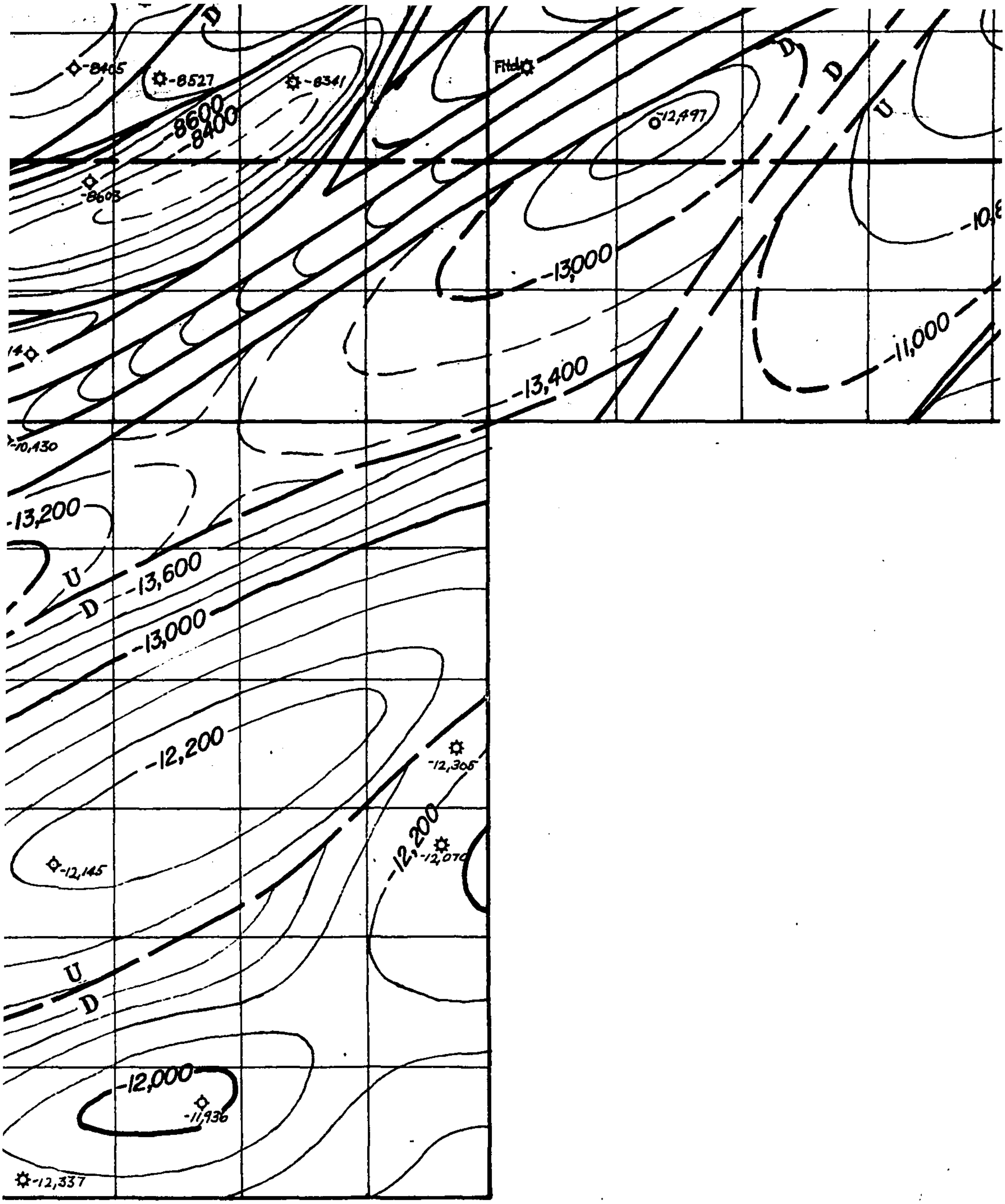

-8405
-8527
-8341
-8600
-8400
-8608
-12,497
D
U
-13,000
-11,000
-13,400
-10,430
-13,200
-13,600
-13,000
-12,200
-12,305
-12,200
-12,070
-12,145
-12,000
-11,936
-12,337

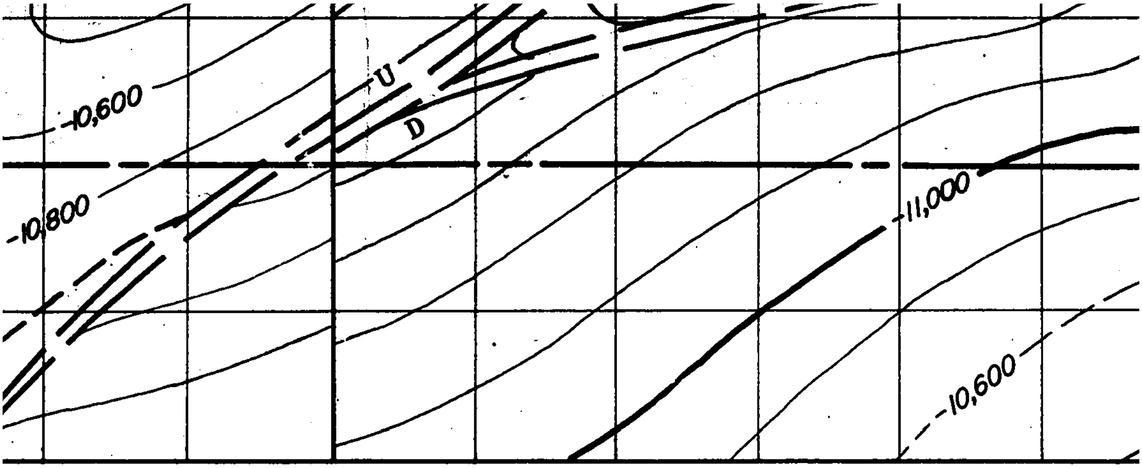

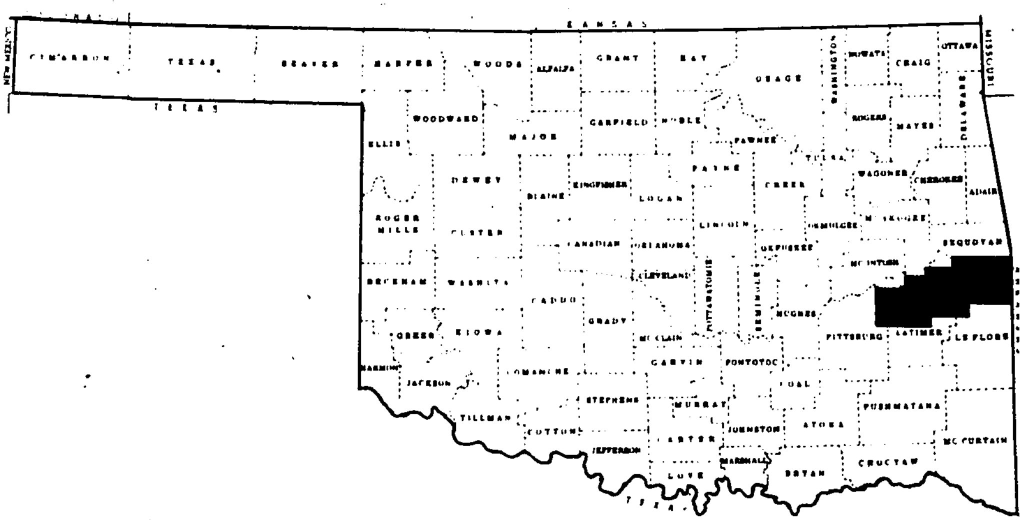

Index map showing study area mapped.

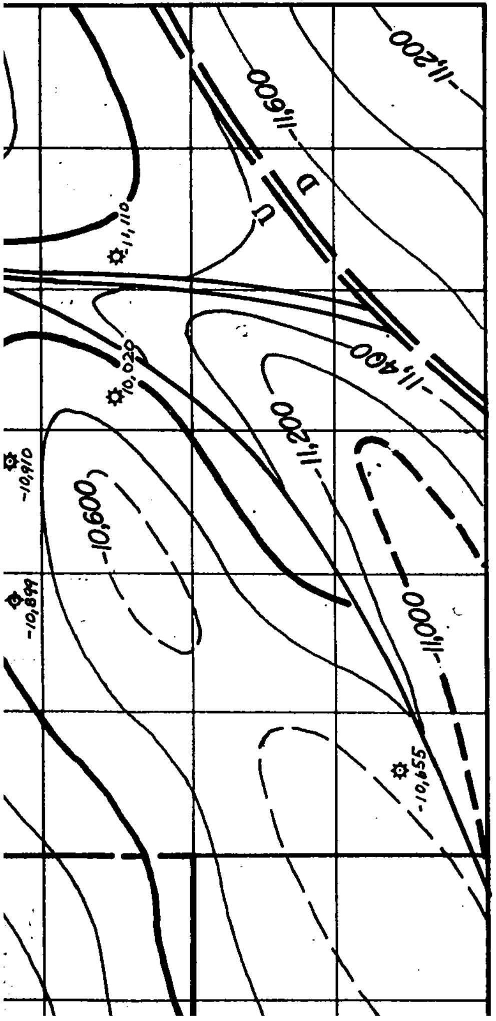
-11,200
-11,600
U
D
-11,110
-11,400
-10,020
-11,200
-10,910
-10,600
-10,899
-11,000
-10,655

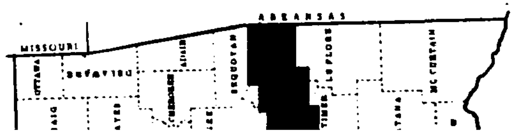
MISSOURI
ARKANSAS

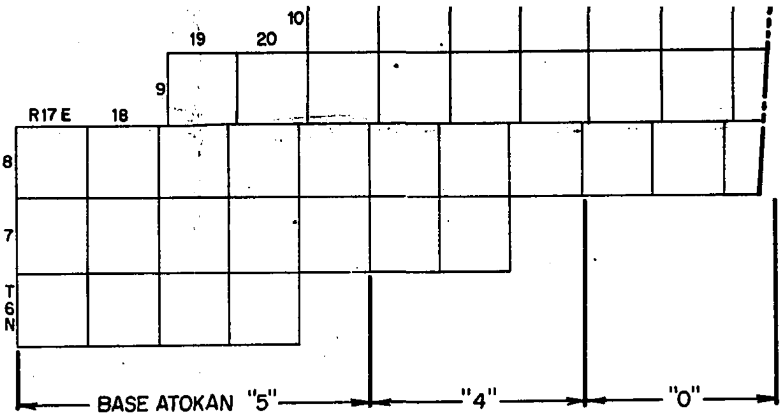

-5000 Subsea value of mapped datum

Synclinal area

Fault

PLAT

STRUCTU

BASAL

ARKOMA BASIN, E

CONTOUR INTE

0 1 2

Scale

University of Oklahoma Ph.D. 1977

_ATE VII

TURE MAP OF

L ATOKAN

I, EASTERN OKLAHOMA

NTERVAL: 200 FEET

3 4 5 6

Scale in miles

77

M. W. Mc Quillan

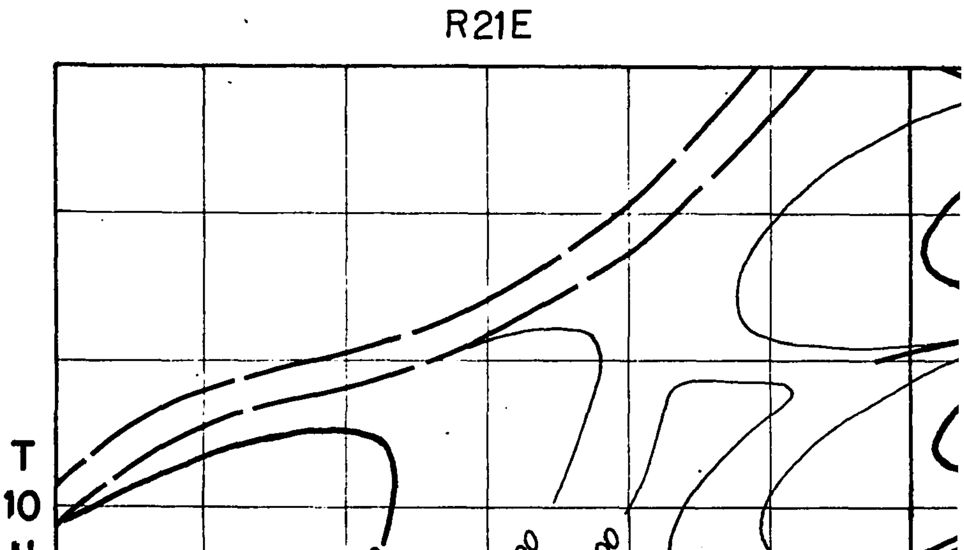
R21E
T
10

R22E

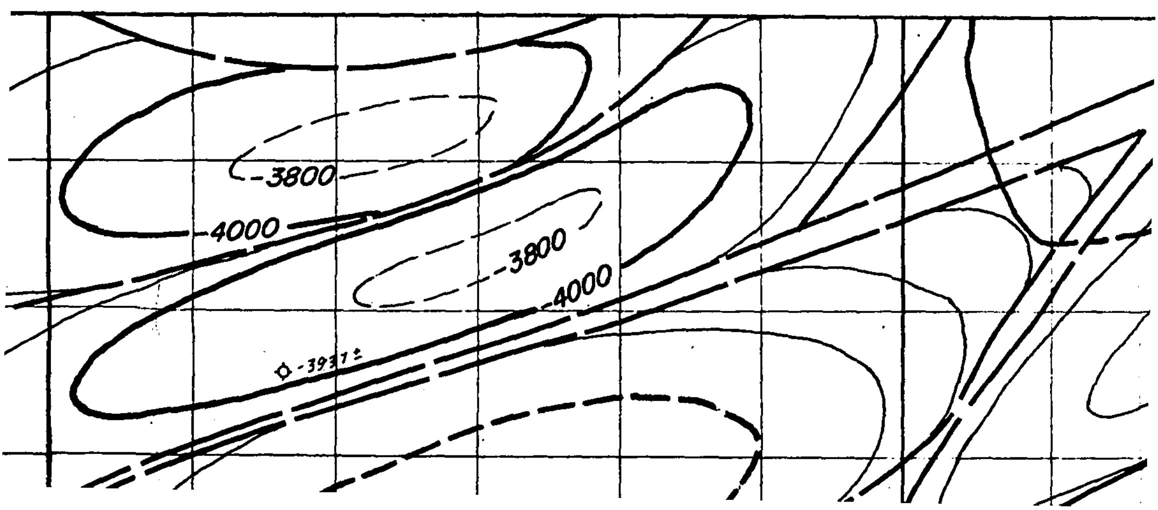

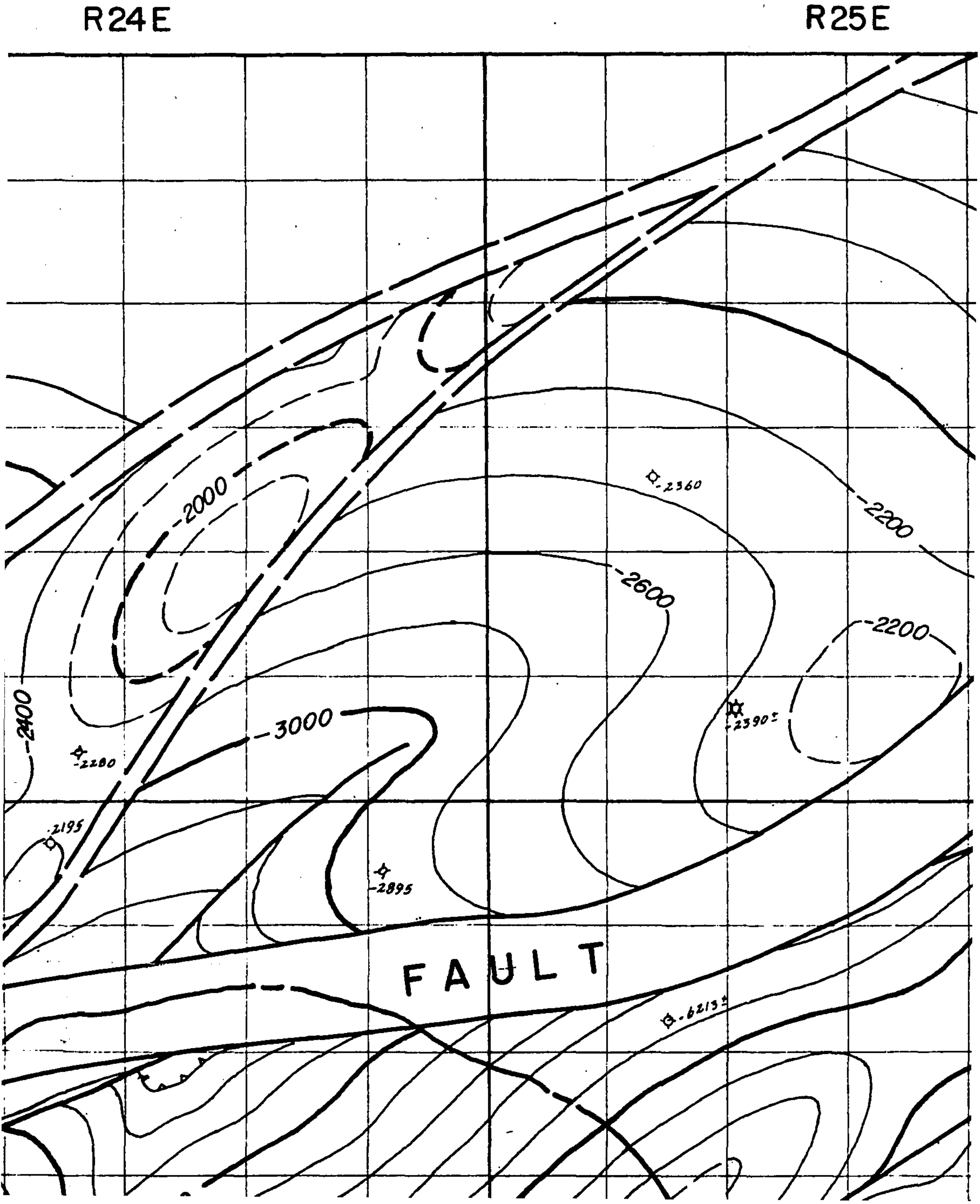
R24E
R25E
-2000
-2200
-2200
-2600
-3000
-2400
-2360
-2390±
-2280
-2195
-2895
-6213±
FAULT

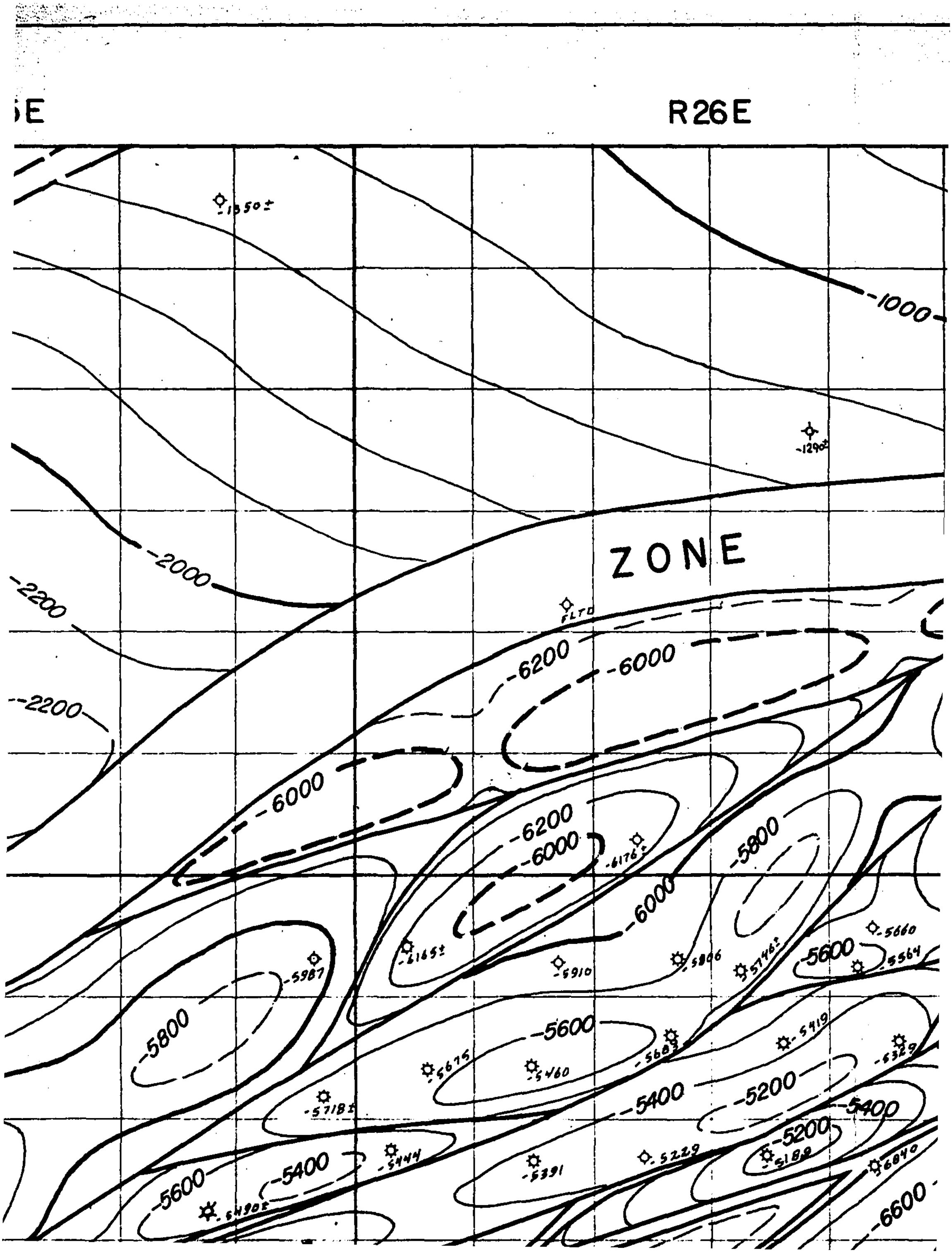

E
R26E
-1350±
-1000
-1290±
-2000
-2200
-2200
ZONE
FLTD
-6200
-6000
-6000
-6200
-6000
-6176±
-5800
-6000
-5660
-5600
-5564
-5987
-6165±
-5910
-5806
-5746±
-5800
-5600
-5419
-5683
-6329
-5675
-5460
-5718±
-5400
-5200
-5400
-5200
-5444
-5400
-5391
-5229
-5189
-6840
-5600
-5490±
-6600

R17E

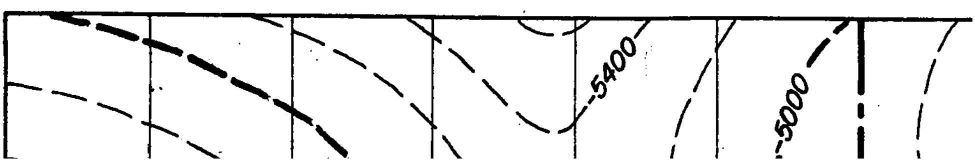

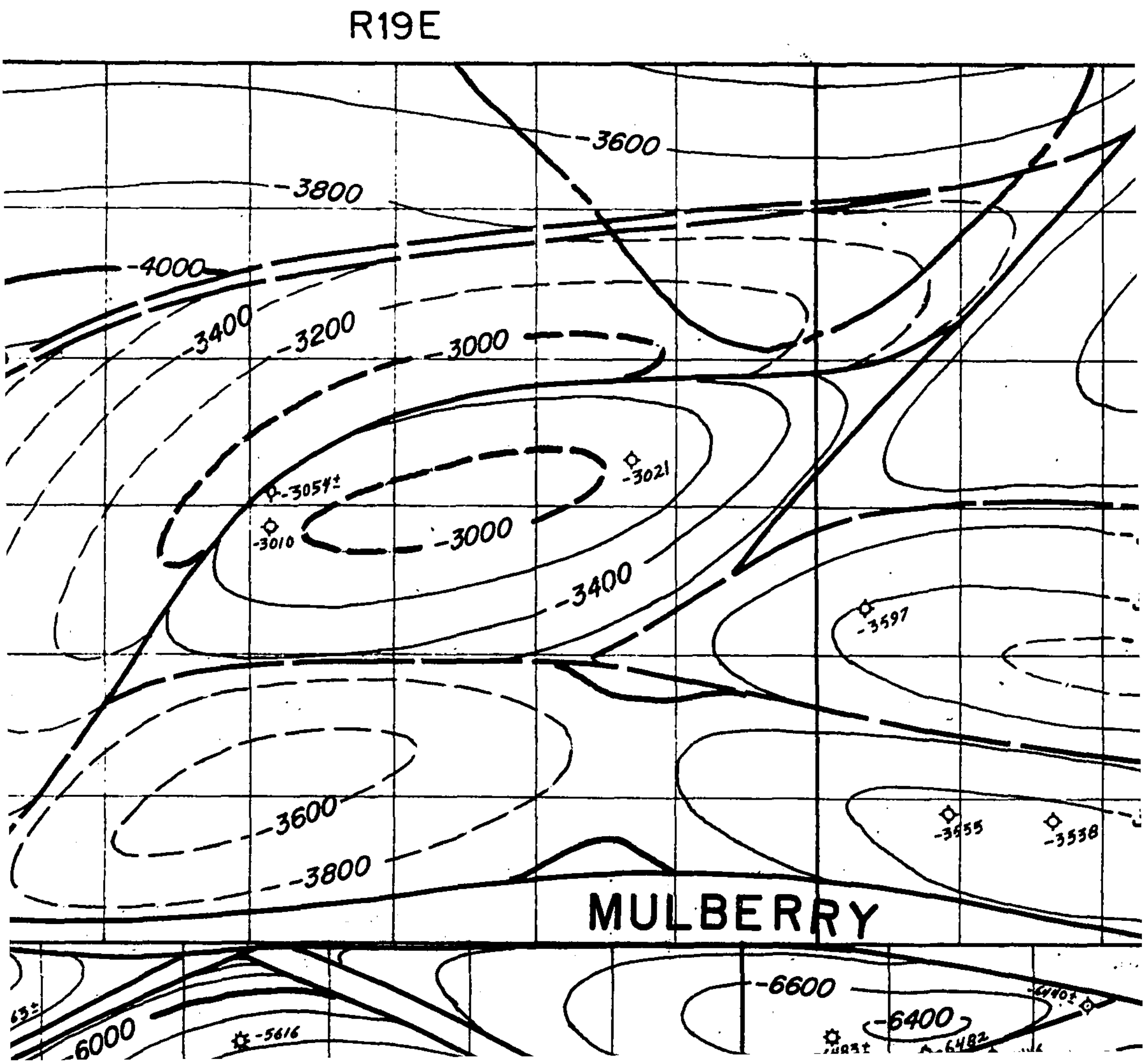
R19E
3600
3800
4000
3400
3200
3000
-3054±
-3021
-3010
-3000
-3400
-3597
3600
3800
-3555
-3538
MULBERRY
-6600
-6400
-6000
-5616
-6482

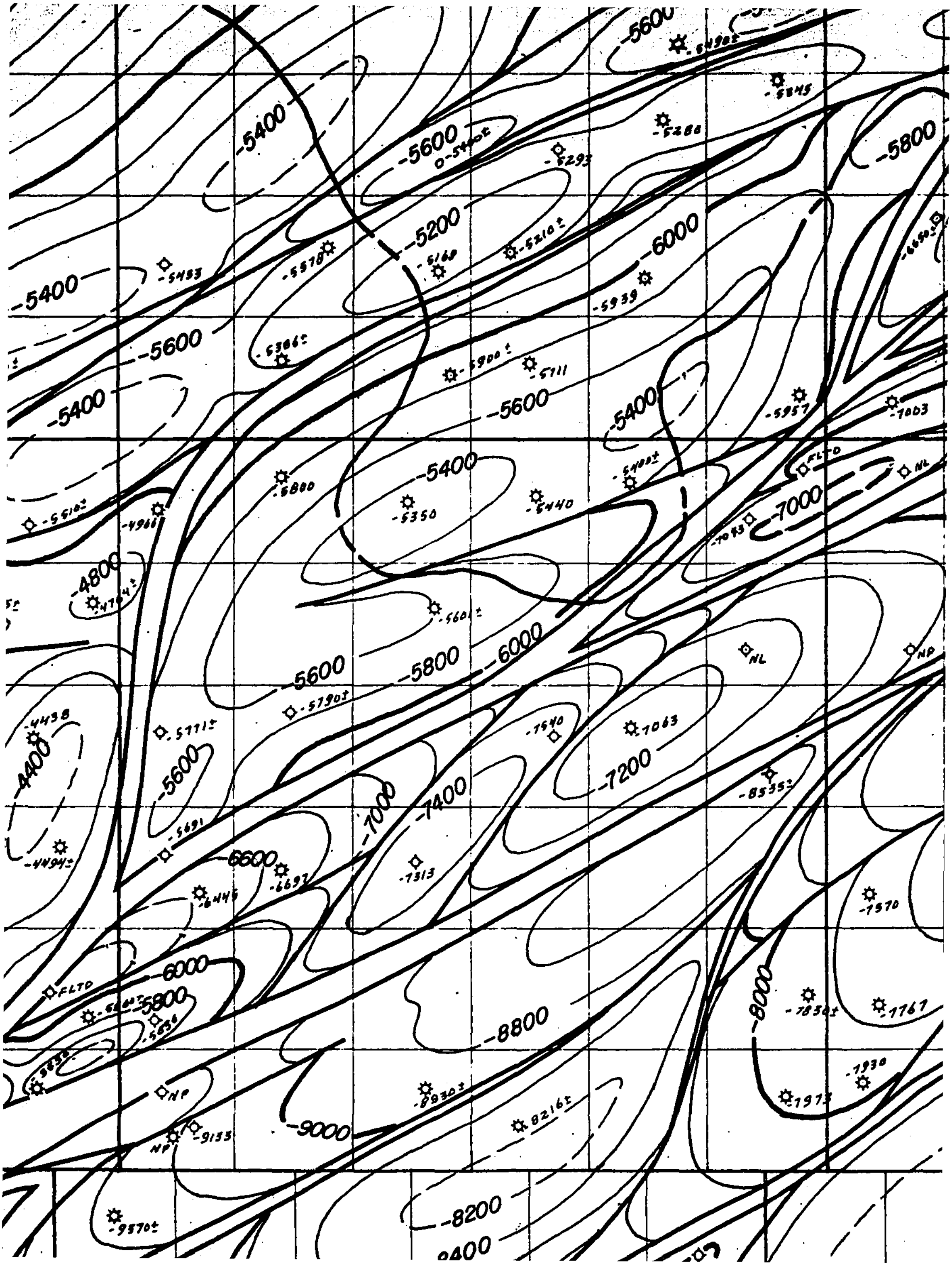

-5600
-5400
-5600
-5800
-5200
-6000
-5400
-5600
-5400
-5600
-5400
-5400
-4800
-7000
-5600
-5800
-6000
-4400
-5600
-7200
-7400
-7000
-6600
-6000
-5800
-8000
-8800
-9000
-8200
-5293
-5288
-5845
-5453
-5939
-5711
-5880
-5350
-5440
-5957
-7063
-4966
-5601±
-5790±
-5771±
-4438
-4494±
-5691
-7540
-7063
-8535±
-7313
-6693
-6445
-7570
-7836±
-7767
-7930
-7973
-8930±
-8216±
-9133
-9370±

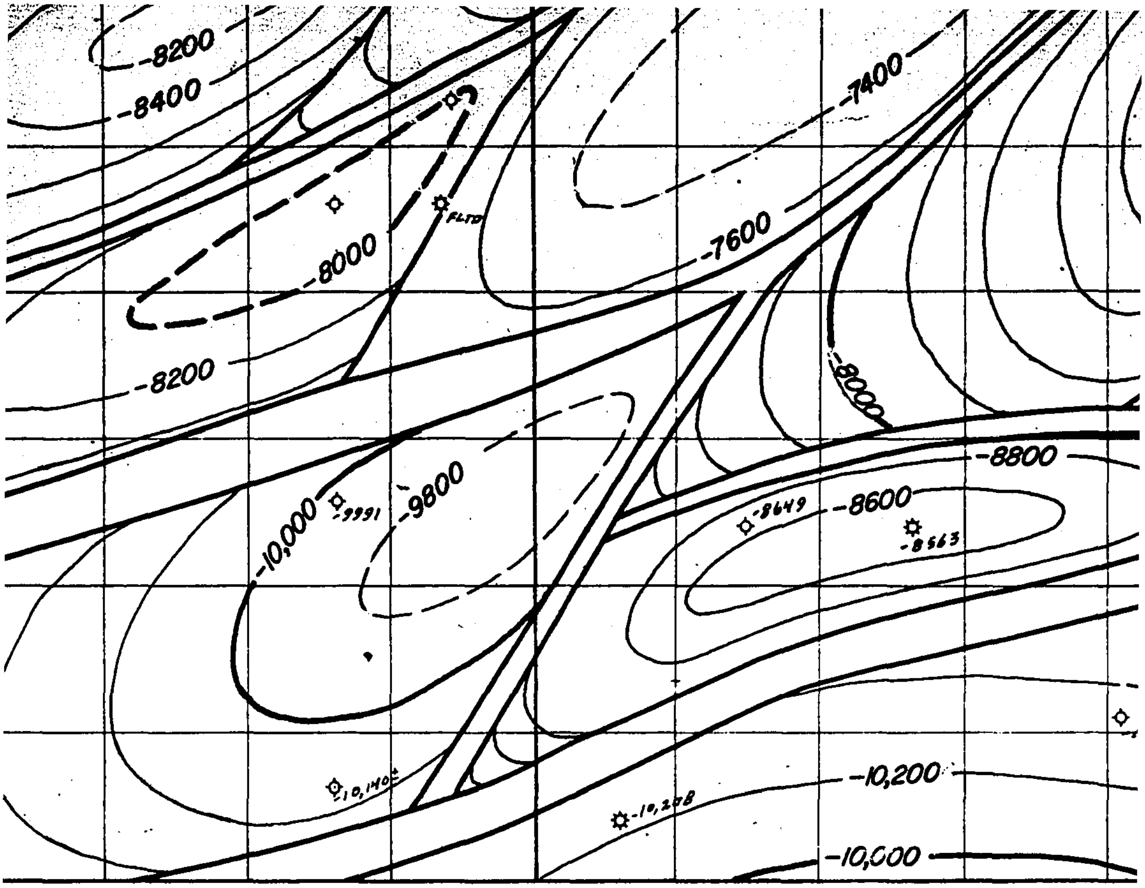
-8200
-8400
-8000
FLTD
-8200
-7400
-7600
-8000
-8800
-8649
-8600
-8563
-9800
-9991
-10,000
-10,140±
-10,278
-10,200
-10,000

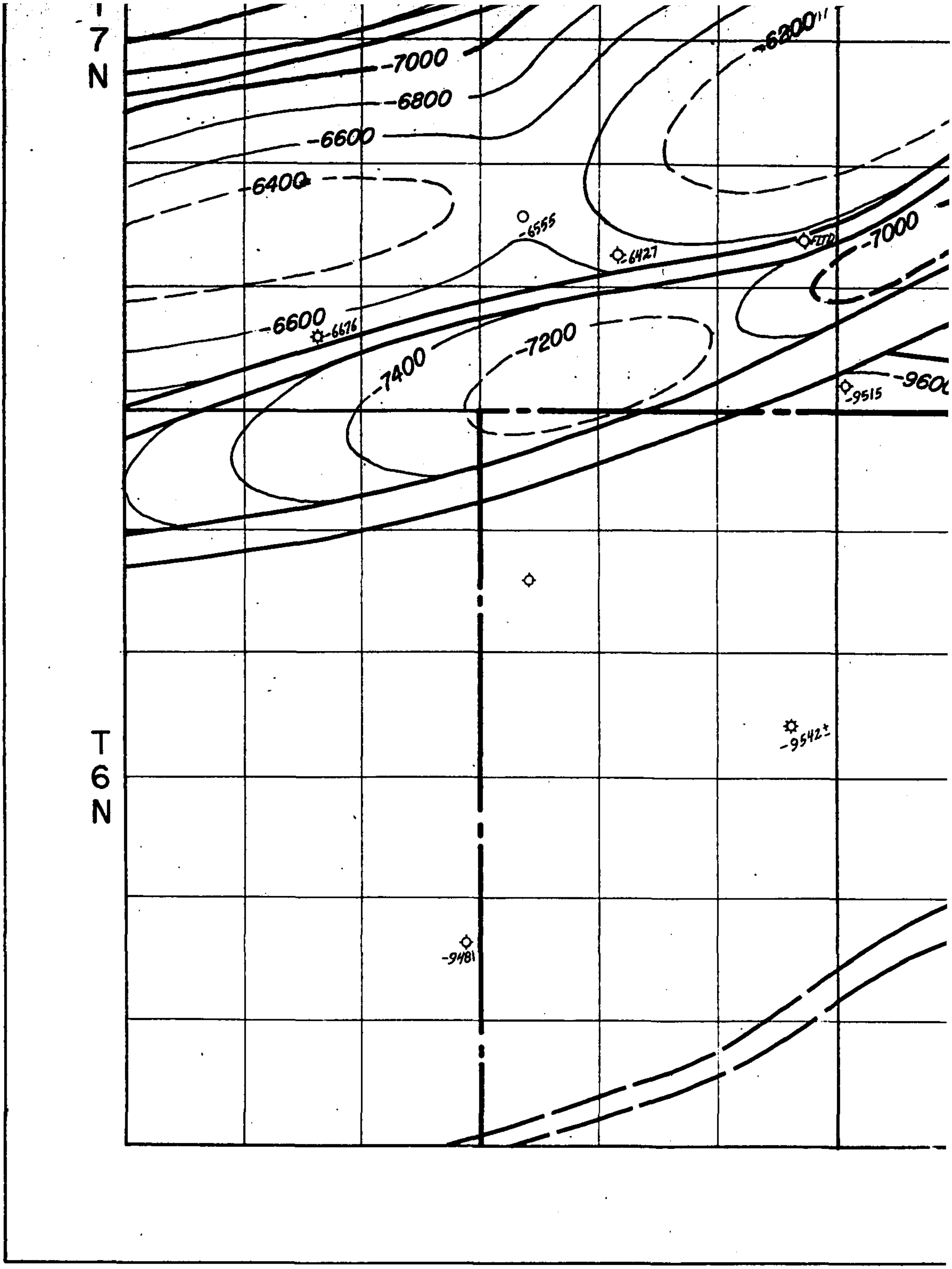

T 7 N
-7000
-6800
-6600
-6400
-6200
-6555
-6427
-6600
-6676
-7000
-7200
-7400
-9600
-9515
T 6 N
-9542±
-9481

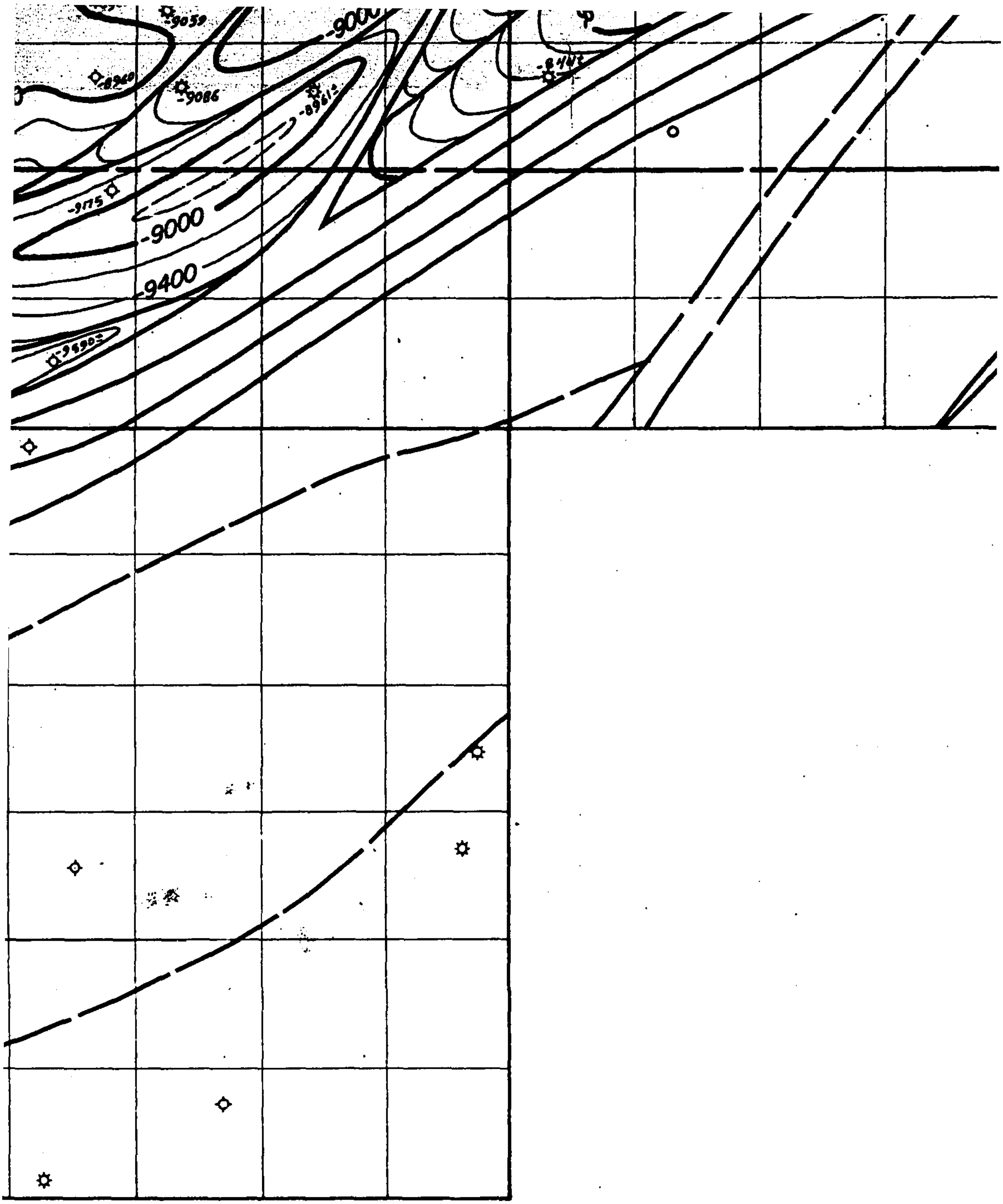
-9059
-9000
-8940
-9086
-8961
-8442
-9175
-9000
-9400

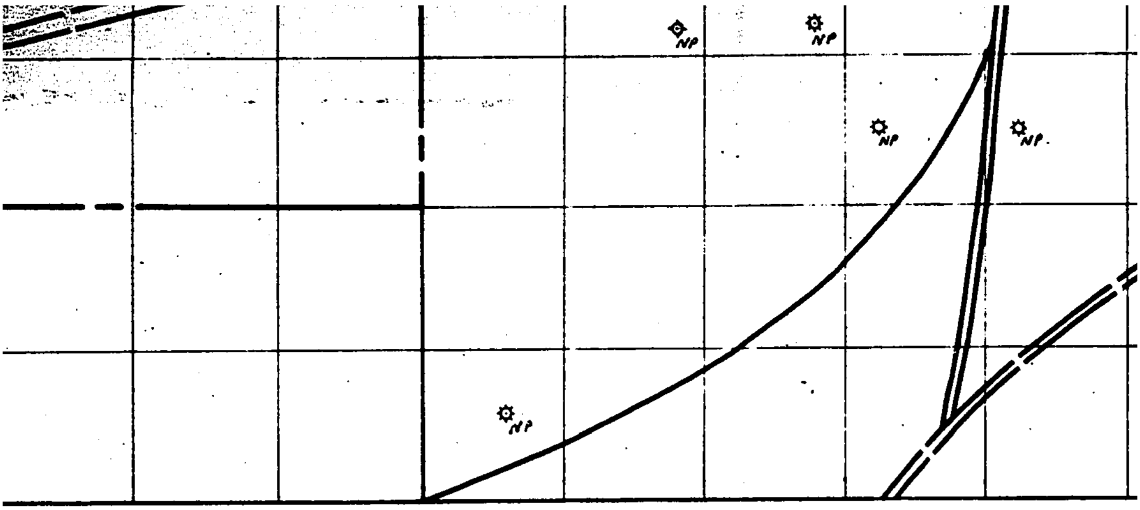
NP
NP
NP
NP
NP

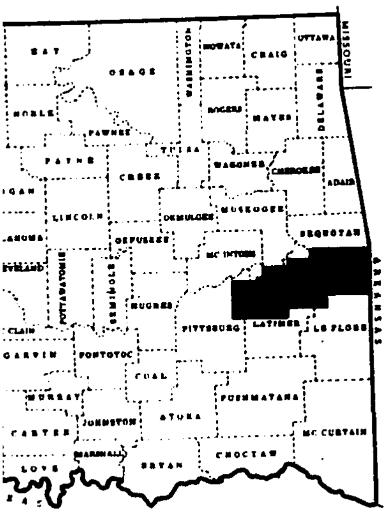
KAY
OSAGE
WASHINGTON
NOWATA
CRAIG
OTTAWA
MISSOURI
NOBLE
PAWNEE
ROGERS
MAYES
DELAWARE
PAYNE
CREEK
WAGONER
CHEROKEE
ADAIR
LINCOLN
OKMULGEE
MUSKOGEE
SEQUOYAH
OKFUSKEE
MC INTOSH
POTTAWATOMIE
SEMINOLE
HUGHES
PITTSBURG
LATIMER
LE FLORE
ARKANSAS
GARVIN
PONTOTOC
COAL
MURRAY
PUSHMATAHA
JOHNSTON
ATOKA
CARTER
MC CURTAIN
MARSHALL
LOVE
BRYAN
CHOCTAW

area mapped.

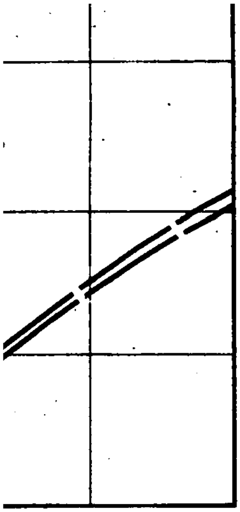

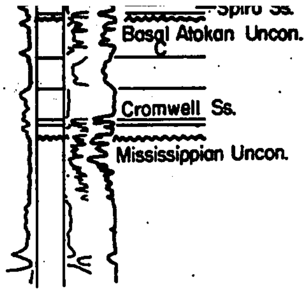

TYPE LOG

-6000 Subsea value of mapped datum

Synclinal area

Fault

PLATE VIII

RUCTURE MAP OF

MARKER (MORROW)

ASIN, EASTERN OKLAHOMA

TOUR INTERVAL: 200 FEET

2 3 4 5 6

Scale in miles

h. D. 1977 M. W. McQuillan

R21E

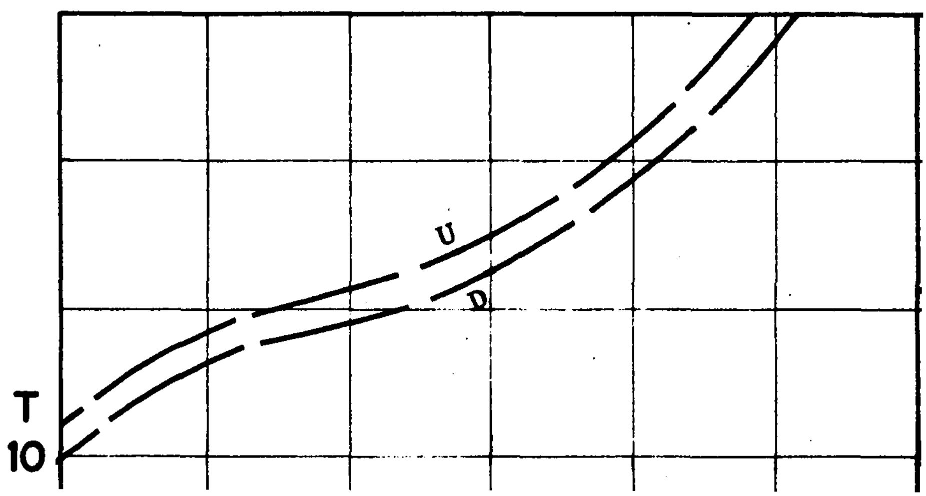

R22E

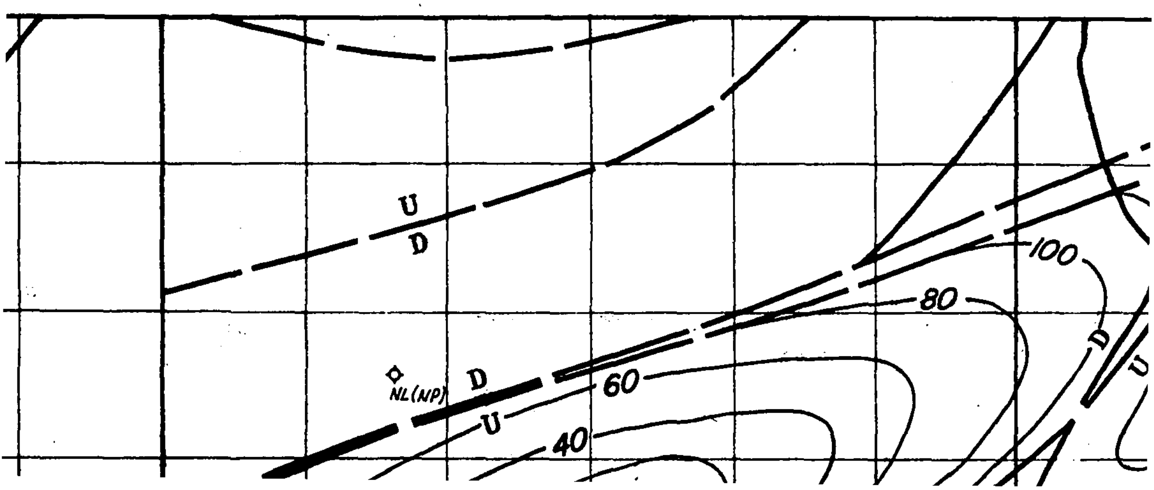

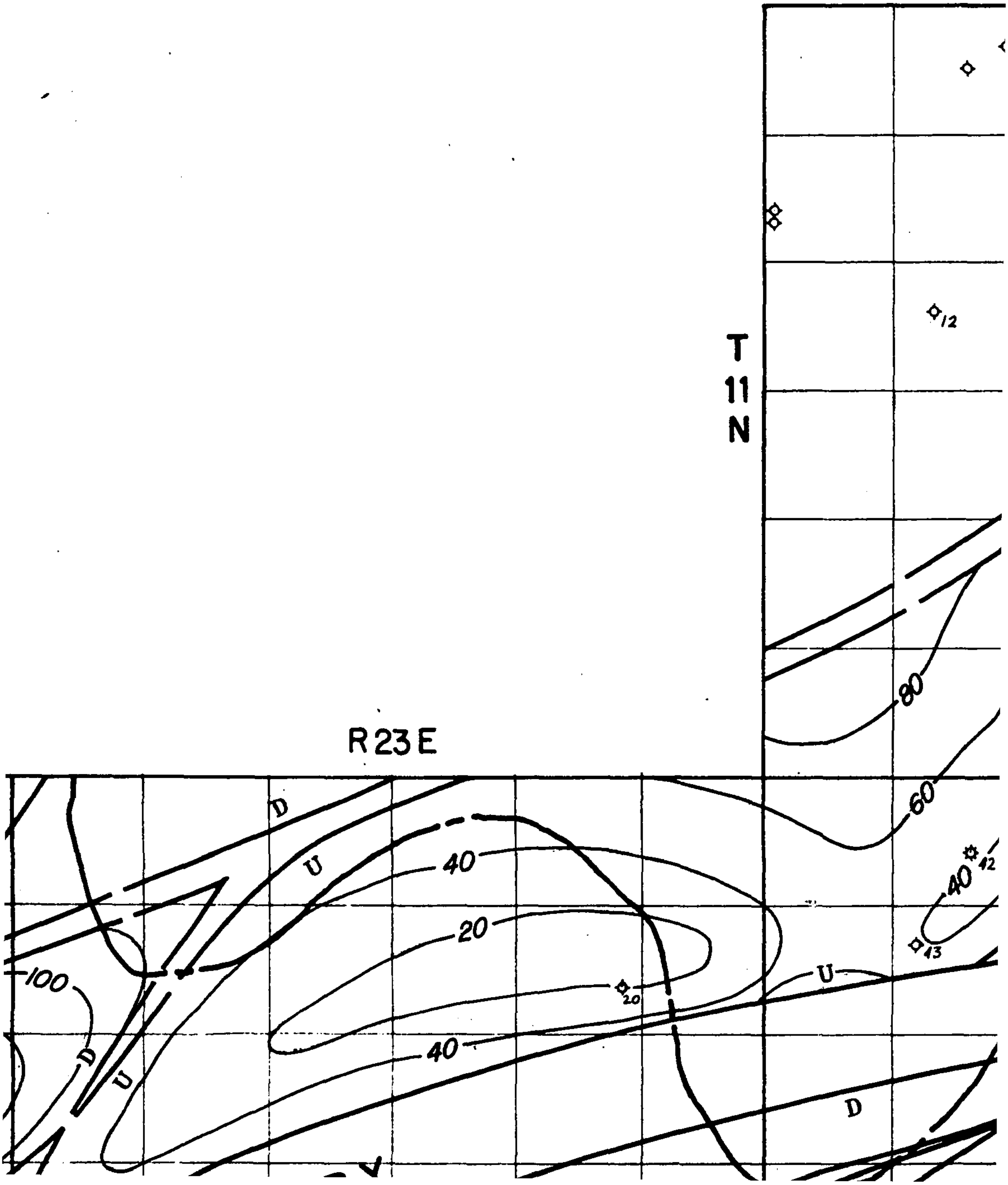

R23E
T
11
N
D
U
40
20
100
80
60
40
20
D
U
40
12
42
43
U
D

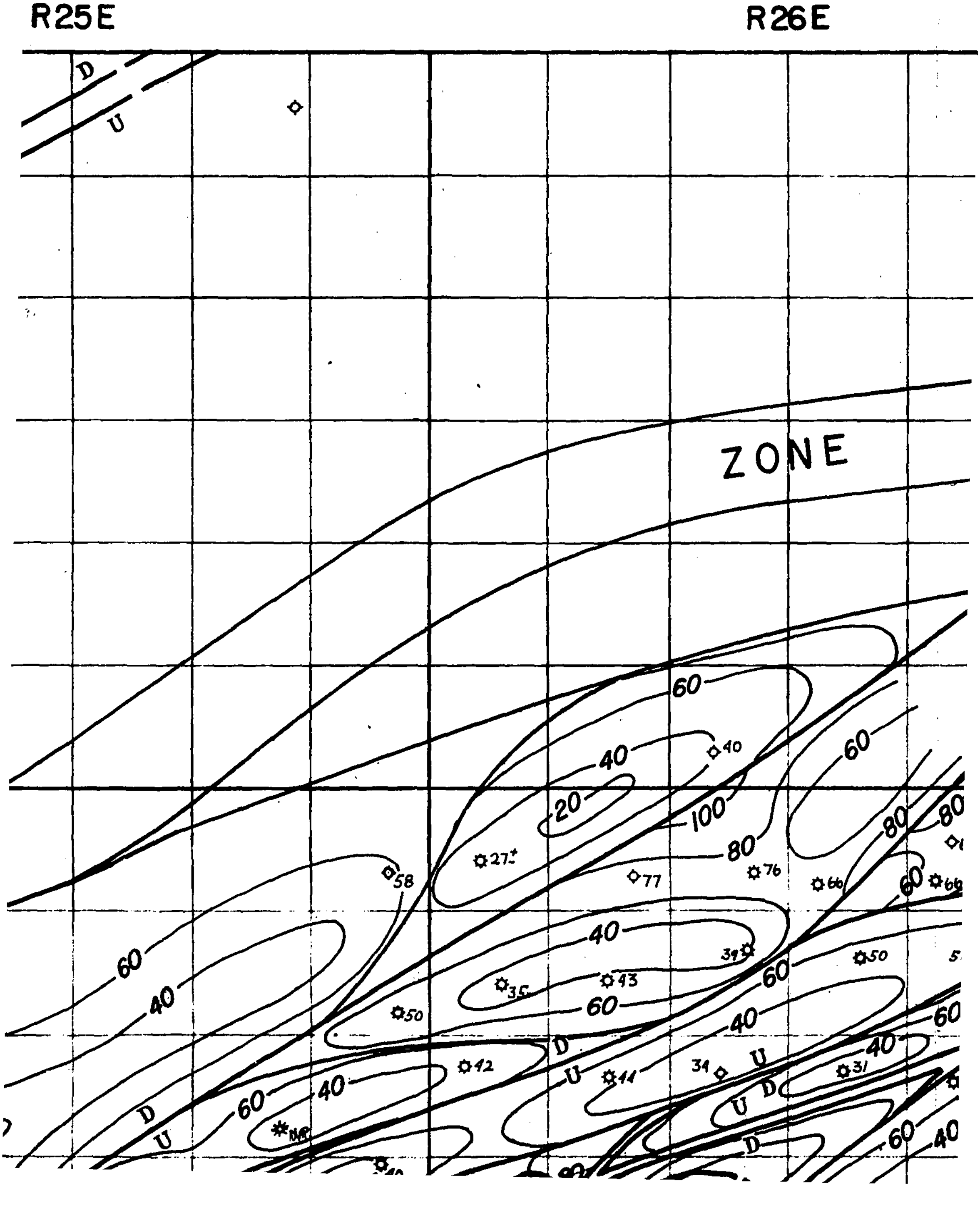
R25E
R26E
ZONE
D
U
60
40
20
100
80
27±
40
58
77
76
66
35
43
50
42
44
34
31
NP

R17E

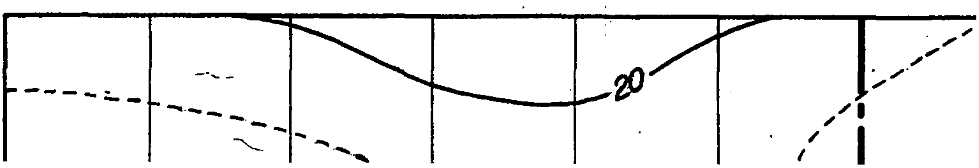

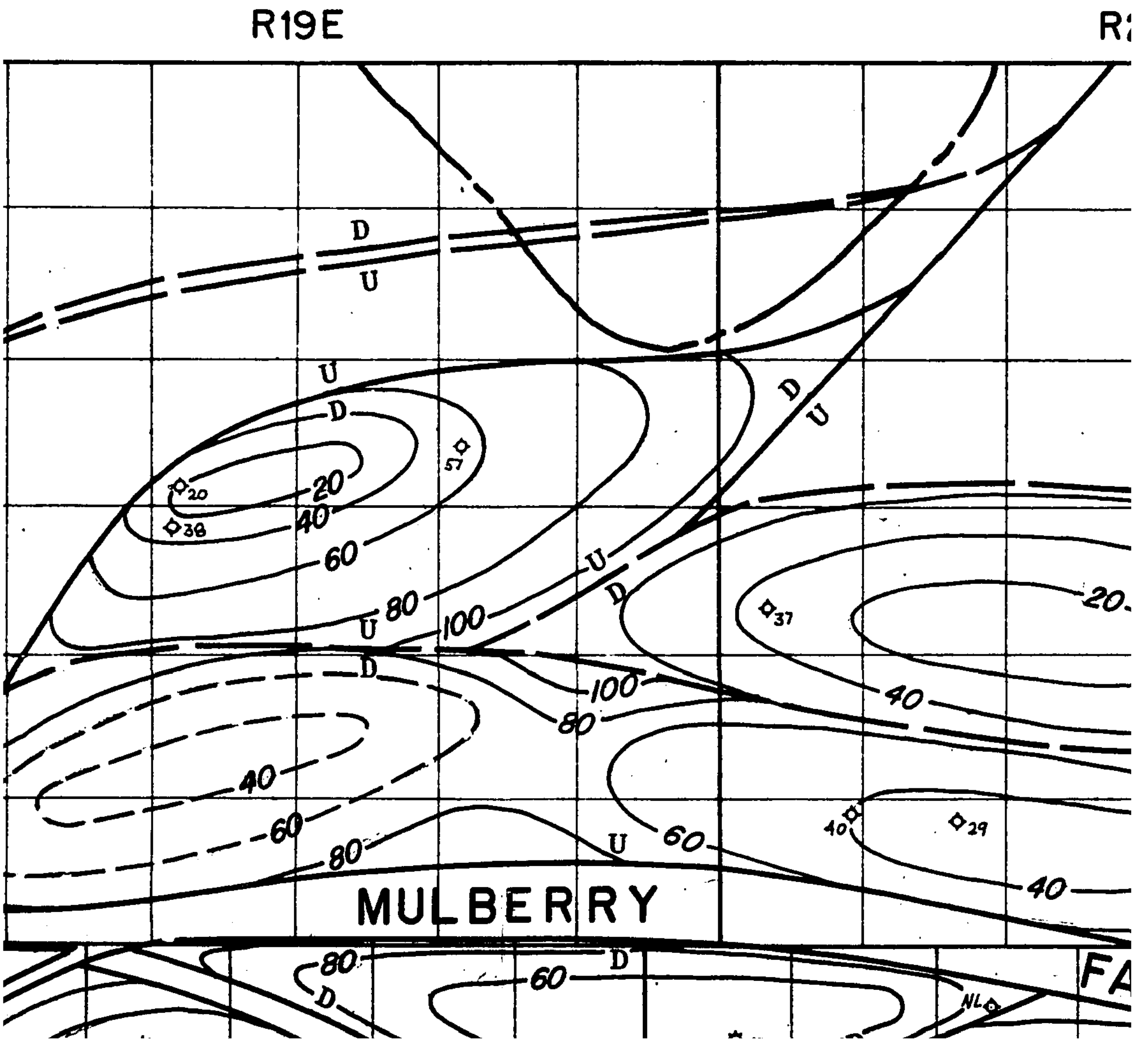
R19E
D
U
U
D
20
40
60
80
100
U
D
D
U
U
D
20
40
100
80
40
60
80
U
60
40
MULBERRY
80
60
D
D

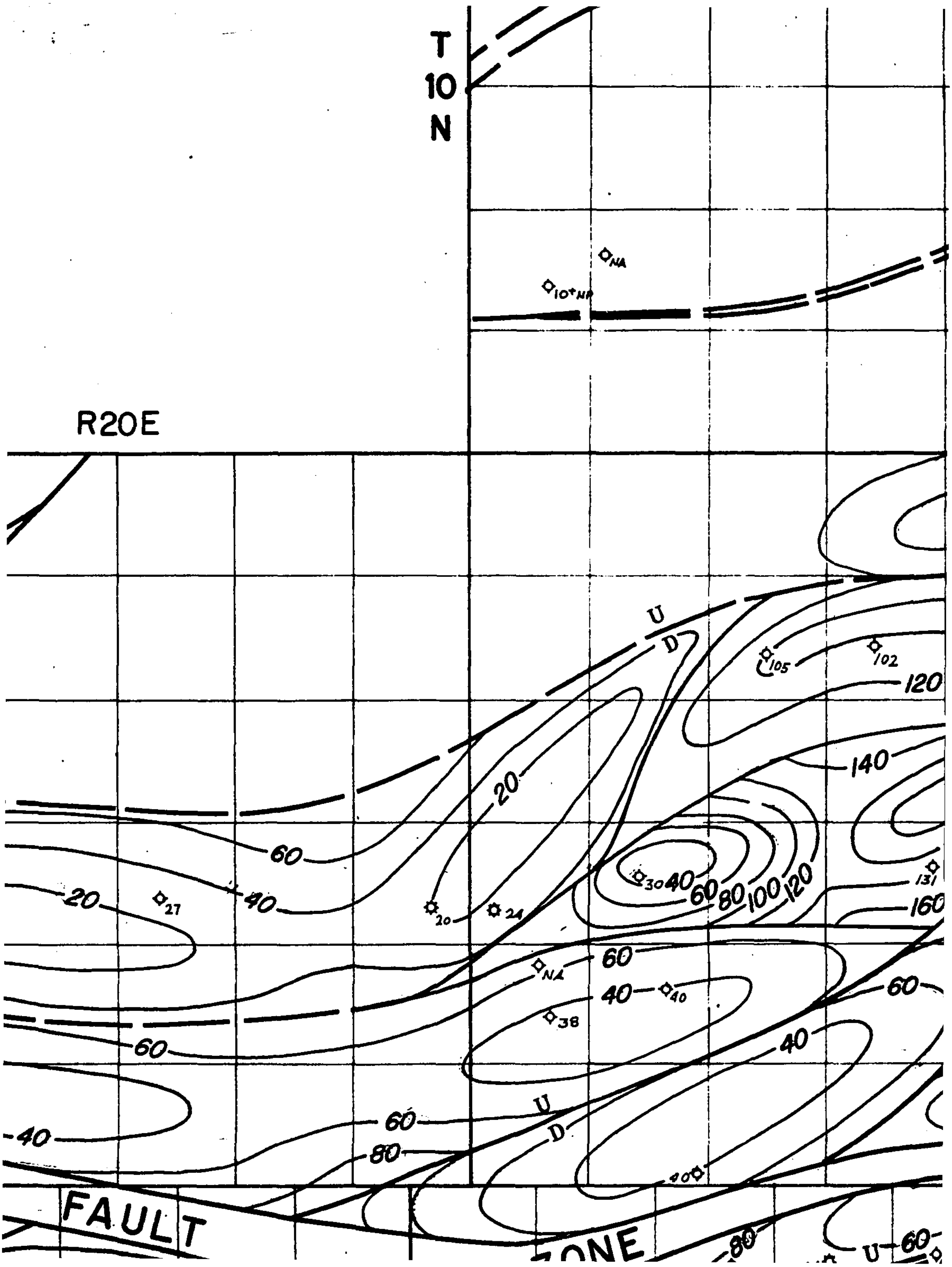

T
10
N
R20E
NA
U
D
105
102
120
140
20
60
40
20
27
20
24
30
40
60
80
100
120
131
160
60
NA
40
40
38
60
40
60
U
D
40
60
80
40
FAULT
ZONE
80
U
60

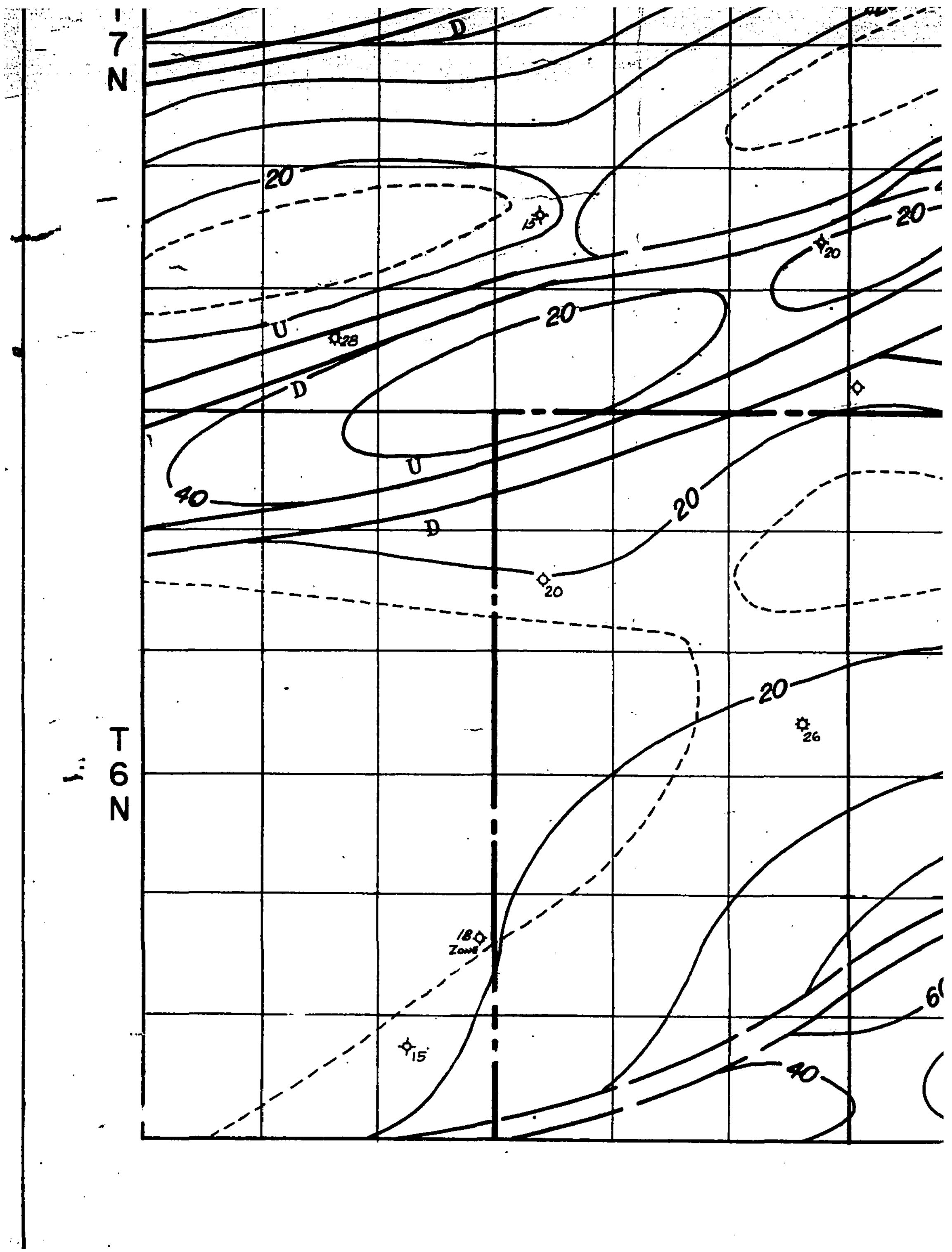
T
7
N
T
6
N
20
20
20
20
20
20
20
40
40
60
U
U
D
D
D
15
28
20
26
18
Zone
15

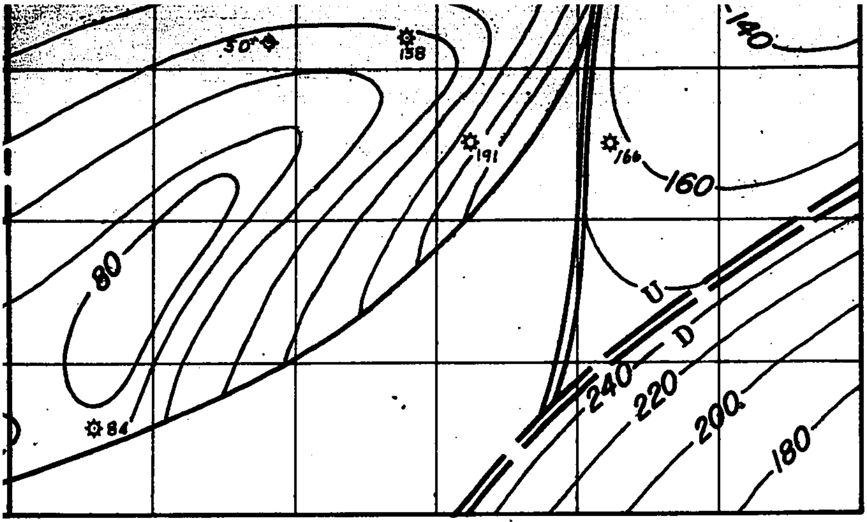

140
160
80
U
D
240
220
200
180
158
191
166
84

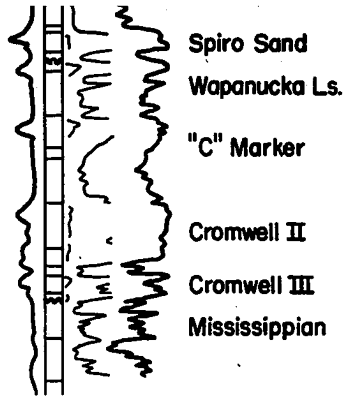

Key Straigraphic Section

ϕ_{40} Thickness in feet
Zn Shaley and mapped as zone
Brkn Interbedded sand and shale
NP Not penetrated
NL Not logged
NA Log not available

Area where Spiro Sand is shaley

Fault

PLATE IX

ISOPACHOUS MAP OF

SPIRO "A" SAND

ARKOMA BASIN, EASTERN OKL

CONTOUR INTERVAL: 20 FEET

0 1 2 3 4 5

Scale in miles

University of Oklahoma Ph.D. 1977

K

MAP OF

SAND

ERN OKLAHOMA

.: 20 FEET

4 5 6

M. W. Mc Quillan

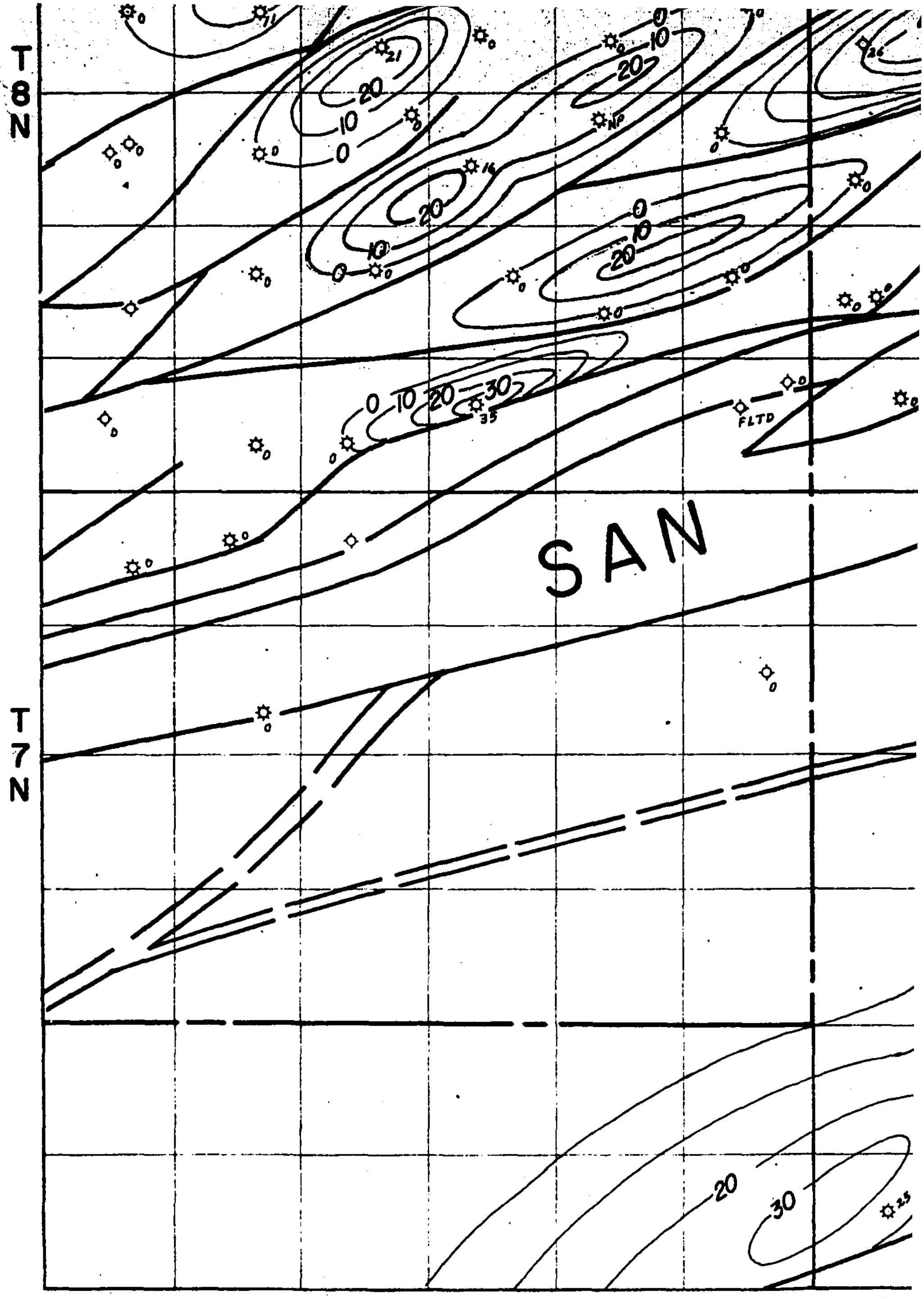

T 8 N
T 7 N
SAN
FLTD
NP
0
10
20
30
35

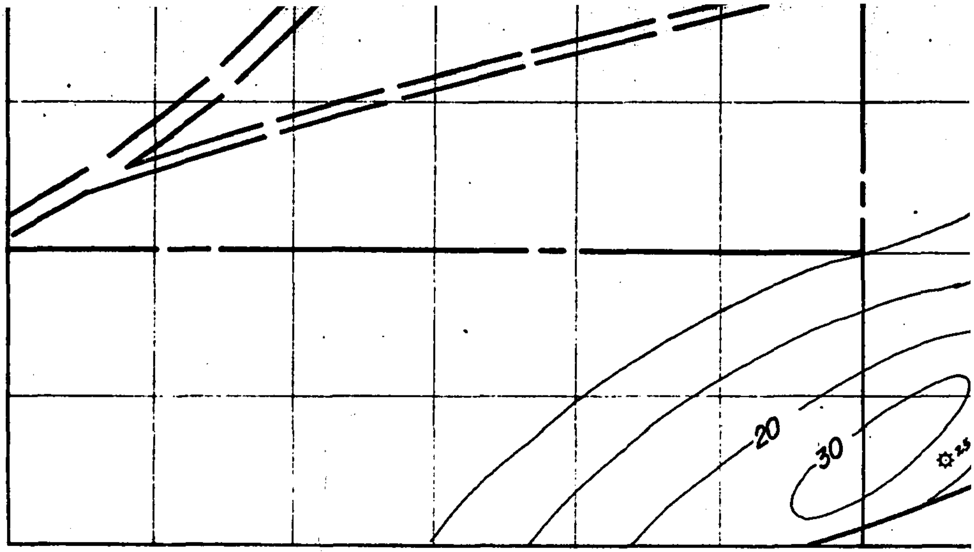

S

ARKO

0

University of Okl

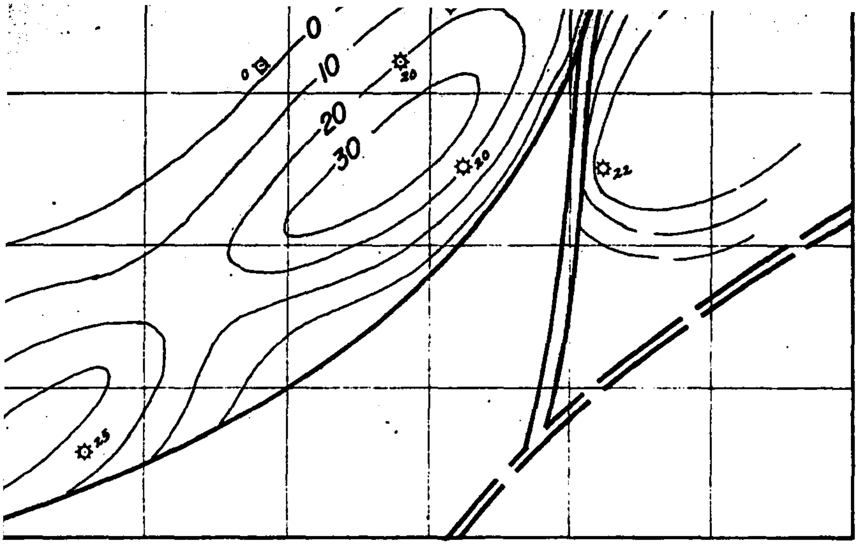

PLATE X

ISOPACHOUS MAP OF

SPIRO "B" SAND

ARKOMA BASIN, EASTERN OKLAHOMA

CONTOUR INTERVAL: 10 FEET

0 1 2 3 4 5 6

Scale in miles

y of Oklahoma Ph.D. 1977 M. W. McQuillan

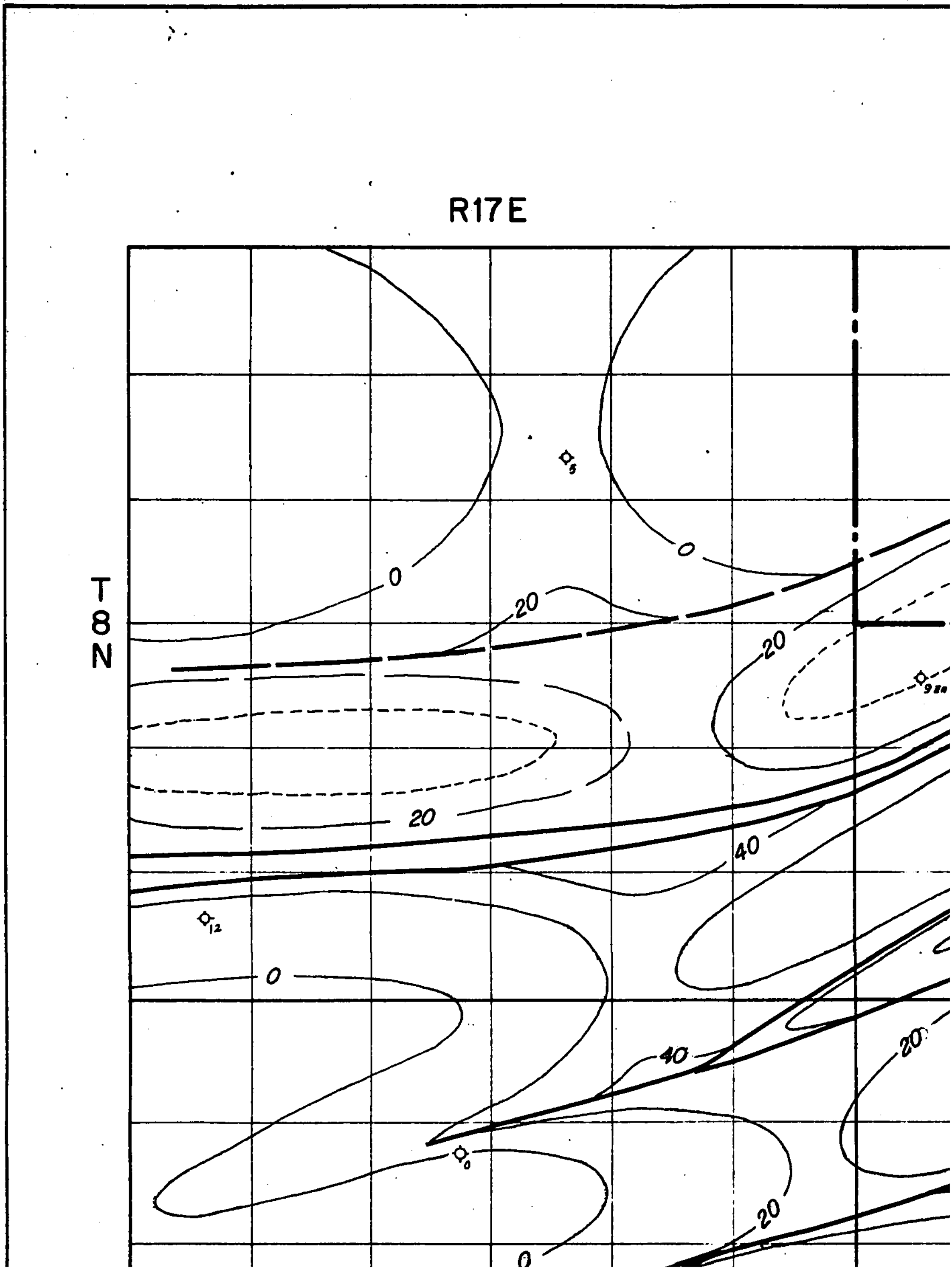
R17E
T 8 N
0
0
20
20
20
40
0
40
20
20
0

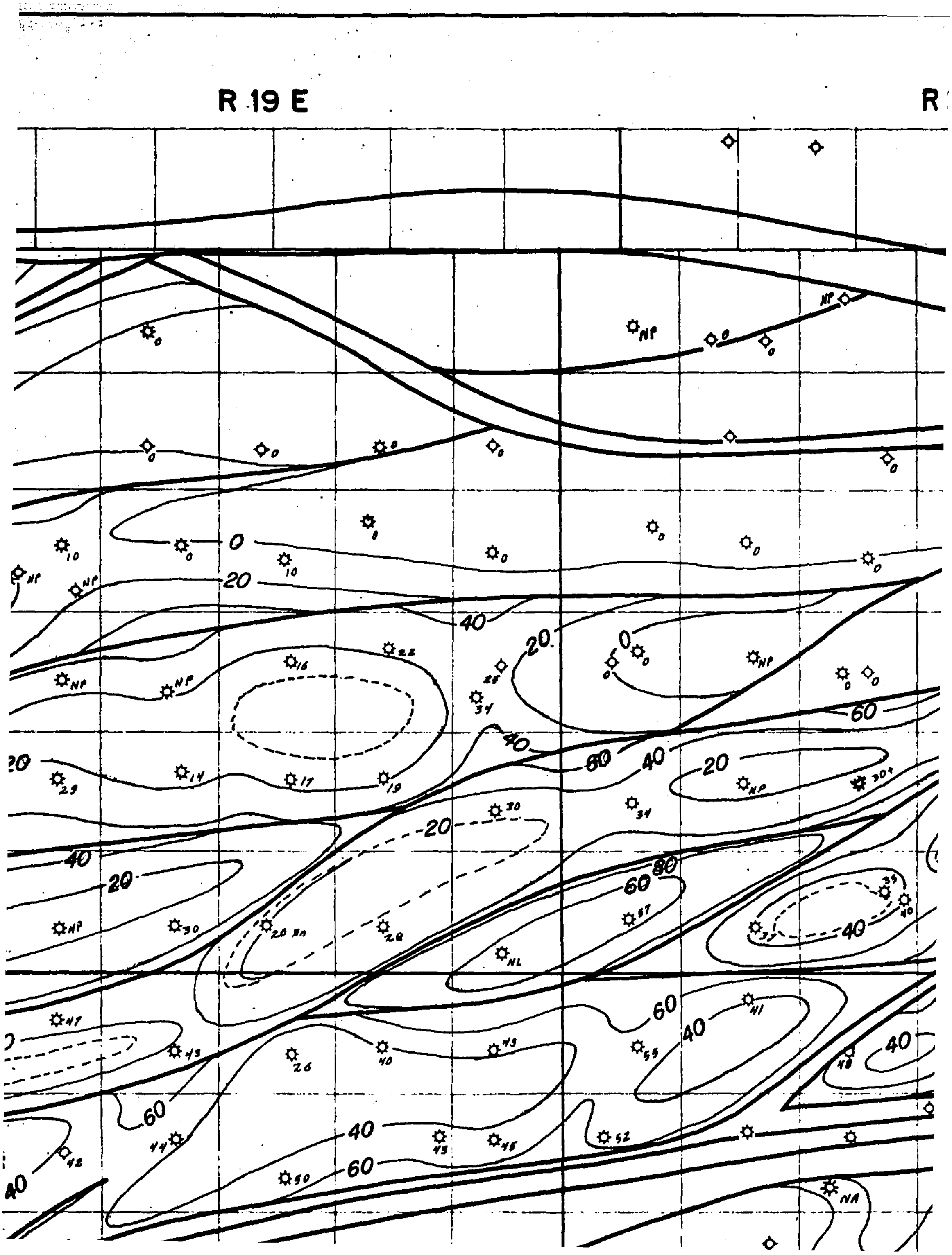
R 19 E
R
0
20
40
20
0
60
40
80
40
20
20
20
40
20
80
60
40
60
40
40
60
40
60
40
NP
0
10
NP
NP
NP
14
17
19
29
22
16
25
34
30
34
30
NP
57
NL
28
37
35
40
47
43
26
40
43
55
41
48
44
42
50
43
46
52
NA

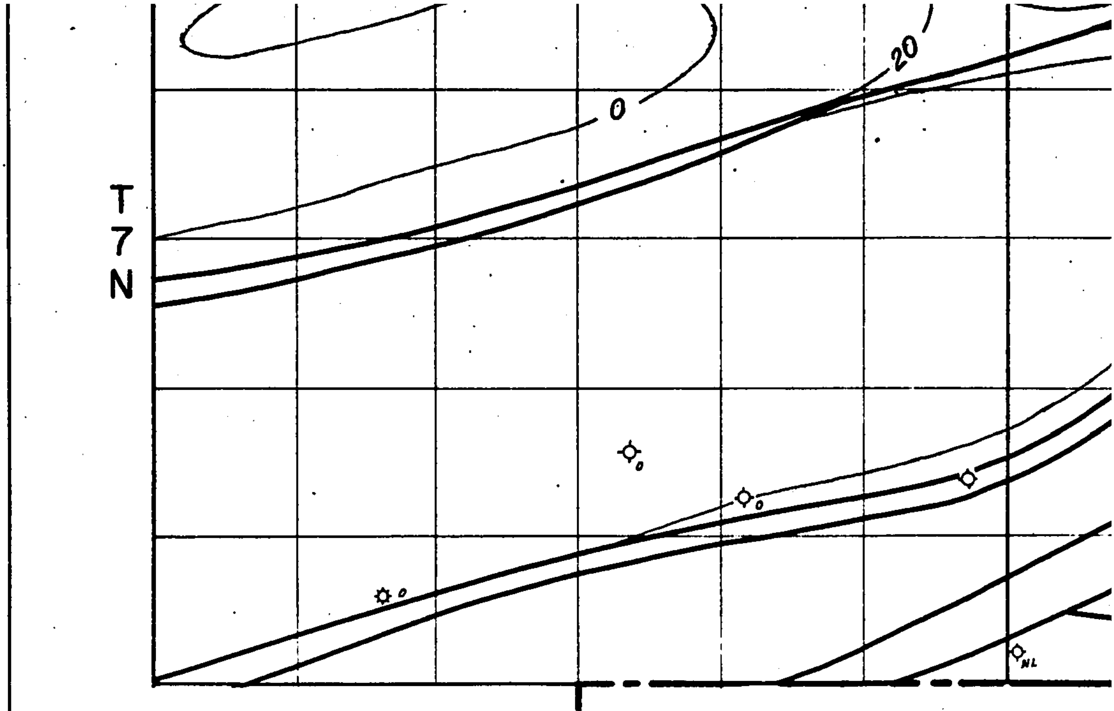

☼40 Thickness in feet
Zn Interval shaley mapped as zone
Brkn Interval consist of interbedded sand and shaley
NP Interval not penetrated
NL Interval not logged
NA Log not available

Fault

Area where Cro

Key Str

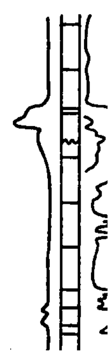

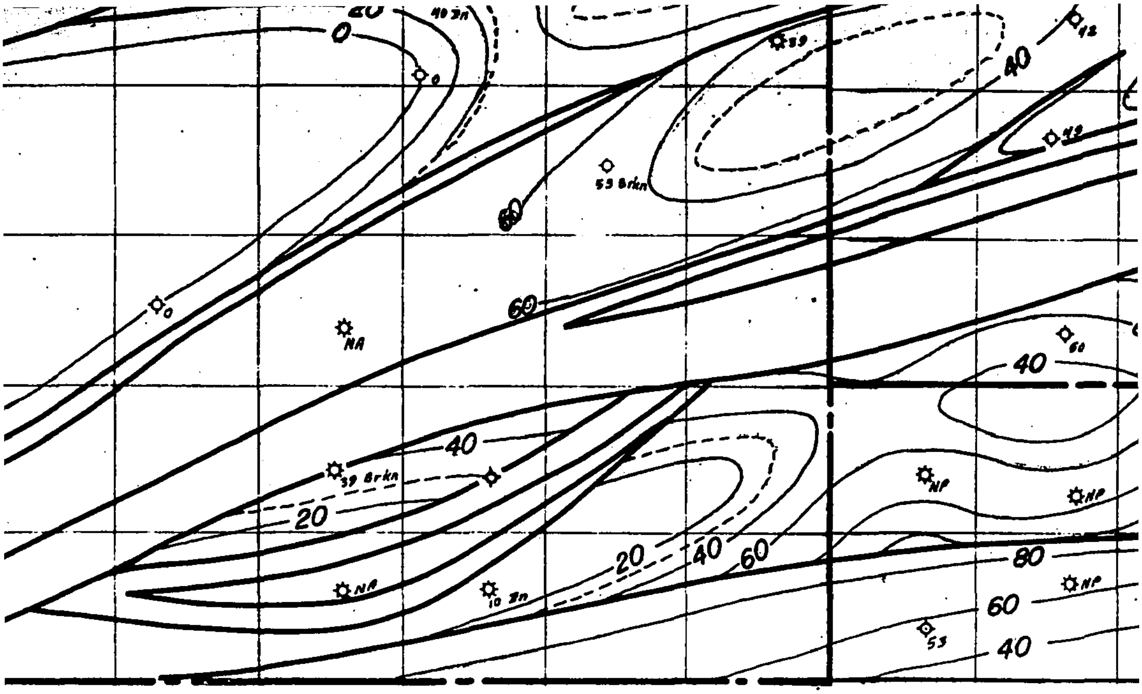

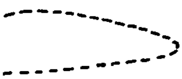

re Cromwell I shaley

ey Stratigraphic Subdivisions

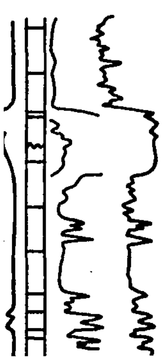

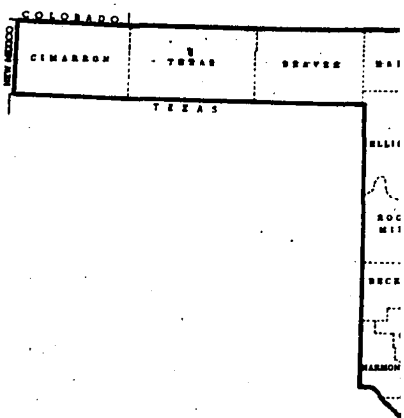

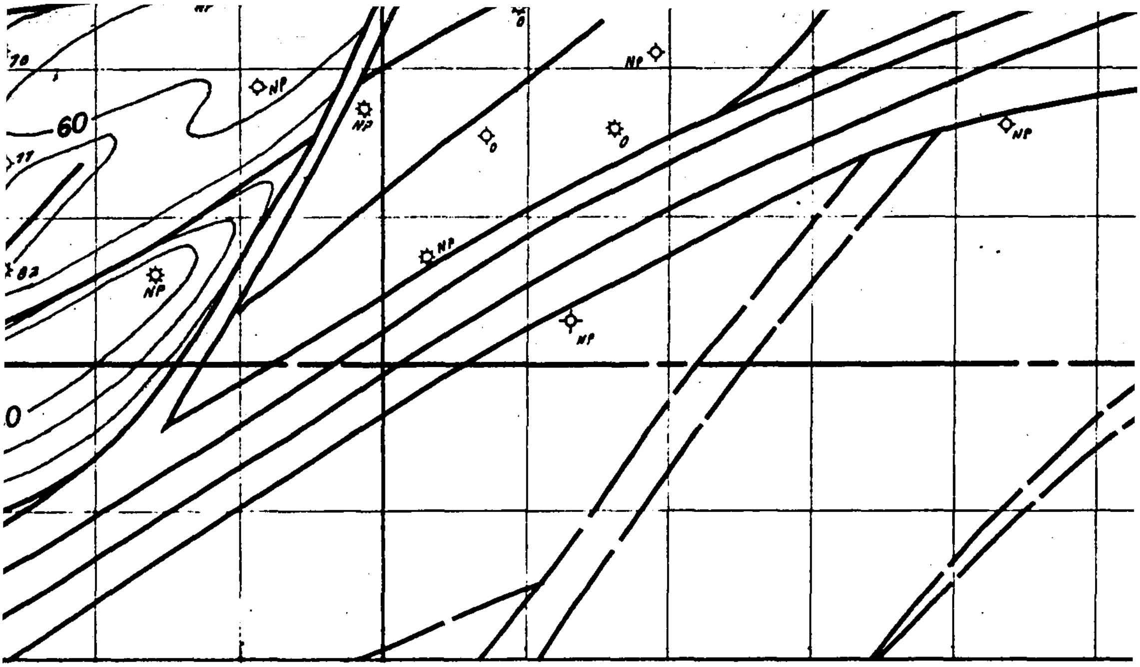

PLATE XI

ISOPACHOUS MAP OF

CROMWELL I SAND

ARKOMA BASIN, EASTERN OKLAHOMA

CONTOUR INTERVAL: 20 FEET

0 1 2 3 4 5 6

Scale in miles

University of Oklahoma Ph.D. 1977 M. W. Mc G

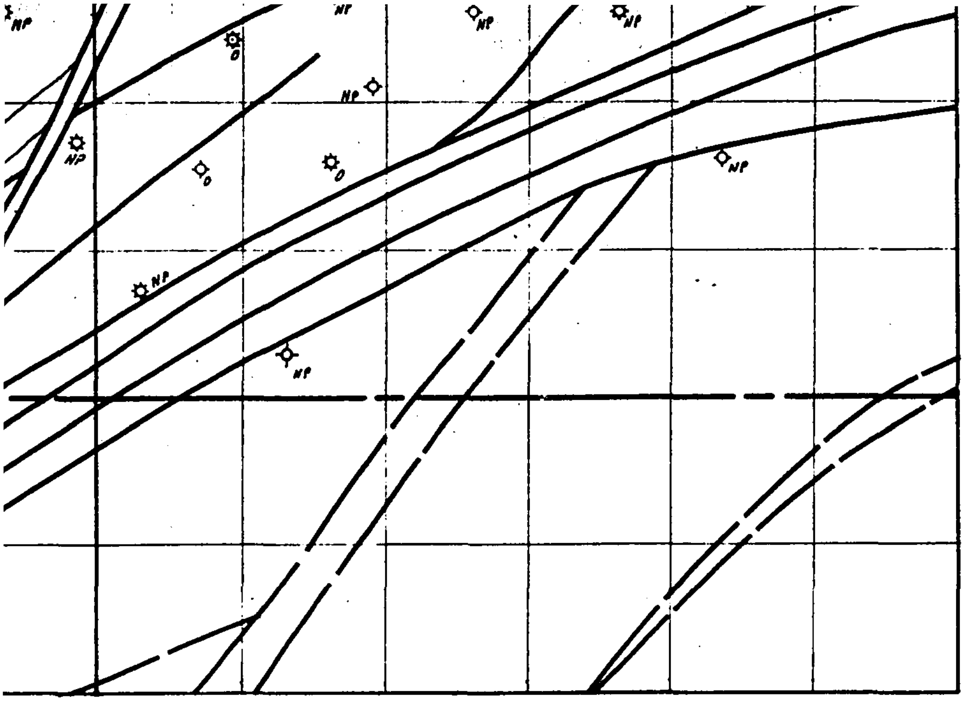

PLATE XI

ISOPACHOUS MAP OF

ROMWELL I SAND

OMA BASIN, EASTERN OKLAHOMA

CONTOUR INTERVAL: 20 FEET

1 2 3 4 5 6

Scale in miles

ahoma Ph.D. 1977 M. W. McQuillan

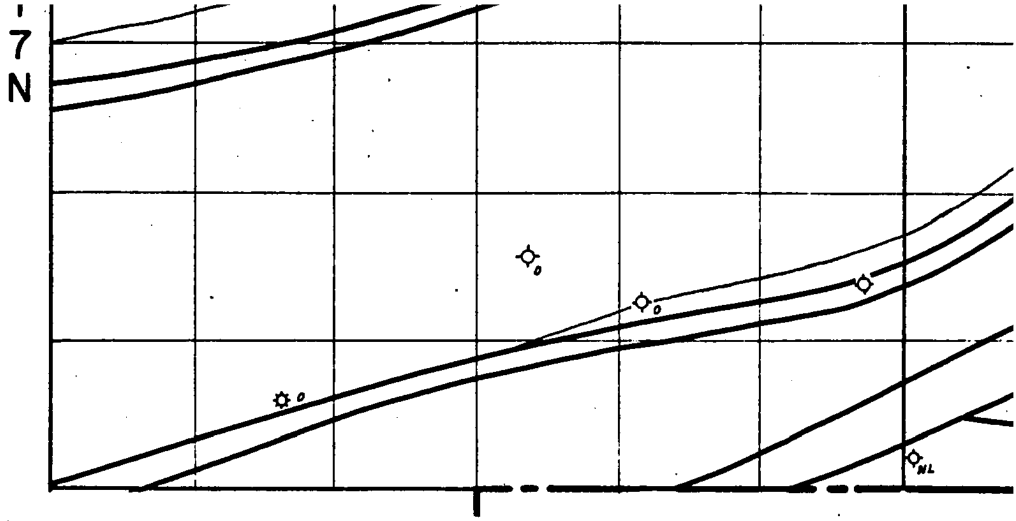

40 Thickness in feet
Zn Interval shaley mapped as zone
Brkn Interval consist of interbedded sand and shaley
NP Interval not penetrated
NL Interval not logged
NA Log not available

Fault

Area where Cror

Key Stra

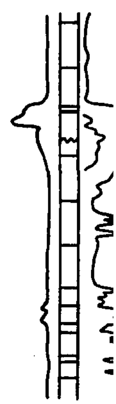

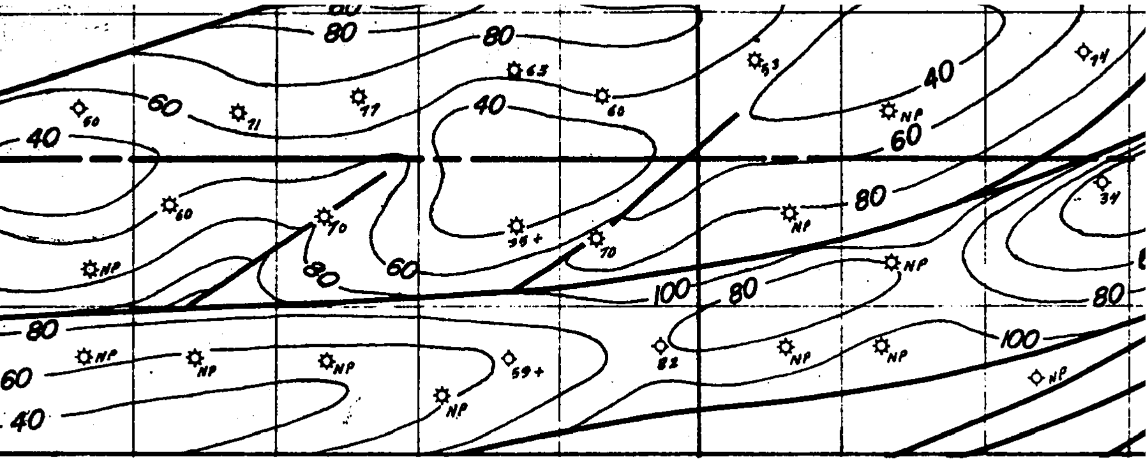

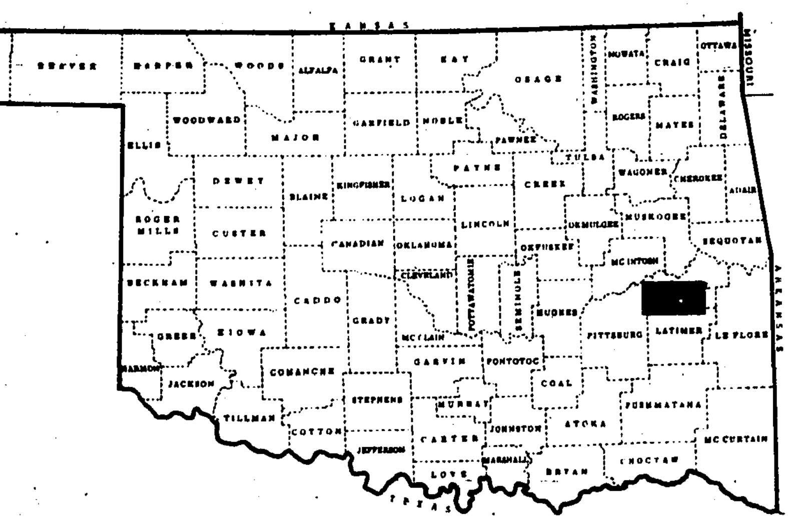

Index map showing study area mapped.

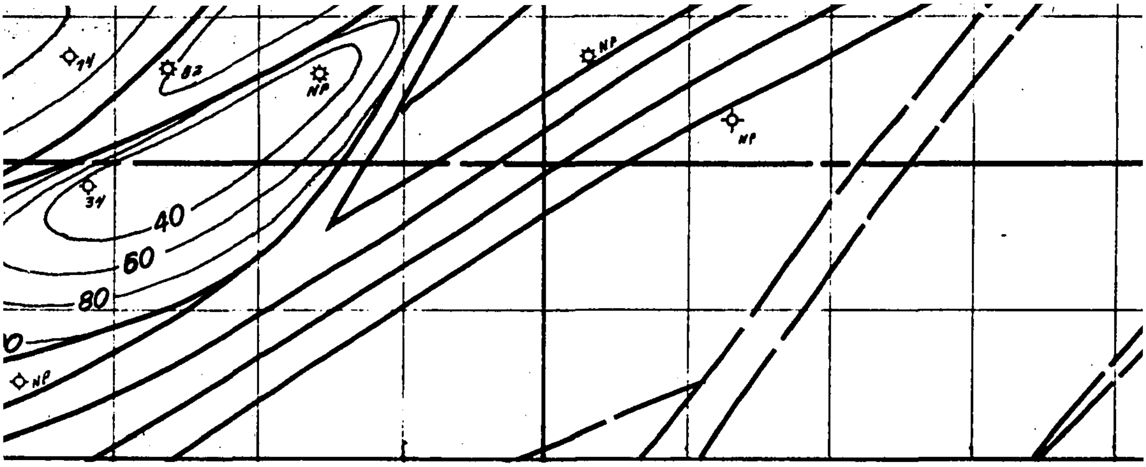

PLATE XI

ISOPACHOUS MAP OF

CROMWELL I SAN

ARKOMA BASIN, EASTERN OKLAH

CONTOUR INTERVAL: 20 FEET

0 1 2 3 4 5

Scale in miles

University of Oklahoma Ph.D. 1977 M.

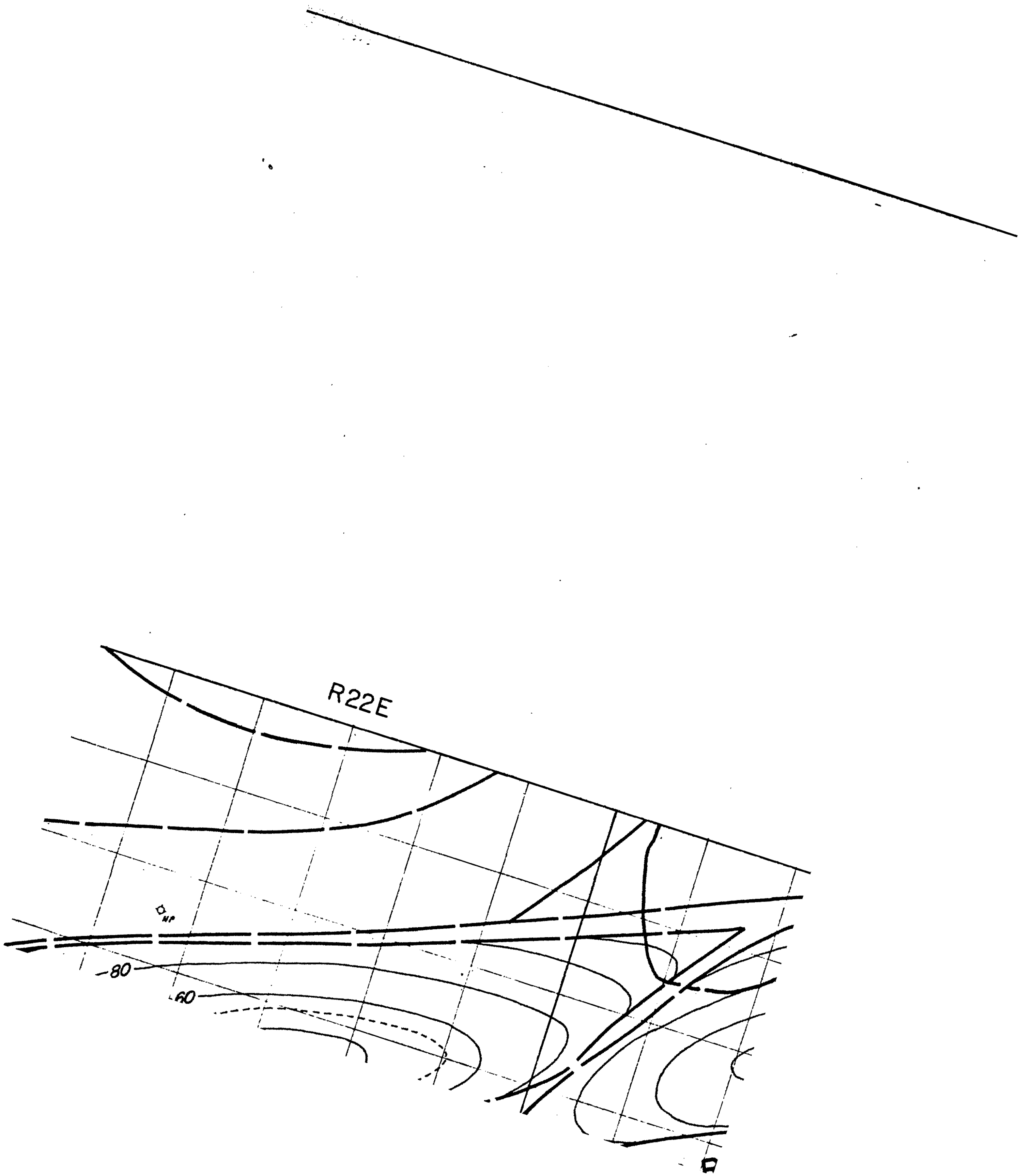
R22E
-80
60

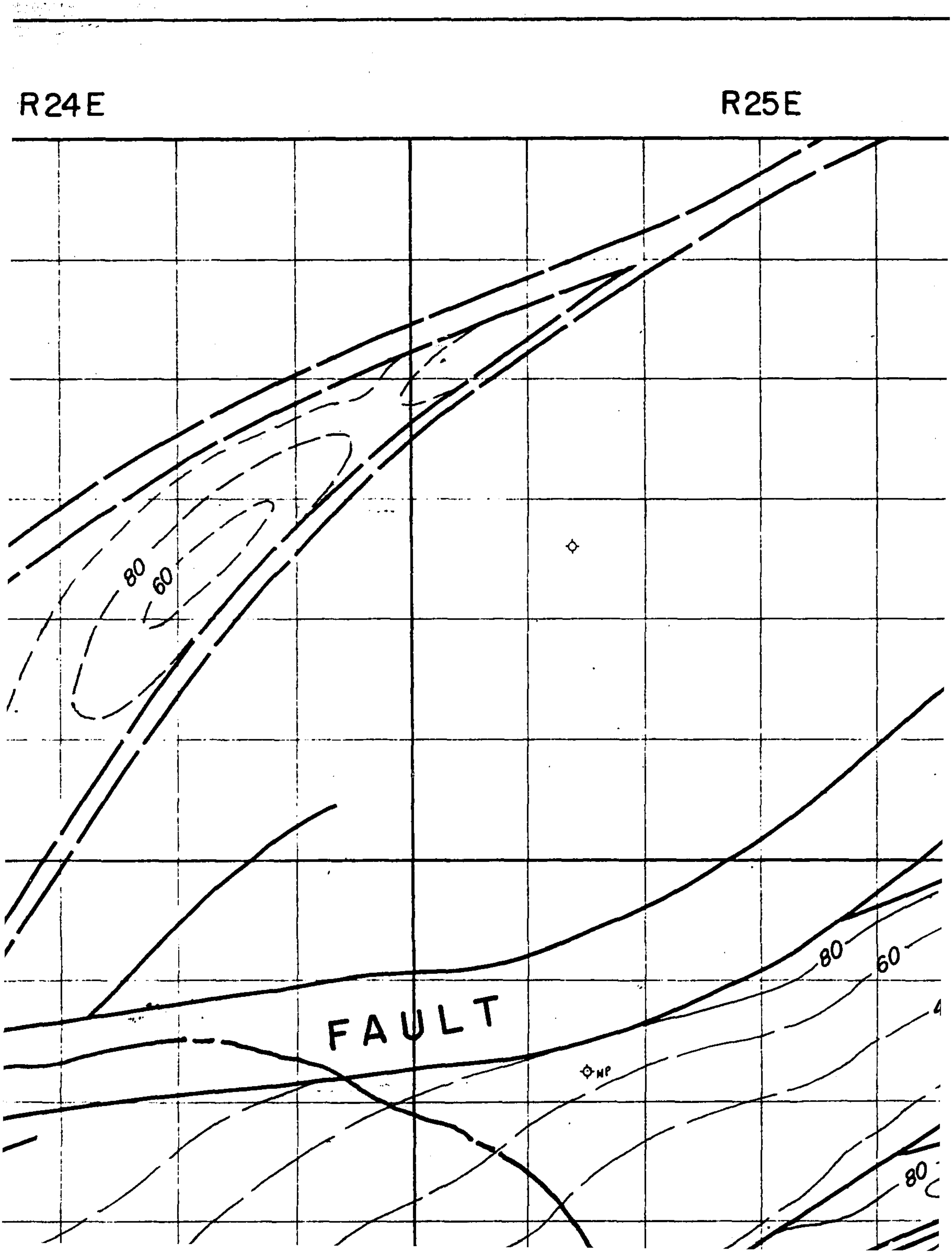
R24E
R25E
80
60
FAULT
80
60
NP
80

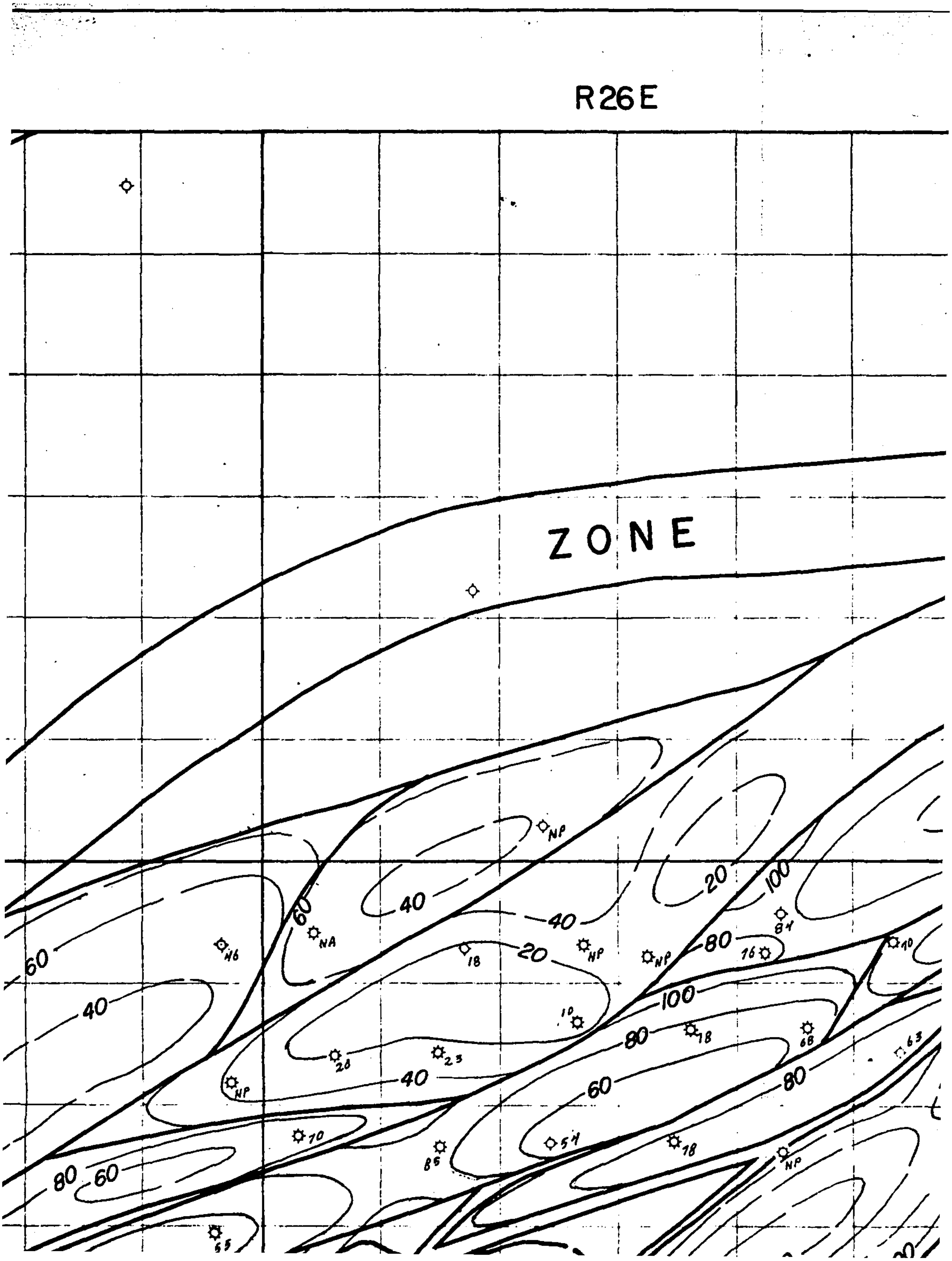

R26E
ZONE
20
100
40
60
80
NP
NA
18
10
23
28
70
85
54
65
84
16
68
63
46

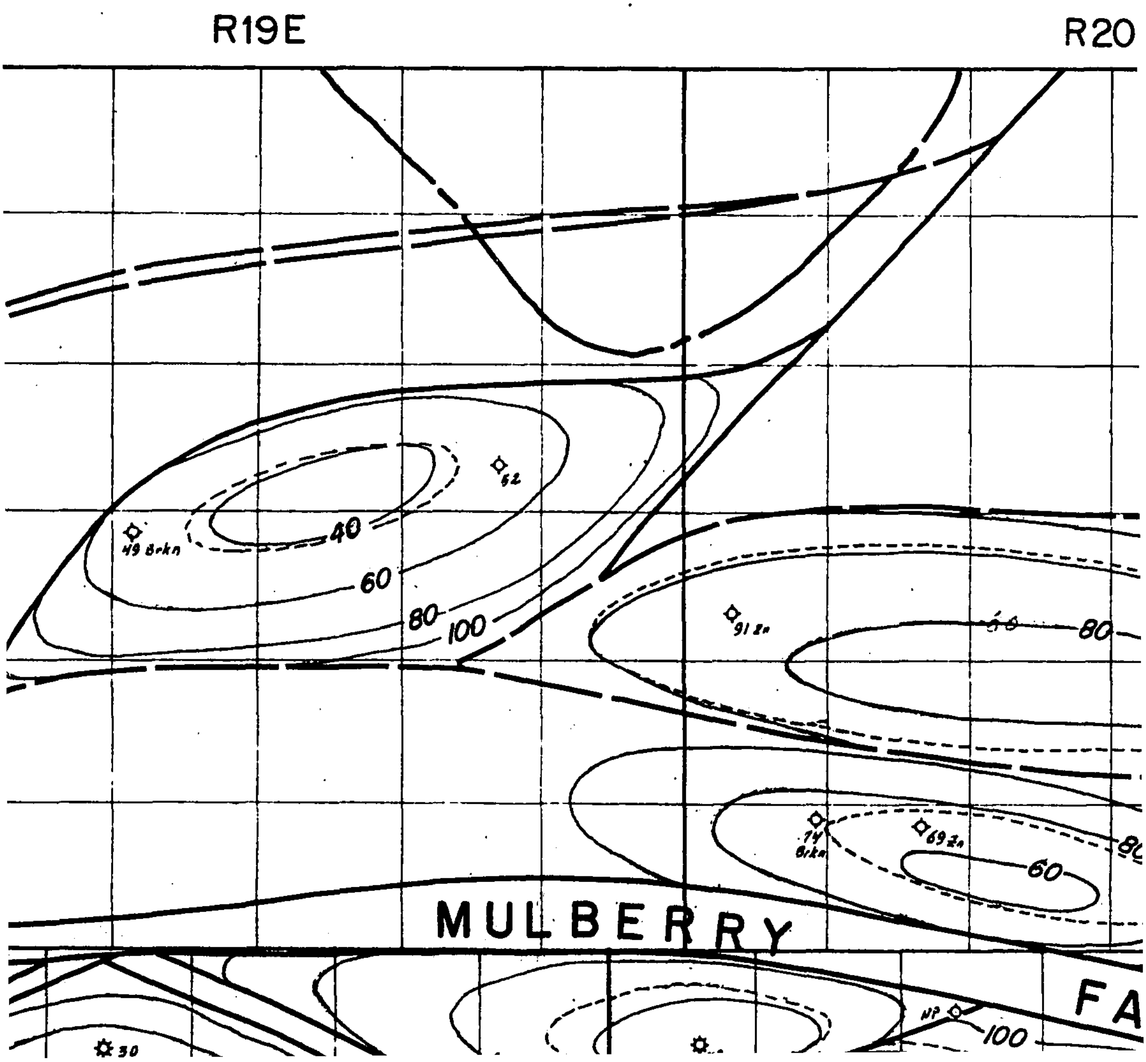

R19E
R20
40
60
80
100
80
60
80
100
49 Brkn
62
91 Zn
74 Brkn
69 Zn
NP
30
MULBERRY
FA

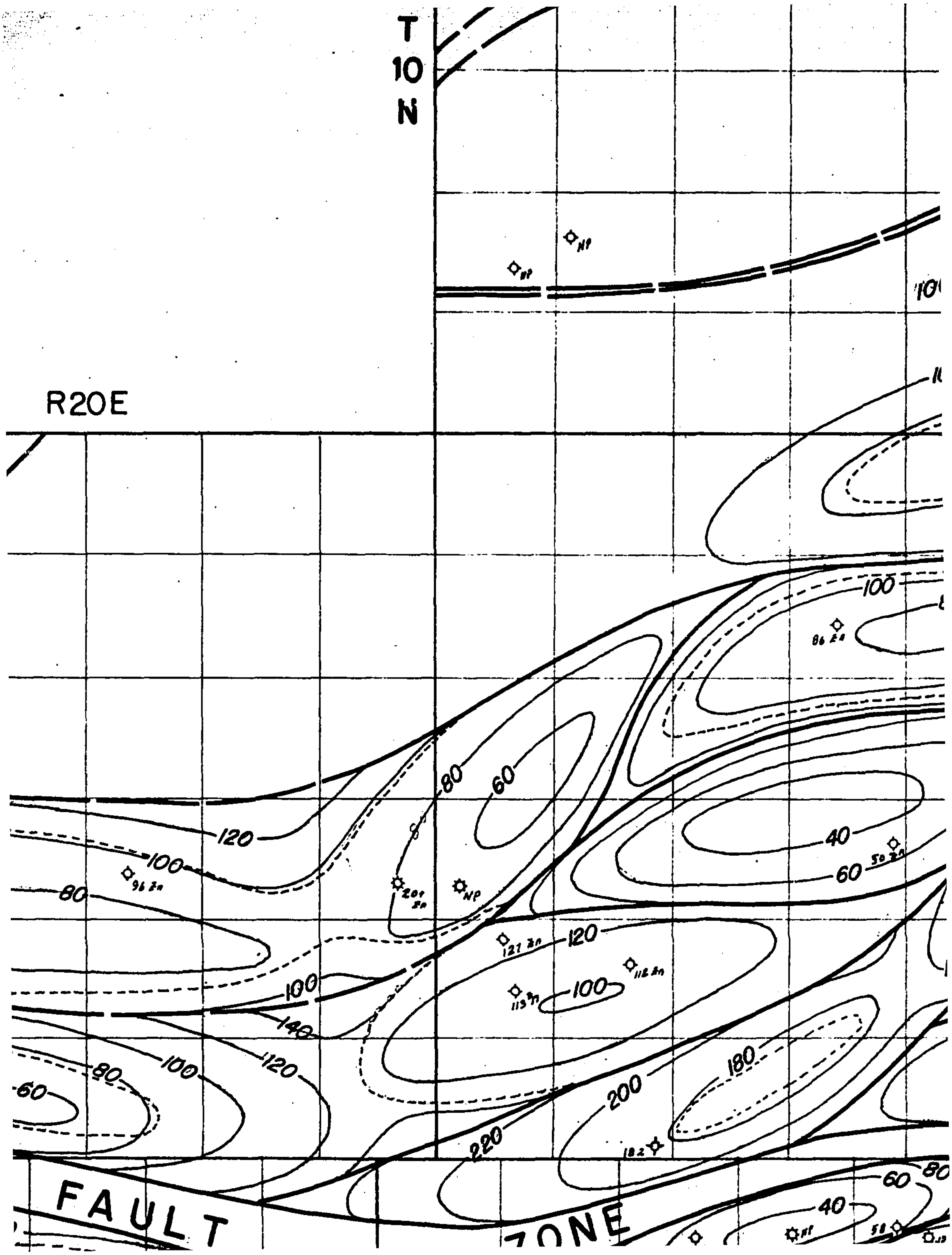
T
10
N
R20E
FAULT
ZONE
120
100
80
60
40
140
180
200
220

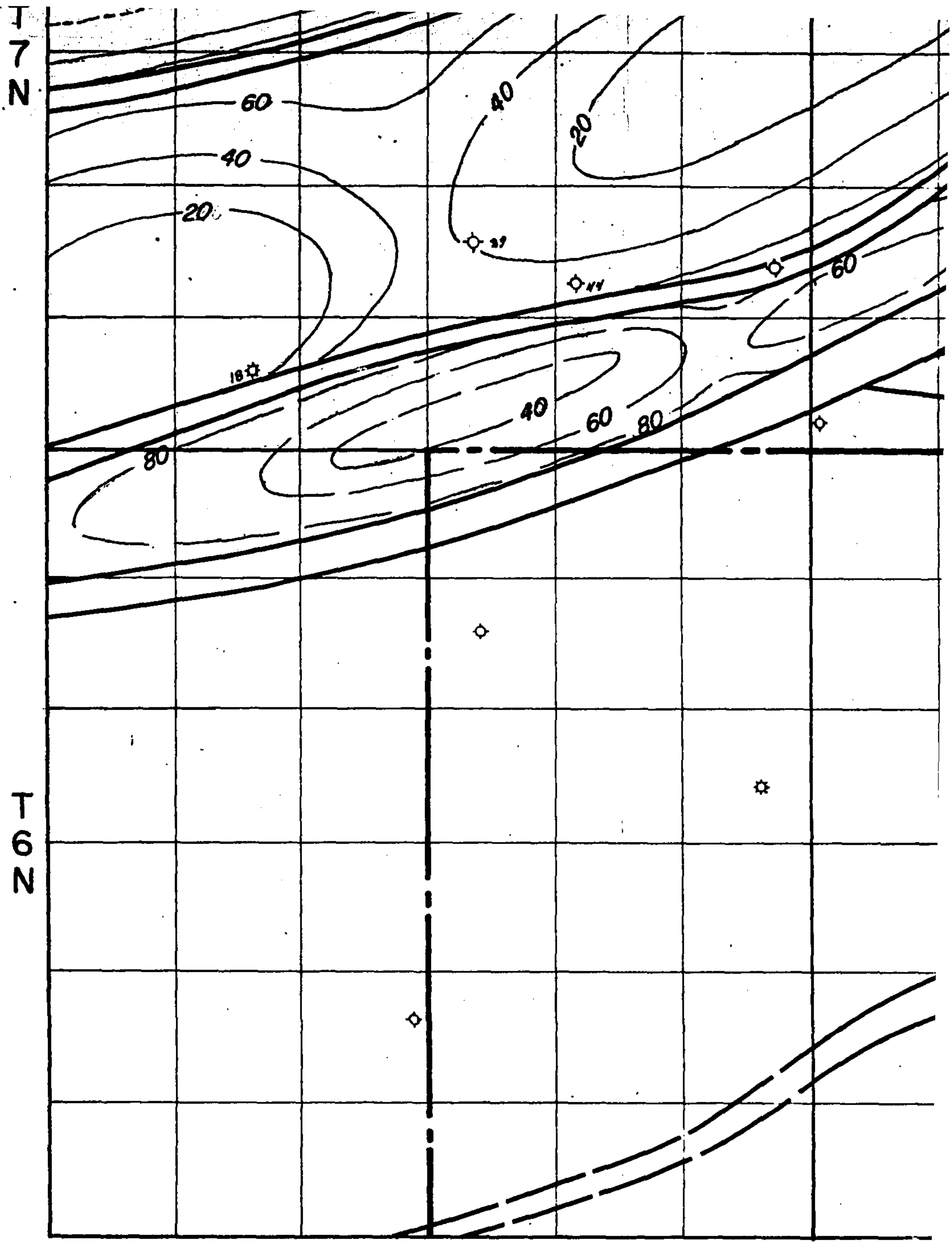
T
7
N
60
40
20
40
20
60
18
80
40
60
80
T
6
N

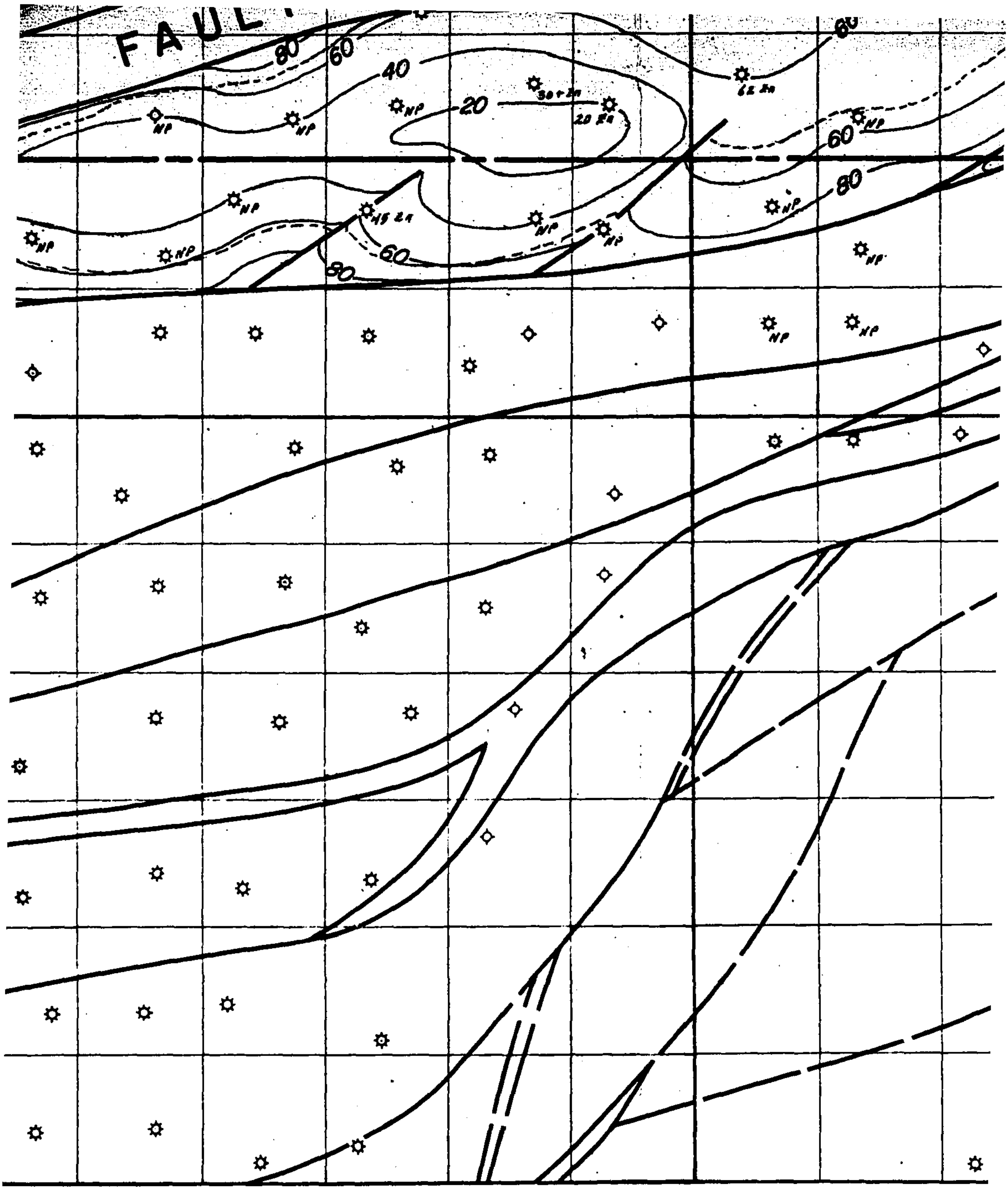

FAUL
80
60
40
20
NP
60
80
60
80
NP

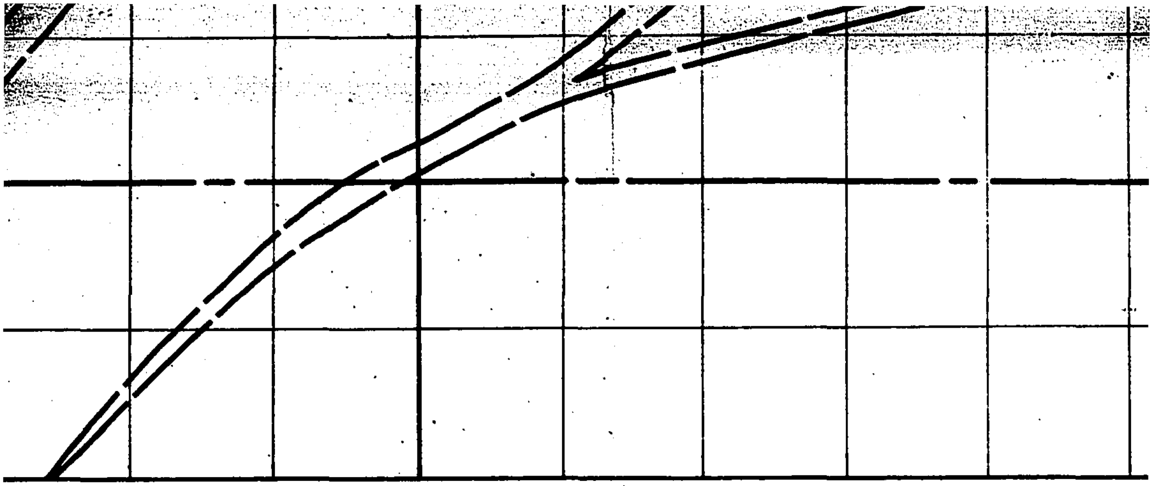

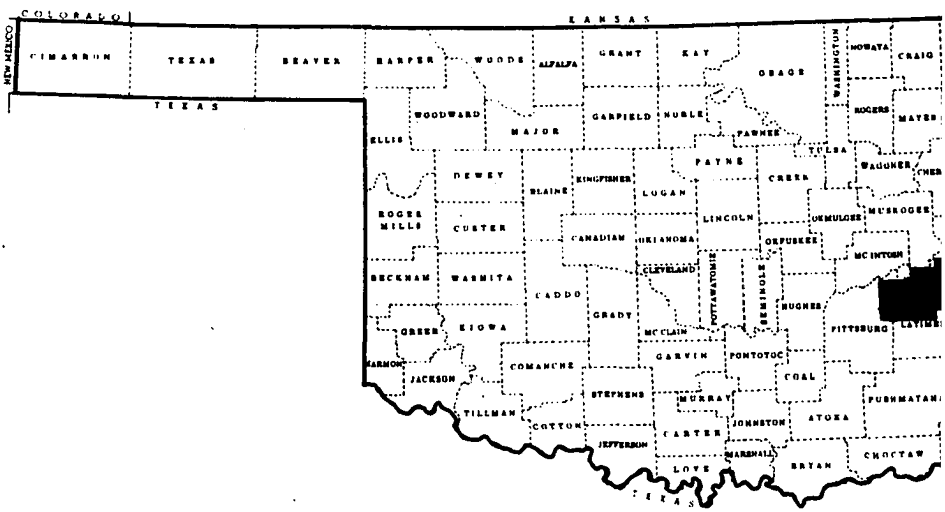

Index map showing study area mapped.

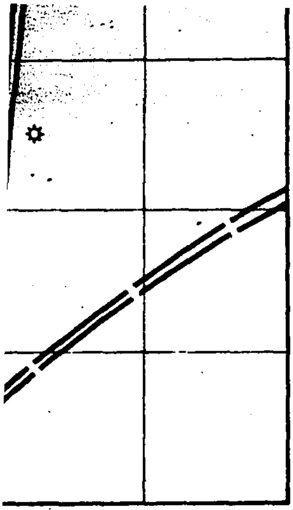

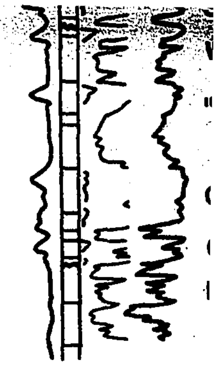

Key Straigraphic

40 Thickness in feet
Zn Shaley and mapped as zone
Brkn Interbedded sand and shale
NP Not penetrated
NL Not logged
NA Log not available

Area where Cromw

Fault

Spiro Sand

Wapanucka Ls.

"C" Marker

Cromwell II

Cromwell III

Mississippian

ıphic Section

ISOPA(

CROMWELL

ARKOMA BAS

CONTOU

0 1 2

romwell is shaley

ult

University of Oklahoma Ph.D.

R22E

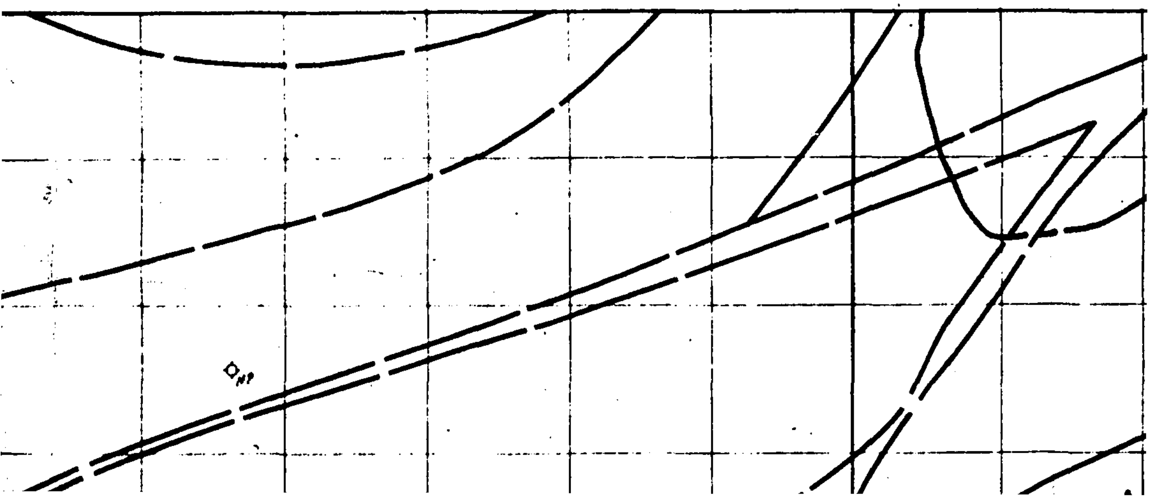

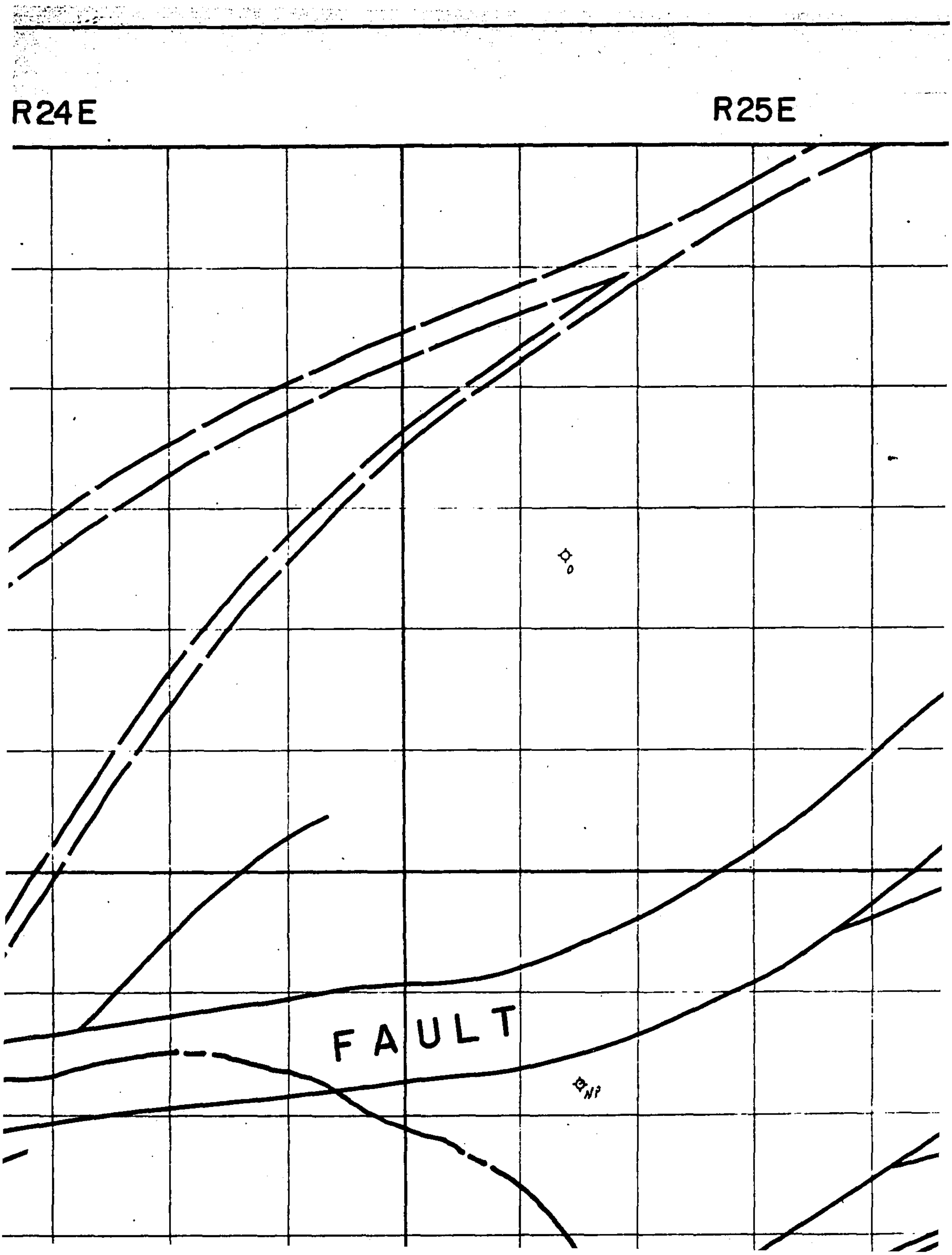
R24E
R25E
FAULT

R17E

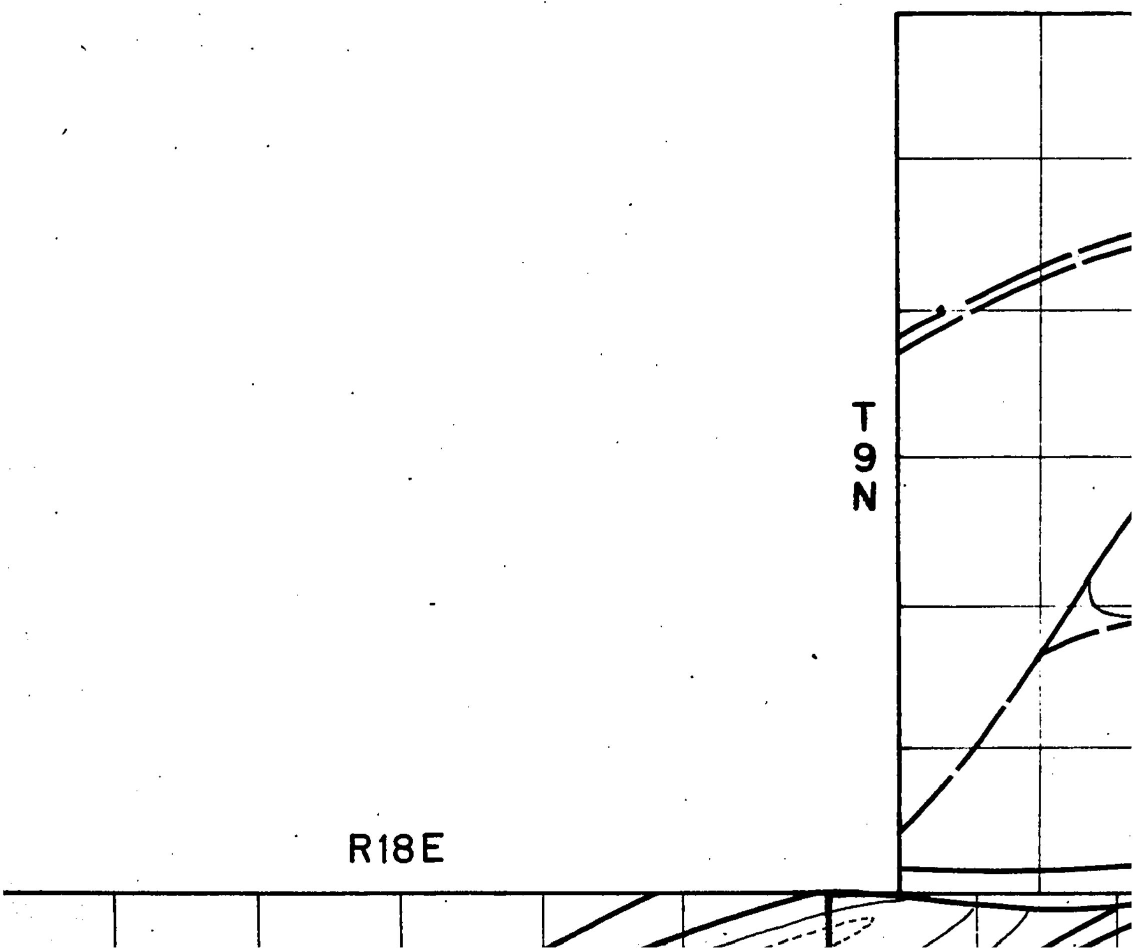
T9N
R18E

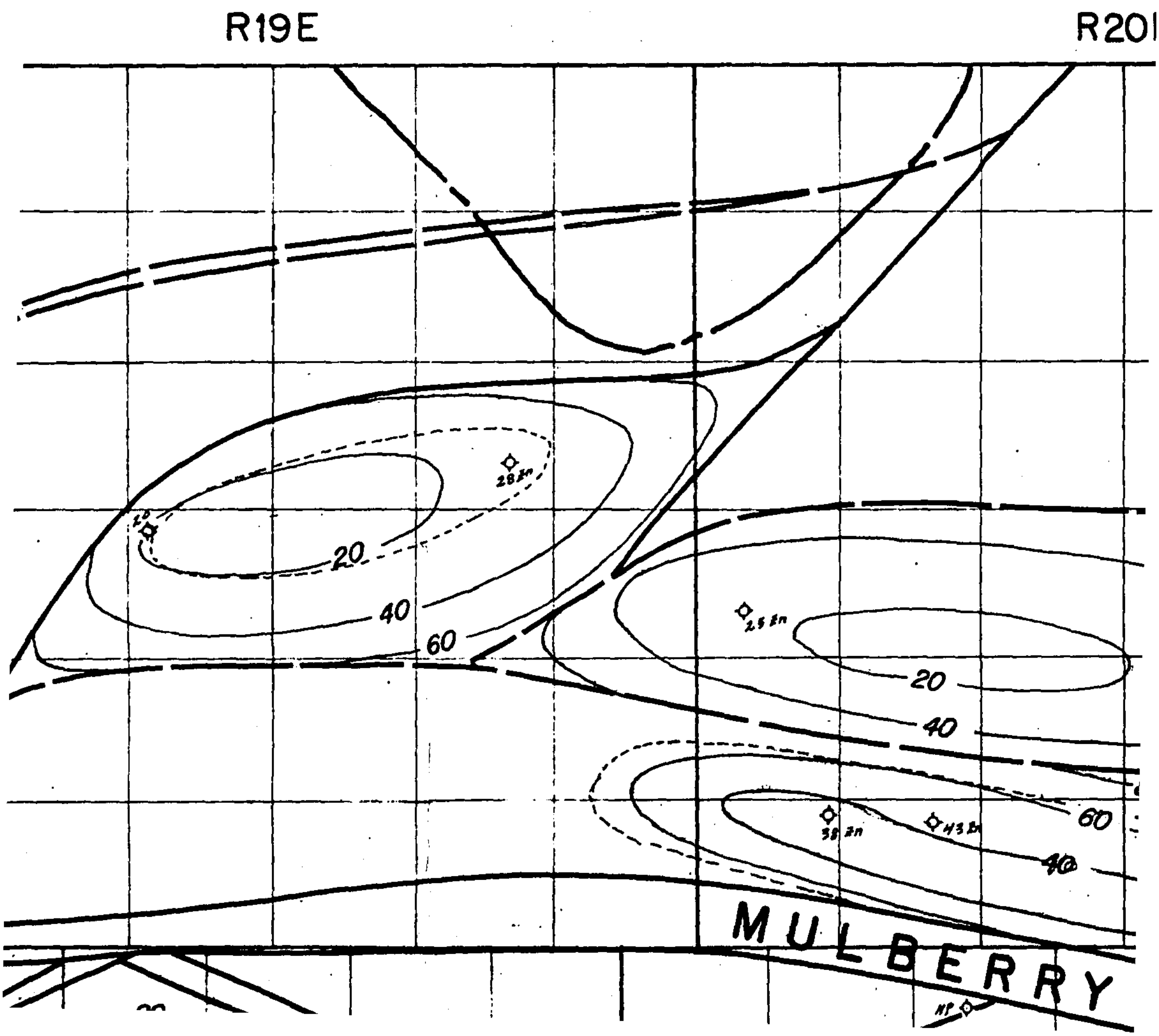
R19E
R20I
20
40
60
20
40
60
40
MULBERRY

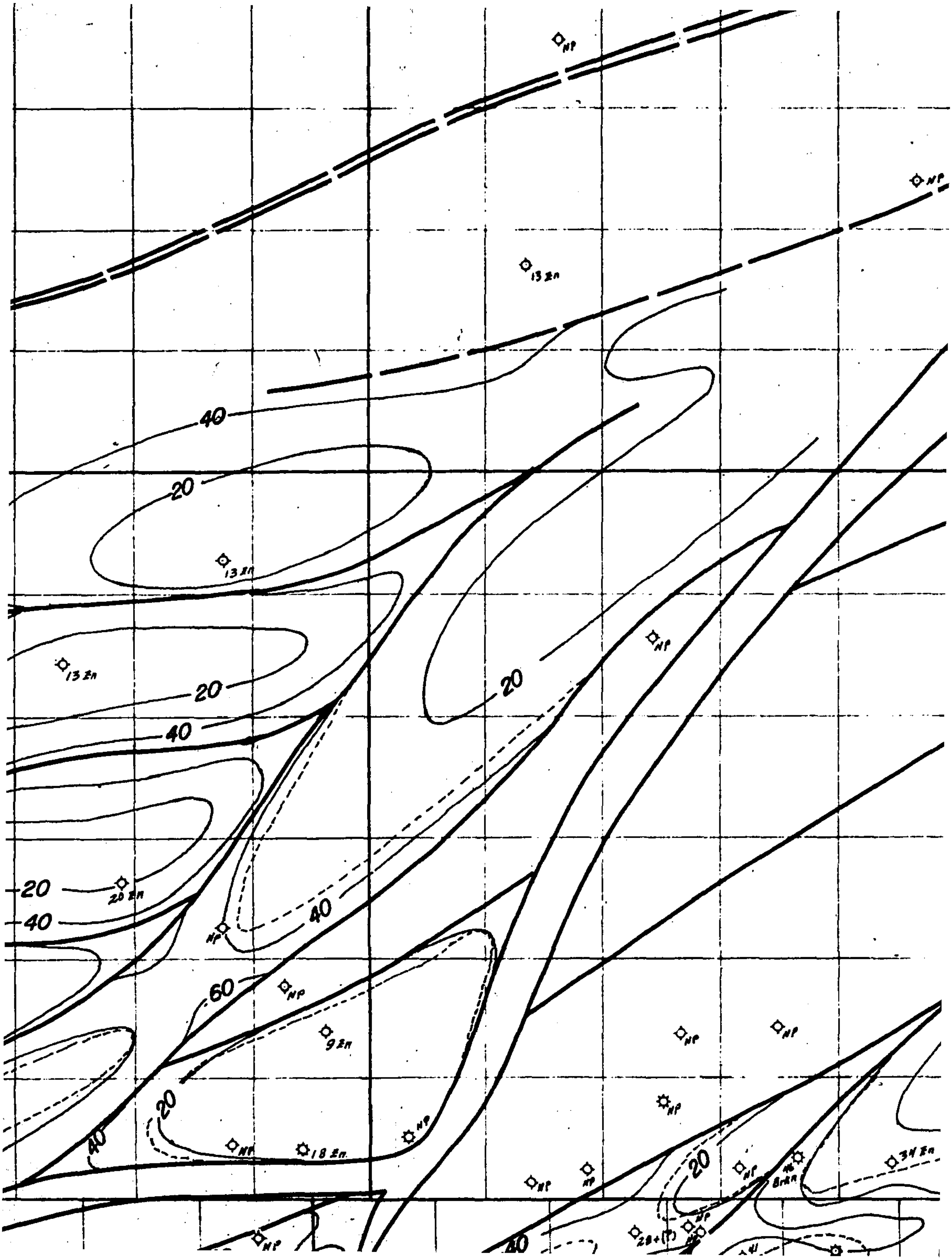

NP
13 Zn
40
20
13 Zn
13 Zn
20
40
NP
20
20 Zn
40
NP
40
60
NP
9 Zn
NP
NP
NP
20
40
NP
18 Zn
NP
NP
NP
20
NP
34 Zn
NP
40

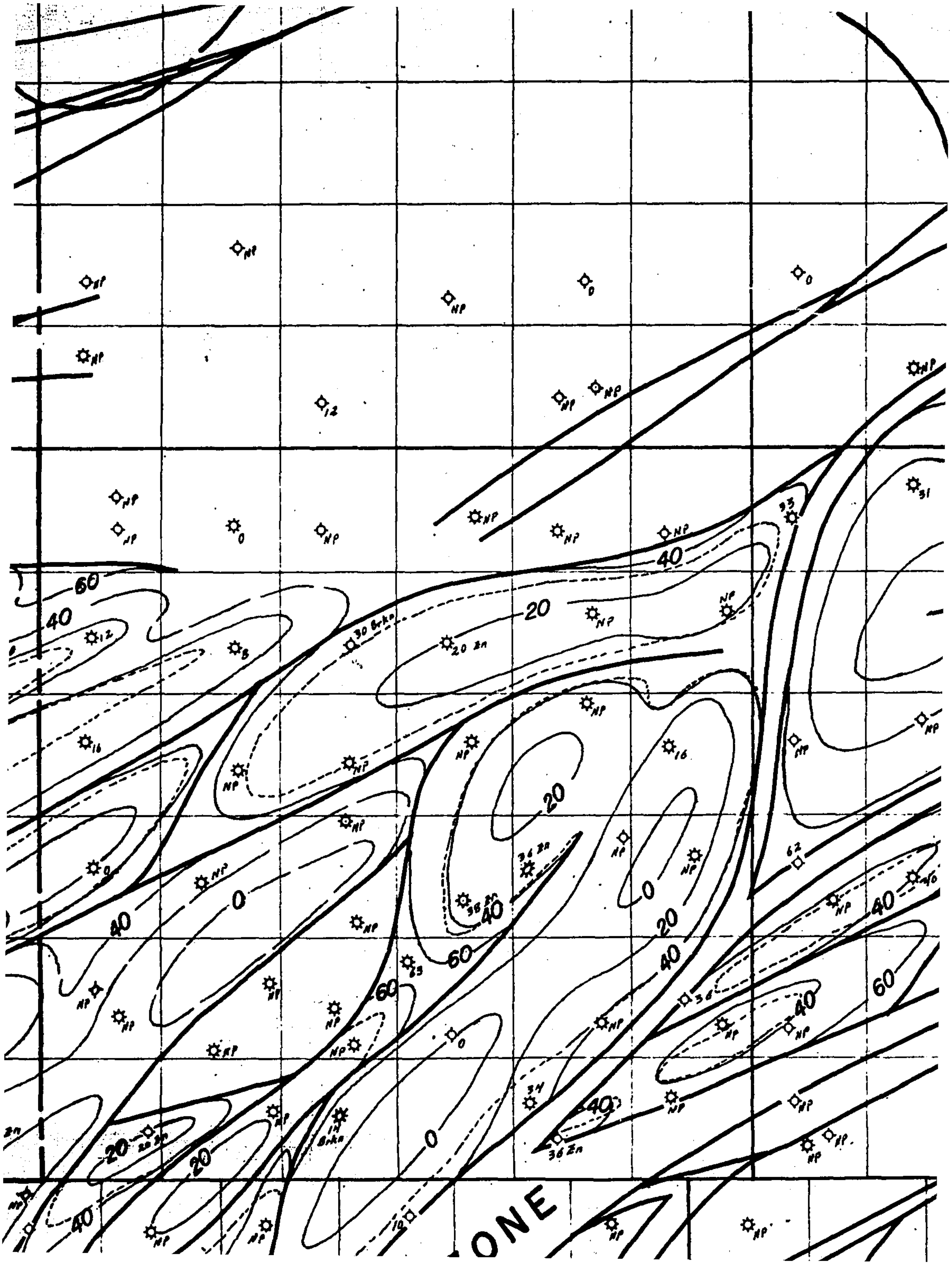
ONE

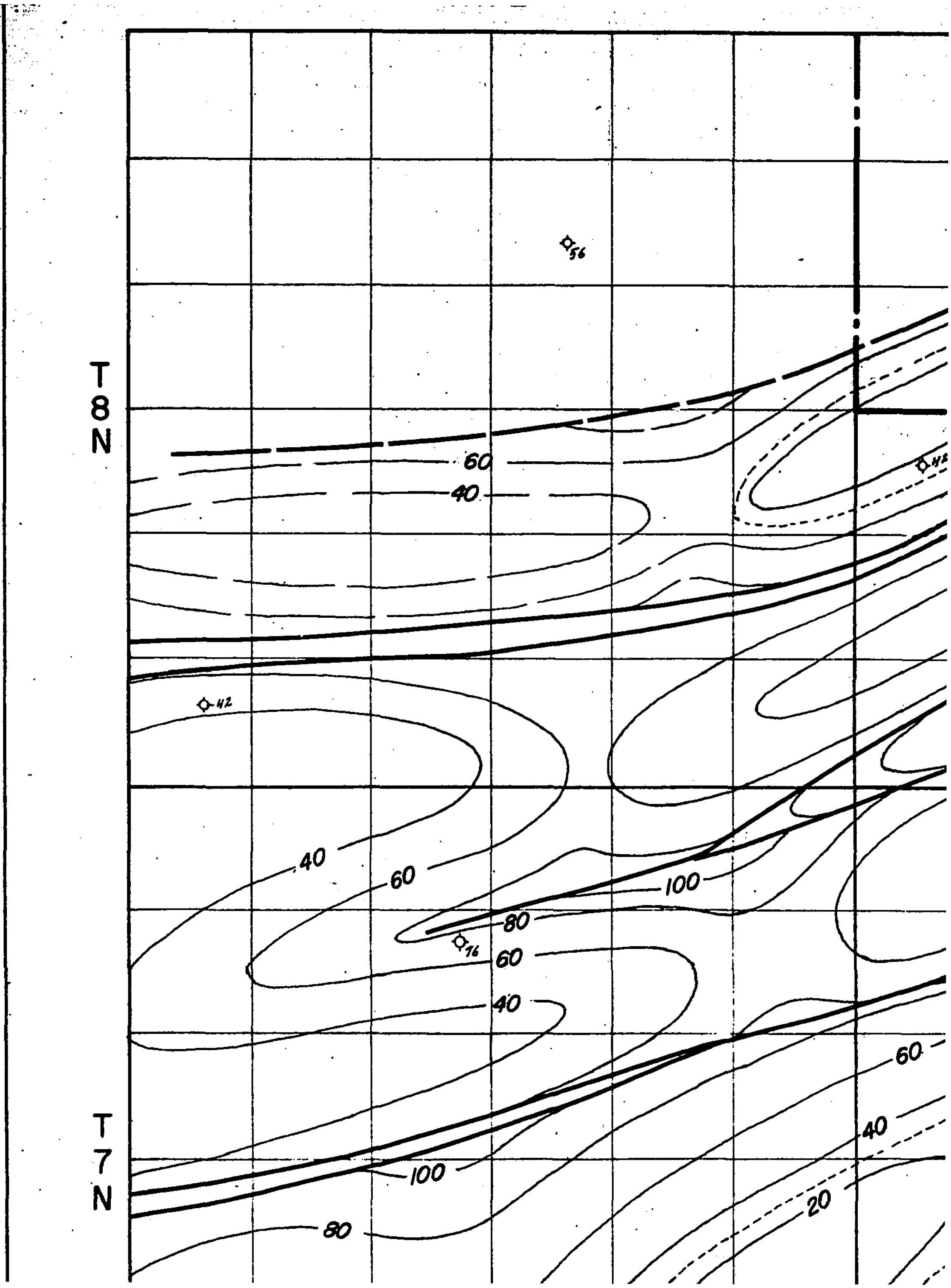

T 8 N
T 7 N
60
40
40
60
100
80
60
40
60
40
20
100
80

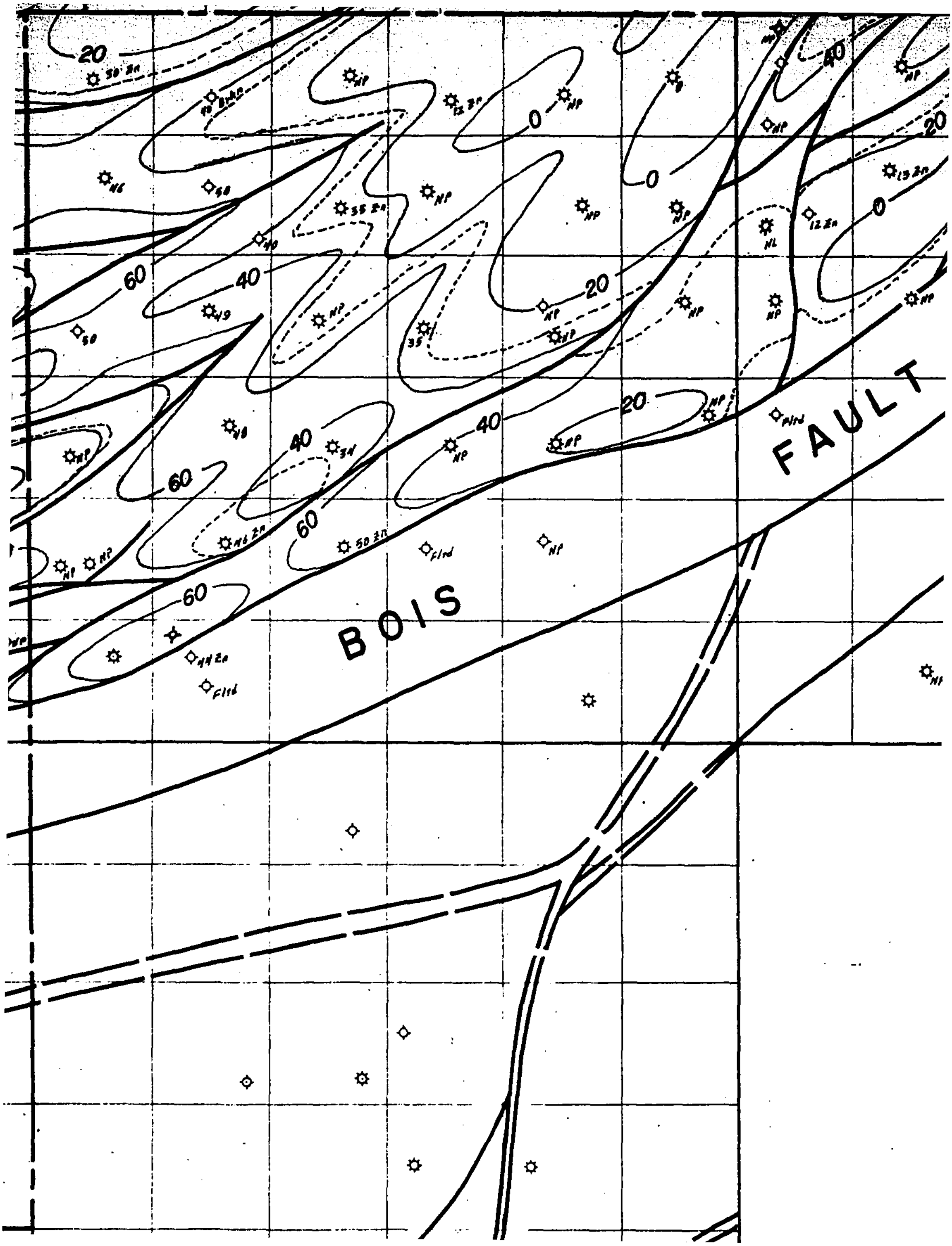

BOIS
FAULT
20
0
20
40
60

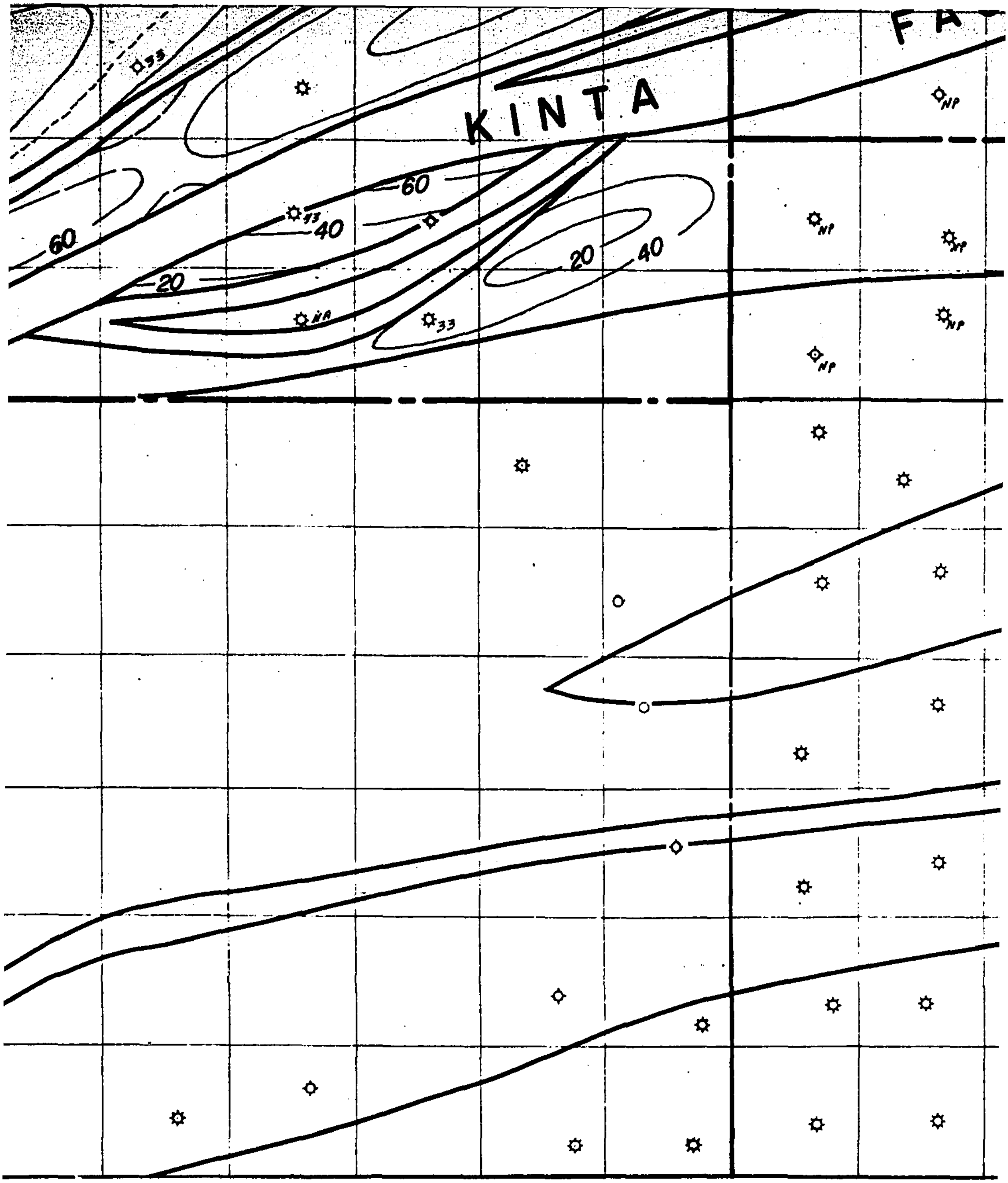
KINTA
FA
60
40
20
20
40
60
20
40
60

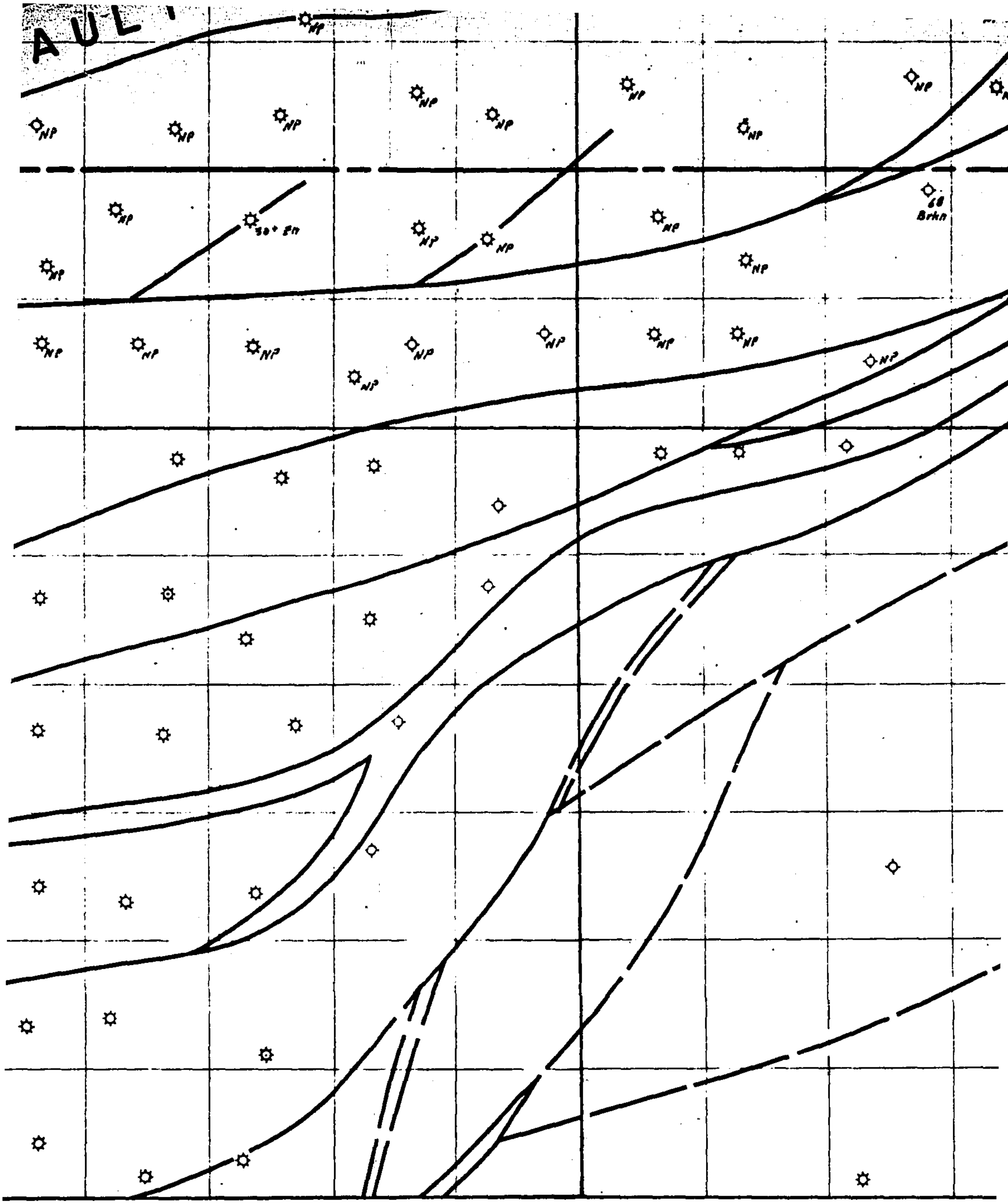
AULT
NP
50+ Zn
68
Brkn

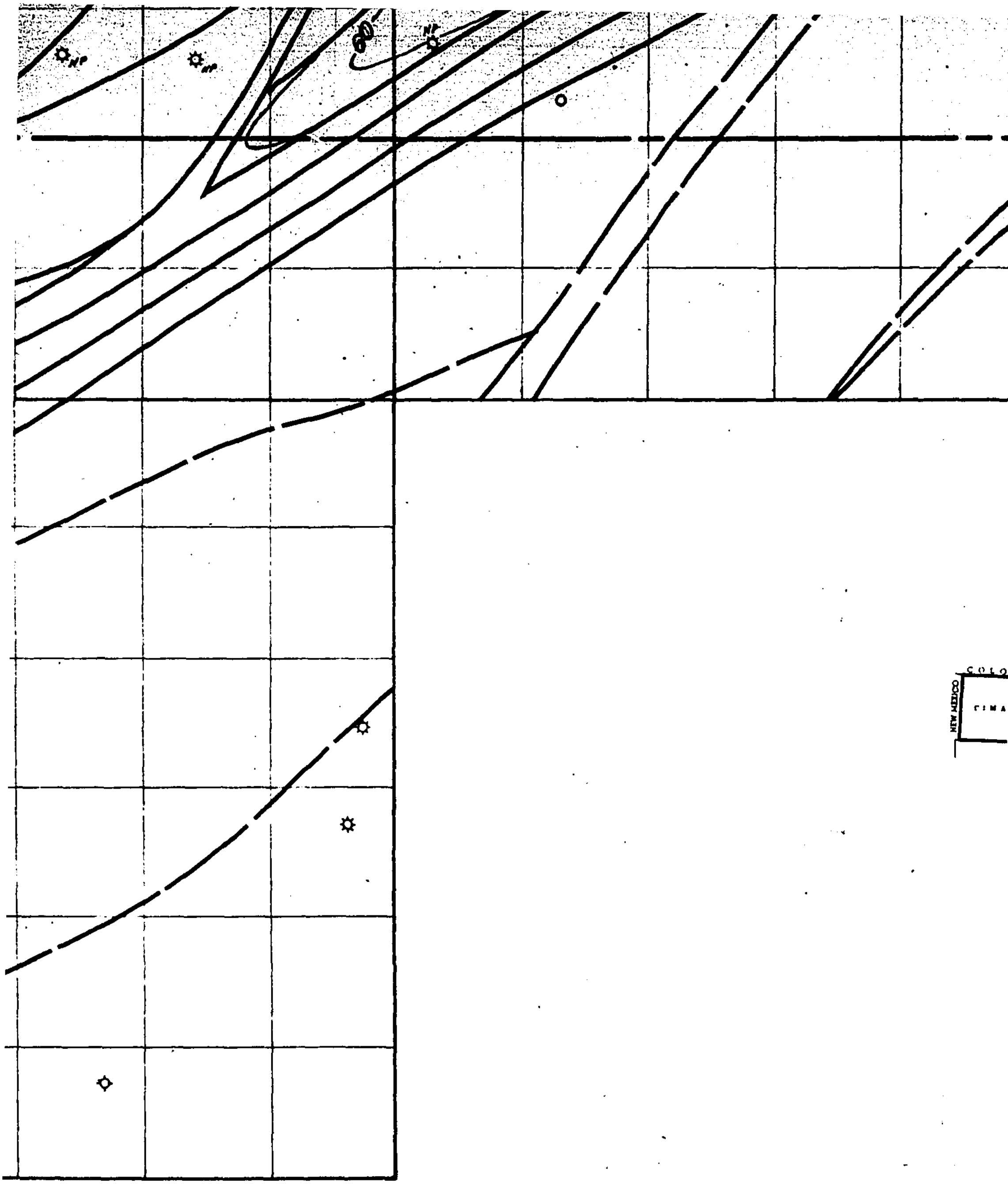
NP
NP
NP
COLO
NEW MEXICO
CIMA

PLATE XIII

ISOPACHOUS MAP OF

CROMWELL III (GROSS

ARKOMA BASIN, EASTERN OKL

CONTOUR INTERVAL: 20 FEET

0 1 2 3 4 5

Scale in miles

University of Oklahoma Ph.D. 1977

LATE XIII

OUS MAP OF

III (GROSS SAND)

, EASTERN OKLAHOMA

INTERVAL: 20 FEET

3 4 5 6

Scale in miles

77 M. W. Mc Quillan

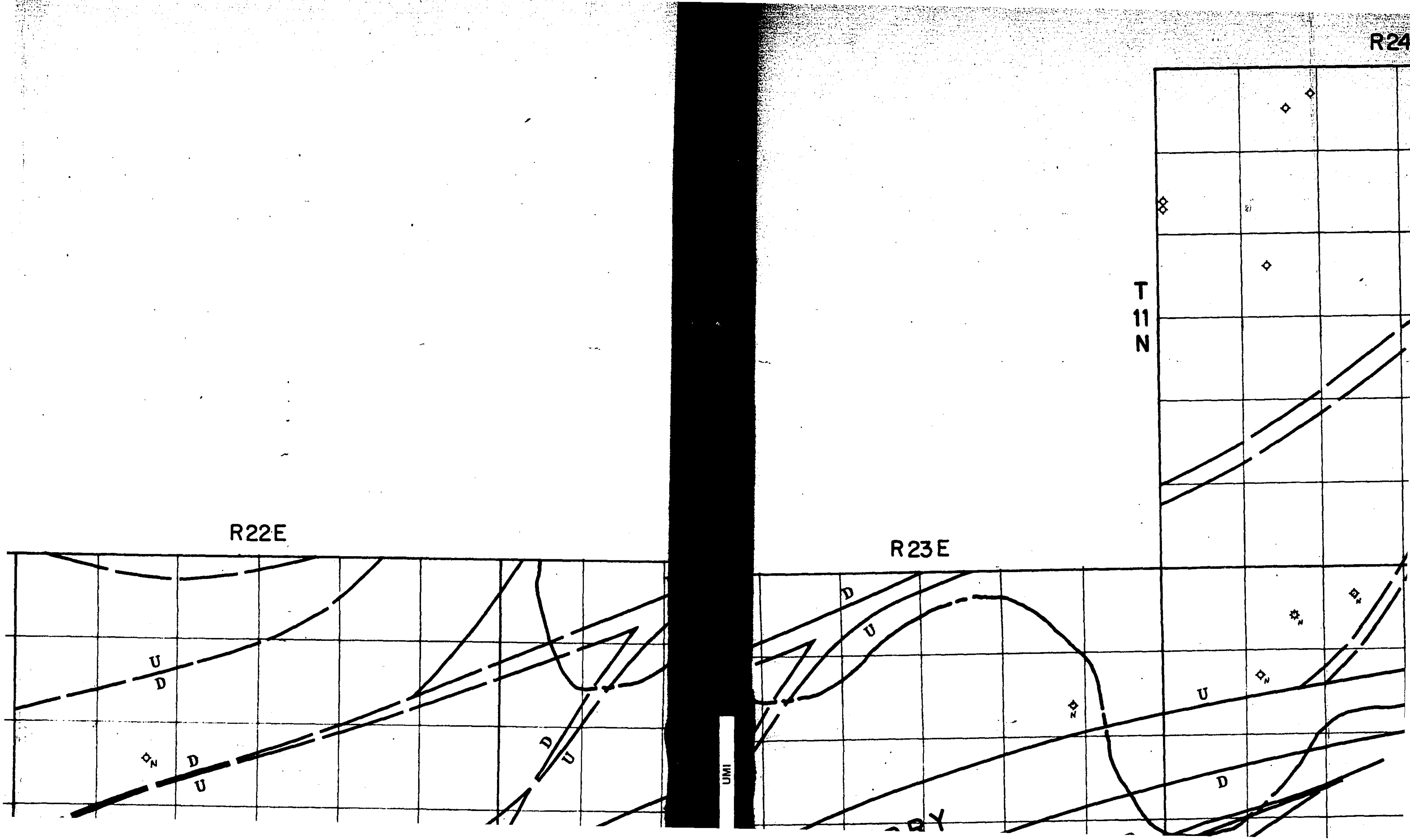
R24
T
11
N
R22E
R23E
U
D
D
U
D
U
D
U
U
D
UMI

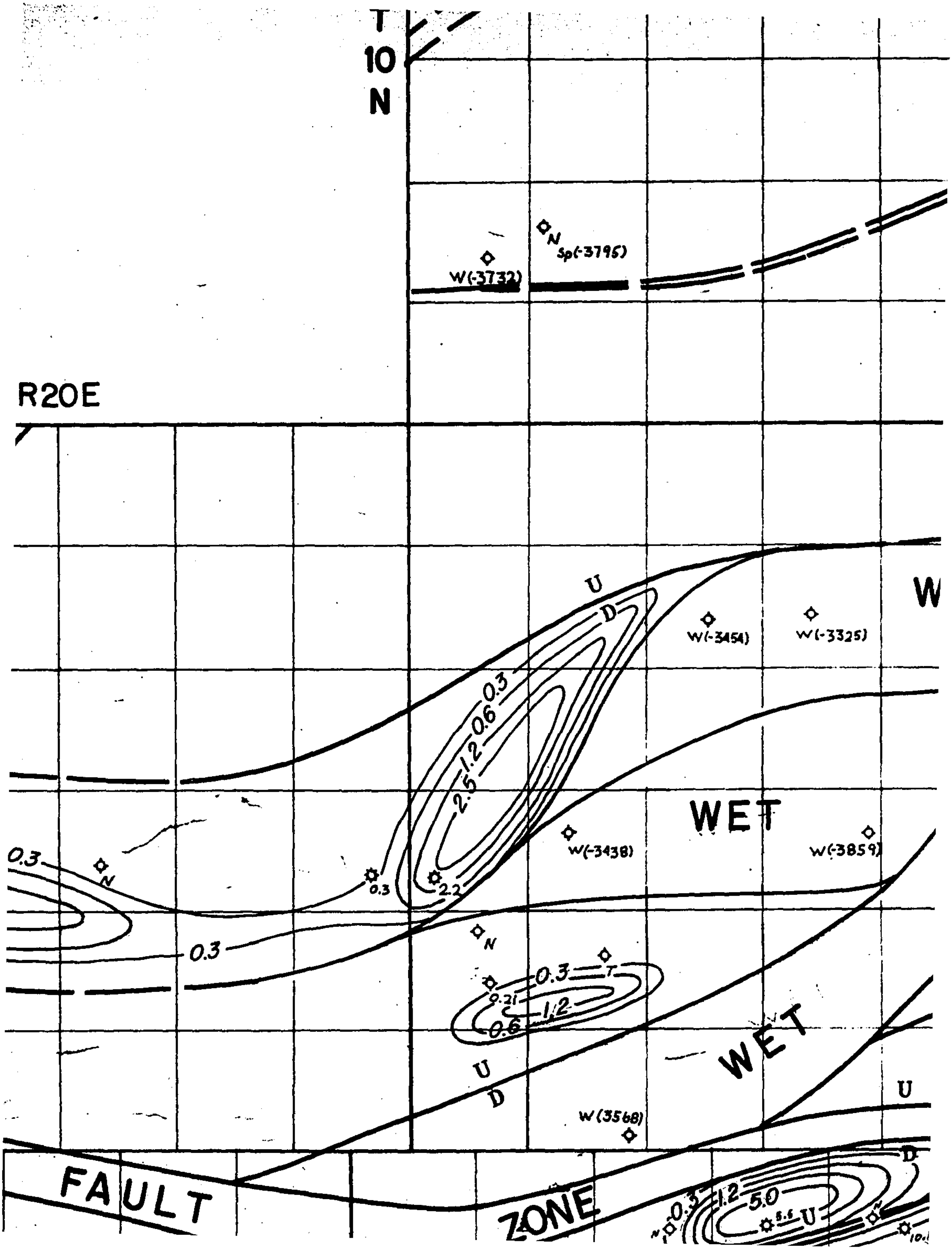
T
10
N
W(-3732)
N Sp(-3795)
R20E
W
U
D
W(-3454)
W(-3325)
0.3
0.6
1.2
2.5
WET
W(-3438)
W(-3859)
0.3
N
0.3
2.2
0.3
N
0.3
T
0.21
1.2
0.6
WET
U
D
W(3568)
U
D
FAULT
ZONE
0.3
1.2
5.0
U

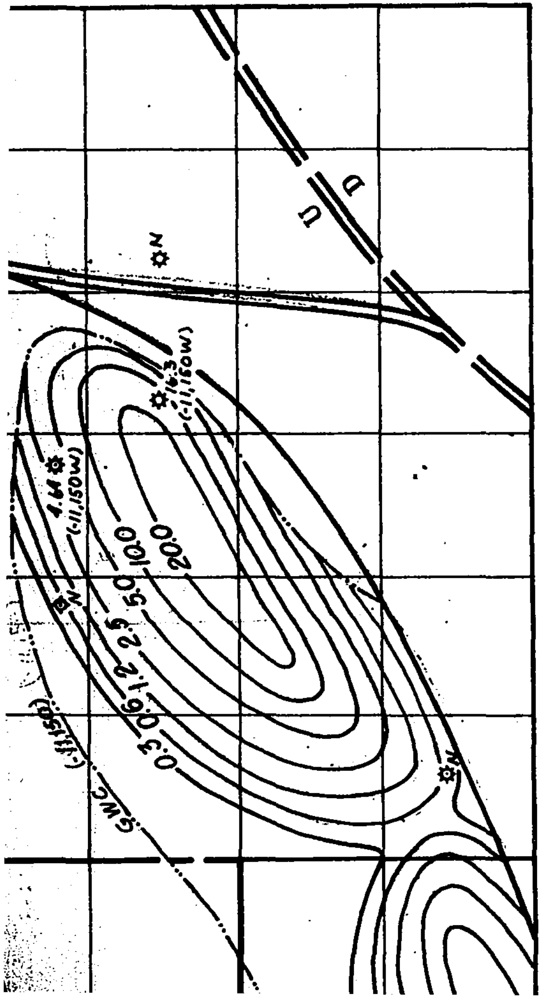
U
D
N
14.3
(-11,150W)
4.64
(-11,150W)
0.3
0.6
1.2
2.5
5.0
10.0
20.0
GWC
(-11,150)

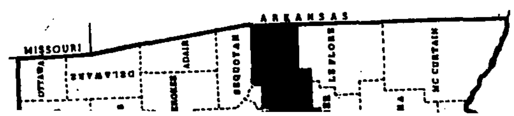
ARKANSAS
MISSOURI
OTTAWA
DELAWARE
ADAIR
SEQUOYAH
LE FLORE
MC CURTAIN

PLATE XIV

ISOPOTENTIAL M

SPIRO "A" S

ARKOMA BASIN, EASTER

CONTOUR INTERVAL GEOMETRIC INTERVA

0 1 2 3

Scale in miles

University of Oklahoma Ph.D. 1977

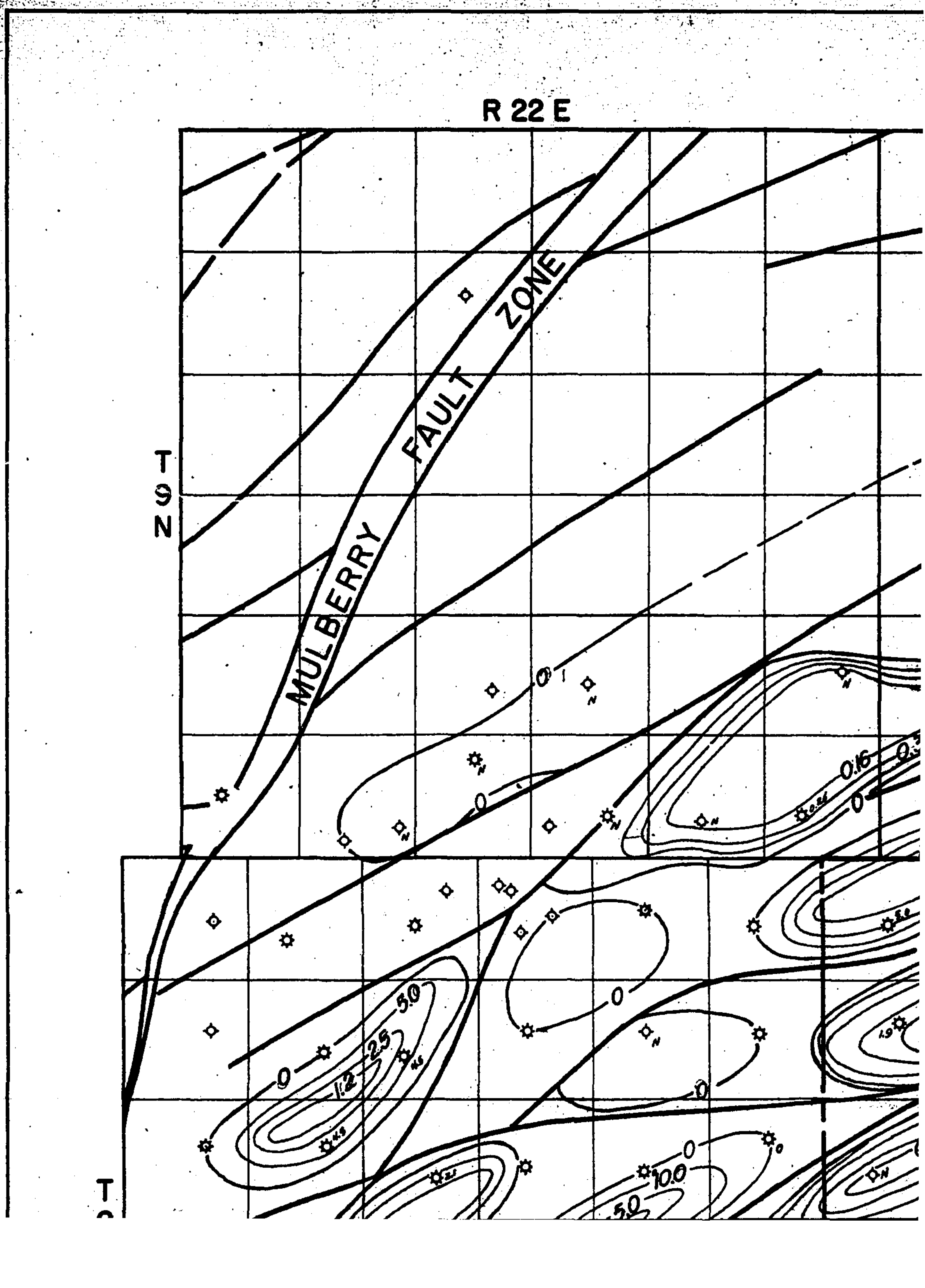
R 22 E
T 9 N
MULBERRY FAULT ZONE
T

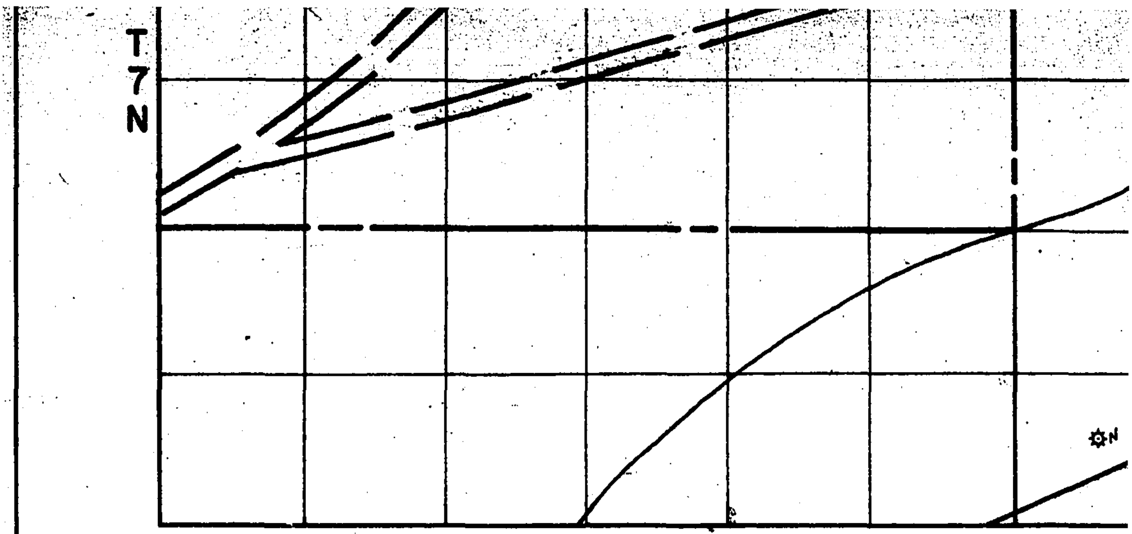

S

ARKO

CONTOUR INTE

0

University of Okl

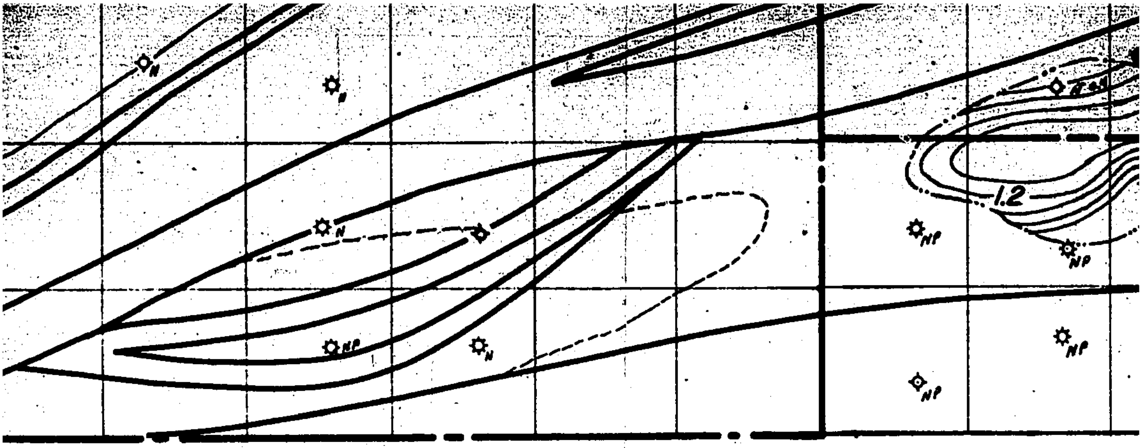

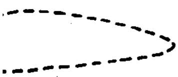

re Cromwell I shaley

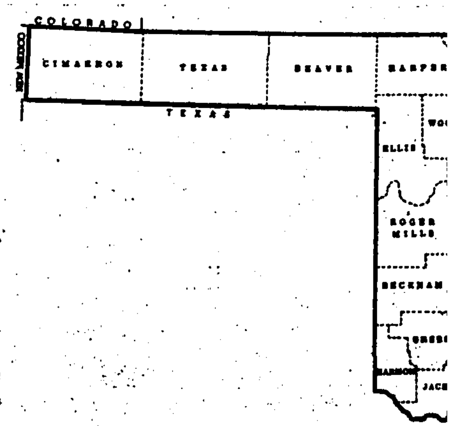

Index map

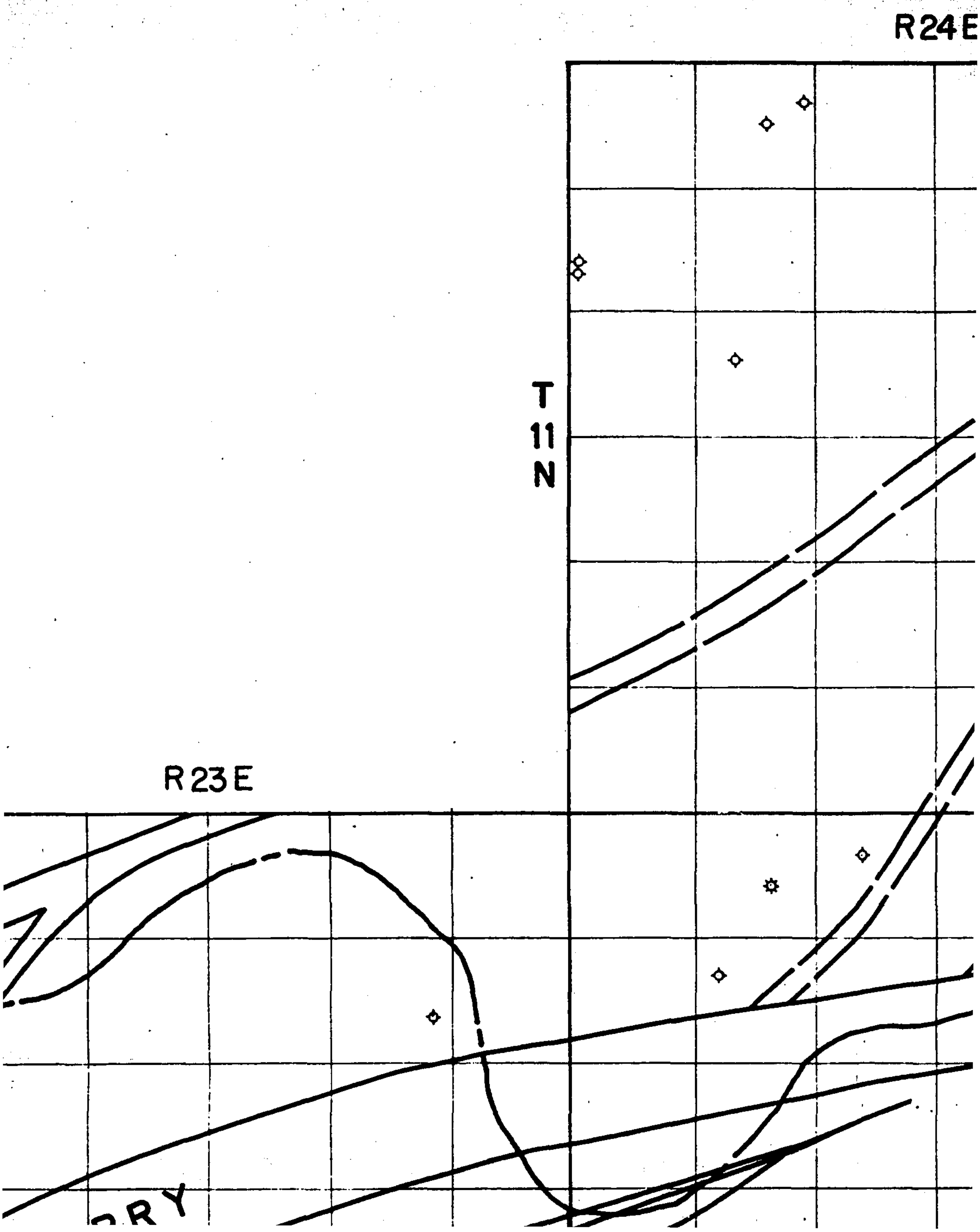
R24E
T
11
N
R23E
RY

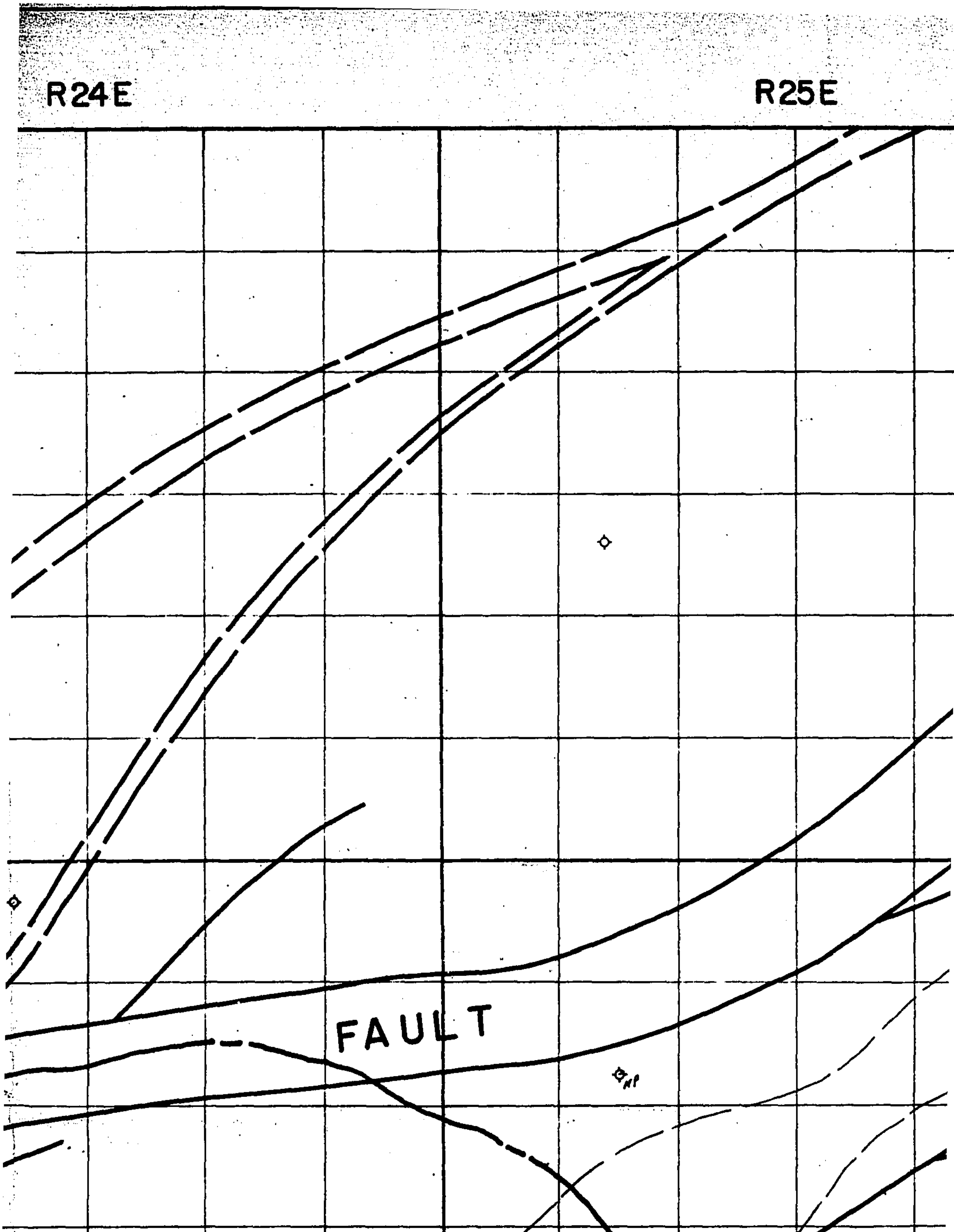
R24E
R25E
FAULT
NP

R17E

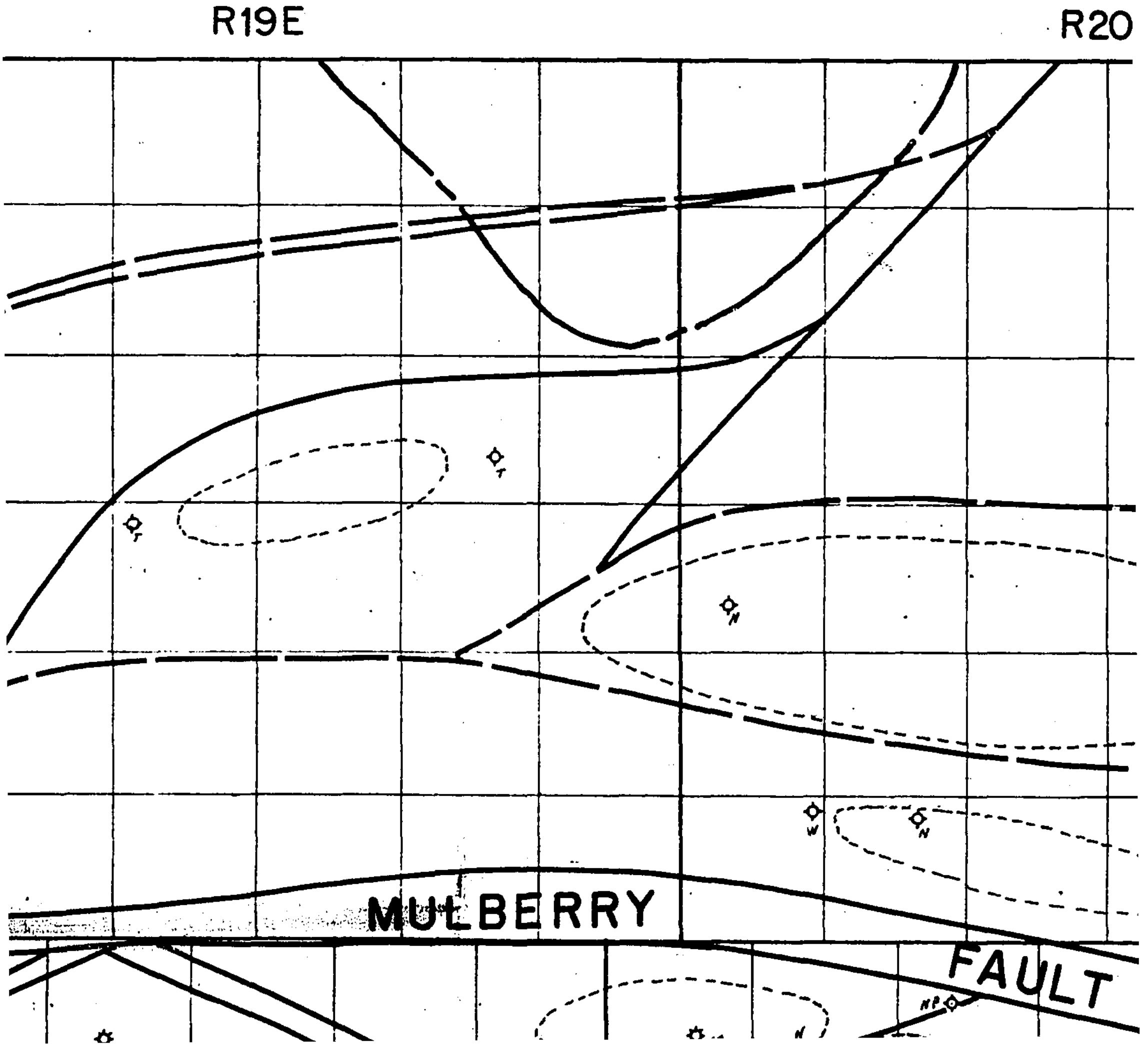
R19E
R20
MULBERRY
FAULT

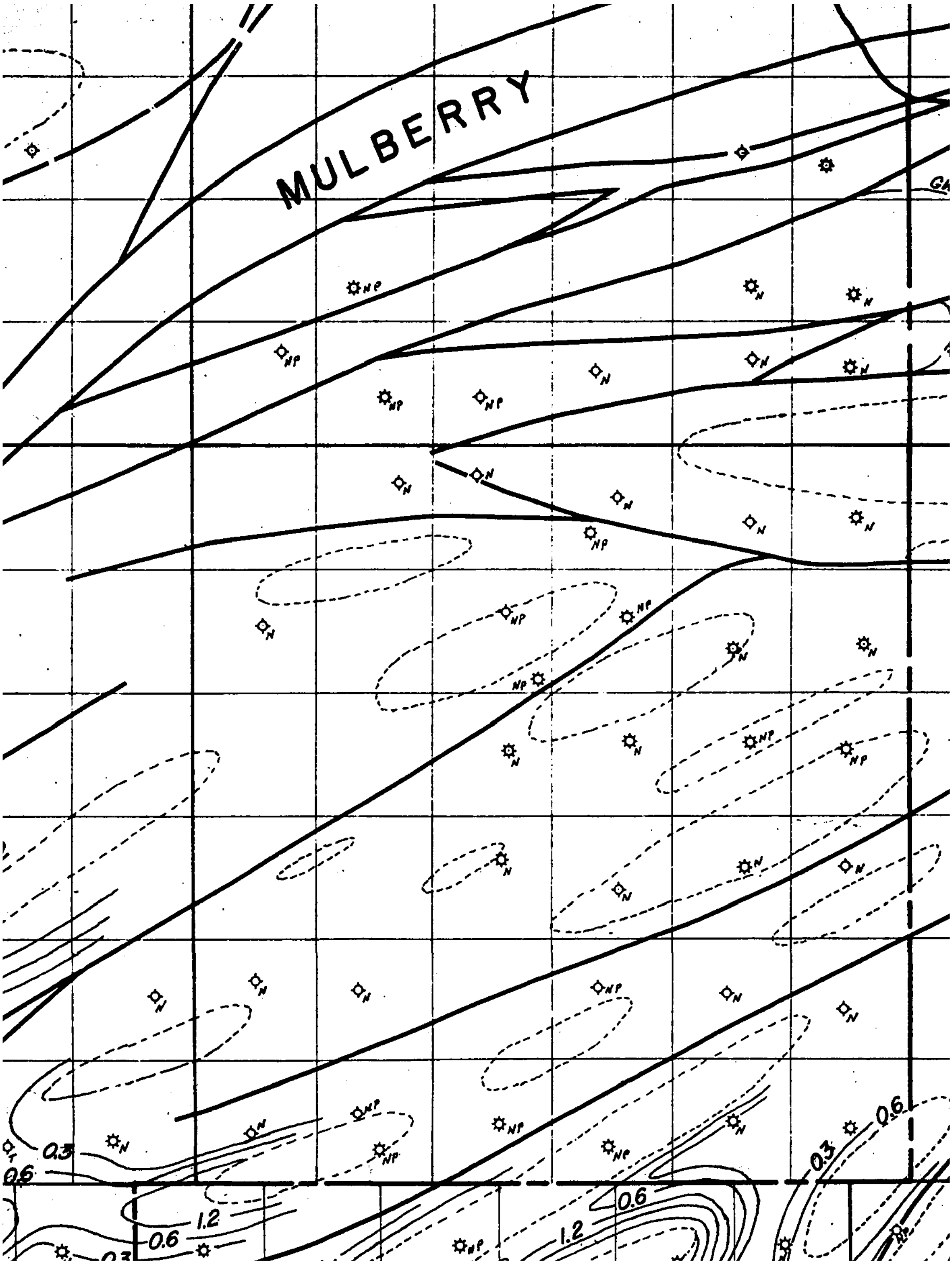
MULBERRY
0.3
0.6
1.2

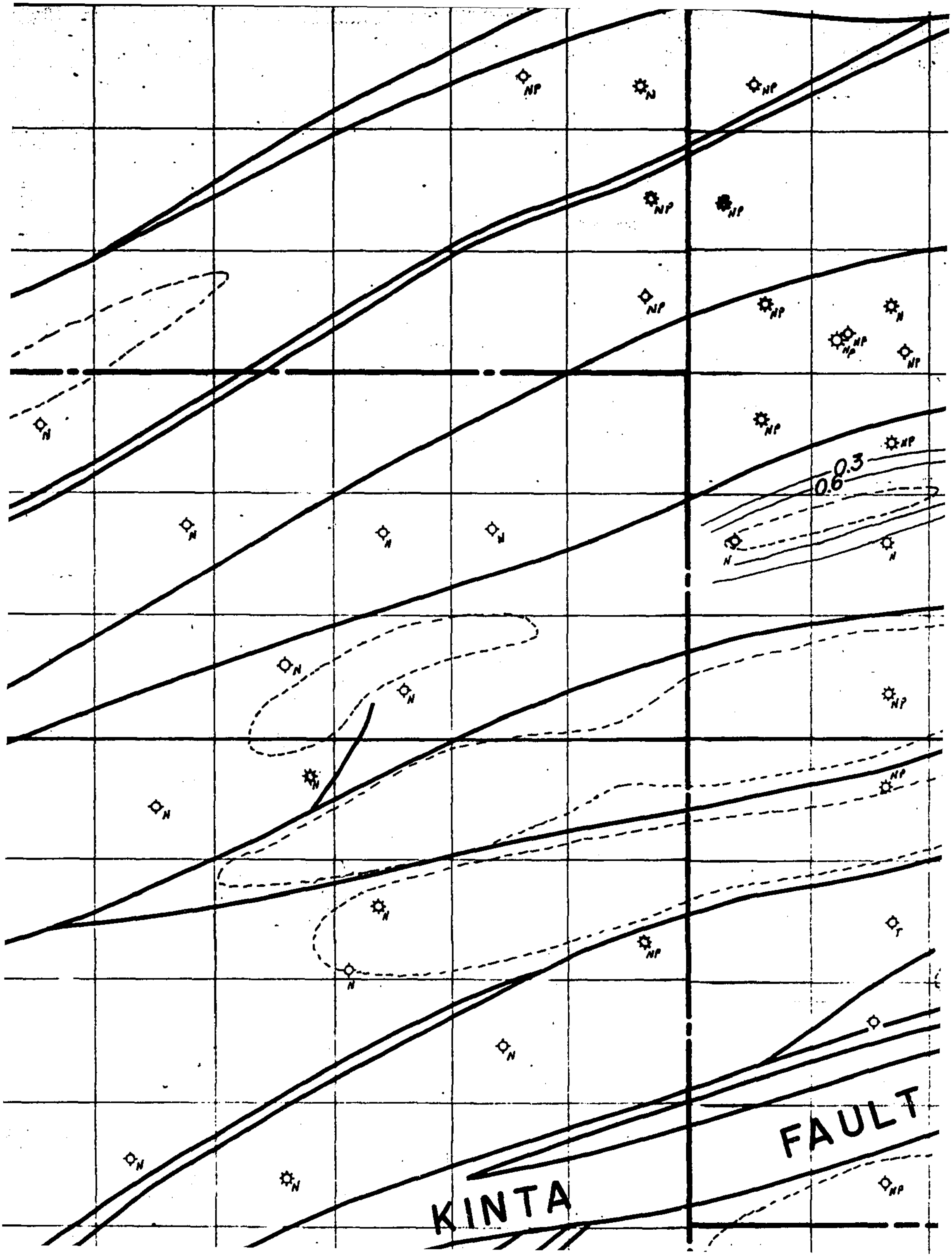

0.3
0.6
KINTA
FAULT

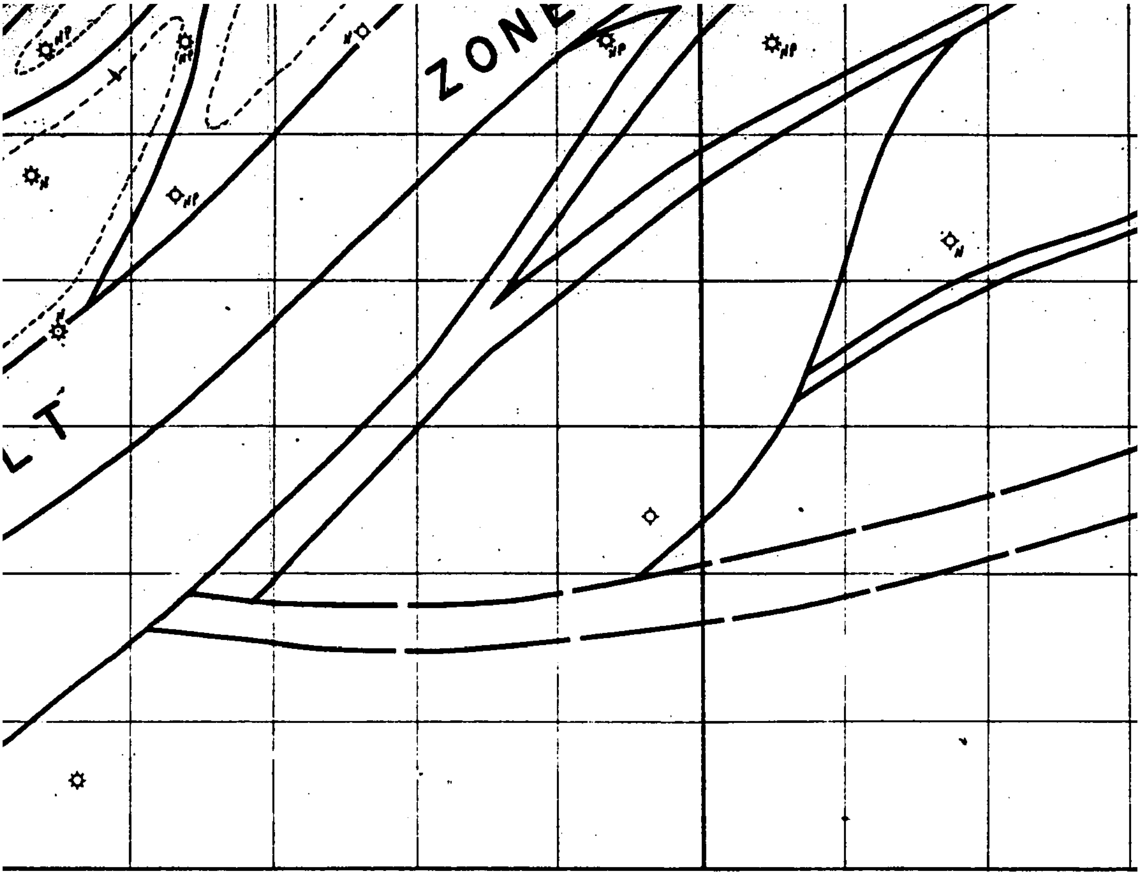
ZONE
LT

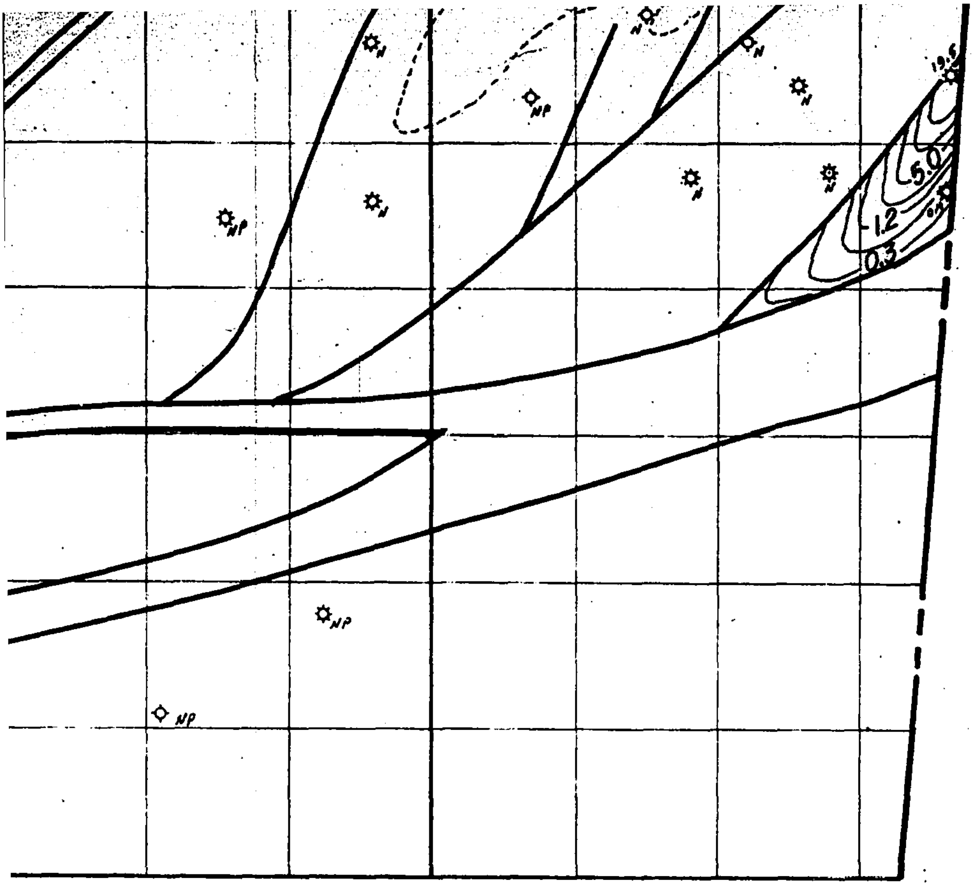

19.5
5.0
1.2
0.3
N
NP

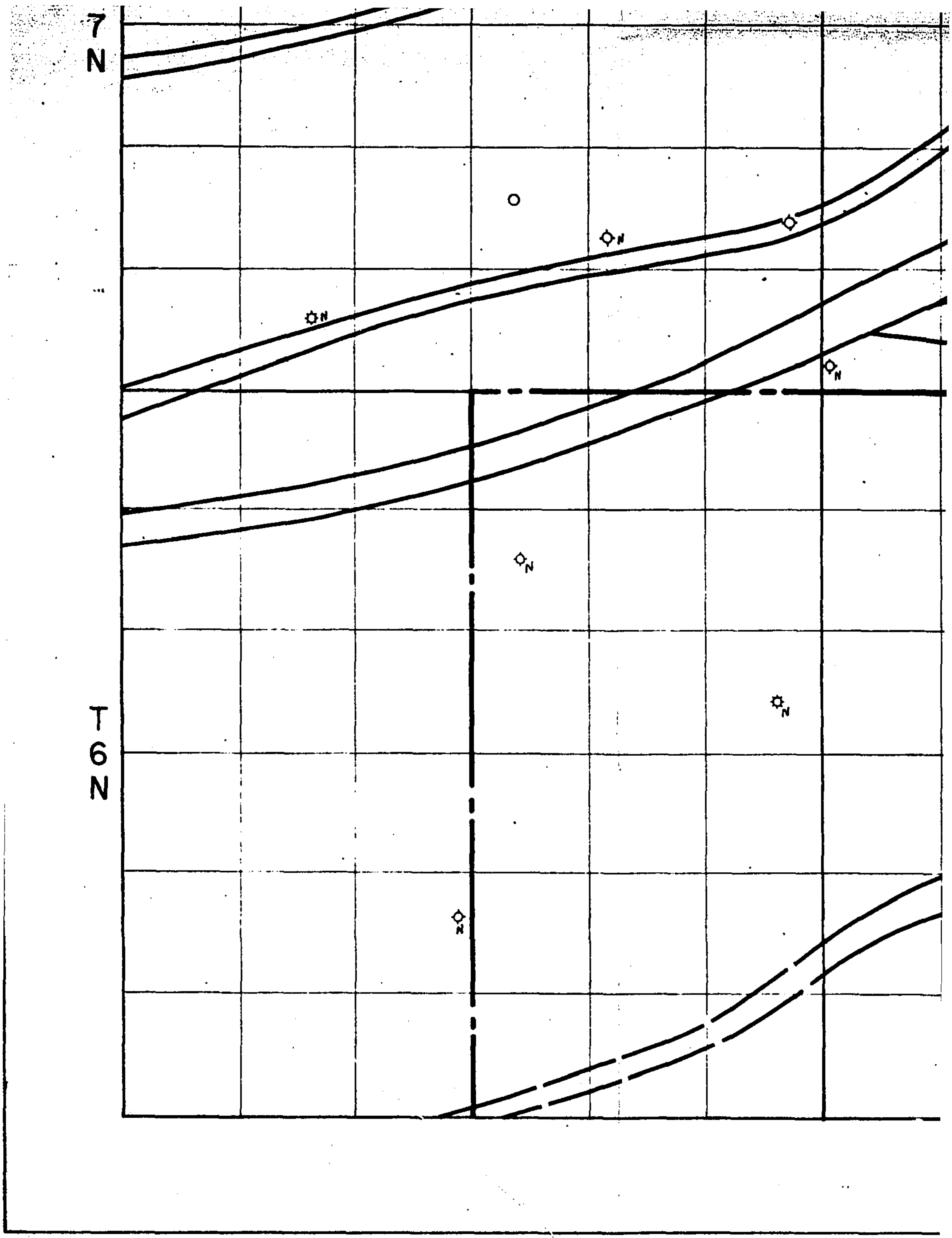

7
N
T
6
N

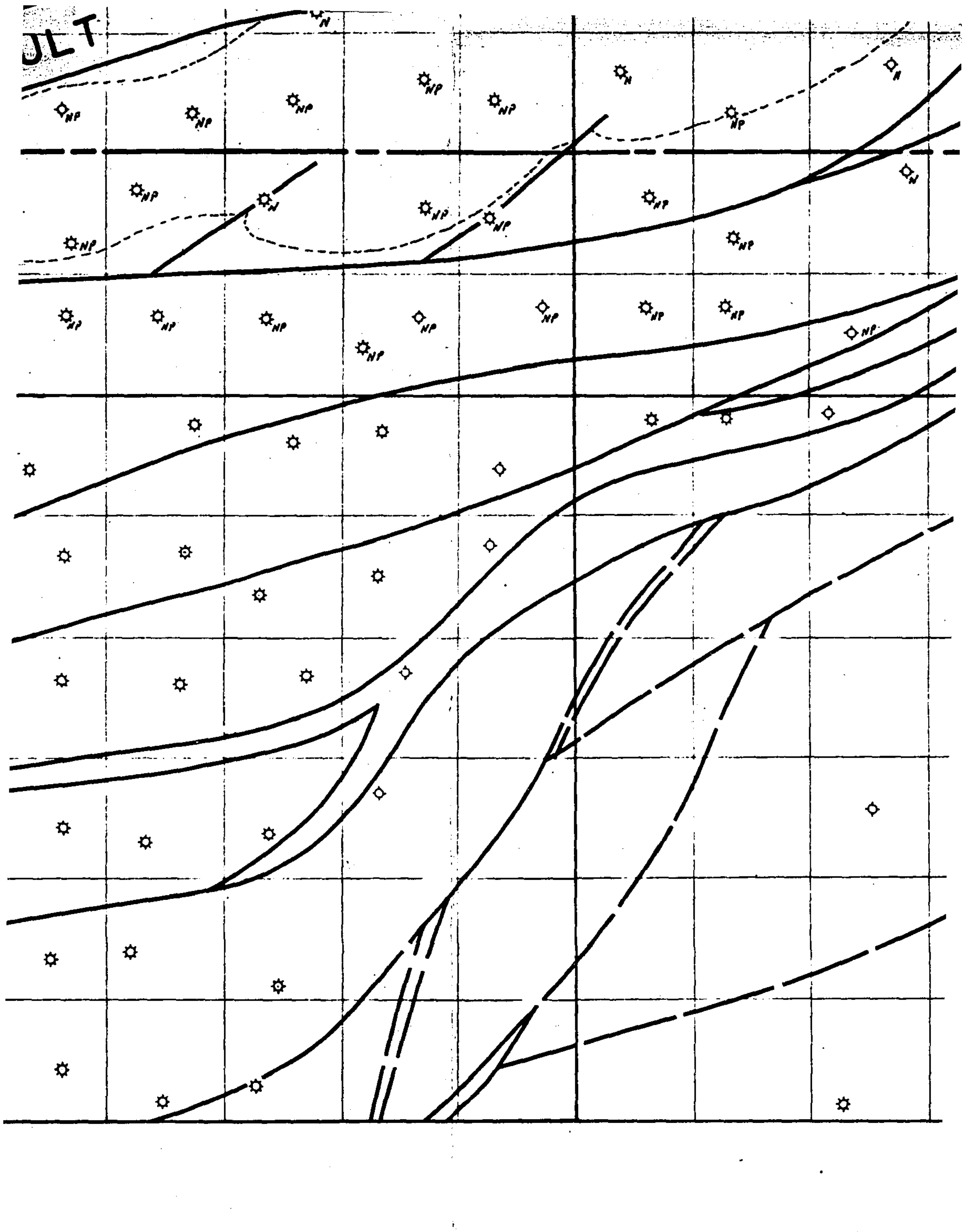

JLT
N
NP

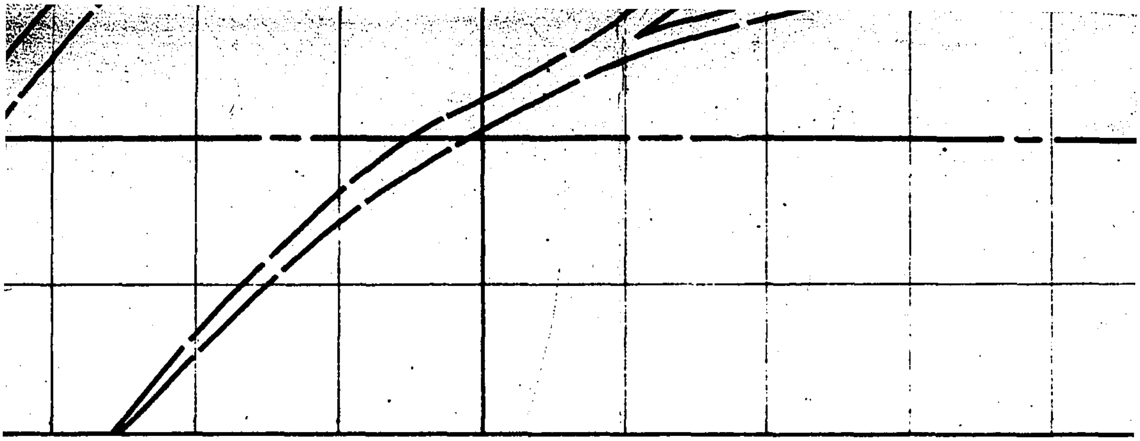

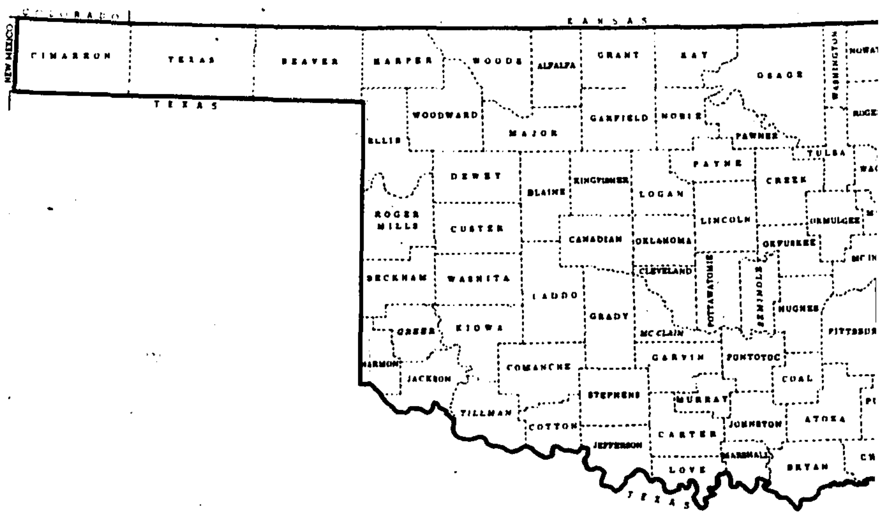

Index map showing study area mapped.

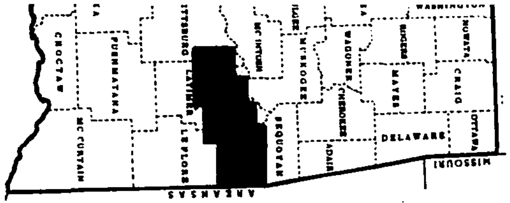
CHOCTAW
PUSHMATAHA
MC CURTAIN
LATIMER
LE FLORE
SEQUOYAH
MC INTOSH
MUSKOGEE
WAGONER
CHEROKEE
ADAIR
ROGERS
MAYES
DELAWARE
NOWATA
CRAIG
OTTAWA
ARKANSAS
MISSOURI

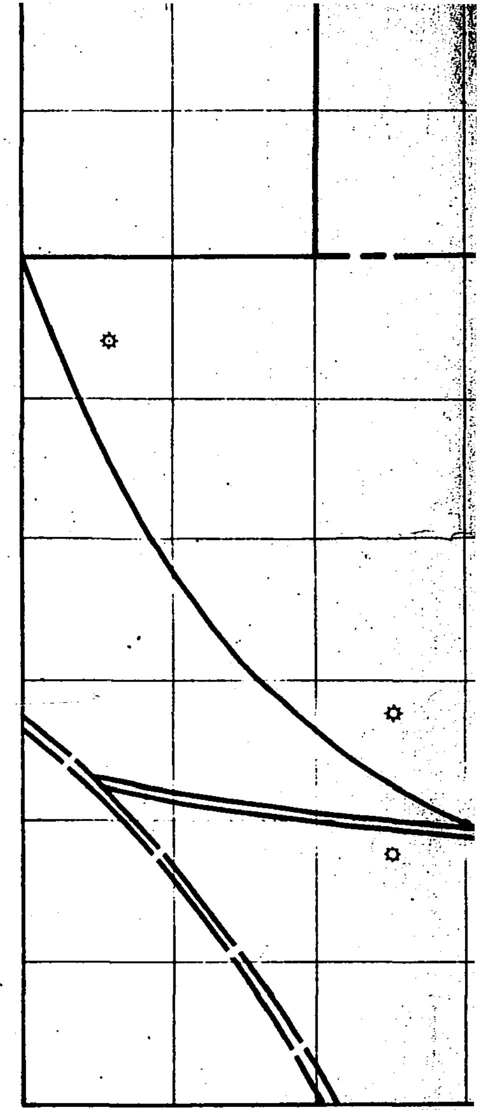

7.0 I.P. (MMCFGPD)
NP Not penetrated
N. No cores or tests
W Wet
T Tight
N̄ Non-commercial test
GWC Gas water contact

Area where Cromwell is shaley

Gas water contact

Fault

7.0 I.P. (MMCFGPD)
NP Not penetrated
N. No cores or tests
W Wet
T Tight
N̄ Non-commercial test
GWC Gas water contact

Area where Cromwell is shaley

Gas water contact

Fault

PLATE

ISOPOTENTIAL

CROMWELL II (

ARKOMA BASIN, EAST

CONTOUR INTERVAL GEOMETRIC INTER

0 1 2 3

Scale in miles

University of Oklahoma Ph.D. 1977

PLATE XVII

ENTIAL MAP OF

. II (GROSS SAND)

IN, EASTERN OKLAHOMA

/IETRIC INTERVAL TO BASE 2 (MMCFGPD)

2 3 4 5 6

Scale in miles

1977

M. W. Mc Quillan